NUMERICAL MODELING OF BUOYANT PLUMES IN A TURBULENT, STRATIFIED ATMOSPHERE

by
Ralph G. Bennett
and
Michael W. Golay

Energy Laboratory Report MIT-EL 79-002
January, 1979

NUMERICAL MODELING OF BUOYANT PLUMES IN A TURBULENT, STRATIFIED ATMOSPHERE

by

Ralph G. Bennett
and
Michael W. Golay

Energy Laboratory
and
Department of Nuclear Engineering
Massachusetts Institute of Technology
Cambridge, Massachusetts 02139

MIT-EL 79-002

January, 1979

Sponsored by

The Consolidated Edison Company of New York, Inc.

Northeast Utilities Service Corporation

MIT-EL 79-002

ERRATA

Page	Line	
64	5	speed
78	8	atmospheres
84	3	library
116	17	uncertainty
122	8	0.50 °F
126	3	analysis
11	19	The name of Pasquill is in common usage today for plume modeling. The bivariate Gaussian plume description was originated by O. G. Sutton (*Proc. Roy. Soc.* A. 135, pp. 143-165).

NUMERICAL MODELING OF BUOYANT PLUMES IN A TURBULENT, STRATIFIED ATMOSPHERE

by

Ralph G. Bennett

and

Michael W. Golay

ABSTRACT

A widely applicable computational model of buoyant, bent-over plumes in realistic atmospheres is constructed. To do this, the two-dimensional, time-dependent fluid mechanics equations are numerically integrated, while a number of important physical approximations serve to keep the approach at a tractable level. A three-dimensional picture of a steady state plume is constructed from a sequence of time-dependent, two-dimensional plume cross sections--each cross section of the sequence is spaced progressively further downwind as it is advected for a progressively longer time by the prevailing wind. The dynamics of the plume simulations are quite general. The buoyancy sources in the plume include the sensible heat in the plume, the latent heat absorbed or released in plume moisture processes, and the heating of the plume by a radioactive pollutant in the plume. The atmospheric state in the simulations is also quite general. Atmospheric variables are allowed to be functions of height, and the ambient atmospheric turbulence (also a function of height) is included in the simulations.

A demonstration of the ability of the model to reproduce the solutions to problems that are known is undertaken. Comparisons to buoyant line-thermal laboratory experiments show that the model calculates the dynamics of the fluid motions to an acceptable accuracy. Comparisons to atmospheric plume rise and dispersion experiments show that the model can simulate individual plumes more accurately than existing correlations because it calculates the effect of the atmospheric turbulence and stratification from first-principles. The comparisons also show that improvements to the model are likely to be made by more accurately describing the anisotropic nature of atmospheric turbulence, and the production of turbulence by the sources of buoyancy.

TABLE OF CONTENTS

ACKNOWLEDGEMENTS

This research was conducted under the sponsorship of Consolidated Edison and Northeast Utilities Service Corp. The authors gratefully acknowledge their support.

Blank Page

1. PROBLEM DESCRIPTION AND SOLUTION

1.1 Introduction

With the rapidly increasing burden of air pollution over recent decades, the engineer's ability to analyze the behavior of an ever-widening assortment of effluents has not kept up with the importance of the consequences of the releases. The reason for this is that the "predictive" models of plume behavior that are currently available universally suffer from a lack of extendability. That is, they need to observe the behavior of an ensemble of the releases that they wish to model before they can form an accurate picture of the release. The models are useful only to the extent that an appropriate ensemble of plumes can be created for study, either as full-scale atmospheric releases, or as scaled-down laboratory experiments. Inasmuch as the important turbulent and thermal characteristics of the atmosphere cannot be simulated in the laboratory, and since an ensemble of plumes with catastrophic consequences (e.g., radioactive plumes from nuclear reactor accidents) may be impractical to produce, plume modeling has needed to take a more universal approach.

The purpose of this work is to construct a widely applicable model of plume behavior in realistic atmospheres. To do this, a "first principles" approach is adopted. A numerical integration of the fluid mechanics equation is undertaken, while a number of important physical approximations to the problem serve to keep the approach at a tractable level. The advantage of the model presented here is the ability to tackle problems outside of the scope of existing models without greatly increasing the resources spent on the analysis.

1.2 Background and Problem Description

1.2.1 Historical Background

Man has produced and observed bent-over buoyant plumes since the discovery of fire. However, the bent-over plume did not have any great impact on society until the advent of large industrial sources near population centers during the industrial revolution. The number of large industrial sources has increased steadily with the industrialization of many countries. In the recent past, the variety of releases from large industrial sources has increased greatly, and now includes the potentially more harmful effluents from chemical refining and combustion processes, nuclear power plants, and large cooling towers. Also, the steady growth of population centers almost always dictates that these new sources will be located in at least moderately populated areas.

Historically, the ability to analyze the effects of large releases and hence to develop technologies for their mitigation has not kept pace with the consequences of the releases. To date, the advances have been quite modest: early observations during the industrial revolution suggested the use of tall stacks for lessening the effects of large releases. The strong influence of the synoptic-scale weather on releases (first investigated in order to increase the effectiveness of chemical warfare agents) has largely motivated the Pasquill-type correlations of plume behavior. The hope of simply reducing the consequences by reducing the amount of effluents has stimulated an abundance of filtering, scrubbing, and effluent control technologies. However, increasingly important releases are certain to occur. A brief review here of the existing approaches to plume modeling can indicate the most promising avenue for study.

1.2.2 Characteristics of Bent-Over Buoyant Plumes

The character of the bent-over buoyant plume is central to all of the available plume models. When an effluent stream with a given upward momentum and initial buoyancy is released from a stack into a windy atmosphere, the plume is deflected downwind. This occurs partly because of pressure forces that develop around the plume, and partly because the plume entrains the ambient air, which mixes a lot of downwind momentum into the plume. The deflection quickly causes the plume to bend over (usually within about one stack height) and then to be carried downstream. The buoyancy of the plume is converted into kinetic energy, and the plume rises under this action for a considerable distance downwind. About 20 years ago it was noted[1] that the motion of the plume in cross section during this rise was essentially that of a two-dimensional turbulent vortex pair. Initially the vortex pair rises and grows without being too dependent upon atmospheric turbulence (although atmospheric stratification is always important). After the kinetic energy of the cross-sectional motions has essentially died out, the plume continues to disperse solely by atmospheric motions. It will be found in the review of plume models that only the detailed numerical plume models provide a method that can easily bridge between the regimes where plume turbulence dominates and where atmospheric turbulence dominates.

1.2.3 Overview of Plume Models

With regard to the detailed three-dimensional nature of plume motions, existing models of plume behavior are found to possess a wide variety of sophistication. The Pasquill-type models, the entrainment models, and the numerical models are considered here.

The Pasquill-type models develop a highly idealized picture of the fluid motions in and around the plume. Pollutants in the plume cross section are assumed to fit Gaussian distributions of height and width. In essence, the model parameters (standard deviations of the Gaussian distributions) are simply an ad-hoc replica of the experimental results; as such, the models are unable to predict in cases for which experiments have not been performed. The wealth of non-passive effluents and the rich variations in the meteorological state of the atmosphere serve to guarantee that cases outside of the Pasquill-type models will always exist.

The entrainment models develop a much less idealized, and much more physical picture of the fluid motions in the plume. In general, the models make use of the very elegant non-dimensional formulations and similarity relationships that are central to the theory of homogeneous isotropic turbulence. Typically the models are successful at analyzing the initial plume behavior, where the self-generated plume turbulence dominates over the atmospheric turbulence. The entrainment models are generally able to analyze plumes only in fairly simple atmospheres when analytical solutions are sought. But this is not the primary limitation of entrainment models, since in some cases their solutions are found on computers. The limitations of the entrainment models are the condition that the plume self-generated turbulence is dominant over the atmospheric turbulence, (which eventually breaks down for all plumes, commonly at downwind distances for which the solution is still needed) and the basic entrainment velocity assumption, which cannot be obtained from fundamental constants and scales in a straightforward way.

Numerical plume models are capable of developing the most detailed picture of the fluid motions in the plume. In general, the models seek to integrate a closed set of Reynolds-averaged fluid mechanics equations, either in two or three dimensions. Turbulence leads to a fundamental closure problem in writing this set of equations, so that each model will have a collection of closure assumptions that together form a turbulence model, aside from other assumptions that are made concerning the plume behavior. Numerical plume models are becoming capable of analyzing the most detailed cases, yet they are often limited by the large computing costs. Aside from the computer costs, the tasks of initializing and validating the problem with fully two- or three-dimensional data can also quickly become intractable. Until computer costs are reduced greatly, the most useful numerical plume models will likely have to be two-dimensional. The greatest benefit that comes from such models is the wider range of application of the models, and the ease of extending them to new cases.

1.2.4 Scope of the Work

This work constructs a three-dimensional solution of a steady state plume from a sequence of time-dependent two-dimensional plume cross sections; each plume cross section of the sequence being spaced progressively further downwind as it is advected for a progressively longer time by the prevailing wind. The two-dimensional cross sections are simulated with a time-dependent turbulent fluid mechanics code which integrates the time-averaged equations of continuity, momentum, energy, moisture, and pollutant. The behavior of an individual plume is modeled in this way until the height or radius of the plume reaches several hundred meters, which roughly corresponds to the plume cross section being tens of kilometers downwind of the source.

The dynamics of the plume simulations are quite general. The buoyancy sources in the plume encompass the sensible heat in the plume, the latent heat absorbed or released in plume moisture processes, and the radioactive decay heating of the plume by a radioactive pollutant species in the plume. Buoyancy from chemical reactions could be easily included. The atmospheric state in the simulations accepts atmospheric wind, temperature, water vapor, liquid water, background pollutant, turbulent eddy viscosity, and turbulent kinetic energy as functions of height. The turbulence is treated with the sophisticated second-order closure model of Stuhmiller[2], which allows the turbulent recirculation and entrainment of the plume cross section to be treated in a very natural way.

The model is validated against the Pasquill model[3] and the entrainment model of Richards[4] for idealized cases in which these models apply, and for several cases from the LAPPES[5] field data for actual large power plant stacks. Simulations are obtained for cases outside of the Pasquill and entrainment models, and while no specific field data for these cases exists, the behavior of the simulation agrees with the physical changes imposed on the problems.

2. LITERATURE REVIEW

The literature review in this work undertakes a broad survey of plume modeling. In the first section, existing numerical plume models are discussed, along with the experimental data base that is available for the validation of these detailed plume models. The first section also includes the research that has been done on computational and experimental modeling of two-dimensional line vortex pairs. It is important to include them since the results of such work are very easily interpreted in the context of air pollution problems. In the second section, existing numerical models of the planetary boundary layer are discussed. Again, these models are very easily extended to air pollution problems (with the inclusion of a pollutant transport equation and pollutant source), so it is important to include them in the review.

2.1 Numerical Plume Models

A large number of plume models have been developed that are available as computer programs. Several recent reviews[6-8] have reported dozens of such models, and it is important to make a distinction regarding them. A majority of the models employ the Gaussian plume assumption; as such, the computer is simply being used to look up and present the standard handbook calculations, with minor modifications in some cases. These are not"numerical plume models" in the sense that the primitive equations are not being integrated to show the plume development, although computers are being used. Such models are not considered further here. The remaining models in the reviews are truly numerical plume models, and they will be considered next, along with several models that were reported elsewhere.

2.1.1 Three-Dimensional Models

The most sophisticated numerical plume models to date have not yet attempted a second-order turbulence closure to the fully three-dimensional flow field for non-passive pollutants. Some of these features are found in each of the models discussed here, but not all of them. The notes of Rao[9] and Nappo[10] discuss the desirable features of three-dimensional numerical plume models, and provide a good introduction to future work that may be undertaken.

Donaldson's modeling[11] has concentrated on a second-order turbulence closure for a three-dimensional planetary boundary layer simulation with a passive pollutant. Because the pollutant is passive, and hence does not affect the flow field or its turbulence, the turbulence closure only addresses PBL turbulence, and is independent of the behavior of buoyant plumes. This is in contrast to the method in this work, where the second-order closure is "tuned" to the development of turbulent buoyant plumes, and is largely independent of PBL turbulence development. Lewellen's modeling[12] begins with a second-order closure to the passive pollutant transport equation, and then adopts the PBL flow field and turbulence from Donaldson's model.[11] Only integrations of the pollutant transport equation are needed in Lewellen's model because of the adoption of a complete PBL solution. Patankar's model[13] of a deflected turbulent jet in three-dimensions also uses a second-order closure model, but does not allow for buoyancy and stratification, although it does allow for non-isotropic turbulent transports in the vertical and horizontal directions. A fundamentally different approach to three-dimensional modeling is found in the Atmospheric Release Advisory Capability (ARAC) system.[15-22] A mass-consistent three-dimensional wind field is interpolated from a small set of local tower wind measurements and used to predict the advection of a passive pollutant. Turbulent diffusion is modeled with a zero equation model, although many other important features such as rainout, wet and dry deposition, and surface terrain have been added.

2.1.2 Two-Dimensional Models

Two two-dimensional numerical plume models have been found in the literature. Henninger's model[23] solves continuity, momentum, energy, and moisture with a less-sophisticated zero-equation turbulence closure, and with a more sophisticated treatment of moisture. For plumes in a wind, the model chooses the mesh alignment shown in Fig. 3.3.2.1b of Sec. 3.3.2, which is felt to be a less satisfactory choice than that of the present work. Taft's model[24] is much closer to the model in this work, since it adopts the same mesh alignment (see Fig. 3.3.2.1c in Sec. 3.3.2). The principal differences are that Taft's model employs a one-equation turbulence model, uses a more complex moisture model, and does not make any attempt to describe ambient atmospheric turbulence.

A number of two-dimensional numerical buoyant thermal models have evolved in the literature of meteorology, usually in support of efforts to parameterize the growth of rain clouds. The models have not been applied to air pollution directly, but could be easily converted. Lilly's model[25] seeks a self-preserving solution for the (dry) buoyant line thermal, and as such, would only be applicable for the early plume behavior when plume self-turbulence is dominating. Johnson's model[26] is used to study fog clearing on runways with helicopter downwash; while the moisture equations are more complex than that in this work, the eddy viscosity is assumed to be constant. Ogura's model[27] of rain cloud development also assumes a constant eddy viscosity, while Arnason's model[28] ignores eddy transports altogether. Liu's model[29] employs a stratification of atmospheric turbulence into two constant eddy viscosity layers. While the treatment of turbulence in these models is very simple, it should be emphasized that these models are focussed on precipitation modeling, and they are likely to be helpful in the improvement of the moisture model in this work. A recent review of precipitation modeling is found in Cotton.[30]

2.1.3 Experimental Studies

The field study that the model in this work is validated against is the Large Power Plant Effluent Study (LAPPES).[5] Complete field data for stack plumes from three mine-mouth coal-fired plants are found in the four volumes of the study: wind, temperature, and humidity profiles, plant operating characteristics, and plume SO_2 concentration cross sections are of the most interest in this work. The Chalk Point Cooling Tower Project (CPCTP)[31] is also of interest to this work since it provides cooling tower plume cross sections, but plant operating data[32] was not available during this work.

The experimental laboratory studies that this work is validated against are the papers of Tsang[33] and Richards.[4] The experiments study the behavior of two-dimensional line thermals released in a water tank. The ambient receiving fluid in the tank is both laminar and unstratified, and the thermals are fully turbulent.

2.2 Numerical Planetary Boundary Layer Modeling

A three-dimensional numerical model of the planetary boundary layer has been reported by Deardorff[34-36] that could easily be adapted to local air pollution studies, although the expense is likely to be prohibitive. The model solves the complete set of primitive equations (with an eighteen-equation model of turbulence) in a box that ranges 5 km on a side and 2 km deep. The numerical experiments to date have compared very favorably with several well-documented planetary boundary layer field studies.

To apply the model to a single source of pollutant, a single mesh cell could be initialized with sources of momentum, heat, moisture, pollutant, and turbulence. To accommodate this, a pollutant transport equation would have to be added, and an additional three-equation model of turbulent pollutant fluxes would need to be developed. Time-dependent or steady-state releases could be modeled in great detail in this way.

However, the model currently requires 15 seconds of CPU on a CDC-7600 to simulate 1 second of flow in the atmosphere. Also, the specification of boundary conditions on a three-dimensional mesh with accurate time-dependent micrometeorological data would require a very elaborate reporting network. Nonetheless, the model represents a more sophisticated and potentially more accurate approach than the model in this work.

3. HYDRODYNAMIC MODEL DEVELOPMENT

3.1 Introduction

In order to model buoyant plumes in the atmosphere, the equation set contained in the VARR-II computer code is reinterpreted and expanded. A reinterpretation of the hydrodynamic variables is necessary in order to satisfactorily account for the compressible nature of an atmosphere that is at rest. The equations are expanded in Sec. 3.2.1 to include the transport of a pollutant and radioactive decay heating by the pollutant, and in Sec. 3.2.2, where the transport of water vapor, cloud liquid water, and the energy released or absorbed during the phase changes of water substance are considered. Since so many fundamental changes are made here in reinterpreting the VARR-II equation set, this discussion of the model development undertakes a derivation of the equations; for completeness it reiterates the important assumptions contained in the VARR-II code which were developed outside of this work.

3.2 Hydrodynamic Model Equation Sets

3.2.1 Equations for Dry Atmospheres

The equations for a dry atmosphere are derived in this section. When the potential temperature is simply reinterpreted as the virtual potential temperature, these equations are applicable to moist plumes in moist atmospheres if none of the moisture undergoes a change of phase, and if the turbulent diffusion coefficients of heat and moisture are equal. A further discussion of virtual potential temperature is found in Sec. 3.2.2.1.

3.2.1.1 Reference State Decomposition

As a starting point for the model development, consider the three-dimensional compressible fluid mechanics equations, where the six primitive variables $\tilde{p}$, $\tilde{\rho}$, $\tilde{T}$, and $\tilde{u}_i$ are physically measurable values of the fluctuating pressure, density, temperature, and velocity, respectively:

Continuity Eq:

$$\frac{\partial\tilde{\rho}}{\partial t} + \frac{\partial}{\partial x_j}(\tilde{\rho}\tilde{u}_j) = 0 \tag{3.1}$$

Momentum Eq:

$$\frac{\partial}{\partial t}(\tilde{\rho}\tilde{u}_i) + \frac{\partial}{\partial x_j}(\tilde{\rho}\tilde{u}_i\tilde{u}_j) = -\frac{\partial\tilde{p}}{\partial x_i} - \tilde{\rho}g_i + \mu\frac{\partial^2\tilde{u}_i}{\partial x_j^2} \tag{3.2}$$

Energy Eq:

$$\frac{\partial}{\partial t}(\tilde{\rho}\tilde{T}) + \frac{\partial}{\partial x_j}(\tilde{\rho}\tilde{u}_j\tilde{T}) = \frac{\tilde{u}_j}{c_p}\frac{\partial\tilde{p}}{\partial x_j} + \frac{\partial}{\partial x_j}k\frac{\partial\tilde{T}}{\partial x_j} + \frac{1}{c_p}\frac{\partial\tilde{p}}{\partial t} \tag{3.3}$$

Equation of State:

$$\tilde{p} = \tilde{\rho} R_d \tilde{T} \qquad (3.4)$$

These equations have property values μ, c_p, and k, which may depend upon temperature in general. The energy equation has neglected the kinetic energy in the fluid motions, and the equation of state is that for an ideal dry gas.

The variations of temperature, pressure, and density in a static atmosphere are usually "subtracted out" of these equations in meteorological analyses by a reference state decomposition. That is, equations of motion for perturbations about an adiabatic atmosphere are sought by decomposing the primitive variables as

$$\left\{\begin{array}{l}\text{the value}\\ \text{of a primi-}\\ \text{tive variable}\end{array}\right\} = \left\{\begin{array}{l}\text{its value in}\\ \text{an adiabatic}\\ \text{atmosphere}\\ \text{(function of}\\ \text{height only)}\end{array}\right\} + \left\{\begin{array}{l}\text{a departure}\\ \text{from the}\\ \text{state at}\\ \text{rest}\end{array}\right\} \qquad (3.5)$$

or, in terms of the notation in this work

$$\tilde{p} \rightarrow p_o + p \qquad (3.6)$$

$$\tilde{\rho} \rightarrow \rho_o + \rho \qquad (3.7)$$

$$\tilde{T} \rightarrow T_o + T \qquad (3.8)$$

$$\tilde{u}_i \rightarrow 0 + u_i \qquad (3.9)$$

The state of the dry, adiabatic atmosphere is found by making the substitutions Eq. 3.6-Eq. 3.9 into Eq. 3.1-Eq. 3.4, and setting the time derivatives and the perturbations p, ρ, T, and u_i to zero. The continuity and energy equations become trivial under this substitution. The momentum equation becomes the hydrostatic equation:

$$\frac{dp_o}{dz} = -\rho_o g \tag{3.10}$$

The equation of state is simply

$$p_o = \rho_o R_d T_o \tag{3.11}$$

The First Law of Thermodynamics for an adiabatic process is

$$dQ = 0 = c_p dT_o - dp_o/\rho_o \tag{3.12}$$

Dividing by a displacement dz gives

$$\frac{dp_o}{dz} = \rho_o c_p \frac{dT_o}{dz} \tag{3.13}$$

and substitution of Eq. 3.13 into Eq. 3.10 gives Γ_d, the lapse rate of the dry adiabatic atmosphere:

$$\Gamma_d \equiv -\frac{dT_o}{dz} = \frac{g}{c_p} = 9.76\ ^{\circ}C/\mathrm{km} \tag{3.14}$$

To this point the solution of the adiabatic atmosphere has been presented. Substituting the reference state decomposition, Eq. 3.6-Eq. 3.9 into the equations of motion, Eq. 3.1-Eq. 3.4, and using the results of the adiabatic atmosphere, Eq. 3.10 and Eq. 3.14, gives the equations of motion for the perturbations:

Continuity Equation

$$\frac{\partial u_j}{\partial x_j} = - \frac{u_j}{\rho_o} \frac{\partial \rho_o}{\partial x_j} + \frac{R_d}{c_p} \frac{k}{\rho_o} \frac{\partial^2 T}{\partial x_j^2} \simeq 0 \qquad (3.15)$$

Momentum Equation:

$$\rho_o \frac{\partial u_i}{\partial t} + \rho_o u_j \frac{\partial u_i}{\partial x_j} = - \frac{\partial p}{\partial x_i} - \rho g_i + \mu_o \frac{\partial^2 u_i}{\partial x_j^2} \qquad (3.16)$$

Energy Equation:

$$\rho_o \frac{\partial T}{\partial t} + \rho_o u_j \frac{\partial T}{\partial x_j} = \frac{R_d}{c_p} \frac{\partial^2 T}{\partial x_j^2} \qquad (3.17)$$

Equation of State:

$$\frac{p}{p_o} = \frac{T}{T_o} + \frac{\rho}{\rho_o} + \frac{\rho T}{\rho_o T_o} \qquad (3.18)$$

The fluid perturbations will generally be assumed to be incompressible in the Boussinesq sense. That is, changes in fluid density are assumed to be produced only by temperature changes, and not by pressure fluctuations. Neglecting the pressure fluctations in the equation of state, and noting that generally $\rho T << \rho_o T_o$, the equation of state becomes

$$\rho/\rho_o \simeq -T/T_o \qquad (3.19)$$

which is the familiar Boussinesq equation of state. This equation allows the buoyancy term $(-\rho g_i/\rho_o)$ in the momentum equation (Eq. 3.16) to be similarly approximated. The continuity equation (Eq. 3.15) becomes that of an incompressible fluid, assuming that the fluid motions do not rapidly mix deep layers of the fluid,[37] e.g., comparing length scales of velocity and density:

$$\left(\frac{1}{|u_j|}\left|\frac{\partial u_j}{\partial x_j}\right|\right)^{-1} << \left(\frac{1}{\rho_o}\left|\frac{\partial \rho_o}{\partial x_j}\right|\right)^{-1} \tag{3.20}$$

and[11] that the heat conduction term in Eq. 3.1 is a small contribution to the divergence. Making these approximations, the equations for the perturbations may be written as

Continuity Eq.:

$$\frac{\partial u_j}{\partial x_j} = 0 \tag{3.21}$$

Momentum Eq:

$$\frac{\partial u_i}{\partial t} + u_j \frac{\partial u_i}{\partial x_j} = -\frac{1}{\rho_o}\frac{\partial p}{\partial x_i} - \frac{\rho}{\rho_o} g_i + \frac{\mu_o}{\rho_o}\frac{\partial^2 u_i}{\partial x_j^2} \tag{3.22}$$

Energy Eq:

$$\frac{\partial T}{\partial t} + u_j \frac{\partial T}{\partial x_j} = Pr^{-1}\frac{\mu_o}{\rho_o}\frac{\partial^2 T}{\partial x_j^2} \tag{3.23}$$

Define the potential temperature, θ, as

$$\theta \equiv \tilde{T} \left(\frac{1000\text{mb}}{\tilde{p}}\right)^{R_d/c_p} \tag{3.24}$$

Differentiating with respect to height finds that the adiabatic atmosphere has a lapse rate of potential temperature of zero,

$$\frac{d\theta_o}{dz} = 0 \tag{3.25}$$

or that the potential temperature is a constant in an adiabatic atmosphere. Errors introduced by evaluating density with θ instead of $\tilde{T}$ are assumed to be small (this is investigated in Sec. 3.3.4). Neglecting the perturbation p with respect to p_o in Eq. 3.24, and approximating ρ_o as $\rho(\theta_o)$ in Eq. 3.22, the use of θ instead of T in the primitive equations (Eq. 3.21-Eq. 3.23) gives

Continuity Eq:

$$\frac{\partial u_j}{\partial x_j} = 0 \tag{3.26}$$

Momentum Eq:

$$\frac{\partial u_i}{\partial t} + u_j \frac{\partial u_i}{\partial x_j} = - \frac{1}{\rho(\theta_o)} \frac{\partial p}{\partial x_i} - \frac{\rho(\theta)-\rho(\theta_o)}{\rho(\theta_o)} g_i + \nu \frac{\partial^2 u_i}{\partial x_j^2} \tag{3.27}$$

Energy Eq:

$$\frac{\partial \theta}{\partial t} + u_j \frac{\partial \theta}{\partial x_j} = \nu \mathrm{Pr}^{-1} \frac{\partial^2 \theta}{\partial x_j^2} \tag{3.28}$$

The utility of the potential temperature formulation is that strong variations of pressure and density with height in the hydrostatic approximation of Eq. 3.10 are no longer present in the primitive equations. Initialization errors to the hydrostatic state, if included in the primitive equations, lead to strong transient fluid motions.[38] The transients are neatly avoided by this formulation.

To this point the fully three-dimensional fluid mechanics equations have been decomposed into an adiabatic reference state, and a flow field of perturbations about this state. A number of approximations have simplified the equations for the perturbations to those of a Boussinesq incompressible flow. The equations need to be ensemble-averaged and a turbulence closure formulated, and then the set must be finite-differenced for computer solution.

3.2.1.2 Reynolds Decomposition and Closure

To model the effects of turbulence on the mean flow, each primitive variable in the equation set is decomposed into its time-averaged and fluctuating parts as

$$\left\{\begin{array}{l}\text{the value of the}\\ \text{perturbation of}\\ \text{a primitive}\\ \text{variable}\end{array}\right\} = \left\{\begin{array}{l}\text{its ensemble-}\\ \text{averaged}\\ \text{value}\\ \end{array}\right\} + \left\{\begin{array}{l}\text{any fluctua-}\\ \text{tions about}\\ \text{its ensemble-}\\ \text{average value}\end{array}\right\} \tag{3.29}$$

which is represented here by the decompositions

$$p \rightarrow \bar{p} + p' \tag{3.30}$$

$$\theta \rightarrow \bar{\theta} + \theta' \tag{3.31}$$

$$\rho \rightarrow \bar{\rho} + \rho' \tag{3.32}$$

$$u_i \rightarrow \bar{u}_j + u_j' \tag{3.33}$$

Under this transformation, by selectively ensemble-averaging and subtracting the equations, and by making use of the continuity equation, the primitive equations become

Continuity Equations

$$\partial \bar{u}_j / \partial x_j = 0 \tag{3.34}$$

$$\partial u_j' / \partial x_j = 0 \tag{3.35}$$

Momentum Equations:

$$\frac{\partial \bar{u}_i}{\partial t} + \bar{u}_j \frac{\partial \bar{u}_i}{\partial x_j} = -\frac{1}{\rho(\theta_o)} \frac{\partial \bar{p}}{\partial x_i} + \frac{\rho(\bar{\theta}) - \rho(\theta_o)}{\rho(\theta_o)} g_i + \nu \frac{\partial^2 \bar{u}_i}{\partial x_j^2} - \frac{\partial}{\partial x_j} (\overline{u_i' u_j'}) \tag{3.36}$$

$$\frac{\partial u'_i}{\partial t} + \bar{u}_j \frac{\partial u_i'}{\partial x_j} + u_j' \frac{\partial \bar{u}_i}{\partial x_j} + u_j' \frac{\partial u_i'}{\partial x_j} - \frac{\partial}{\partial x_j} (\overline{u_i' u_j'}) = \frac{-1}{\rho(\theta_o)} \frac{\partial p'}{\partial x_i} - \frac{\rho(\theta') - \rho(\theta_o)}{\rho(\theta_o)} g_i + \nu \frac{\partial^2 u_i'}{\partial x_j^2} \tag{3.37}$$

Energy Equations:

$$\frac{\partial \bar{\theta}}{\partial t} + \bar{u}_j \frac{\partial \bar{\theta}}{\partial x_j} = \nu Pr^{-1} \frac{\partial^2 \bar{\theta}}{\partial x_j^2} - \frac{\partial}{\partial x_j} (\overline{u_j' \theta'}) \tag{3.38}$$

$$\frac{\partial \theta'}{\partial t} + \bar{u}_j \frac{\partial \theta'}{\partial x_j} + u_j \frac{\partial \bar{\theta}}{\partial x_j} + u_j \frac{\partial \theta'}{\partial x_j} - \frac{\partial}{\partial x_j} (\overline{u_j' \theta'}) = \nu Pr^{-1} \frac{\partial^2 \theta'}{\partial x_j^2} \tag{3.39}$$

The set of ensemble-averaged equations (i.e., Eq. 3.34, Eq. 3.36 and Eq. 3.38) suffer from the well-known closure problem due to the generation of the $\overline{u_i' u_j'}$ and $\overline{u_i' \theta'}$ terms by the non-linear advection terms in Eq. 3.27 and Eq. 3.28. Equations 3.37 and 3.39 may be manipulated to produce transport equations for these two new variables:

$$\frac{D}{Dt}(\overline{u_i' u_j'}) = - \overline{u_i' u_k'} \frac{\partial \overline{u_j}}{\partial x_k} - \overline{u_j' u_k'} \frac{\partial \overline{u_i}}{\partial x_k} \qquad \text{production terms}$$

$$- \frac{\partial}{\partial x_k} (\overline{u_i' u_j' u_k'}) \qquad \text{turbulent transport term}$$

$$-\frac{1}{\rho_o} \frac{\partial}{\partial x_i} (\overline{p' u_j'}) - \frac{1}{\rho_o} \frac{\partial}{\partial x_j} (\overline{p' u_i'}) \qquad \text{pressure diffusion terms}$$

$$+ \frac{1}{\rho_o} \overline{p' \left(\frac{\partial u_i'}{\partial x_j} + \frac{\partial u_j'}{\partial x_i} \right)} \qquad \text{tendency toward isotropy term}$$

$$+ \frac{1}{\theta_o} (g_i \overline{u_j' \theta'} + g_j \overline{u_i' \theta'})$$
buoyant production terms

$$+ \nu \frac{\partial^2 (\overline{u_i' u_j'})}{\partial x_k^2}$$
molecular diffusion terms

$$-2\nu \overline{\frac{\partial u_i'}{\partial x_k} \frac{\partial u_j'}{\partial x_k}}$$
dissipation term

(3.40)

$$\frac{D}{Dt} (\overline{u_i' \theta'}) = -\overline{u_j' u_i'} \frac{\partial \overline{\theta}}{\partial x_j} - \overline{u_j \theta'} \frac{\partial \overline{u_i}}{\partial x_j}$$
production terms

$$- \frac{\partial}{\partial x_j} (\overline{u_i' u_j' \theta'})$$
turbulent transport term

$$- \frac{1}{\rho_o} \frac{\partial}{\partial x_i} (\overline{p' \theta'})$$
pressure diffusion term

$$+ \frac{1}{\rho_o} \overline{p' \frac{\partial \theta'}{\partial x_i}}$$
tendency toward isotropy term

$$+ \frac{1}{\theta_o} g_i \overline{\theta' \theta'}$$
buoyant production term

$$+\nu \frac{\partial^2 (\overline{u_i' \theta'})}{\partial x_j^2}$$
molecular diffusion term

$$- 2\nu \overline{\frac{\partial u_i'}{\partial x_j} \frac{\partial \theta'}{\partial x_j}}$$

dissipation term

(3.41)

A discussion of the individual terms noted in Eq. 3.40 and Eq. 3.41 can be found elsewhere.[11] These equations were closed by Stuhmiller[2] and the results are listed here for completeness. In Eq. 3.40, the tendency toward isotropy term is neglected, because the turbulence is assumed to be homogeneous, and the molecular diffusion term is neglected because the flow is expected to be highly turbulent. The buoyant production term is also neglected, mainly in order to see how well the turbulence model can do without it, since it was neglected in Stuhmiller's turbulence model. It is found that the incorporation of this term would probably aid the model in reproducing the buoyant line-thermal results (see Sec. 5.2.2). By further making the assumption that the <u>average</u> flow is two-dimensional in the y-z axes of Fig. 3.1, the following closure is made for the trace of Eq. 3.40, which is the turbulence kinetic energy, q, $q \equiv \overline{u_i' u_i'}$,

$$\frac{Dq}{Dt} = 2\sigma\left(\left(\frac{\partial v}{\partial y}\right)^2 + \frac{1}{2}\left(\frac{\partial v}{\partial z} + \frac{\partial w}{\partial y}\right)^2 + \left(\frac{\partial w}{\partial z}\right)^2\right) - 4\alpha q^2 \sigma^{-1}$$
$$+ \Gamma\left(\frac{\partial}{\partial y}\sigma \frac{\partial q}{\partial y} + \frac{\partial}{\partial z}\sigma \frac{\partial q}{\partial z}\right) \qquad (3.42)$$

Figure 3.1

Flow Field Orientation

The flow field of Eqs. 3.42-3.47 is time-dependent and two-dimensional in the y-z axes. The relationship of the time-dependence to the (downwind) x-axis is discussed in Sec. 3.3.3.

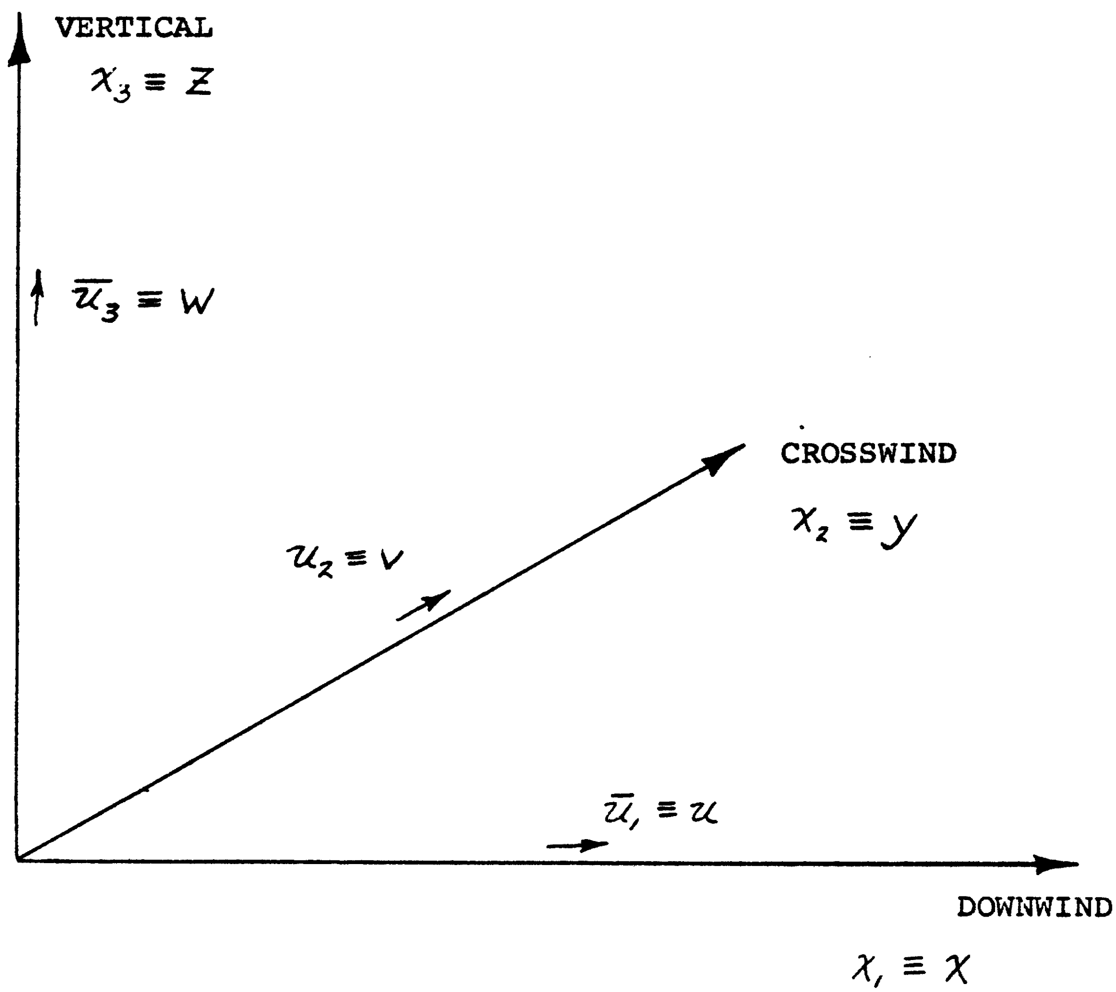

The off-diagonal terms of the Reynolds stress tensor are related to a <u>scalar</u> eddy viscosity, σ, where $\overline{u_i'u_j'} = \frac{\sigma}{2}\left(\frac{\partial \bar{u}_i}{\partial x_j} + \frac{\partial \bar{u}_j}{\partial x_i}\right)$, and σ has the following transport equation:

$$\frac{D\sigma}{Dt} = \frac{\sigma^2}{q}\left(\left(\frac{\partial v}{\partial y}\right)^2 + \frac{1}{2}\left(\frac{\partial v}{\partial z} + \frac{\partial w}{\partial y}\right)^2 + \left(\frac{\partial w}{\partial z}\right)^2\right) - \alpha q$$

$$+ \Gamma \frac{\sigma}{q}\left(\frac{\partial}{\partial y} \sigma\frac{\partial q}{\partial y} + \frac{\partial}{\partial z} \sigma \frac{\partial q}{\partial z}\right) - \Gamma_1 \left(\frac{\sigma^3}{q^2}\left(\frac{\partial}{\partial y} q \frac{\partial}{\partial y}\left(\frac{q}{\sigma}\right) + \frac{\partial}{\partial z} q \frac{\partial}{\partial z}\left(\frac{q}{\sigma}\right)\right)\right) \tag{3.43}$$

Finally, the turbulent fluxes of heat in Eq. 3.41 are related to the turbulent momentum fluxes through a reciprocal turbulent Prandtl number, γ_T, which is specified along with the three other turbulence constants α, Γ, and Γ_1. With this turbulence closure, the continuity, momentum, and energy equations become, in a two-dimensional flow

$$\frac{\partial v}{\partial y} + \frac{\partial w}{\partial z} = 0 \tag{3.44}$$

$$\frac{\partial v}{\partial t} + \frac{\partial}{\partial y}(v^2) + \frac{\partial}{\partial z}(vw) = -\frac{1}{\rho(\theta_o)}\frac{\partial \bar{p}}{\partial y} + \frac{\partial}{\partial y}\left(\sigma\frac{\partial v}{\partial y}\right) + \frac{\partial}{\partial z}\left(\sigma \frac{\partial v}{\partial z}\right) \tag{3.45}$$

$$\frac{\partial w}{\partial t} + \frac{\partial}{\partial y}(vw) + \frac{\partial}{\partial z}(w^2) = \frac{-1}{\rho(\theta_o)}\frac{\partial \bar{p}}{\partial z} + \frac{\partial}{\partial y}\left(\sigma\frac{\partial w}{\partial y}\right) + \frac{\partial}{\partial z}\left(\sigma\frac{\partial w}{\partial z}\right) - \left(\frac{\rho(\bar{\theta}) - \rho(\theta_o)}{\rho(\theta_o)}\right) g_z \tag{3.46}$$

$$\frac{\partial \bar{\theta}}{\partial t} + \frac{\partial}{\partial y}(\bar{\theta} v) + \frac{\partial}{\partial z}(\bar{\theta} w) = \frac{\partial}{\partial y}(\gamma_T \sigma \frac{\partial \bar{\theta}}{\partial y}) + \frac{\partial}{\partial z}(\gamma_T \sigma \frac{\partial \bar{\theta}}{\partial z}) \tag{3.47}$$

With an internal energy variable, I, defined as $I \equiv c_p \bar{\theta}$, equations 3.42-3.47 are solved by the VARR-II code. Additional pollutant and moisture transport equations are discussed in the next two sections, and possible modifications to these equations are discussed in section 6.2.

3.2.1.2 Pollutant Species Transport Equation

A transport equation for a pollutant species density, χ is added to the set of Eqs. 3.42-3.47. The pollutant is assumed to be a neutrally buoyant, passive species, although it may be contained in a buoyant stream of effluent. The assumption that the species is neutrally buoyant could be relaxed, but the model is felt to be useful in modeling most dilute pollutants in its present form. The turbulent diffusion of the pollutant is related to the eddy viscosity of momentum by a reciprocal turbulent Schmidt number, γ_χ. The transport equation may be written down as

$$\begin{bmatrix}\text{substantial derivative}\\ \text{of } \chi\end{bmatrix} = \begin{bmatrix}\text{turbulent transport}\\ \text{of } \chi\end{bmatrix} - \begin{bmatrix}\text{rate of}\\ \text{destruction}\\ \text{of } \chi\end{bmatrix} \tag{3.48}$$

which is represented here as

$$\frac{\partial \chi}{\partial t} + v\frac{\partial \chi}{\partial y} + w\frac{\partial \chi}{\partial t} = \frac{\partial}{\partial y}\left(\gamma_\chi \sigma \frac{\partial \chi}{\partial y}\right) + \frac{\partial}{\partial z}\left(\gamma_\chi \sigma \frac{\partial \chi}{\partial z}\right) - \sum_{i=1}^{N} \lambda_\chi^{(i)} \chi \qquad (3.49)$$

in the notation of Fig. 3.1.

The destruction of χ is assumed to be by radioactive decay into any of N decay channels, so that the rate of destruction of χ is the product of χ and the sum of its radioactive decay constants $\lambda_\chi^{(i)}$, in Eq. 3.49. This formulation makes no account of sources of the pollutant species through decay of radioactive precursors. It also ignores chemical reactions which could alter the pollutant concentration. However, the extension of the model to include these effects is straightforward.

3.2.1.4 Radioactive Decay Heating

The thermal energy released by radioactive decay of the pollutant is added to the specific internal energy of the fluid. Pollutants may decay by any one of N different decay channels with decay constant $\lambda_\chi^{(i)}$ and energy $E_\chi^{(i)}$. A fraction $F_\chi^{(i)}$ of the energy is deposited within the plume, yielding an energy release rate of

$$\left(c_p \frac{\partial \bar{\theta}}{\partial t}\right)_{\text{radioactive}} = \frac{4.151\text{x}10^{10} \ \frac{\text{BTU-atoms}}{\text{MeV-lb}_m\text{-mole}}}{\rho W_{mol\chi} / \chi} \sum_{i=1}^{N} F_{\chi}^{(i)} E_{\chi}^{(i)} \lambda_{\chi}^{(i)} \tag{3.50}$$

where $W_{mol\chi}$ is the molecular weight of χ in lb_m/lb_m-mole. Daughter radiations have been ignored in this formulation, but could be included with their own transport equation. Similarly, alterations of the energy balance caused by chemical reactions has not been treated in this work, but would be easy to address in extensions of this work.

3.2.2 Moist Equations

The inclusion of moisture is considered in this section with the purpose of pointing out the assumptions that allow the equations to be formulated with the concept of virtual potential temperature, in addition to two other moisture variables. The assumptions that are made in this section are important--the moisture model is not meant to be perfectly general; it is expected to do poorly when these assumptions are not valid.

3.2.2.1 Reference State Decomposition

Atmospheric moisture is assumed to be in either the liquid or vapor phases. The amount of vapor is described by the vapor density moisture variable, $\tilde{\rho}_{vap}$, and the amount of cloud liquid water is described by the liquid density moisture variable, $\tilde{\rho}_{liq}$. Transport equations for these two variables are written that take note of the turbulent transports of vapor and liquid, and the processes of evaporation and condensation that cause the interchange of vapor and liquid. First, however, the effect of moisture on the buoyancy of a parcel of air is developed and applied to the description of a hydrostatic reference state.

The density of a parcel of moist air is the sum of the dry air, vapor, and liquid densities:

$$\tilde{\rho} = \tilde{\rho}_{dry} + \tilde{\rho}_{vap} + \tilde{\rho}_{liq} \tag{3.51}$$

In this work the contribution to the density of the typically small amount of cloud liquid water is ignored, (there is usually no liquid water present in the simulations, and when it is present, it is typically less than 1% of the mass of the fluid), so that the concept of virtual potential temperature can be explored. Dropping the $\tilde{\rho}_{liq}$ term and applying the perfect gas law to $\tilde{\rho}_{dry}$ and $\tilde{\rho}_{vap}$ yields:

$$\tilde{\rho} = \frac{\tilde{p}_{dry}}{R_d \tilde{T}} + \frac{\tilde{p}_{vap}}{R_v \tilde{T}} \equiv \frac{(\tilde{p}_{dry} + \tilde{p}_{vap})}{R_d \tilde{T}_v} = \frac{\tilde{p}}{R_d \tilde{T}_v} \tag{3.52}$$

where $\tilde{p}$ is the total pressure, m_{vap} and m_{dry} are molecular weights and the virtual temperature, $\tilde{T}_v$, is

$$\tilde{T}_v \equiv \tilde{T} \left[\frac{1 + m_{dry}\tilde{\rho}_{vap}/m_{vap}\rho_{dry}}{1 + \tilde{\rho}_{vap}/\tilde{\rho}_{dry}} \right] \tag{3.53}$$

It is very important to note in Eq. 3.52 that the virtual temperature is a fictitious temperature that is used in the dry gas equation of state to give the density of moist air. Generally the virtual temperature is no more than a few degrees higher than the thermodynamic temperature for typical atmospheric conditions.

Following the development in Sec. 3.2.1.1, the variations of virtual temperature, pressure, and density of a static atmosphere are "subtracted out" by making a reference state decomposition:

$$\left\{\begin{array}{l}\text{the value of}\\ \text{a primitive}\\ \text{variable}\end{array}\right\} = \left\{\begin{array}{l}\text{its value in a uni-}\\ \text{formly moist adiabatic}\\ \text{atmosphere (function}\\ \text{of height only)}\end{array}\right\} + \left\{\begin{array}{l}\text{a departure}\\ \text{from the}\\ \text{state at}\\ \text{rest}\end{array}\right\} \tag{3.54}$$

Or, in the notation of this work:

$$\tilde{p} \rightarrow p_o + p \tag{3.55}$$

$$\tilde{\rho} \rightarrow \rho_o + \rho \tag{3.56}$$

$$\tilde{T}_v \rightarrow T_{vo} + T_v \tag{3.57}$$

$$\tilde{u}_i \rightarrow 0 \quad + u_i \tag{3.58}$$

the only difference here to the reference state decomposition of Eqs. 3.6-3.9 is in the use of the (fictitious) virtual temperature in order to allow the use of an equation of state that is analogous to Eq. 3.4:

$$\tilde{\rho} = \tilde{p}/R_d\tilde{T}_v \qquad (3.59)$$

Substituting Eqs. 3.55-3.58 into the primitive equation set (Eqs. 3.1-3.3 and Eq. 3.59), and setting the time derivatives and perturbations to zero yields the state of the moist adiabatic atmosphere. The continuity and energy equations are trivial (as before), and the momentum equation becomes the moist hydrostatic equation:

$$\frac{dp_o}{dz} = -\rho_o g \qquad (3.60)$$

The equation of state is simply

$$p_o = \rho_o R_d T_{vo} \qquad (3.61)$$

The first Law of Thermodynamics for an unsaturated adiabatic process in this atmosphere is

$$dQ = 0 = c_p^{moist}\, dT_{vo} - dp_o/\rho_o \qquad (3.62)$$

Approximating the heat capacity for a moist gas, c_p^{moist}, as that of a dry gas, c_p, dividing by dz and substituting Eq. 3.62 into 3.60 yields an approximate lapse rate for a moist, unsaturated atmosphere which is the same as that for a dry adiabatic atmosphere:

$$\frac{-dT_{vo}}{dz} = \frac{g}{c_p} = 9.76^{o}\mathrm{C/km} \tag{3.63}$$

To this point the resting state of a moist adiabatic atmosphere has been presented. The neglect of the effect of the liquid water on the total density has allowed the treatment of moisture to duplicate the dry atmosphere equations after the transformation of temperature to virtual temperature. The equations for the perturbations are identical to those of the dry atmosphere developed in Sec. 3.2.1.1, except that temperature is replaced by virtual temperature, and a latent heat release term is included:

Continuity Eq.

$$\frac{\partial u_j}{\partial x_j} = 0 \tag{3.64}$$

Momentum Eq.

$$\frac{\partial u_i}{\partial t} + u_j \frac{\partial u_i}{\partial x_j} = - \frac{1}{\rho_o} \frac{\partial p}{\partial x_i} + \frac{T_v}{T_{vo}} g_i + \frac{\mu_o}{\rho_o} \frac{\partial^2 u_i}{\partial x_j^2} \tag{3.65}$$

Energy Eq.

$$\frac{\partial T_v}{\partial t} + u_j \frac{\partial T_v}{\partial x_j} = \nu \mathrm{Pr}^{-1} \frac{\partial^2 T_v}{\partial x_j^2} - \frac{L}{\rho c_p} \left(\frac{D\rho_{vap}}{Dt} \right)_{\mathrm{phase}} \tag{3.66}$$

The latent heat release term is considered in Sec. 3.2.2.4.

Define the virtual potential temperature, θ_v, as

$$\theta_v \equiv \tilde{T}_v \left(\frac{1000}{p}\right)^{R_d/c_p^{moist}} \tag{3.67}$$

Again assume that c_p^{moist} is essentially equal to c_p. Differentiating with respect to height finds that the moist unsaturated adiabatic atmosphere has a lapse of virtual potential temperature that vanishes:

$$\frac{d\theta_{vo}}{dz} = 0 \tag{3.68}$$

The result here is that the virtual potential temperature is a constant in the reference state.

Neglecting the perturbation pressure, p, with respect to p_o in Eq. 3.56, the use of θ_v instead of T_v in the primitive equations (Eq. 3.64-Eq. 366) gives

Continuity Eq:

$$\frac{\partial u_j}{\partial x_j} = 0 \tag{3.69}$$

Momentum Eq:

$$\frac{\partial u_i}{\partial t} + u_j \frac{\partial u_i}{\partial x_j} = \frac{-1}{\rho(\theta_{vo})} \frac{\partial p}{\partial x_i} - \frac{\rho(\theta_v)-\rho(\theta_{vo})}{\rho(\theta_{vo})} g_i + \nu \frac{\partial^2 u_i}{\partial x_j^2} \tag{3.70}$$

Energy Eq:

$$\frac{\partial \theta_v}{\partial t} + u_j \frac{\partial \theta_v}{\partial x_j} = \nu Pr^{-1} \frac{\partial^2 \theta_v}{\partial x_j^2} - \frac{L}{\rho c_p} \left(\frac{D\rho_{vap}}{Dt}\right)_{phase} \tag{3.71}$$

The result here is the same as in Sec. 3.2.1.1: the strong variation of pressure with height is no longer present in the primitive equations. This formulation is common (although in slightly different forms) among papers in meteorology.

Transport equations may be written down for the water vapor and liquid water densities according to the conservation scheme:

$$\left\{\begin{array}{l}\text{Eulerian time}\\ \text{rate of change}\\ \text{of vapor or}\\ \text{liquid}\end{array}\right\} = \left\{\begin{array}{l}\text{Diffusion of}\\ \text{vapor or}\\ \text{liquid}\end{array}\right\} + \left\{\begin{array}{l}\text{Gain or loss of}\\ \text{vapor or liquid}\\ \text{due to phase}\\ \text{changes}\end{array}\right\} \tag{3.72}$$

or, in the notation of this work:

$$\frac{\partial \rho_{vap}}{\partial t} + u_j \frac{\partial \rho_{vap}}{\partial x_j} = \nu Sc_{vap}^{-1} \frac{\partial^2 \rho_{vap}}{\partial x_j^2} + \left(\frac{D\rho_{vap}}{Dt}\right)_{phase} \tag{3.73}$$

$$\frac{\partial \rho_{liq}}{\partial t} + u_j \frac{\partial \rho_{liq}}{\partial x_j} = \nu Sc_{liq}^{-1} \frac{\partial^2 \rho_{liq}}{\partial x_j^2} - \left(\frac{D\rho_{vap}}{Dt}\right)_{phase} \tag{3.74}$$

where the gain or loss of vapor due to phase changes, $(D\rho_{vap}/Dt)_{phase}$, identically shows up as a loss or gain of liquid, and Schmidt numbers that describe the molecular diffusion of vapor and liquid are introduced, respectively. The terminal fall velocities of the liquid water droplets are ignored. The $\left(\frac{D\rho_{vap}}{Dt}\right)_{phase}$ term is discussed in Sec. 3.2.2.3.

Note that any constant background (ambient atmospheric) value of ρ_{vap} and ρ_{liq} trivially satisfied these equations, so that no new information would be brought into the specification of the reference state by decomposing the variables in these transport equations. That is, ρ_{vap} and ρ_{liq} do not have a reference state "subtracted away" from them, unlike the other primitive variables $\tilde{p}$, $\tilde{\theta}_v$, and $\tilde{\rho}$.

3.2.2.2 Reynolds Decomposition and Closure

A Reynolds decomposition of the primitive equations is made as in Sec. 3.2.1.2. Each primitive variable in the equation set is decomposed into its ensemble-averaged and fluctuating parts:

$$p \rightarrow \bar{p} + p' \tag{3.75}$$

$$\theta \rightarrow \bar{\theta} + \theta_v' \tag{3.76}$$

$$\rho \rightarrow \bar{\rho} + \rho' \tag{3.77}$$

$$u_j \rightarrow 0 \quad + u_j' \tag{3.78}$$

$$\rho_{vap} \rightarrow \bar{\rho}_{vap} + \rho_{vap}' \tag{3.79}$$

$$\rho_{liq} \rightarrow \bar{\rho}_{liq} + \rho_{liq}' \tag{3.80}$$

By selectively ensemble-averaging and subtracting the equations, and by making use of the continuity equation, the primitive equations yield the following relationships:

Continuity Eq:

$$\frac{\partial \bar{u}_j}{\partial x_j} = 0 \tag{3.81}$$

Momentum Eq:

$$\frac{\partial u_i}{\partial t} + u_j \frac{\partial u_i}{\partial x_j} = \frac{-1}{\rho(\theta_{vo})} \frac{\partial \bar{p}}{\partial x_i} - \frac{\rho(\bar{\theta}_v) - \rho(\theta_{vo})}{\rho(\theta_{vo})} g_i + \nu \frac{\partial^2 u_i}{\partial x_j^2}$$

$$- \frac{\partial}{\partial x_j} (\overline{u_i' u_j'}) \tag{3.82}$$

Energy Eq:

$$\frac{\partial \bar{\theta}_v}{\partial t} + u_j \frac{\partial \bar{\theta}_v}{\partial x_j} = \nu Pr^{-1} \frac{\partial^2 \theta_v}{\partial x_j^2} - \frac{\partial}{\partial x_j} (\overline{u_j' \theta_v'}) - \frac{L}{\rho(\theta_v) c_p} \left(\frac{D\bar{\rho}_{vap}}{Dt} \right)_{phase} \tag{3.83}$$

and the transport equations for moisture, Eq. 3.73 and Eq. 3.74 yield

Vapor Eq:

$$\frac{\partial}{\partial t} \bar{\rho}_{vap} + u_j \frac{\partial \bar{\rho}_{vap}}{\partial x_j} = \nu Sc_{vap}^{-1} \frac{\partial^2 \bar{\rho}_{vap}}{\partial x_j^2} - \frac{\partial}{\partial x_j} (\overline{\rho_{vap}' u_j'}) + \left(\frac{D\bar{\rho}_{vap}}{Dt} \right)_{phase} \tag{3.84}$$

Liquid Eq:

$$\frac{\partial}{\partial t} \bar{\rho}_{liq} + u_j \frac{\partial \bar{\rho}_{liq}}{\partial x_j} = \nu Sc_{liq}^{-1} \frac{\partial^2 \bar{\rho}_{liq}}{\partial x_j^2} - \frac{\partial}{\partial x_j} (\overline{\rho_{liq}' u_j'}) - \left(\frac{D\bar{\rho}_{vap}}{Dt} \right)_{phase} \tag{3.85}$$

Rather than providing the full equations for the correlated fluctuations $\overline{u_i' u_j'}$, $\overline{u_j' \theta_v'}$, $\overline{u_j' \rho_{vap}}$, and $\overline{u_j' \rho_{liq}}$, the turbulence closure is simply extended from that developed in Sec. 3.2.1.2. The closed set of equations in two-dimensions is, in the notation of Fig. 3.1

Continuity Eq:

$$\frac{\partial v}{\partial y} + \frac{\partial w}{\partial z} = 0 \qquad (3.86)$$

Momentum Eqs:

$$\frac{Dv}{Dt} = \frac{-1}{\rho(\theta_{vo})}\frac{\partial \bar{p}}{\partial y} + \frac{\partial}{\partial y}(\sigma \frac{\partial v}{\partial y}) + \frac{\partial}{\partial z}(\sigma \frac{\partial v}{\partial z}) \qquad (3.87)$$

$$\frac{Dw}{Dt} = \frac{-1}{\rho(\theta_{vo})}\frac{\partial \bar{p}}{\partial z} - \frac{\rho(\bar{\theta}_v) - \rho(\theta_{vo})}{\rho(\theta_{vo})} g_z + \frac{\partial}{\partial y}(\sigma \frac{\partial w}{\partial y}) + \frac{\partial}{\partial z}(\sigma \frac{\partial w}{\partial z})$$

Energy Eq:

$$\frac{D}{Dt}(c_p\bar{\theta}_v) = \frac{\partial}{\partial y}(\gamma_T \sigma \frac{\partial (c_p\bar{\theta}_v)}{\partial y}) + \frac{\partial}{\partial z}(\gamma_T \sigma \frac{\partial (c_p\bar{\theta}_v)}{\partial z}) - \frac{L}{\rho(\theta_v)}\left(\frac{D\bar{\rho}_{vap}}{Dt}\right)_{phase} \qquad (3.88)$$

Vapor Eq:

$$\frac{D}{Dt}\bar{\rho}_{vap} = \frac{\partial}{\partial y}(\gamma_v \sigma \frac{\partial \bar{\rho}_{vap}}{\partial y}) + \frac{\partial}{\partial z}(\gamma_v \sigma \frac{\partial \bar{\rho}_{vap}}{\partial z}) + \left(\frac{D\bar{\rho}_{vap}}{Dt}\right)_{phase} \qquad (3.89)$$

Liquid Eq:

$$\frac{D}{Dt}\bar{\rho}_{liq} = \frac{\partial}{\partial y}(\gamma_L \sigma \frac{\partial \bar{\rho}_{liq}}{\partial y}) + \frac{\partial}{\partial z}(\gamma_L \sigma \frac{\partial \bar{\rho}_{liq}}{\partial z}) - \left(\frac{D\bar{\rho}_{vap}}{Dt}\right)_{phase} \qquad (3.90)$$

Eddy Viscosity Eq:

$$\frac{D\sigma}{Dt} = \frac{\sigma^2}{q}\left(\left(\frac{\partial v}{\partial y}\right)^2 + \frac{1}{2}\left(\frac{\partial v}{\partial z} + \frac{\partial w}{\partial y}\right)^2 + \left(\frac{\partial w}{\partial z}\right)^2\right) - \alpha q +$$

$$+ \Gamma\frac{\sigma}{q}\left(\left(\frac{\partial}{\partial y}\sigma\frac{\partial q}{\partial y}\right)+\left(\frac{\partial}{\partial z}\sigma\frac{\partial q}{\partial z}\right)\right) - \Gamma_1\left(\frac{\sigma^3}{q^2}\frac{\partial}{\partial y}q\frac{\partial}{\partial y}\left(\frac{q}{\sigma}\right)+\frac{\partial}{\partial z}q\frac{\partial}{\partial z}\left(\frac{q}{\sigma}\right)\right) \tag{3.91}$$

Turbulence Kinetic Energy Eq:

$$\frac{Dq}{Dt} = 2\sigma\left(\left(\frac{\partial v}{\partial y}\right)^2 + \frac{1}{2}\left(\frac{\partial v}{\partial z}+\frac{\partial w}{\partial y}\right)^2 + \left(\frac{\partial w}{\partial z}\right)^2\right) - 4\alpha q\sigma^{-1}$$

$$+ \Gamma\left(\frac{\partial}{\partial y}\sigma\frac{\partial q}{\partial y}+\frac{\partial}{\partial z}\sigma\frac{\partial q}{\partial z}\right) \tag{3.92}$$

Pollutant Eq:

$$\frac{D\chi}{Dt} = \frac{\partial}{\partial y}\left(\gamma_\chi\sigma\frac{\partial \chi}{\partial y}\right) + \frac{\partial}{\partial z}\left(\gamma_\chi\sigma\frac{\partial \chi}{\partial z}\right) - \sum_{i=1}^{N}\lambda_\chi^{(i)}\chi \tag{3.93}$$

where reciprocal turbulent Prandtl and Schmidt numbers have been introduced, and are assumed to be constants.

3.2.2.3 Equilibrium Cloud Microphysics Model

The cloud microphysics model simply assumes that water vapor and liquid are always in equilibrium. Further, the surface tension of the liquid droplets is ignored. That is, phase equilibrium over a flat surface of water is assumed to exist. A phase diagram that illustrates this equilibrium is sketched in Fig. 3.2.2.3.1. The liquid-vapor equilibrium curve above $273^{\circ}K$ is the locus of points that the saturation vapor pressure, $e_{sat}(T)$, may take. The vapor density, ρ_{vap}, in the presence of liquid water would be $e_{sat}(T)/R_{vap}T$. If there is no liquid available to evaporate, then the vapor density may be less than this saturation value. Below $273^{\circ}K$ the subcooled liquid-vapor equilibrium (dashed line) is obeyed. No ice formation is allowed. The entire liquid-vapor equilibrium curve is given by Magnus' formula:[39]

$$\log_{10} e_{sat} = - \frac{2937.4}{T} - 4.9283 \log_{10} T + 23.5518 \tag{3.94}$$

The $\left(\frac{D\bar{\rho}_{vap}}{Dt}\right)_{phase}$ term of Eq. 3.89 and Eq. 3.90 is simply adjusted to make the liquid and vapor coexist. The logic of the moisture model is illustrated in Fig. 3.2.2.3.2. Liquid and vapor are advected and diffused in an initial calculation for each computer cell. This generally results in a non-equilibrium moisture state in the cell, so the cell is allowed to evaporate or condense water in order to restore the equilibrium. The amount of evaporation or condensation in each cell is noted in order to provide the latent heat release term in the energy equation.

3.2.2.4 Latent Heat Source Term

The latent heat source term is calculated in each cell

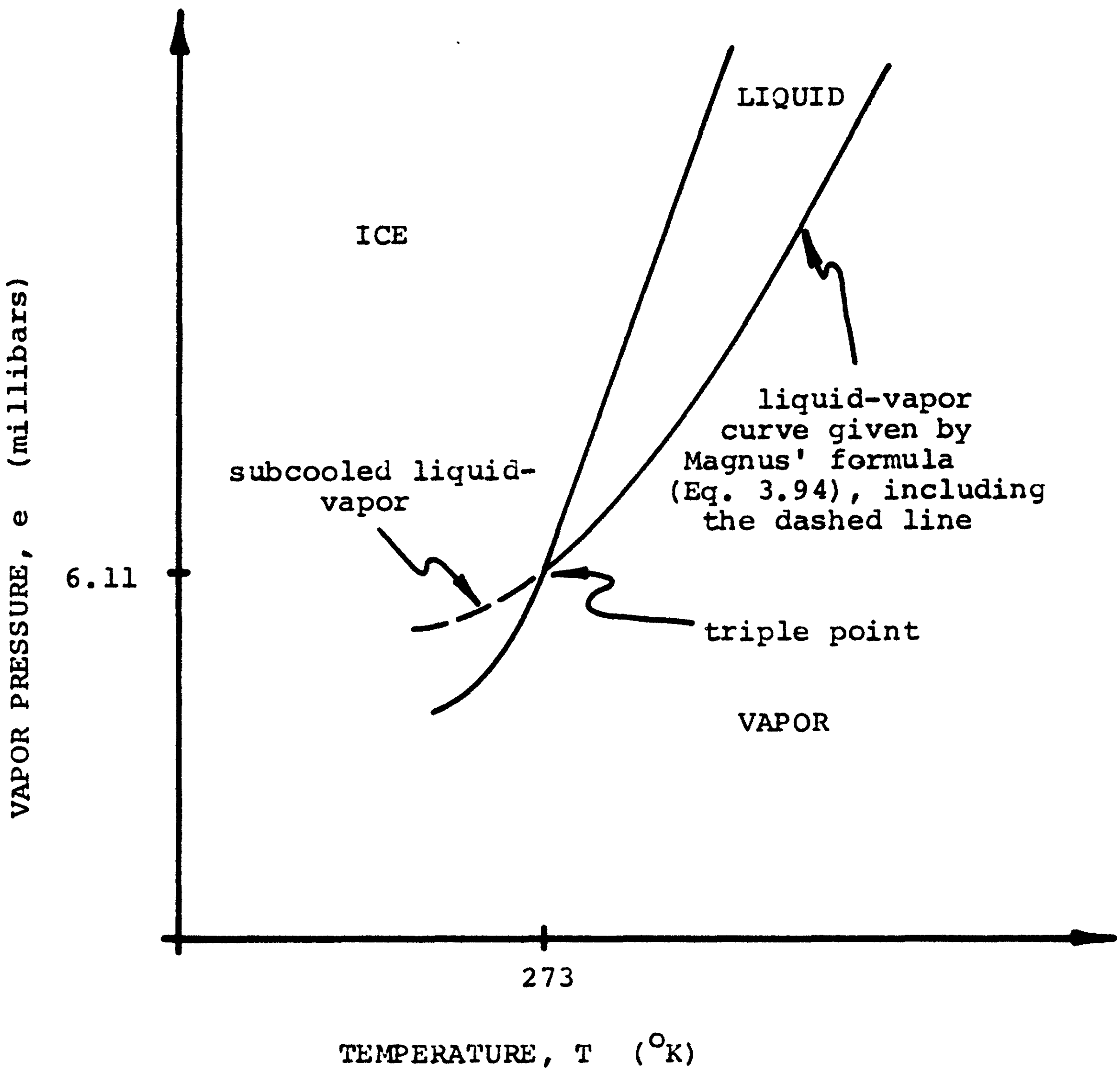

Fig. 3.2.2.3.1 Phase Diagram for Water Substance

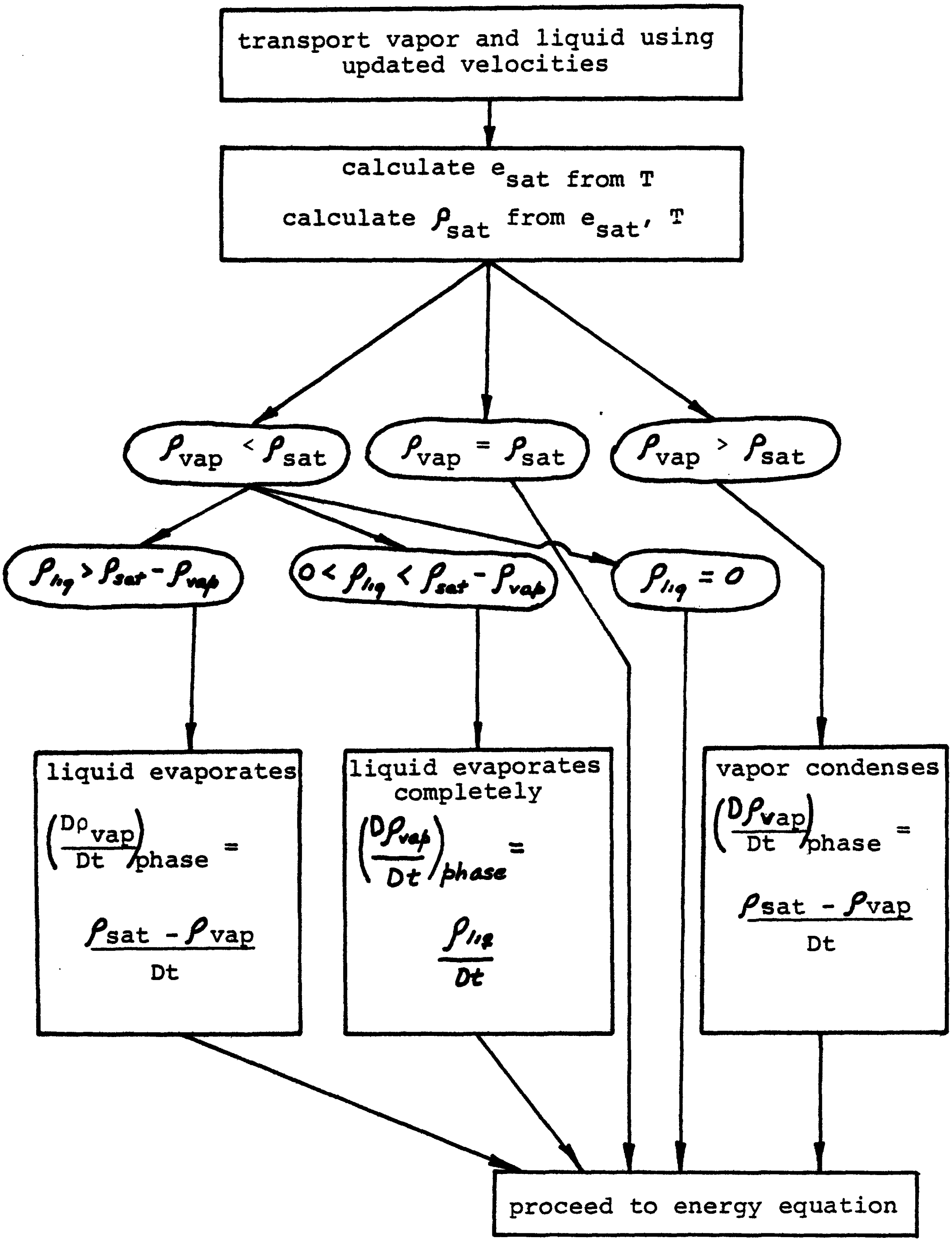

Fig. 3.2.2.3.2 Logic Diagram for the Equilibrium Moisture Calculation in a Single Cell during a Single Timestep

at every step depending on whether evaporation or condensation takes place. The latent heat release term is calculated as

$$\text{Latent Heat Release}\left[\frac{\text{BTU}}{\text{lb}_m\ \text{sec}}\right] = -\frac{L}{\rho(\theta_v)}\left(\frac{D\bar{\rho}_{vap}}{Dt}\right)_{phase} \tag{3.95}$$

where the latent heat of vaporization, L, is assumed to be a constant, 1075 BTU/lb_m. The $\left(\frac{D\rho_{vap}}{Dt}\right)_{phase}$ is found in the logic diagram of Fig. 3.2.2.3.2.

3.3 Model Solution Methodology

3.3.1 The VARR-II Fluid Mechanics Algorithm

The VARR-II computer code[40] is the starting point for the model development methodology in this work. In its original form, the VARR-II code solves the two-dimensional time-dependent turbulent fluid mechanics equations of continuity, momentum, and energy for a Boussinesq fluid. (The Boussinesq approximation to the momentum equation is considered in Sec. 3.2.1.1.) Two closure variables, the eddy viscosity, σ, and the turbulence kinetic energy, q, are also calculated from their own transport equations. The original VARR-II computer code is quite flexible in the choice of boundary conditions, allowing no-slip, free-slip, continuative inflow/outflow, or prescribed inflow/outflow boundaries.

The VARR-II fluid mechanics algorithm is the Simplified Marker and Cell (SMAC) method.[41] The computer mesh for this method is Eulerian in either Cartesian or cylindrical geometry, and the primitive variables are solved directly, with no transformation to vorticity-stream function variables. The algorithm divides naturally into two sections during each time step: In the first section the velocity field is updated using the previous velocity and pressure fields with mixed central and donor-cell differencing[42] of the equations. These velocities generally do not satisfy the continuity equation, so in a second section a pressure iteration adjusts these velocities until they satisfy continuity. Once the divergence-free updated velocity field is known, the energy and turbulence transport equations are updated, completing the calculational cycle of the time step.

The basic SMAC fluid mechanics algorithm has not been modified in this work. Pollutant and moisture transport equations have been added to the equation set, and they are updated in the same manner as the energy and turbulence variables, using the divergence-free updated velocity field. The stability of the method for problems of an atmospheric scale is considered in Sec. 5.2.1.

3.3.2 Orientation of the Computer Mesh

The optimal orientation of the two-dimensional computer solution mesh is discussed here. Consider the representative three-dimensional plume in Fig. 3.3.2.1a. The plume has bent over in the imposed (one-dimensional) wind field, and the plume boundaries monotonically expand as the plume proceeds downwind. The most natural possibilities of orienting a two-dimensional solution mesh on this flow are: (1) to align the mesh parallel to the wind and through the center of the plume, as in Fig. 3.3.2.1b, or (2) to align the mesh perpendicular to the flow, as in Fig. 3.3.2.1c.

The advantages of the "crosswind" alignment of Fig. 3.3.2.1c over the "downwind" alignment of Fig. 3.3.2.1b are immediately apparent. In the crosswind alignment a three-dimensional simulation results since in the downwind Lagrangian translation of the computational mesh the time variable becomes a surrogate for the downwind position x, where

$x = \int_0^t u(z(t))dt$. The downwind alignment is appropriate only for cases of line-source plumes--in which internal recirculation and entrainment will be of secondary importance to buoyant plume rise and atmospheric turbulent entrainment. Further, the crosswind alignment can take advantage of the centerline symmetry of the turbulent vortex pair to reduce the total mesh area by a factor of two, while the downwind

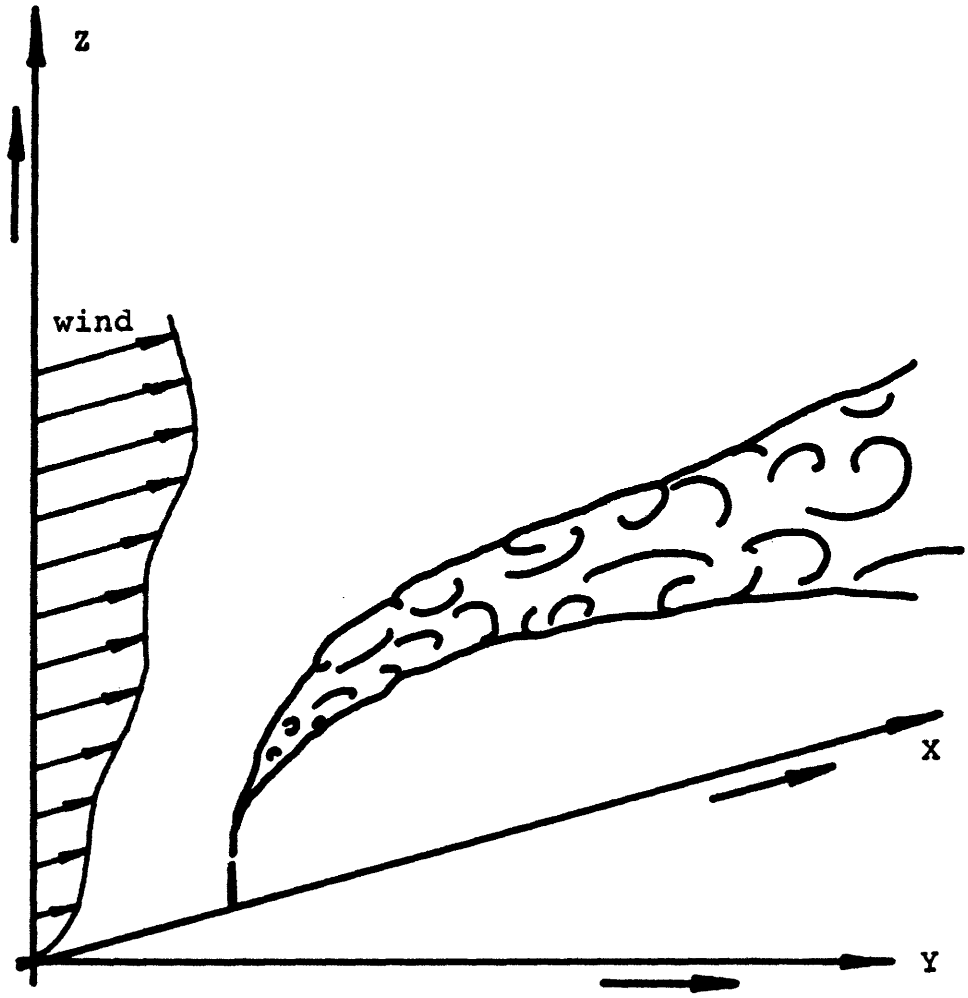

Fig. 3.3.2.1a Bent-Over Buoyant Plume with Ambient Thermal Stratification.

Fig. 3.3.2.1b

Mesh Alignment Appropriate for a Line Source Release

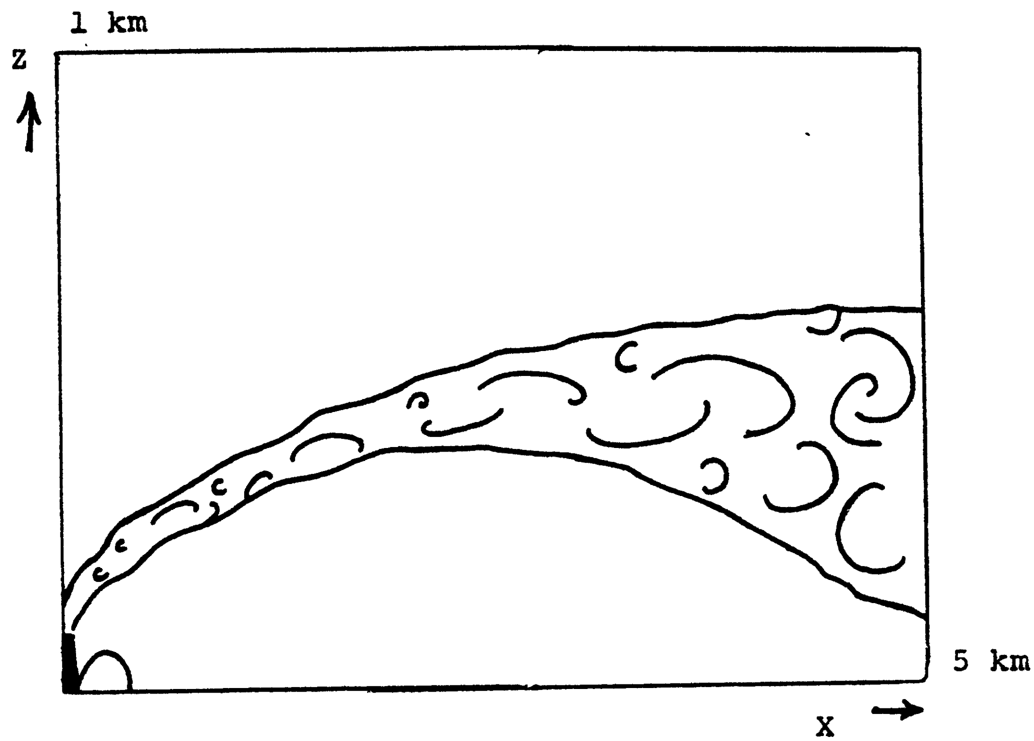

Fig. 3.3.2.1c

Mesh Alignment Appropriate for a Point Source Release

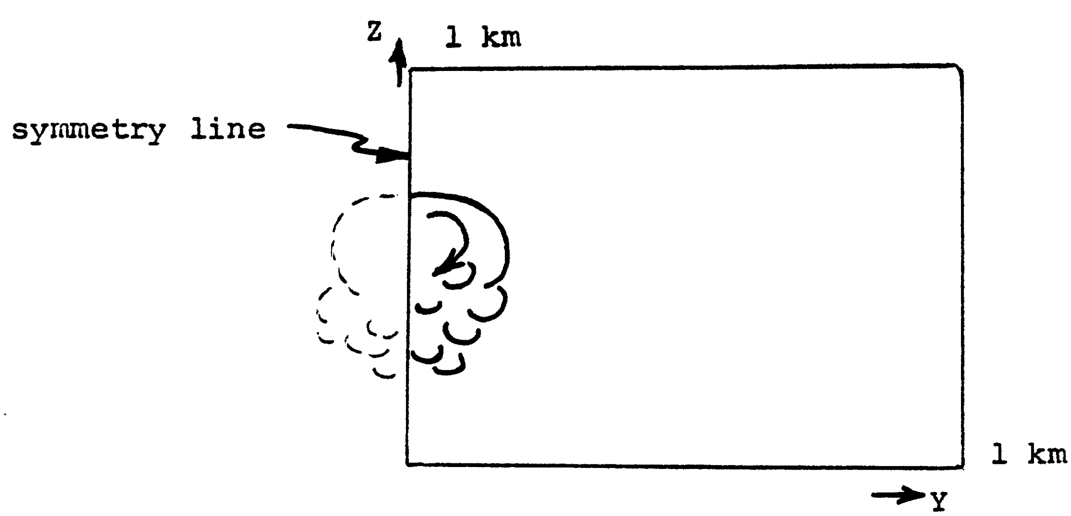

alignment scheme needs an extraordinarily long x-axis to model the same plume. Overall, the crosswind alignment scheme is about five times smaller than the downwind scheme. The velocity field in the crosswind alignment is that of a two-dimensional turbulent vortex, which typically exhibits strong shearing and entrainment of fluid. The velocity field in the downwind alignment is that of a two-dimensional turbulent deflected jet, which over most of the flow field exhibits a much smaller amount of shearing and entrainment. Clearly, the crosswind alignment scheme is expected to simulate the more important features of the flow.

The singular disadvantage of the crosswind alignment scheme is that it cannot explicitly calculate the shear-produced turbulence of the mean wind field, since the mean wind has no component in the y-z plane. The resolution of this problem is discussed in Sec. 4.3.3.

3.3.3 Downwind Advection of the Mesh

From the discussion in Sec. 3.3.2, the computer solution mesh is aligned perpendicular to the wind. The time evolution of the flow field of the plume cross section is drawn in Fig. 3.3.3.1. The choice of an appropriate downwind advection velocity of the computer mesh is needed in order to reconstruct

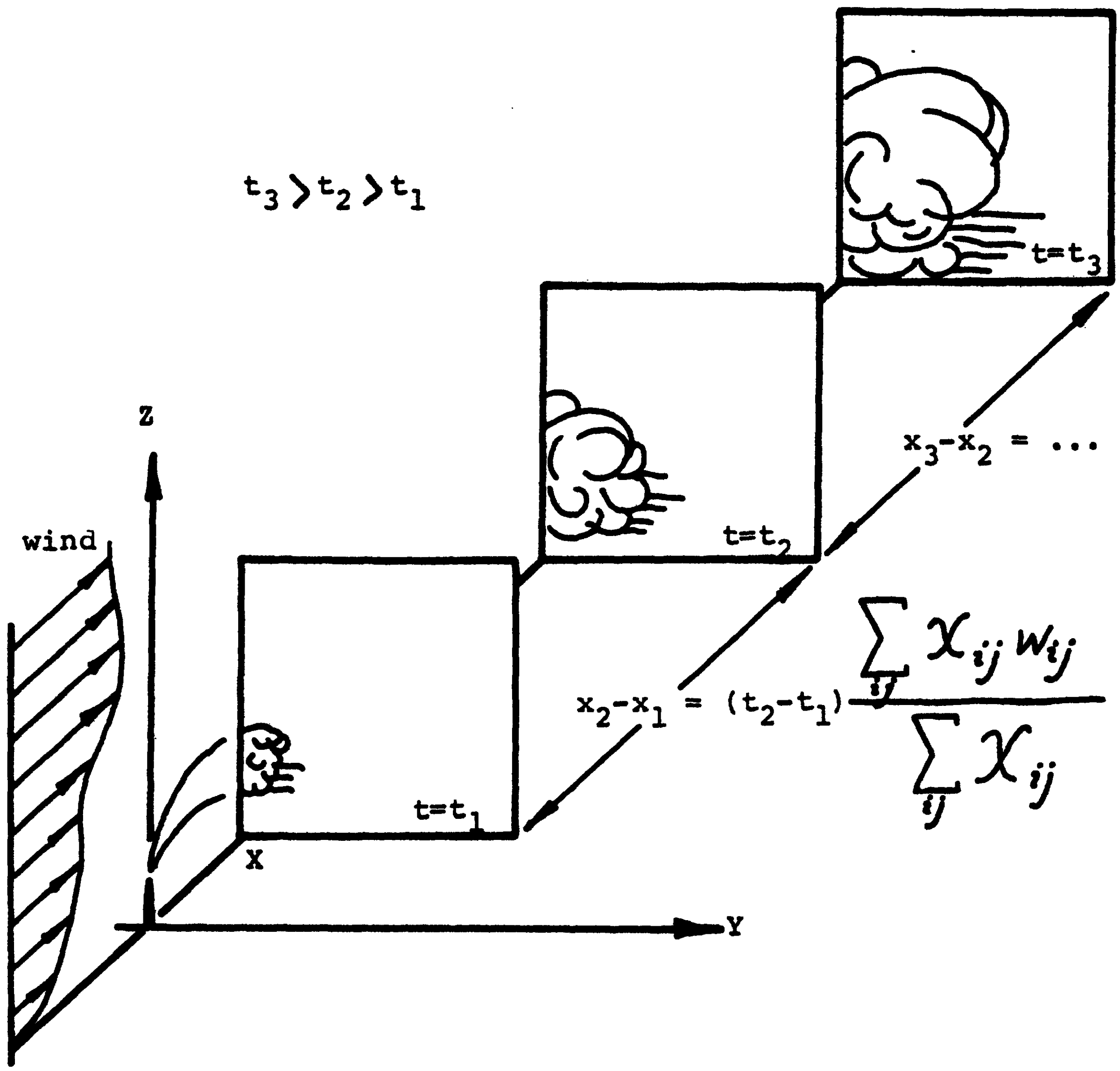

Fig. 3.3.3.1 Reconstruction of the Three-dimensional Plume. Wind vectors as a function of height are shown.

the full steady state plume, i.e., the time of the computer simulation must be related to a downwind distance. The choice is difficult because the wind profile dictates that fluid elements at different heights will advect downwind at different rates. A simple approximation is that the advection velocity should be equal to the "pollutant averaged" wind speed:

$$\frac{\Delta x}{\Delta t} = \frac{\int_0^\infty \int_0^\infty u(z)\ \chi(y,z)\,dy\,dz}{\int_0^\infty \int_0^\infty \chi(y,z)\,dy\,dz} \qquad (3.96)$$

The finite difference form of Eq. 3.96 is written in Fig. 3.3.3.1. The calculation of this quantity is performed in the "statistics package" of Sec. 3.3.7. A further refinement of the solution scheme is discussed in Sec. 6.2.1.

In practice, for plumes that are released from tall stacks, the amount of wind shear that the plume encounters is ordinarily moderate and does not greatly alter the plume behavior.

3.3.4 Property Data

The original VARR-II computer code allows for quadratic fitting of air property data versus temperature. In view of the fact that potential temperature is substituted for temperature in moist simulations, the scheme of fitting property data to temperature must be examined. The air property data to be fitted includes density, specific internal energy, dynamic viscosity, thermal conductivity, and heat capacity at constant pressure. The coefficients of the quadratic fits for dry air data[43] are listed in Table 3.3.4.1, along with the quadratic form that they are used in. The effect on the property value of the substitution of θ or θ_v for $\tilde{T}$ is considered next.

The use of $\tilde{T}$ or $\tilde{T}_v$ in the perfect gas law yields, by definition, the correct density of a dry or moist parcel of air, respectively. A quadratic fit of the perfect gas law over a small temperature range of interest would yield essentially exact results for the density as well. The calculation of densities with θ or θ_v substituted into the formula for $\tilde{T}$ is also appropriate because θ or θ_v vary from $\tilde{T}$ by very little compared to the absolute temperature. Recall that θ or θ_v is used in the problem formulation to eliminate the compressible nature of the hydrostatic atmosphere. The relevant density variations in the momentum equation are the relative density variations, and the criteria for the use of, say θ_v for T is that

$$\frac{\rho(\tilde{T})-\rho(T_o)}{\rho(T_o)} \simeq \frac{\rho(\theta_v)-\rho(\theta_{vo})}{\rho(\theta_{vo})} \qquad (3.97)$$

Table 3.3.4.1 Property Values of Air

				Constants		
i	symbol	property	units	a_i	b_i	c_i
1	ρ	density	lb_m/ft^3	2.0×10^{-7}	-1.78×10^{-4}	0.086394
2	I	internal energy	BTU/lb_m	4.3×10^{-6}	1.71×10^{-1}	78.357
3	ν	dynamic viscosity	$lb_m/ft\cdot sec$	-1.0×10^{-6}	1.92×10^{-3}	1.0932
4	K	thermal conductivity	$BTU/ft\ sec\,^oR$	0	2.59×10^{-5}	0.01313
5	C_p	heat capacity at constant pressure	$BTU/lb_m\,^oR$	0	-2.00×10^{-6}	0.24008

$$\text{property } i = a_i\ (T-460^oR)^2 + b_i\ (T-460^oR) + c_i$$

$(T \text{ in } ^oR)$

with a similar condition for θ in dry simulations. This relation holds with about four percent accuracy for the most extreme cases encountered in this work.

The specific internal energy is originally fitted versus T. Again, the fact that θ or θ_v is close to T compared to the absolute temperature allows them to be interchanged without significant error. The specific internal energy is accurate to about 4 percent under this substitution.

The values of dynamic viscosity and thermal conductivity are important only if the flow becomes laminar. None of the simulations in this work are expected to encounter regions of laminar flow, so the fitted values of molecular viscosity and thermal conductivity are unimportant.

The specific heat varies slowly with temperature, and the substitution of θ or θ_v for T results in only a 0.02 percent error for typical cases.

The necessary property data for equilibrium conditions of water vapor and cloud liquid water are included in Secs. 3.2.2.3 and 3.2.2.4. The inclusion of water in the simulations is assumed to have a negligible effect on the property data of the air-water mixture, except for the density, which is corrected through the use of the virtual temperature.

3.3.5 Mesh Initialization and Boundary Conditions

3.3.5.1 Input Profiles

Seven vertical profiles are required for a simulation. Five of the profiles serve to specify the boundary conditions on the computer mesh, one profile (the mean wind wpeed) is needed by the statistics package, and one profile (the hydrostatic pressure) is needed by the equilibrium moisture thermodynamics model. The required profiles are listed in Table 3.3.5.1. Each vertical profile consists of a set of values that are representative of the cell-centered temperature, wind speed, etc. The number of values is obviously equal to the number of fluid cells in the z-direction. The extension of the model to time-dependent vertical profiles is considered in Sec. 6.2.2.

3.3.5.2 Boundary Conditions

Boundary conditions must be specified for each of eight variables on the four walls of the computer mesh. The walls of the computer mesh are numbered in Fig. 3.3.5.1. Wall #1 is in the plume centerline with the real computer simulation to its left. For this purpose, wall #1 is a free-slip solid wall. Wall #4 always represents the earth, and is specified to be a no-slip wall. The earth is assumed to be a perfect

Table 3.3.5.1

Required Input Profiles

Atmospheric Profile	Units
virtual potential temperature	^{o}F
water vapor density	lb_m/ft^3
cloud liquid water density	lb_m/ft^3
eddy viscosity	ft^2/sec
turbulence kinetic energy	ft^2/sec^2
mean wind speed[A]	ft/sec
hydrostatic pressure[B]	millibars

A. The mean wind speed is required by the statistics package of Sec. 3.3.7.

B. The hydrostatic pressure is required by the equilibrium moisture thermodynamics model of Sec. 3.2.2.3.

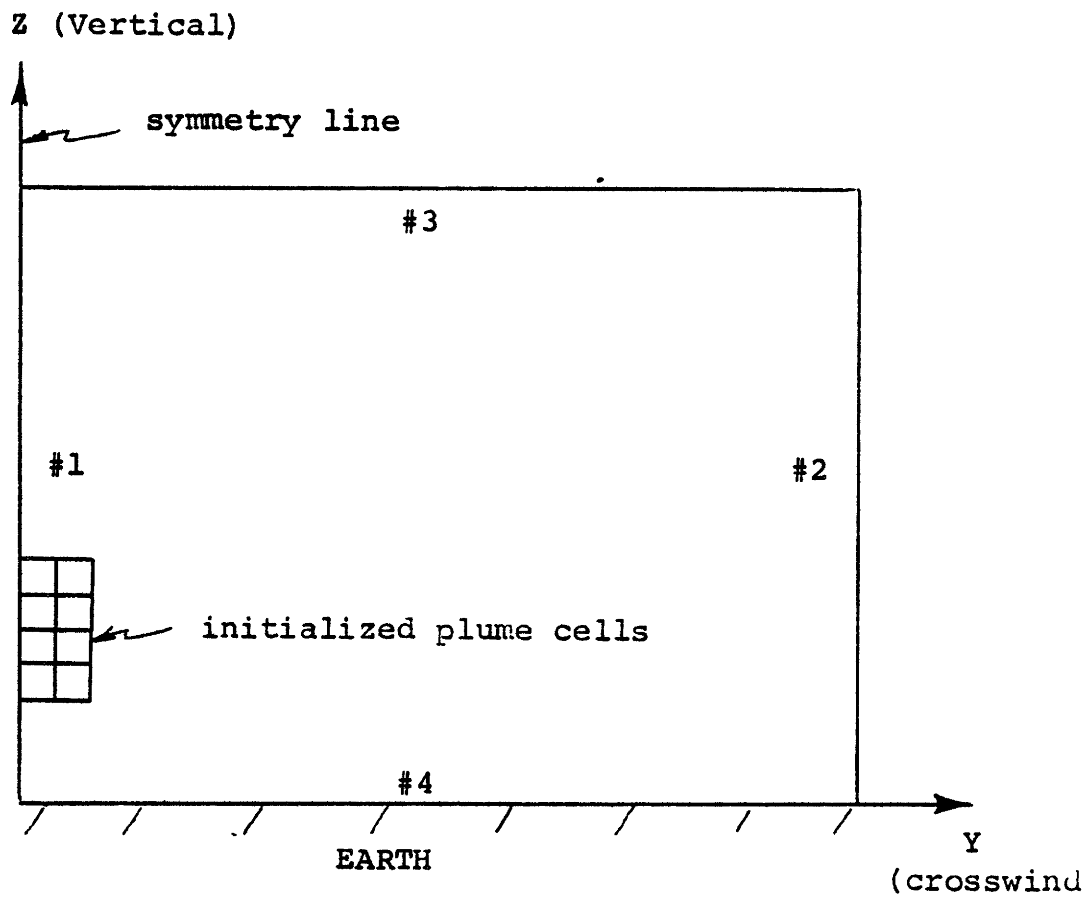

Fig. 3.3.5.1 Wall Numbering Scheme

reflector of pollutant and humidity in this work. This assumption could be easily modified to account for deposition of pollutant, sources of humidity, etc., for any case of specific interest. Walls #2 and #3 are chosen to be sufficiently far away from the plume so that negligible error is introduced in making them solid and free-slip. In practice, the plumes rise toward wall #3 and begin to deflect when their 10% boundary intersects the wall. This serves as a rough criterion on when to stop the computer simulation.

A summary of the boundary conditions is found in Table 3.5.5.2. The solid-wall, no-slip and free-slip conditions are found in the specification of the two velocity components, v and w. The reflective conditions are due to the "perfect reflecting walls" assumption; they are foregone at wall #2 for the five variables that are known as functions of height.

3.3.5.3 Mesh Initialization

The entire computer mesh in Fig. 3.3.5.2 is first initialized with the known atmospheric profiles of virtual potential temperature, eddy viscosity, turbulence kinetic energy, water vapor density, and cloud liquid water content. The entire mesh is initialized with a single background value of pollutant, and the velocity field is initialized to be at rest. The plume cells in the figure are then initialized by volume-averaging

Table 3.3.5.2

Boundary Conditions

Variable	Wall#1	Wall #2	Wall #3	Wall #4
y-velocity, v	S	S	F	N
z-velocity, w	F	F	S	S
virtual potential temperature	R	*	R	R
eddy viscosity	R	*	R	R
turbulence kinetic energy	R	*	R	R
pollutant	R	R	R	R
water vapor density	R	*	R	R
liquid water density	R	*	R	R

S--solid wall (normal velocity = 0)

N--no-slip (tangent velocity = 0)

F--free-slip (normal derivative of tangent velocity = 0)

R--reflective (normal derivative = 0)

*--specified as profiles of height (z)

the plume sources of energy, pollutant, and moisture over those cells, using mean wind speed at that height to define the depth of the cells swept out in one second. The initial eddy viscosity and turbulence kinetic energy in the plume cells are set to about 100 times that of the surrounding atmosphere--in practice, the plume turbulence values very quickly relax into values that are consistent with the flow field. No initial volume-averaged momentum is given to the plume cells. Instead of this, an effective stack height increment due to momentum is added to the actual stack height in specifying the location of the center of the plume cells.

3.3.6 Mesh Coarsening Capability

Model programming has been undertaken to allow the mesh spacing to be doubled periodically during the simulations, while keeping the same number of fluid cells on the whole computer mesh. The motivation for this is the desire to keep the growing plume cross section away from the unphysical (solid wall) top and right mesh boundaries. When the simulation is "coarsened," the mesh spacing doubles, which reduces the plume cross section by a factor of four. The calculation is restarted, and the simulation proceeds on a mesh that has four times the area of the old mesh, but the same number of fluid cells.

The coarsening procedure is outlined in Fig. 3.3.6.1. In

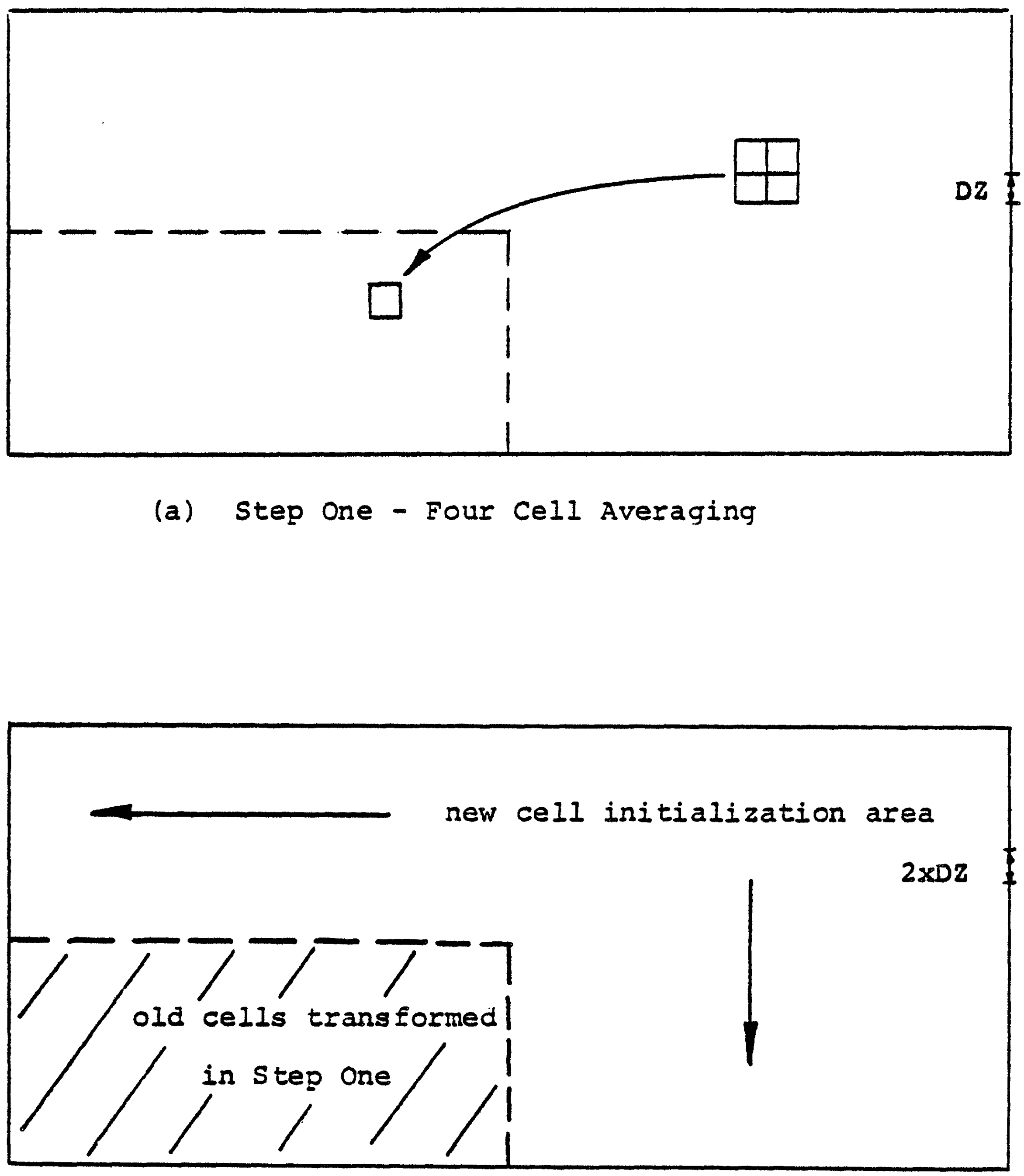

(a) Step One - Four Cell Averaging

(b) Step Two - Initialization of New Cells

Figure 3.3.6.1 Mesh Coarsening Procedure Steps a first step (a) the entire mesh is swept over, four cells at a time. Note that the number of cells vertically or horizontally must be even in order to do this. The fluid variables in these four cells are averaged in the following way: the cell specific internal energy, momenta, and turbulence kinetic energy are mass-averaged over the four cells, since these variables are defined on a per unit mass of air basis. The cell pollutant, eddy viscosity, and moisture variables are simply averaged over the four cells, since these variables are not defined on a per unit mass of air basis. The cell pressure is set to zero, which conforms with the usual starting guess procedures in running VARR-II. The average cell made up from these four cells is now stored in its proper place on the larger mesh, which is half of the distance to the origin vertically and horizontally. When the entire mesh has been swept, four cells at a time, the old mesh has now been relocated in the lower left corner, and is one-fourth of its old size.

In a second step (b) the remaining three-quarters of the mesh needs to be initialized. This "new" area is swept row-by-row in ascending order. The velocity field is assumed to be initially at rest, and the pressure field is initially set to zero. The remaining atmospheric state variables are all specified from a master library of profiles. When the "new" area has been initialized, the calculation is restarted with the vertical and horizontal mesh spacings doubled.

The computer mesh may be coarsened up to five times during a simulation--this would result in a final mesh that is $2^5 \times 2^5 = 1024$ times as large as the original mesh. The five times are user specified, and need not take place at regular intervals.

3.3.7 Plume Statistics Package

At regular intervals specified by the user, the program calls on a statistics package to calculate a number of important plume statistics without printing out the data of the entire computer mesh. The quantities that are reported by the statistics package are listed in Table 3.3.7.1. The average plume advection velocity is the feature discussed in Sec. 3.3.3, and is defined in Eq. 3.96.

Table 3.3.7.1

Data Reported by the Plume Statistics Package

Quantity	Units
Time of Simulation	sec
Total Number of Problem Iterations	(none)
Current Number of Pressure Iterations	(none)
Current Time Step Size	sec
Center Height of Pollutant Field	ft
Total Specific Internal Energy on Mesh	BTU
Average Downwind Advection Velocity	ft/sec
Plume Downwind Distance	ft

4. DESCRIPTION OF ATMOSPHERIC TURBULENCE

4.1 Introduction

This chapter describes in detail how atmospheric turbulence is represented in the model. The description begins with the knowledge (e.g., from a set of measurements) of the common atmospheric variables as functions of height: the set includes the wind speed and direction, virtual potential temperature, water vapor density, and cloud liquid water density. The important processes that are responsible for the characteristic shapes of these profiles are outlined, and the concept of layers in the atmosphere arises naturally in the explanation of the interdependencies of the profiles. With a working knowledge of the dominant phenomena in the atmospheric layers, the problem of prescribing the atmospheric turbulence is undertaken. For the model in this work, the atmospheric turbulence is specified with profiles of eddy viscosity and turbulence kinetic energy. The relation of these two variables to the other profiles, and their inclusion into the model occupies most of this chapter.

4.2 Atmospheric Profiles of Wind, Temperature, and Humidity

The vertical atmospheric profiles considered in this work are assumed to have been measured with some appropriate meteorological instruments over a flat terrain. For instance, a tower with a series of instruments at various heights would produce essentially pointwise values of the variables, which could then be linearly interpolated between the measurement heights to produce the full profiles. It is assumed that the measurements were time-averaged for at least 20 minutes so that there is very little time-dependence in the profiles. Alternatively, a radiosonde (balloon) ascent is commonly used for measuring vertical profiles, although the measurement averaging times are not long enough to completely average over the larger atmospheric eddies.

The measured atmospheric wind profiles have several common features. First, the atmospheric wind vanishes at the ground. This is in accord with the no-slip velocity boundary condition of real fluids. Second, the time-averaged (i.e., averaged over about 20 minutes) <u>vertical</u> velocity is very small at any height. This is because the very low frequency (of the order of 1 per day) vertical velocities are due to the synoptic scale subsiding or lifting motions associated with fronts; these velocities are usually only about 10 cm/sec. Because the average vertical velocities are small, the wind at any height is assumed to be parallel to the ground. Generally, the wind speed increases with height and commonly exhibits some turning with height--

especially in the first several hundred feet of elevation, where pressure gradient, Coriolis, and frictional forces are all important.

The fact that the wind vector may very roughly approximate a logarithmic profile,[44] an Ekman spiral,[45] or a thermal wind relation,[46] is only of minor interest here since the actual wind profile determines the behavior of an individual plume. In this work, the turning of the wind with height is not represented in the hydrodynamic simulations, although the prospect of including it is considered among the extensions of the model outlined in Sec. 6.2. Also, the difficulty of defining an average wind direction when there are only light, variable winds at a station dictates that the computer simulations are not expected to be accurate for winds of less than about 5 knots.

The temperature and humidity profiles directly provide the information about the local stability of vertical atmospheric and plume motions. No approximations to the temperature or humidity profiles are needed to incorporate them into the simulations. The temperature and humidity profiles are used to evaluate the virtual potential temperature profile: Note that in defining equations for virtual potential temperature (Eq. 3.53 and Eq. 3.67) the temperature, humidity, and pressure are required at any height. To this end the pressure profile could have been measured by itself, or calculated with any of a number of approximations (dry hydrostatic, moist hydrostatic, various interpolations between points, etc.) Whatever assumptions are made, the pressure profile consistent with these assumptions must be input to the simulation where it is used to recalculate the correct temperature from the virtual potential temperature and humidity for the equilibrium moisture thermodynamics model.

4.3 Turbulence in the Planetary Boundary Layer

4.3.1 Introduction

The planetary boundary layer (PBL) is a boundary layer in a rotating, stratified, multi-component fluid whose moisture component can undergo changes of phase. Further, the boundary conditions on fluxes of momentum, sensible and latent heats, and radiant energy can vary greatly over large and small distances (i.e., distances that are large or small in comparison to the depth of the boundary layer), and are typically strongly coupled to the flow. Although a number of excellent reviews have been written[47-57] at many levels of detail, the basic notions of turbulence in the planetary boundary layer are developed here with the aim of pointing out the limitations of the description of the PBL turbulence embodied in the computer simulations.

4.3.2 Layers in the PBL and Important Processes

Without much loss in generality, it is assumed in this work that all of the energy in turbulent atmospheric motions ultimately comes from the sun. Although it is possible to conceive of special situations where this is not quite true (for example, the turbulence near a busy expressway, much of which is caused by mechanical stirring and buoyant exhausts), the atmopsheres which are encountered in this work are free of man-made turbulence, except for the buoyant plumes themselves! For the purposes of illustration, the solar energy which produces atmospheric turublence may be divided into two streams: (1) that part of the solar energy that produces the large synoptic-scale pressure patterns on the earth, which in turn drives the wind and produces turbulence in regions of the atmosphere of sufficiently large wind shear, and (2) that part of the solar energy that produces the local thermal stratification of the atmopshere, which in turn produces turbulence in regions of sufficiently unstable stratification. The turbulence that is produced by the first stream is called "mechanically produced turbulence," and that produced by the second stream is called "buoyancy produced turbulence." The thermal stratification that is produced by the second stream is usually formulated in terms of virtual potential temperature, so that moisture and latent heat effects are naturally included in the "buoyancy produced turbulence." There are two mechanisms that destroy atmospheric turbulence: (1) viscous dissipation, which is always at work in a turbulent flow, and (2) buoyant destruction, which is present in regions of stable thermal stratification.

From the preceding discussion it is expected that in a region in steady state the mechanisms of turbulence production and destruction will be balanced, and that the turbulence kinetic energy will maintain a value that is commensurate with the destruction rate. Very commonly in micrometeorological studies, the regions that these processes are studied in are simplified to layers, so that the description of atmospheric turbulence becomes one-dimensional--the single dimension is then height. The situation is illustrated in Fig. 4.3.2.1. In the uppermost layer of laminar flow, the strong geostrophic winds usually have very small wind shears with height, and are usually associated with stably stratified air, so that there is little or no turbulence. The next layer down usually is a region of buoyancy produced turbulence with only small wind shear--the buoyancy is typically from solar heating at the ground and latent heat release in cloud formation (clouds obviously affect the amount of solar heating at the ground, so that these effects are strongly coupled). The layer nearest

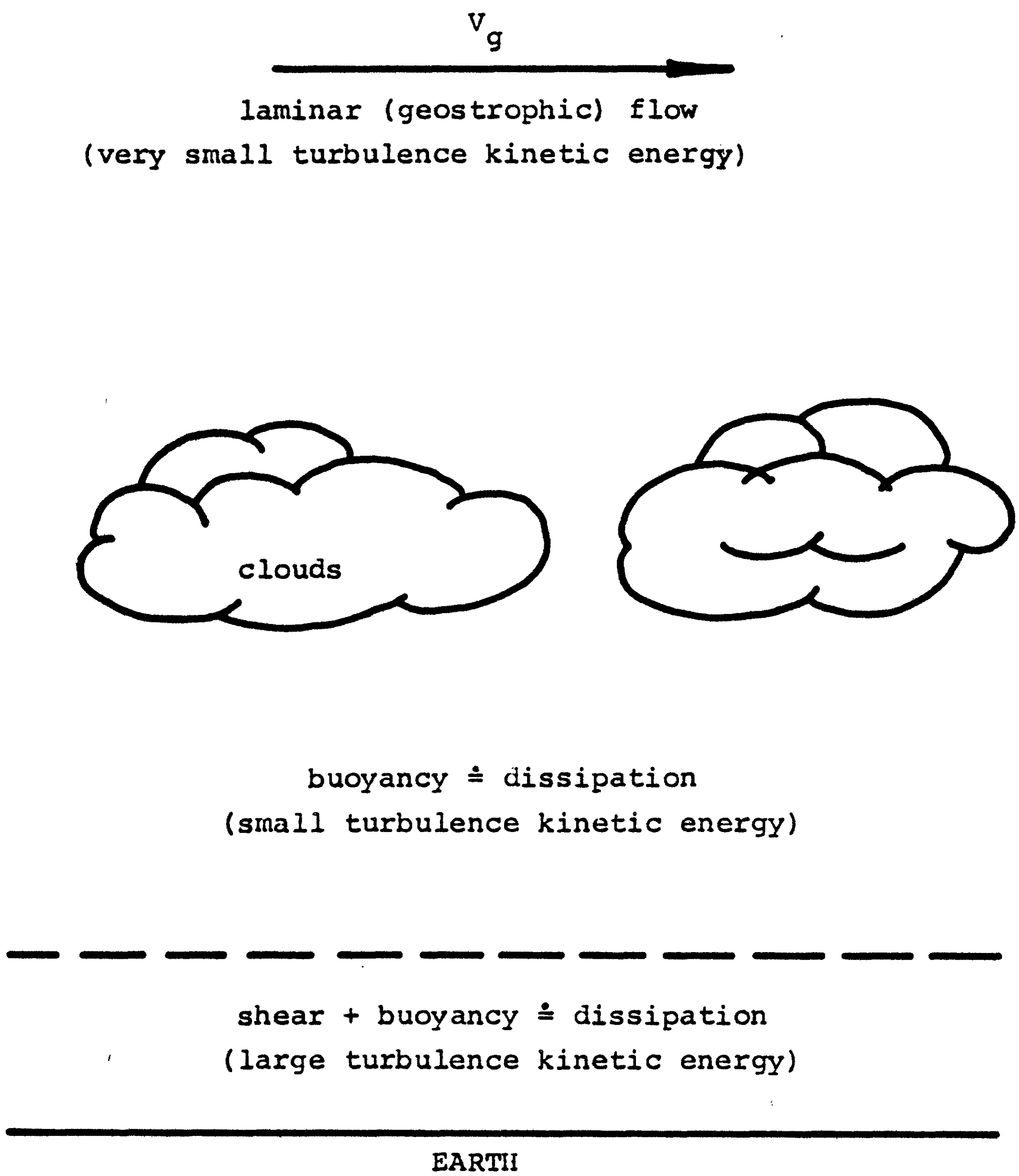

Fig. 4.3.2.1 The Concept of Layers in the Planetary Boundary Layer. Atmospheric turbulence is assumed to be variable in one-dimension only in this figure. The turbulence is steady-state.

to the ground typically exhibits a lot of wind shear due to the no-slip condition at the ground, so that mechanically produced turbulence is present in addition to buoyant production, and turbulence kinetic energy is usually a maximum somewhere in this layer.

The particular illustration of atmospheric layers in Fig. 4.3.2.1 is certainly not unique. Many investigators have coined names for layers to illustrate different refinements on the processes in the PBL. Such terms as the surface layer, Ekman layer, subcloud layer, cloud layer, inner layer, outer layer, tower layer, convection layer, inversion layer, superadiabatic layer, and viscous sublayer are common, but they do not represent anything more sophisticated than treating the atmosphere as one-dimensional.

The prospect of treating the atmospheric state as two-dimensional--now including its downwind development as well as its profile with height--is considered in Sec. 5.4.1 in conjunction with the modeling of a fumigation episode.

4.3.3 Prescription of the Eddy Viscosity

The prescription of the eddy viscosity in the two-dimensional mesh of the crosswind alignment scheme of Fig. 3.3.2.1c is considered in this section. It was mentioned in Sec. 3.3.2

that the absence of any mean wind component (by definition) in the crosswind direction means that, away from the plume, and as far as the computer simulation is concerned, there is no explicit mechanical production of turbulence in the atmosphere. In fact, what takes place in the atmosphere is that the turbulence kinetic energy component, $\overline{u'^2}$, and the Reynolds stress, $\overline{u'w'}$, of the downwind x-z plane are feeding into the crosswind y-z plane turbulence kinetic energy component, $\overline{v'^2}$, and Reynolds stress, $\overline{v'w'}$, through the return to isotropy term in Eq. 3.40. For this work, the assumption is made that the return to isotropy term is very strong, so that the turbulence is <u>isotropic</u>. Experiments on atmospheric return to isotropy indicate that this assumption is reasonably good.[58] It is seen in the discussion of the results in Chapter Five that this is probably the most limiting assumption in the work with regard to being able to model real atmospheres. The eddy viscosity as a function of height in the downwind x-z plane is estimated from a number of prescriptions for eddy viscosity that are correlated from mean wind and temperature profiles, then the eddy viscosity in the crosswind y-z plane is assumed to be the same as in the x-z plane under the assumption of isotropy.

The incorporation of an ambient eddy viscosity profile on the simulation mesh finds two problems. First, any arbitrary eddy viscosity imposed on the mesh cells at the start of the simulation will, in the absence of sufficient mechanical and buoyant production, rapidly decay down to the molecular kinematic viscosity. Second, the turbulence field inside the plume must be allowed to develop on its own. The method of incorporating the ambient eddy viscosity profile in light of these problems is as follows: to start the simulation, the cells outside of the initial plume cells are initialized with the eddy viscosity profile, depending on their height in the mesh. After each time step, each cell on the mesh is tested to see if it has fallen below the prescribed eddy viscosity profile at its height. If it has, its eddy viscosity is simply reset to the ambient value. If it has not fallen below the ambient value, presumably because either the plume-induced turbulence or the turbulently diffused turbulence from neighboring cells is dominating, then the cell eddy viscosity value is left alone. In this way, the far field always maintains the ambient atmospheric turbulence values, and the plume turbulence, if greater than the ambient turbulence, is left to develop on its own. Overall, this method has the effect of adding a non-uniform source term to the eddy viscosity equation--the term always adjusts itself to yield the original eddy viscosity in the far field, and to "turn itself off" if the plume turbulence is dominating. Mathematically, the inequality

$$\sigma(y,z,t) \geq \sigma_{library}(z) \qquad (4.1)$$

has been added to the equation set, where $\sigma_{libary}(z)$ is the prescribed eddy viscosity profile as a function of height.

Before discussing the available prescriptions of eddy viscosity, it should be noted that the potentially most accurate method of prescribing the eddy viscosity for an individual release would be to actually measure it in the field--perhaps simply by estimating it from bivane wind fluctuation data. The effort in this work to arrive at workable prescriptions from the micrometeorological literature is motivated by the total absence of these measurements in existing plume field data. The particular prescriptions that are recommended here are used only because they offer a simple way to estimate the eddy viscosity profile.

A number of prescriptions for the eddy viscosity in the outer boundary layer of the atmosphere as a function of height have been reviewed.[59-64] A summary of the various prescriptions is presented in Table 4.3.3.1, where they are separated into two major groups--those that require wind speed and direction profiles, and those that do not. Those which do not require wind profiles as input are easier to use because the wind profiles need not be measured (e.g., with instrumented towers or

Table 4.3.3.1 Comparison of Eddy Viscosity Prescriptions

Author(s)	Atmospheric Stability in which the Prescription is Applicable		
	Neutral	Stable	Unstable
* * Prescriptions that require wind speed and direction versus height:			
Blackadar[59]	yes	no	no
Blackadar and Ching[60]	no	no	yes
Yamamoto and Shimanuki[61]	yes	yes	yes
Nieuwstadt[64]	yes	yes	yes
Prescriptions that do not require wind profiles:			
O'Brien[62]	yes	yes	yes
Bornstein[63]	yes	yes	yes

balloons). However, they are not expected to be as accurate, since the wind profile has taken an ideal shape. All of the models in Table 4.3.3.1 are searched for applicability to neutral, stable, and unstable atmospheres.

It is recommended that if the wind speed and direction profiles have been measured, the prescriptions of Blackadar,[59,60] and Yamamoto and Shimanuki[61] should be used. If the wind speed and direction profiles have not been measured, the prescriptions of Bornstein[63] or O'Brien[62] should be used. The prescription of Nieuwstadt[64] requires a substantial numerical analysis of the profiles and has not been tested.

Any of these prescriptions must be used with caution since all of them are only capable of providing an estimate to the eddy viscosity. The greatest difficulty in using these prescriptions is that they typically require values for quantities that were not measured, such as the heat flux at the ground, the roughness height, geostrophic velocity, etc.

4.3.4 Prescription of the Turbulence Kinetic Energy

The prescription of the turbulence kinetic energy (TKE) in the two-dimensional mesh of the crosswind alignment scheme of Fig. 3.3.2.1c is considered in this section. The turbulence kinetic energy suffers from exactly the same problem as the eddy viscosity in Sec. 4.3.3.: in the absence of explicit buoyant and mechanical production of turbulence on the two-dimensional mesh, the turbulence kinetic energy would gradually decay away entirely. To satisfactorily avoid this problem, the concept of the turbulent "return to isotropy" is again invoked to allow the turbulent kinetic energy produced by the mean flow shearing and buoyancy to be fed into the crosswind motions. A turbulence kinetic energy profile is needed, so that it may maintain the turbulence for mesh cells that lack the sufficient turbulence production in exactly the same way that an eddy viscosity profile maintains the eddy viscosity for the mesh.

Ideally, the TKE profile should be measured or deduced from other profiles for an actual atmosphere. In fact, however, prescriptions for the turbulence kinetic energy from mean wind and temperature profiles are not generally available in the literature. The actual prescription of the turbulence kinetic energy profile in this work has had to come from the following, very approximate analysis of the transport equations.

Consider the TKE transport equation in a region away from the plume. The vertical and horizontal velocities, v and w, are zero, and the eddy viscosity, σ , and TKE, q, are functions of height, z, only; with the resulting expression being

$$\frac{\partial q}{\partial t} = \frac{-4\alpha q^2}{\sigma} + \Gamma \frac{\partial}{\partial z} \left(\sigma \frac{\partial q}{z}\right) \tag{4.2}$$

For a properly time-independent TKE, there must be a balance of dissipation and diffusion in Eq. 4.2; or

$$\frac{4\alpha q^2}{\sigma} = \Gamma \frac{\partial}{\partial z} \left(\sigma \frac{\partial q}{\partial z}\right) \tag{4.3}$$

Performing a scale analysis of the terms, noting that $\Gamma/_{4\alpha} \simeq 10$ and that the depth of the planetary boundary layer is taken equal to L_{eddy} , one obtains the result

$$q \sim 10 \frac{\sigma^2}{L_{eddy}^2} \tag{4.4}$$

For typical values in the atmosphere, $\sigma \sim 100$ ft^2/sec and $L_{eddy} \sim 10^3$ ft, giving the value

$$\frac{q}{\sigma} \sim 10^{-3} \text{ sec}^{-1} . \tag{4.5}$$

Note that for a highly idealized picture of turbulence,[65] with eddies of a single size, L_{eddy}, and velocity, u_{eddy},

$$q \sim u_{eddy}^2 , \tag{4.6}$$

$$\sigma \sim u_{eddy} L_{eddy} , \tag{4.7}$$

and therefore

$$\frac{q}{\sigma} \sim \frac{u_{eddy}}{L_{eddy}} \quad [\text{sec}^{-1}] . \tag{4.8}$$

This states that q/σ is simply the inverse of the eddy turn-over time. The scale analysis (Eq. 4.5) of the q transport equation shows that the choice $q \sim 10^{-3} \sec^{-1} \sigma$ should roughly allow q to have a constant value. The fact that this choice of q agrees with the eddy turnover time of roughly the most diffusive atmospheric eddies[66] (10^3 seconds, or about 15 minutes) lends support to the idea that σ and q have been chosen consistently in this scheme.

The crude specification of $q_{library}(z)$ has been found to be satisfactory in this work primarily because the turbulence kinetic energy only indirectly influences the eddy viscosity, so that errors in estimating TKE are tolerated much more than the errors in estimating the eddy viscosity. The preceding analysis, since it is a scale analysis, only provides a very approximate estimate of the turbulence kinetic energy profile. Mathematically, the inequality

$$q(y,z,t) > q_{library}(z) = 10^{-3} \sec^{-1} \sigma_{library}(z) \qquad (4.9)$$

has been added to the equation set, where $q_{library}(z)$ is the prescribed turbulence kinetic energy profile as a function of height.

5. RESULTS

5.1 Introduction

The discussion of the results of the computer plume simulations is very naturally divided into two sections corresponding to the two regimes of plume behavior outlined in Sec. 1.2.2. To illustrate the two regimes, typical values of effluent temperature, velocity, and pollutant are shown in Fig. 5.1.1 for several stations downwind of a large combustion source. At the stack exit, the plume rushes upward at 20m/sec, is about $100^{\circ}C$ above the ambient air temperature, and has an SO_2 concentration of about 100 000 pphm (parts per hundred million). At the second station the plume has become diluted about 200 times. Without a detailed picture of its cross section, it may be stated generally that its average temperature excess is now only about $0.5^{\circ}C$ and its turbulent velocity fluctuations (disregarding those induced by its buoyancy) are about 10 cm/sec--and these are just about on the level of observed atmospheric fluctuations. However, the plume SO_2 concentration is still many times higher than the background SO_2 level, so that the plume is recognizable by its SO_2 concentration field, but not by its temperature or velocity fields. Throughout this first regime the plume

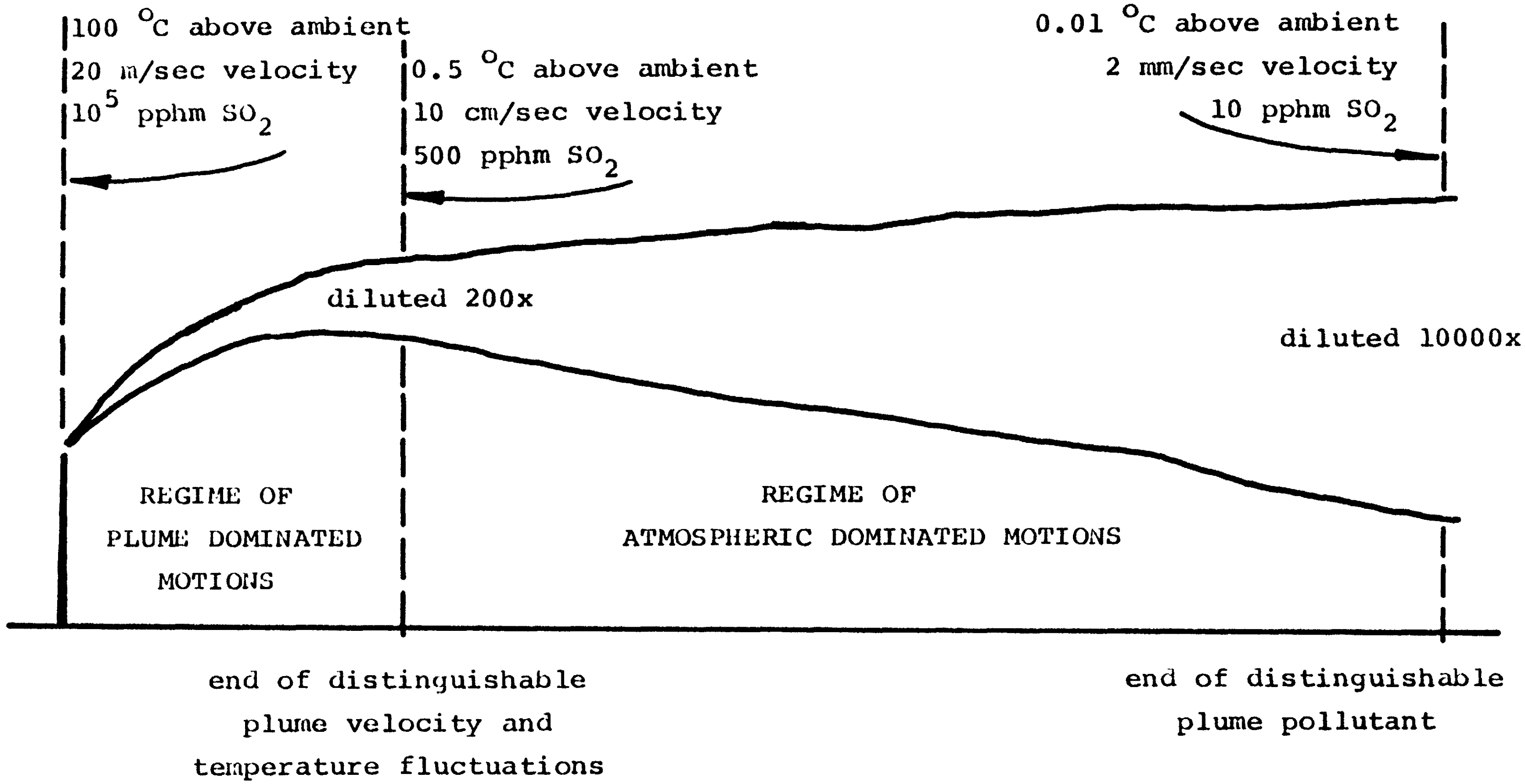

Fig. 5.1.1 Plume Regimes. The plume behavior is divided at the point at which the plume temperature and velocity fluctuations are reduced to levels that are indistinguishable from atmospheric fluctuations.

velocity and temperature fluctuations have been stronger than the atmospheric fluctuations, so that in a large part the plume motions have been dominated by the plume properties. Throughout the second regime the atmospheric motions are responsible for the plume dilution to the point where the pollutant becomes indistinguishable from the background level, and the plume disappears.

The selection of these regimes is very natural in the discussion of the results. The results that are applicable in the plume dominated stage will address the question of how adequately the dynamics of a buoyant, deflected plume are simulated. Such results are found in Sec. 5.2. The results that are applicable in the atmospheric dominated stage will address the question of how adequately the atmospheric turbulence is being simulated. Such results are found in Sec. 5.3. The results in Sec. 5.4 are essentially model extensions that are applicable in the atmospheric dominated regime for Sec. 5.4.1, and the plume dominated regime for Sec. 5.4.2, but which do not have a body of experimental results to be compared with.

The plume simulations that are presented in this chapter have been included for several different reasons. The general simulation in Sec. 5.2.1 is included to acquaint the reader with the general features of the buoyant line-vortex. The detailed comparison of simulations like the one in Sec. 5.2.1 with experimental results is made in Sec. 5.2.2. The effect of thermal stratification on the buoyant line vortex is then developed in the simulation of Sec. 5.2.3. The simulations for comparison with actual field studies again considers the neutral atmosphere case in Sec. 5.3.1. The effect of thermal stratification is then developed in the simulation of Sec. 5.3.2, where a large stack plume in a low-level inversion is studied. Simulations that demonstrate the model extensions are found in Sec. 5.4.

5.2 Comparisons to Analytical Models

5.2.1 General Nature of the Solutions

The general nature of all the computer solutions in this work is discussed in this section. All of the simulations are performed on a 20 cell by 20 cell mesh, although the cell height and width vary between different simulations. The time step size is selected by the program at each time step, and is usually from one-tenth of a second to several seconds. The selection of a time step size is performed by the code,[67] where it always chooses the smallest step size from a choice of a diffusion condition,

$$DT = \frac{TSTEP}{\max(\sigma)\left(\frac{1}{Dy^2} + \frac{1}{Dz^2}\right)} , \tag{5.1}$$

a Courant condition,

$$DT = \frac{TSTEP \ \ \min(Dx,Dz)}{\max(v,w)} , \tag{5.2}$$

or a simple rate of change condition,

$$DT = \frac{.2 \max\ (v,w)}{(\max(v,w) - \max(v_{old},w_{old}) + 10^{-6})} , \tag{5.3}$$

where TSTEP usually has a value of 0.01. As a practical matter, it is found that the time steps have to be reduced beyond these conditions by about a factor of 25 for the mesh cell sizes encountered in this work. This allows the code to conserve energy in the computer mesh cells within an acceptable tolerance. The non-conservation of energy arises from the first order accuracy of the differencing scheme for the advection terms. Full donor cell differencing of the advection terms is found to give the best answers in the simulations--less than full donor cell differencing produces noticeable nonlinear instabilities in the flow.

A simple plume development is found in Figures 5.2.1.1 to 5.2.1.6. Figure 5.2.1.1 interprets the mesh cell quantities found in the following figures. In Fig. 5.2.1.2, the

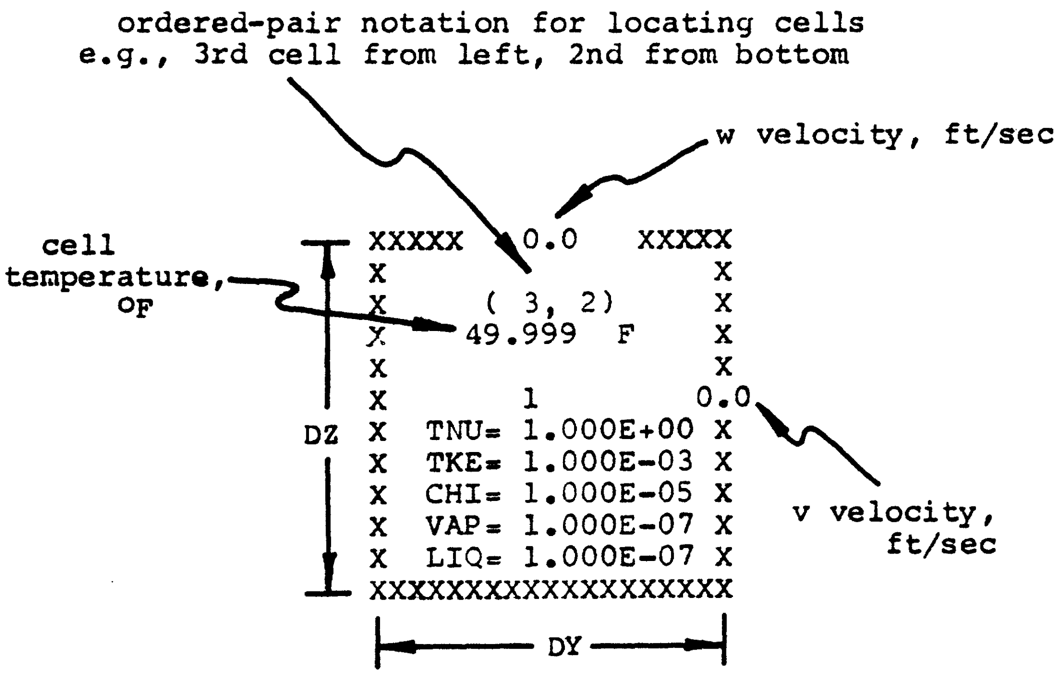

TNU is eddy viscosity in ft^2/sec

TKE is turbulence kinetic energy in ft^2/sec^2

CHI is pollutant concentration in lbm/ft^3

VAP is water vapor density in lbm H_2O/ft^3

LIQ is liquid water density in lbm H_2O/ft^3

Fig. 5.2.1.1 Key to Cellwise Quantities for Figs. 5.2.1.2, 5.2.1.3, 5.2.1.4, 5.2.1.6, and 5.3.2.1.

```
XXXXX   0.0   XXXXXXXXX   0.0   XXXXXXXXX   0.0   XXXXXXXXX   0.0   XXXXXXXXX   0.0   XXXXX
X                   X                   X                   X                   X                   X
X      ( 2, 8)      X      ( 3, 8)      X      ( 4, 8)      X      ( 5, 8)      X      ( 6, 8)      X
X    49.999  F      X    49.999  F      X    49.999  F      X    49.999  F      X    49.999  F      X
X                   X                   X                   X                   X                   X
O      1       0.0       1       0.0       1       0.0       1       0.0       1       0.0
X  TNU= 1.000E+00 X  TNU= 1.000E+00 X  TNU= 1.000E+00 X  TNU= 1.000E+00 X  TNU= 1.000E+00 X
X  TKE= 1.000E-03 X  TKE= 1.000E-03 X  TKE= 1.000E-03 X  TKE= 1.000E-03 X  TKE= 1.000E-03 X
X  CHI= 1.000E-05 X  CHI= 1.000E-05 X  CHI= 1.000E-05 X  CHI= 1.000E-05 X  CHI= 1.000E-05 X
X  VAP= 1.000E-07 X  VAP= 1.000E-07 X  VAP= 1.000E-07 X  VAP= 1.000E-07 X  VAP= 1.000E-07 X
X  LIQ= 1.000E-07 X  LIQ= 1.000E-07 X  LIQ= 1.000E-07 X  LIQ= 1.000E-07 X  LIQ= 1.000E-07 X
XXXXX   0.0   XXXXXXXXX   0.0   XXXXXXXXX   0.0   XXXXXXXXX   0.0   XXXXXXXXX   0.0   XXXXX
X                   X                   X                   X                   X                   X
X      ( 2, 7)      X      ( 3, 7)      X      ( 4, 7)      X      ( 5, 7)      X      ( 6, 7)      X
X    49.999  F      X    49.999  F      X    49.999  F      X    49.999  F      X    49.999  F      X
X                   X                   X                   X                   X                   X
O      1       0.0       1       0.0       1       0.0       1       0.0       1       0.0
X  TNU= 1.000E+00 X  TNU= 1.000E+00 X  TNU= 1.000E+00 X  TNU= 1.000E+00 X  TNU= 1.000E+00 X
X  TKE= 1.000E-03 X  TKE= 1.000E-03 X  TKE= 1.000E-03 X  TKE= 1.000E-03 X  TKE= 1.000E-03 X
X  CHI= 1.000E-05 X  CHI= 1.000E-05 X  CHI= 1.000E-05 X  CHI= 1.000E-05 X  CHI= 1.000E-05 X
X  VAP= 1.000E-07 X  VAP= 1.000E-07 X  VAP= 1.000E-07 X  VAP= 1.000E-07 X  VAP= 1.000E-07 X
X  LIQ= 1.000E-07 X  LIQ= 1.000E-07 X  LIQ= 1.000E-07 X  LIQ= 1.000E-07 X  LIQ= 1.000E-07 X
XXXXX   0.0   XXXXXXXXX   0.0   XXXXXXXXX   0.0   XXXXXXXXX   0.0   XXXXXXXXX   0.0   XXXXX
X                   X                   X                   X                   X                   X
X      ( 2, 6)      X      ( 3, 6)      X      ( 4, 6)      X      ( 5, 6)      X      ( 6, 6)      X
X    49.999  F      X    49.999  F      X    49.999  F      X    49.999  F      X    49.999  F      X
X                   X                   X                   X                   X                   X
O      1       0.0       1       0.0       1       0.0       1       0.0       1       0.0
X  TNU= 1.000E+00 X  TNU= 1.000E+00 X  TNU= 1.000E+00 X  TNU= 1.000E+00 X  TNU= 1.000E+00 X
X  TKE= 1.000E-03 X  TKE= 1.000E-03 X  TKE= 1.000E-03 X  TKE= 1.000E-03 X  TKE= 1.000E-03 X
X  CHI= 1.000E-05 X  CHI= 1.000E-05 X  CHI= 1.000E-05 X  CHI= 1.000E-05 X  CHI= 1.000E-05 X
X  VAP= 1.000E-07 X  VAP= 1.000E-07 X  VAP= 1.000E-07 X  VAP= 1.000E-07 X  VAP= 1.000E-07 X
X  LIQ= 1.000E-07 X  LIQ= 1.000E-07 X  LIQ= 1.000E-07 X  LIQ= 1.000E-07 X  LIQ= 1.000E-07 X
XXXXX   0.0   XXXXXXXXX   0.0   XXXXXXXXX   0.0   XXXXXXXXX   0.0   XXXXXXXXX   0.0   XXXXX
X                   X                   X                   X                   X                   X
X      ( 2, 5)      X      ( 3, 5)      X      ( 4, 5)      X      ( 5, 5)      X      ( 6, 5)      X
X    49.999  F      X    49.999  F      X    49.999  F      X    49.999  F      X    49.999  F      X
X                   X                   X                   X                   X                   X
O      1       0.0       1       0.0       1       0.0       1       0.0       1       0.0
X  TNU= 1.000E+00 X  TNU= 1.000E+00 X  TNU= 1.000E+00 X  TNU= 1.000E+00 X  TNU= 1.000E+00 X
X  TKE= 1.000E-03 X  TKE= 1.000E-03 X  TKE= 1.000E-03 X  TKE= 1.000E-03 X  TKE= 1.000E-03 X
X  CHI= 1.000E-05 X  CHI= 1.000E-05 X  CHI= 1.000E-05 X  CHI= 1.000E-05 X  CHI= 1.000E-05 X
X  VAP= 1.000E-07 X  VAP= 1.000E-07 X  VAP= 1.000E-07 X  VAP= 1.000E-07 X  VAP= 1.000E-07 X
X  LIQ= 1.000E-07 X  LIQ= 1.000E-07 X  LIQ= 1.000E-07 X  LIQ= 1.000E-07 X  LIQ= 1.000E-07 X
XXXXX   0.0   XXXXXXXXX   0.0   XXXXXXXXX   0.0   XXXXXXXXX   0.0   XXXXXXXXX   0.0   XXXXX
X                   X                   X                   X                   X                   X
X      ( 2, 4)      X      ( 3, 4)      X      ( 4, 4)      X      ( 5, 4)      X      ( 6, 4)      X
X    68.088  F      X    49.999  F      X    49.999  F      X    49.999  F      X    49.999  F      X
X                   X                   X                   X                   X                   X
O      1       0.0       1       0.0       1       0.0       1       0.0       1       0.0
X  TNU= 1.000E+02 X  TNU= 1.000E+00 X  TNU= 1.000E+00 X  TNU= 1.000E+00 X  TNU= 1.000E+00 X
X  TKE= 1.000E+02 X  TKE= 1.000E-03 X  TKE= 1.000E-03 X  TKE= 1.000E-03 X  TKE= 1.000E-03 X
X  CHI= 1.000E+00 X  CHI= 1.000E-05 X  CHI= 1.000E-05 X  CHI= 1.000E-05 X  CHI= 1.000E-05 X
X  VAP= 1.000E-07 X  VAP= 1.000E-07 X  VAP= 1.000E-07 X  VAP= 1.000E-07 X  VAP= 1.000E-07 X
X  LIQ= 1.000E-07 X  LIQ= 1.000E-07 X  LIQ= 1.000E-07 X  LIQ= 1.000E-07 X  LIQ= 1.000E-07 X
XXXXX   0.0   XXXXXXXXX   0.0   XXXXXXXXX   0.0   XXXXXXXXX   0.0   XXXXXXXXX   0.0   XXXXX
X                   X                   X                   X                   X                   X
X      ( 2, 3)      X      ( 3, 3)      X      ( 4, 3)      X      ( 5, 3)      X      ( 6, 3)      X
X    49.999  F      X    49.999  F      X    49.999  F      X    49.999  F      X    49.999  F      X
X                   X                   X                   X                   X                   X
O      1       0.0       1       0.0       1       0.0       1       0.0       1       0.0
X  TNU= 1.000E+00 X  TNU= 1.000E+00 X  TNU= 1.000E+00 X  TNU= 1.000E+00 X  TNU= 1.000E+00 X
X  TKE= 1.000E-03 X  TKE= 1.000E-03 X  TKE= 1.000E-03 X  TKE= 1.000E-03 X  TKE= 1.000E-03 X
X  CHI= 1.000E-05 X  CHI= 1.000E-05 X  CHI= 1.000E-05 X  CHI= 1.000E-05 X  CHI= 1.000E-05 X
X  VAP= 1.000E-07 X  VAP= 1.000E-07 X  VAP= 1.000E-07 X  VAP= 1.000E-07 X  VAP= 1.000E-07 X
X  LIQ= 1.000E-07 X  LIQ= 1.000E-07 X  LIQ= 1.000E-07 X  LIQ= 1.000E-07 X  LIQ= 1.000E-07 X
XXXXX   0.0   XXXXXXXXX   0.0   XXXXXXXXX   0.0   XXXXXXXXX   0.0   XXXXXXXXX   0.0   XXXXX
X                   X                   X                   X                   X                   X
X      ( 2, 2)      X      ( 3, 2)      X      ( 4, 2)      X      ( 5, 2)      X      ( 6, 2)      X
X    49.999  F      X    49.999  F      X    49.999  F      X    49.999  F      X    49.999  F      X
X                   X                   X                   X                   X                   X
O      1       0.0       1       0.0       1       0.0       1       0.0       1       0.0
X  TNU= 1.000E+00 X  TNU= 1.000E+00 X  TNU= 1.000E+00 X  TNU= 1.000E+00 X  TNU= 1.000E+00 X
X  TKE= 1.000E-03 X  TKE= 1.000E-03 X  TKE= 1.000E-03 X  TKE= 1.000E-03 X  TKE= 1.000E-03 X
X  CHI= 1.000E-05 X  CHI= 1.000E-05 X  CHI= 1.000E-05 X  CHI= 1.000E-05 X  CHI= 1.000E-05 X
X  VAP= 1.000E-07 X  VAP= 1.000E-07 X  VAP= 1.000E-07 X  VAP= 1.000E-07 X  VAP= 1.000E-07 X
X  LIQ= 1.000E-07 X  LIQ= 1.000E-07 X  LIQ= 1.000E-07 X  LIQ= 1.000E-07 X  LIQ= 1.000E-07 X
XXXXX   0.0   XXXXXXXXX   0.0   XXXXXXXXX   0.0   XXXXXXXXX   0.0   XXXXXXXXX   0.0   XXXXX
```

Fig. 5.2.1.2 Initialized Plume Cross Section at 0 sec.
DY = 100 ft, DZ = 200 ft.
Disregard moisture values.

entire 400 mesh cells are initialized at rest and at 50°F, except for one warm cell (2,4) centered 500 ft/high (and on the left boundary) which is at rest and at 68°F. Each mesh cell is 200 ft high and 100 ft wide. The ambient turbulence is set uniformly to 1 ft^2/sec in eddy viscosity and $10^{-3} ft^2/sec^2$ in turbulence kinetic energy, which are essentially laminar values compared to the values that develop inside the plume cell.

After 20 seconds of development (see Fig. 5.2.1.3) a vortex circulation has formed in the vicinity of the warm fluid, and mixing has brought the warmest fluid cell (2,4) from 68°F to 61.24°F. The strongest updraft (6.57 ft/sec) occurs in the warmest cell, and the downdrafts tend to be weaker, since they are spread over a larger area.

After 80 seconds of development (see Fig. 5.2.1.4) the plume has risen 379 ft. Considerable mixing has reduced the warmest cell temperature to 52.9°F from 68°F, and the updraft has now increased to 10.8 ft/sec. Again, the vortex circulation is very easy to identify and it occupies a progressively larger area as the plume cross section grows. The turbulence kinetic energy field at this point in time is illustrated in Fig. 5.2.1.5, where the maximum TKE occurs in the updraft region and is about 1600 times that of the ambient field.

After 200 seconds of development (see Fig. 5.2.1.6), the

```
XXXXX   0.215 XXXXXXXXX   0.107 XXXXXXXXX   0.142 XXXXXXXXX   0.073 XXXXXXXXX   0.041 XXXXX
X                   X                   X                   X                   X                   X
X      ( 2, 8)      X      ( 3, 8)      X      ( 4, 8)      X      ( 5, 8)      X      ( 6, 8)      X
X     49.992  F     X     50.019  F     X     50.137  F     X     49.922  F     X     49.922  F     X
X                   X                   X                   X                   X                   X
O       1       0.073       1       0.120       1       0.148       1       0.121       1       0.126
X  TNU= 1.005E+00 X  TNU= 1.007E+00 X  TNU= 1.005E+00 X  TNU= 1.003E+00 X  TNU= 1.001E+00 X
X  TKE= 1.039E-03 X  TKE= 1.014E-03 X  TKE= 1.009E-03 X  TKE= 1.006E-03 X  TKE= 1.001E-03 X
X  CHI= 1.084E-05 X  CHI= 1.001E-05 X  CHI= 1.000E-05 X  CHI= 9.999E-06 X  CHI= 9.999E-06 X
X  VAP= 2.000E-07 X  VAP= 2.000E-07 X  VAP= 2.001E-07 X  VAP= 2.000E-07 X  VAP= 2.000E-07 X
X  LIQ= 0.0        X  LIQ= 0.0        X  LIQ= 0.0        X  LIQ= 0.0        X  LIQ= 0.0        X
XXXXX   0.348 XXXXXXXXX   0.232 XXXXXXXXX   0.209 XXXXXXXXX   0.005 XXXXXXXXX   0.029 XXXXX
X                   X                   X                   X                   X                   X
X      ( 2, 7)      X      ( 3, 7)      X      ( 4, 7)      X      ( 5, 7)      X      ( 6, 7)      X
X     50.109  F     X     49.964  F     X     49.957  F     X     49.777  F     X     50.089  F     X
X                   X                   X                   X                   X                   X
O       1       0.209       1       0.294       1       0.277       1       0.254       1       0.218
X  TNU= 1.000E+00 X  TNU= 1.039E+00 X  TNU= 1.024E+00 X  TNU= 1.010E+00 X  TNU= 1.004E+00 X
X  TKE= 7.111E-03 X  TKE= 1.239E-03 X  TKE= 1.050E-03 X  TKE= 1.019E-03 X  TKE= 1.007E-03 X
X  CHI= 2.144E-04 X  CHI= 1.398E-05 X  CHI= 1.004E-05 X  CHI= 9.996E-06 X  CHI= 1.000E-05 X
X  VAP= 2.000E-07 X  VAP= 2.000E-07 X  VAP= 2.000E-07 X  VAP= 1.999E-07 X  VAP= 2.000E-07 X
X  LIQ= 0.0        X  LIQ= 0.0        X  LIQ= 0.0        X  LIQ= 0.0        X  LIQ= 0.0        X
XXXXX   0.791 XXXXXXXXX   0.380 XXXXXXXXX   0.150 XXXXXXXXX  -0.045 XXXXXXXXX  -0.028 XXXXX
X                   X                   X                   X                   X                   X
X      ( 2, 6)      X      ( 3, 6)      X      ( 4, 6)      X      ( 5, 6)      X      ( 6, 6)      X
X     50.172  F     X     49.985  F     X     50.012  F     X     50.040  F     X     50.068  F     X
X                   X                   X                   X                   X                   X
O       1       0.875       1       0.756       1       0.543       1       0.430       1       0.276
X  TNU= 2.255E+00 X  TNU= 1.018E+00 X  TNU= 1.047E+00 X  TNU= 1.028E+00 X  TNU= 1.027E+00 X
X  TKE= 3.841E-01 X  TKE= 1.945E-02 X  TKE= 1.626E-03 X  TKE= 1.061E-03 X  TKE= 1.052E-03 X
X  CHI= 1.611E-02 X  CHI= 5.960E-04 X  CHI= 2.124E-05 X  CHI= 1.012E-05 X  CHI= 1.000E-05 X
X  VAP= 2.000E-07 X  VAP= 2.000E-07 X  VAP= 2.000E-07 X  VAP= 2.000E-07 X  VAP= 2.000E-07 X
X  LIQ= 0.0        X  LIQ= 0.0        X  LIQ= 0.0        X  LIQ= 0.0        X  LIQ= 0.0        X
XXXXX   2.530 XXXXXXXXX   0.153 XXXXXXXXX  -0.260 XXXXXXXXX  -0.266 XXXXXXXXX  -0.345 XXXXX
X                   X                   X                   X                   X                   X
X      ( 2, 5)      X      ( 3, 5)      X      ( 4, 5)      X      ( 5, 5)      X      ( 6, 5)      X
X     54.088  F     X     50.324  F     X     50.061  F     X     50.234  F     X     49.888  F     X
X                   X                   X                   X                   X                   X
O       1       2.009       1       1.302       1       0.711       1       0.392       1       0.180
X  TNU= 1.840E+01 X  TNU= 3.753E+00 X  TNU= 1.141E+00 X  TNU= 1.084E+00 X  TNU= 1.078E+00 X
X  TKE= 4.772E+00 X  TKE= 7.725E-01 X  TKE= 5.368E-02 X  TKE= 2.722E-03 X  TKE= 1.176E-03 X
X  CHI= 2.405E-01 X  CHI= 3.218E-02 X  CHI= 1.717E-03 X  CHI= 4.576E-05 X  CHI= 1.032E-05 X
X  VAP= 2.000E-07 X  VAP= 1.999E-07 X  VAP= 2.000E-07 X  VAP= 2.001E-07 X  VAP= 2.000E-07 X
X  LIQ= 0.0        X  LIQ= 0.0        X  LIQ= 0.0        X  LIQ= 0.0        X  LIQ= 0.0        X
XXXXX   6.566 XXXXXXXXX  -1.302 XXXXXXXXX  -1.462 XXXXXXXXX  -0.889 XXXXXXXXX  -0.738 XXXXX
X                   X                   X                   X                   X                   X
X      ( 2, 4)      X      ( 3, 4)      X      ( 4, 4)      X      ( 5, 4)      X      ( 6, 4)      X
X     61.240  F     X     50.768  F     X     49.888  F     X     49.908  F     X     49.770  F     X
X                   X                   X                   X                   X                   X
O       1      -0.536       1      -0.461       1      -0.319       1      -0.260       1      -0.157
X  TNU= 4.347E+01 X  TNU= 2.428E+01 X  TNU= 4.466E+00 X  TNU= 1.035E+00 X  TNU= 1.071E+00 X
X  TKE= 1.122E+01 X  TKE= 3.101E+00 X  TKE= 9.614E-02 X  TKE= 1.592E-03 X  TKE= 1.146E-03 X
X  CHI= 6.256E-01 X  CHI= 6.555E-02 X  CHI= 1.012E-03 X  CHI= 1.180E-05 X  CHI= 9.999E-06 X
X  VAP= 2.000E-07 X  VAP= 1.999E-07 X  VAP= 2.000E-07 X  VAP= 2.000E-07 X  VAP= 1.999E-07 X
X  LIQ= 0.0        X  LIQ= 0.0        X  LIQ= 0.0        X  LIQ= 0.0        X  LIQ= 0.0        X
XXXXX   5.434 XXXXXXXXX  -1.077 XXXXXXXXX  -1.117 XXXXXXXXX  -0.775 XXXXXXXXX  -0.582 XXXXX
X                   X                   X                   X                   X                   X
X      ( 2, 3)      X      ( 3, 3)      X      ( 4, 3)      X      ( 5, 3)      X      ( 6, 3)      X
X     49.735  F     X     50.207  F     X     49.860  F     X     49.943  F     X     50.116  F     X
X                   X                   X                   X                   X                   X
O       1      -2.248       1      -1.472       1      -0.924       1      -0.626       1      -0.426
X  TNU= 3.361E+00 X  TNU= 3.074E+00 X  TNU= 1.050E+00 X  TNU= 1.151E+00 X  TNU= 1.073E+00 X
X  TKE= 8.053E-01 X  TKE= 2.349E-01 X  TKE= 5.556E-03 X  TKE= 1.337E-03 X  TKE= 1.148E-03 X
X  CHI= 1.297E-02 X  CHI= 3.665E-03 X  CHI= 4.321E-05 X  CHI= 1.004E-05 X  CHI= 1.000E-05 X
X  VAP= 1.999E-07 X  VAP= 2.001E-07 X  VAP= 1.999E-07 X  VAP= 2.000E-07 X  VAP= 2.000E-07 X
X  LIQ= 0.0        X  LIQ= 0.0        X  LIQ= 0.0        X  LIQ= 0.0        X  LIQ= 0.0        X
XXXXX   1.012 XXXXXXXXX   0.435 XXXXXXXXX  -0.102 XXXXXXXXX  -0.217 XXXXXXXXX  -0.154 XXXXX
X                   X                   X                   X                   X                   X
X      ( 2, 2)      X      ( 3, 2)      X      ( 4, 2)      X      ( 5, 2)      X      ( 6, 2)      X
X     49.659  F     X     49.999  F     X     49.957  F     X     49.915  F     X     49.964  F     X
X                   X                   X                   X                   X                   X
O       1      -0.492       1      -0.710       1      -0.678       1      -0.583       1      -0.50
X  TNU= 1.008E+00 X  TNU= 1.000E+00 X  TNU= 1.147E+00 X  TNU= 1.068E+00 X  TNU= 1.038E+00 X
X  TKE= 4.085E-03 X  TKE= 1.958E-03 X  TKE= 1.323E-03 X  TKE= 1.139E-03 X  TKE= 1.075E-03 X
X  CHI= 2.747E-05 X  CHI= 1.101E-05 X  CHI= 1.005E-05 X  CHI= 9.997E-06 X  CHI= 9.999E-06 X
X  VAP= 1.999E-07 X  VAP= 2.000E-07 X  VAP= 2.000E-07 X  VAP= 2.000E-07 X  VAP= 2.000E-07 X
X  LIQ= 0.0        X  LIQ= 0.0        X  LIQ= 0.0        X  LIQ= 0.0        X  LIQ= 0.0        X
XXXXX   0.0   XXXXXXXXX   0.0   XXXXXXXXX   0.0   XXXXXXXXX   0.0   XXXXXXXXX   0.0   XXXXX
```

Fig. 5.2.1.3 Plume Cross Section at 20 sec.
DY = 100 ft, DZ = 200 ft.
Disregard moisture values.

```
XXXXX   2.792 XXXXXXXXX   1.C4C XXXXXXXXX   0.609 XXXXXXXXX   0.168 XXXXXXXXX  -0.170 XXXXX
X             X                 X                 X                 X                 X
X   ( 2, 8)   X    ( 3, 8)      X    ( 4, 8)      X    ( 5, 8)      X    ( 6, 8)      X
X  50.809  F  X   5C.137  F     X   50.082  F     X   49.999  F     X   49.936  F     X
X             X                 X                 X                 X                 X
O     1     1.592     1     1.860     1     1.585     1     1.118     1     0.843
X TNU= 5.087E+00 X TNU= 2.169E+00 X TNU= 1.658E+00 X TNU= 2.012E+CC X TNU= 1.370E+CC X
X TKE= 4.702E-01 X TKE= 1.135E-01 X TKE= 2.026E-02 X TKE= 6.234E-C3 X TKE= 2.047E-C3 X
X CHI= 4.895E-02 X CHI= 1.078E-02 X CHI= 1.448E-03 X CHI= 1.383E-C4 X CHI= 1.682E-C5 X
X VAP= 2.000E-07 X VAP= 2.000E-07 X VAP= 2.000E-07 X VAP= 2.000E-07 X VAP= 2.000E-C7 X
X LIQ= 0.0       X LIQ= 0.0       X LIQ= 0.0       X LIQ= 0.0       X LIQ= 0.0       X
XXXXX   5.963 XXXXXXXXX   1.573 XXXXXXXXX   0.074 XXXXXXXXX  -0.752 XXXXXXXXX  -0.714 XXXXX
X             X                 X                 X                 X                 X
X   ( 2, 7)   X    ( 3, 7)      X    ( 4, 7)      X    ( 5, 7)      X    ( 6, 7)      X
X  52.397  F  X   50.927  F     X   50.165  F     X   49.888  F     X   49.999  F     X
X             X                 X                 X                 X                 X
O     1     1.790     1     2.327     1     1.898     1     1.345     1     0.966
X TNU= 1.364E+01 X TNU= 6.094E+00 X TNU= 2.564E+00 X TNU= 1.746E+CC X TNU= 1.560E+CC X
X TKE= 1.420E+00 X TKE= 5.864E-01 X TKE= 1.550E-01 X TKE= 3.042E-02 X TKE= 5.690E-C3 X
X CHI= 1.422E-01 X CHI= 5.942E-02 X CHI= 1.527E-02 X CHI= 2.390E-03 X CHI= 2.289E-C4 X
X VAP= 2.000E-07 X VAP= 2.000E-07 X VAP= 2.000E-07 X VAP= 1.999E-07 X VAP= 2.000E-C7 X
X LIQ= 0.0       X LIQ= 0.0       X LIQ= 0.0       X LIQ= 0.0       X LIQ= 0.0       X
XXXXX   9.535 XXXXXXXXX   2.644 XXXXXXXXX  -0.778 XXXXXXXXX  -1.852 XXXXXXXXX  -1.471 XXXXX
X             X                 X                 X                 X                 X
X   ( 2, 6)   X    ( 3, 6)      X    ( 4, 6)      X    ( 5, 6)      X    ( 6, 6)      X
X  52.903  F  X   51.870  F     X   50.733  F     X   50.137  F     X   50.006  F     X
X             X                 X                 X                 X                 X
O     1     0.651     1     1.127     1     0.740     1     C.562     1     0.313
X TNU= 1.802E+01 X TNU= 1.130E+01 X TNU= 4.335E+00 X TNU= 1.775E+CC X TNU= 1.98CE+0C X
X TKE= 1.815E+00 X TKE= 1.200E+00 X TKE= 3.780E-01 X TKE= 7.838E-02 X TKE= 1.715E-C2 X
X CHI= 1.763E-01 X CHI= 1.146E-01 X CHI= 4.295E-02 X CHI= 8.167E-03 X CHI= 9.445E-04 X
X VAP= 1.999E-07 X VAP= 2.000E-07 X VAP= 2.000E-07 X VAP= 2.000E-07 X VAP= 2.000E-07 X
X LIQ= 0.0       X LIQ= 0.0       X LIQ= 0.0       X LIQ= 0.0       X LIQ= 0.0       X
XXXXX  10.833 XXXXXXXXX   3.637 XXXXXXXXX  -1.545 XXXXXXXXX  -2.236 XXXXXXXXX  -1.998 XXXXX
X             X                 X                 X                 X                 X
X   ( 2, 5)   X    ( 3, 5)      X    ( 4, 5)      X    ( 5, 5)      X    ( 6, 5)      X
X  52.119  F  X   51.607  F     X   50.324  F     X   50.096  F     X   49.943  F     X
X             X                 X                 X                 X                 X
O     1    -1.157     1    -1.622     1    -1.372     1    -C.988     1    -0.833
X TNU= 1.677E+01 X TNU= 1.198E+01 X TNU= 2.832E+00 X TNU= 1.397E+0C X TNU= 1.922E+CC X
X TKE= 1.643E+00 X TKE= 1.242E+00 X TKE= 2.058E-01 X TKE= 3.337E-C2 X TKE= 8.061E-03 X
X CHI= 1.300E-01 X CHI= 1.046E-01 X CHI= 2.520E-02 X CHI= 2.410E-03 X CHI= 1.479E-C4 X
X VAP= 2.000E-07 X VAP= 1.999E-07 X VAP= 2.000E-07 X VAP= 2.000E-07 X VAP= 2.000E-C7 X
X LIQ= 0.0       X LIQ= 0.0       X LIQ= 0.0       X LIQ= 0.0       X LIQ= 0.0       X
XXXXX   8.533 XXXXXXXXX   2.676 XXXXXXXXX  -1.061 XXXXXXXXX  -1.458 XXXXXXXXX  -1.665 XXXXX
X             X                 X                 X                 X                 X
X   ( 2, 4)   X    ( 3, 4)      X    ( 4, 4)      X    ( 5, 4)      X    ( 6, 4)      X
X  50.858  F  X   50.394  F     X   50.061  F     X   49.902  F     X   49.811  F     X
X             X                 X                 X                 X                 X
O     1    -1.958     1    -2.552     1    -2.173     1    -1.733     1    -1.269
X TNU= 1.359E+01 X TNU= 1.141E+01 X TNU= 4.348E+00 X TNU= 2.004E+00 X TNU= 2.577E+CC X
X TKE= 1.267E+00 X TKE= 8.776E-01 X TKE= 1.592E-01 X TKE= 1.617E-02 X TKE= 8.188E-03 X
X CHI= 5.792E-02 X CHI= 3.061E-02 X CHI= 8.101E-03 X CHI= 5.101E-04 X CHI= 2.975E-C5 X
X VAP= 2.000E-07 X VAP= 2.CC0E-07 X VAP= 2.000E-07 X VAP= 2.000E-07 X VAP= 1.999E-07 X
X LIQ= 0.0       X LIQ= 0.0       X LIQ= 0.0       X LIQ= 0.0       X LIQ= 0.0       X
XXXXX   4.668 XXXXXXXXX   1.477 XXXXXXXXX  -0.350 XXXXXXXXX  -0.614 XXXXXXXXX  -0.739 XXXXX
X             X                 X                 X                 X                 X
X   ( 2, 3)   X    ( 3, 3)      X    ( 4, 3)      X    ( 5, 3)      X    ( 6, 3)      X
X  49.978  F  X   49.735  F     X   49.714  F     X   49.936  F     X   50.103  F     X
X             X                 X                 X                 X                 X
O     1    -1.689     1    -1.970     1    -1.765     1    -1.500     1    -1.166
X TNU= 5.732E+00 X TNU= 3.192E+00 X TNU= 2.453E+00 X TNU= 2.150E+0C X TNU= 2.20CE+CC X
X TKE= 4.311E-01 X TKE= 1.307E-01 X TKE= 4.032E-02 X TKE= 7.152E-03 X TKE= 5.154E-C3 X
X CHI= 6.642E-03 X CHI= 2.758E-03 X CHI= 9.150E-04 X CHI= 5.188E-05 X CHI= 1.138E-05 X
X VAP= 2.000E-07 X VAP= 1.999E-07 X VAP= 1.999E-07 X VAP= 2.000E-07 X VAP= 2.00CE-C7 X
X LIQ= 0.0       X LIQ= 0.0       X LIQ= 0.0       X LIQ= 0.0       X LIQ= 0.0       X
XXXXX   1.202 XXXXXXXXX   0.886 XXXXXXXXX   0.151 XXXXXXXXX   0.018 XXXXXXXXX  -0.036 XXXXX
X             X                 X                 X                 X                 X
X   ( 2, 2)   X    ( 3, 2)      X    ( 4, 2)      X    ( 5, 2)      X    ( 6, 2)      X
X  49.583  F  X   50.061  F     X   50.089  F     X   49.985  F     X   49.874  F     X
X             X                 X                 X                 X                 X
O     1    -0.619     1    -1.082     1    -1.137     1    -1.113     1    -1.078
X TNU= 2.115E+00 X TNU= 2.726E+00 X TNU= 3.230E+00 X TNU= 2.270E+CC X TNU= 1.936E+0C X
X TKE= 2.472E-02 X TKE= 1.924E-02 X TKE= 1.210E-02 X TKE= 5.171E-C3 X TKE= 3.723E-C3 X
X CHI= 7.881E-05 X CHI= 2.391E-05 X CHI= 1.320E-05 X CHI= 1.038E-05 X CHI= 1.001E-05 X
X VAP= 1.998E-07 X VAP= 2.000E-07 X VAP= 2.000E-07 X VAP= 2.000E-07 X VAP= 1.999E-C7 X
X LIQ= 0.0       X LIQ= 0.0       X LIQ= 0.0       X LIQ= 0.0       X LIQ= 0.0       X
XXXXX   0.0   XXXXXXXXX   0.0   XXXXXXXXX   0.0   XXXXXXXXX   0.0   XXXXXXXXX   0.0   XXXXX
```

Fig. 5.2.1.4 Plume Cross Section at 80 sec.
DY = 100 ft, DZ = 200 ft.
Disregard moisture values.

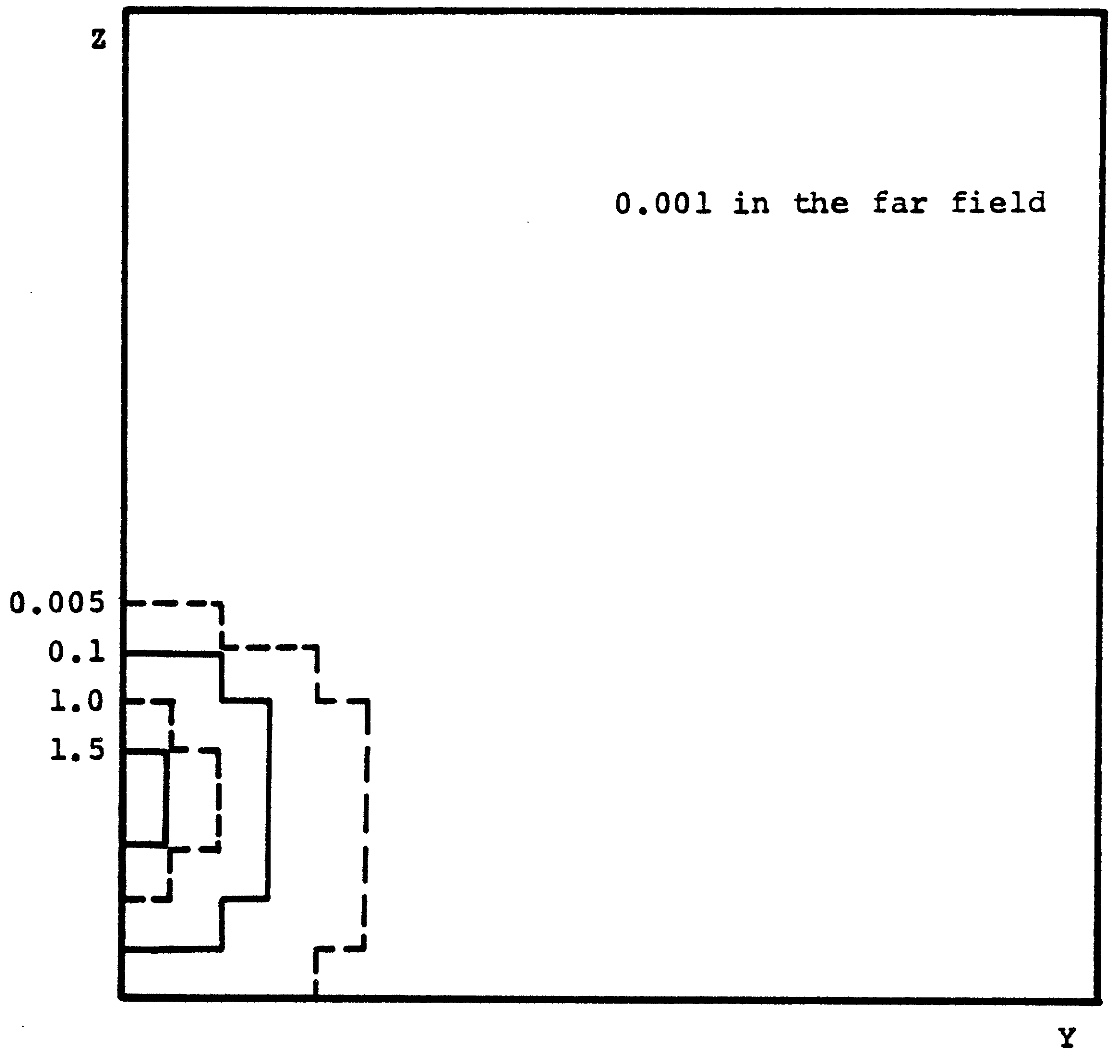

Fig. 5.2.1.5 Turbulence Kinetic Energy Profile at 80 sec. Contours of TKE in ft^2/sec^2. The maximum TKE is 1.82 ft^2/sec^2, and the minimum TKE is 0.001 ft^2/sec^2 (throughout the far field).

```
XXXXX   4.626 XXXXXXXXX   2.064 XXXXXXXXX   0.917 XXXXXXXXX   0.397 XXXXXXXXX   0.014 XXXXX
X                 X                 X                 X                 X                 X
X     ( 2,12)     X     ( 3,12)     X     ( 4,12)     X     ( 5,12)     X     ( 6,12)     X
X    50.588  F    X    50.255  F    X    50.047  F    X    49.950  F    X    49.929  F    X
X                 X                 X                 X                 X                 X
0       1       1.270     1       2.036     1       2.201     1       2.037     1       1.739
X  TNU= 8.396E+00 X  TNU= 6.390E+00 X  TNU= 4.089E+00 X  TNU= 2.994E+00 X  TNU= 2.371E+00 X
X  TKE= 5.049E-01 X  TKE= 3.143E-01 X  TKE= 1.147E-01 X  TKE= 3.513E-02 X  TKE= 1.140E-02 X
X  CHI= 3.858E-02 X  CHI= 1.840E-02 X  CHI= 6.147E-03 X  CHI= 1.435E-03 X  CHI= 2.628E-04 X
X  VAP= 3.857E-02 X  VAP= 1.839E-02 X  VAP= 6.137E-03 X  VAP= 1.425E-03 X  VAP= 2.528E-04 X
X  LIQ= 7.714E-02 X  LIQ= 3.678E-02 X  LIQ= 1.228E-02 X  LIQ= 2.850E-03 X  LIQ= 5.056E-04 X
XXXXX   7.165 XXXXXXXXX   3.601 XXXXXXXXX   1.249 XXXXXXXXX  -0.067 XXXXXXXXX  -0.586 XXXXX
X                 X                 X                 X                 X                 X
X     ( 2,11)     X     ( 3,11)     X     ( 4,11)     X     ( 5,11)     X     ( 6,11)     X
X    50.990  F    X    50.699  F    X    50.352  F    X    50.144  F    X    50.012  F    X
X                 X                 X                 X                 X                 X
0       1       1.191     1       2.153     1       2.442     1       2.207     1       1.784
X  TNU= 1.321E+01 X  TNU= 1.106E+01 X  TNU= 6.546E+00 X  TNU= 4.055E+00 X  TNU= 2.917E+00 X
X  TKE= 8.242E-01 X  TKE= 7.557E-01 X  TKE= 3.537E-01 X  TKE= 1.313E-01 X  TKE= 4.229E-02 X
X  CHI= 6.519E-02 X  CHI= 4.620E-02 X  CHI= 2.292E-02 X  CHI= 8.101E-03 X  CHI= 2.071E-03 X
X  VAP= 6.518E-02 X  VAP= 4.620E-02 X  VAP= 2.291E-02 X  VAP= 8.091E-03 X  VAP= 2.061E-03 X
X  LIQ= 1.304E-01 X  LIQ= 9.239E-02 X  LIQ= 4.582E-02 X  LIQ= 1.618E-02 X  LIQ= 4.123E-03 X
XXXXX   9.549 XXXXXXXXX   5.520 XXXXXXXXX   1.825 XXXXXXXXX  -0.401 XXXXXXXXX  -1.429 XXXXX
X                 X                 X                 X                 X                 X
X     ( 2,10)     X     ( 3,10)     X     ( 4,10)     X     ( 5,10)     X     ( 6,10)     X
X    51.031  F    X    50.962  F    X    50.560  F    X    50.186  F    X    49.999  F    X
X                 X                 X                 X                 X                 X
0       1       0.616     1       1.358     1       1.676     1       1.520     1       1.199
X  TNU= 1.373E+01 X  TNU= 1.449E+01 X  TNU= 9.508E+00 X  TNU= 5.302E+00 X  TNU= 3.155E+00 X
X  TKE= 8.007E-01 X  TKE= 1.077E+00 X  TKE= 6.129E-01 X  TKE= 2.499E-01 X  TKE= 8.170E-02 X
X  CHI= 6.982E-02 X  CHI= 6.276E-02 X  CHI= 3.956E-02 X  CHI= 1.769E-02 X  CHI= 5.453E-03 X
X  VAP= 6.982E-02 X  VAP= 6.275E-02 X  VAP= 3.955E-02 X  VAP= 1.768E-02 X  VAP= 5.443E-03 X
X  LIQ= 1.396E-01 X  LIQ= 1.255E-01 X  LIQ= 7.910E-02 X  LIQ= 3.536E-02 X  LIQ= 1.089E-02 X
XXXXX  10.783 XXXXXXXXX   7.009 XXXXXXXXX   2.458 XXXXXXXXX  -0.720 XXXXXXXXX  -2.077 XXXXX
X                 X                 X                 X                 X                 X
X     ( 2, 9)     X     ( 3, 9)     X     ( 4, 9)     X     ( 5, 9)     X     ( 6, 9)     X
X    50.837  F    X    50.934  F    X    50.657  F    X    50.269  F    X    50.006  F    X
X                 X                 X                 X                 X                 X
0       1      -0.008     1       0.230     1       0.396     1       0.339     1       0.298
X  TNU= 1.243E+01 X  TNU= 1.430E+01 X  TNU= 1.031E+01 X  TNU= 5.267E+00 X  TNU= 2.875E+00 X
X  TKE= 6.941E-01 X  TKE= 1.077E+00 X  TKE= 6.959E-01 X  TKE= 2.578E-01 X  TKE= 7.728E-02 X
X  CHI= 6.017E-02 X  CHI= 6.223E-02 X  CHI= 4.516E-02 X  CHI= 2.060E-02 X  CHI= 6.351E-03 X
X  VAP= 6.016E-02 X  VAP= 6.222E-02 X  VAP= 4.515E-02 X  VAP= 2.059E-02 X  VAP= 6.341E-03 X
X  LIQ= 1.203E-01 X  LIQ= 1.245E-01 X  LIQ= 9.030E-02 X  LIQ= 4.117E-02 X  LIQ= 1.268E-02 X
XXXXX  10.763 XXXXXXXXX   7.474 XXXXXXXXX   2.795 XXXXXXXXX  -0.823 XXXXXXXXX  -2.149 XXXXX
X                 X                 X                 X                 X                 X
X     ( 2, 8)     X     ( 3, 8)     X     ( 4, 8)     X     ( 5, 8)     X     ( 6, 8)     X
X    50.636  F    X    50.754  F    X    50.539  F    X    50.179  F    X    50.026  F    X
X                 X                 X                 X                 X                 X
0       1      -0.501     1      -0.884     1      -0.849     1      -0.739     1      -0.602
X  TNU= 1.112E+01 X  TNU= 1.154E+01 X  TNU= 8.778E+00 X  TNU= 4.489E+00 X  TNU= 2.716E+00 X
X  TKE= 6.304E-01 X  TKE= 8.211E-01 X  TKE= 5.674E-01 X  TKE= 1.970E-01 X  TKE= 6.111E-02 X
X  CHI= 4.694E-02 X  CHI= 5.021E-02 X  CHI= 4.157E-02 X  CHI= 1.996E-02 X  CHI= 6.007E-03 X
X  VAP= 4.693E-02 X  VAP= 5.020E-02 X  VAP= 4.156E-02 X  VAP= 1.995E-02 X  VAP= 5.997E-03 X
X  LIQ= 9.386E-02 X  LIQ= 1.004E-01 X  LIQ= 8.310E-02 X  LIQ= 3.991E-02 X  LIQ= 1.199E-02 X
XXXXX   9.763 XXXXXXXXX   6.718 XXXXXXXXX   2.861 XXXXXXXXX  -0.613 XXXXXXXXX  -1.882 XXXXX
X                 X                 X                 X                 X                 X
X     ( 2, 7)     X     ( 3, 7)     X     ( 4, 7)     X     ( 5, 7)     X     ( 6, 7)     X
X    50.408  F    X    50.498  F    X    50.442  F    X    50.165  F    X    49.971  F    X
X                 X                 X                 X                 X                 X
0       1      -0.865     1      -1.592     1      -1.882     1      -1.710     1      -1.444
X  TNU= 9.805E+00 X  TNU= 8.357E+00 X  TNU= 5.846E+00 X  TNU= 3.547E+00 X  TNU= 2.685E+00 X
X  TKE= 5.612E-01 X  TKE= 5.329E-01 X  TKE= 3.141E-01 X  TKE= 1.221E-01 X  TKE= 4.248E-02 X
X  CHI= 3.381E-02 X  CHI= 3.368E-02 X  CHI= 2.736E-02 X  CHI= 1.410E-02 X  CHI= 3.847E-03 X
X  VAP= 3.381E-02 X  VAP= 3.367E-02 X  VAP= 2.735E-02 X  VAP= 1.409E-02 X  VAP= 3.837E-03 X
X  LIQ= 6.760E-02 X  LIQ= 6.732E-02 X  LIQ= 5.470E-02 X  LIQ= 2.818E-02 X  LIQ= 7.675E-03 X
XXXXX   8.017 XXXXXXXXX   5.265 XXXXXXXXX   [illegible] XXXXXXXXX  -0.257 XXXXXXXXX  -1.348 XXXXX
X                 X                 X                 X                 X                 X
X     ( 2, 6)     X     ( 3, 6)     X     ( 4, 6)     X     ( 5, 6)     X     ( 6, 6)     X
X    50.269  F    X    50.151  F    X    50.033  F    X    49.964  F    X    49.950  F    X
X                 X                 X                 X                 X                 X
0       1      -1.128     1      -1.997     1      -2.373     1      -2.180     1      -1.849
X  TNU= 8.597E+00 X  TNU= 6.132E+00 X  TNU= 4.005E+00 X  TNU= 3.181E+00 X  TNU= 3.128E+00 X
X  TKE= 4.803E-01 X  TKE= 3.263E-01 X  TKE= 1.464E-01 X  TKE= 6.664E-02 X  TKE= 3.131E-02 X
X  CHI= 2.207E-02 X  CHI= 1.786E-02 X  CHI= 1.155E-02 X  CHI= 5.717E-03 X  CHI= 1.660E-03 X
X  VAP= 2.206E-02 X  VAP= 1.785E-02 X  VAP= 1.154E-02 X  VAP= 5.707E-03 X  VAP= 1.650E-03 X
X  LIQ= [illegible] X  LIQ= [illegible] X  LIQ= [illegible] X  LIQ= [illegible] X  LIQ= [illegible] X
XXXXX   5.366 XXXXXXXXX   3.523 XXXXXXXXX   1.523 XXXXXXXXX   [illegible] XXXXXXXXX  -0.693 XXXXX
```

Fig. 5.2.1.6 Plume Cross Section at 200 sec.
DY = 100 ft, DZ = 200 ft.
Disregard moisture values.

plume has risen 1003 feet. The warmest cell in the plume is barely 1^{O}F warmer than the surroundings, and the updraft velocity has remained constant. The plume cross section has grown considerably, and the maximum TKE has dropped by a factor of two from its value at 80 seconds.

The effect of adding an initial internal circulation to the plume cross section is developed in Figures 5.2.1.7 and 5.2.1.8. In Fig. 5.2.1.7, the initial circulation is shown. The mesh cells are not 50 ft by 50 ft, although the same size plume is initialized as in the earlier discussion. The uniform 3 ft/sec circulation pattern is simply a rough guess at the actual circulation. Simulations to 40 seconds with and without the circulation are found in Fig. 5.2.1.8. The presence of an initial circulation makes only a small difference between the runs, as seen in the selected velocity and temperature values. The initialization of all of the subsequent simulations with no initial circulation is presumed to introduce little error into the results, i.e., the dynamics are strongly affected by the buoyancy, and not by the initial circulation.

The effect of ambient atmospheric turbulence is developed in Figures 5.2.1.9 and 5.2.1.10. The initialization is the same as in Fig. 5.2.1.7 without the initial circulation, but with 50 ft square cells. In Figure 5.2.1.9, the ambient

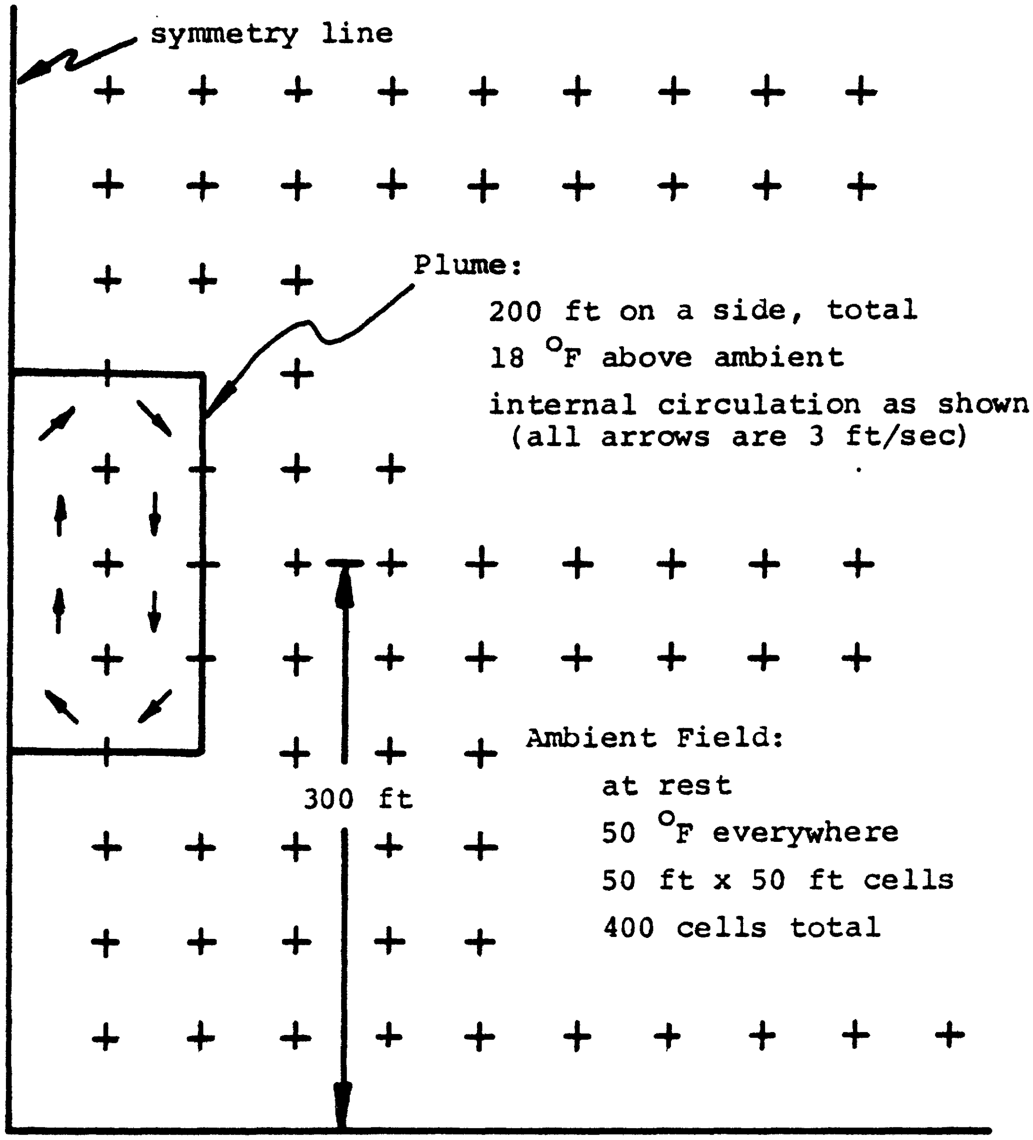

Fig. 5.2.1.7 Initialized Plume Cross Section with Internal Circulation.

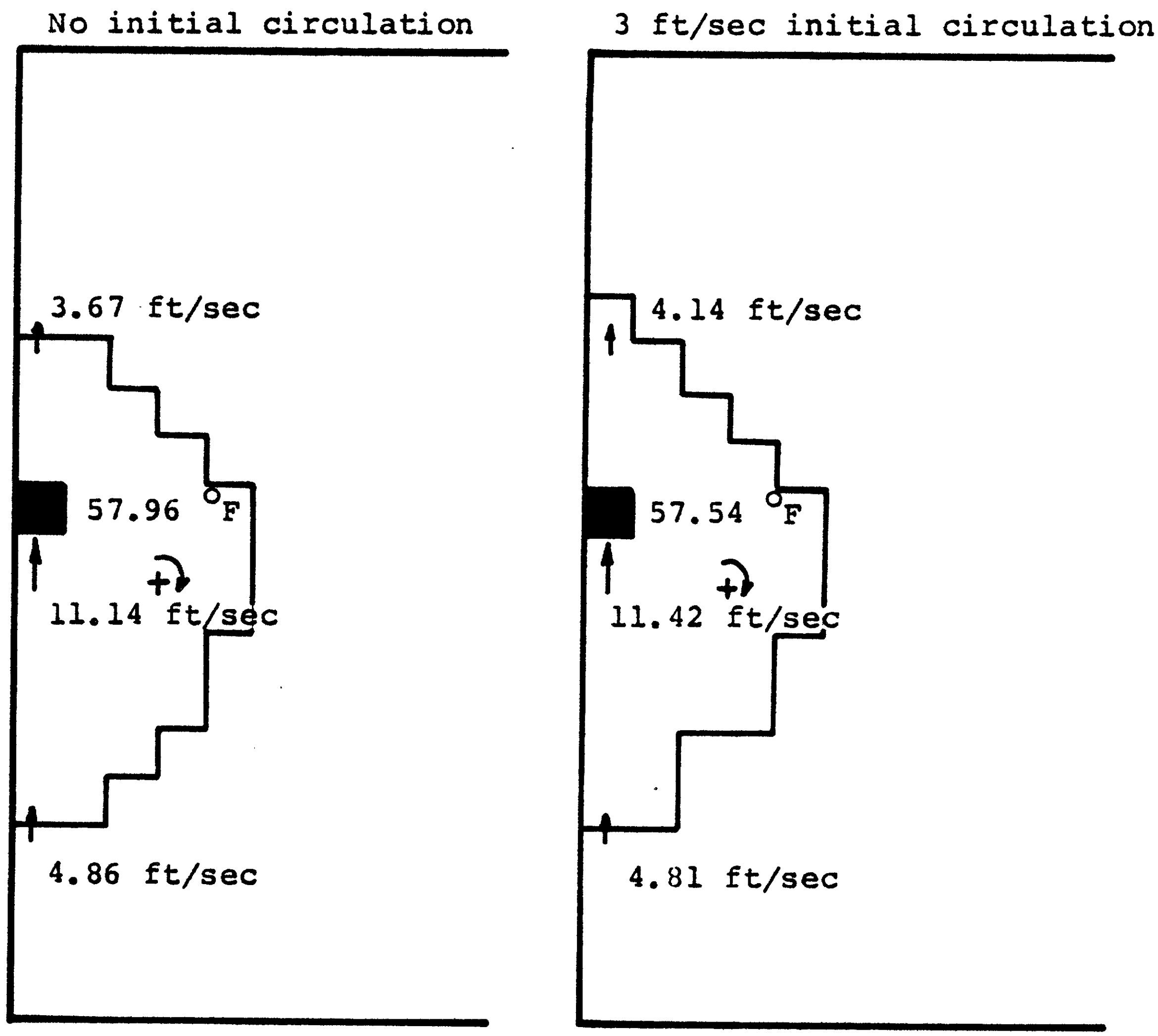

Fig. 5.2.1.8 Plume comparison at 40 sec of simulation showing the small effect of an initial circulation on the plume development.

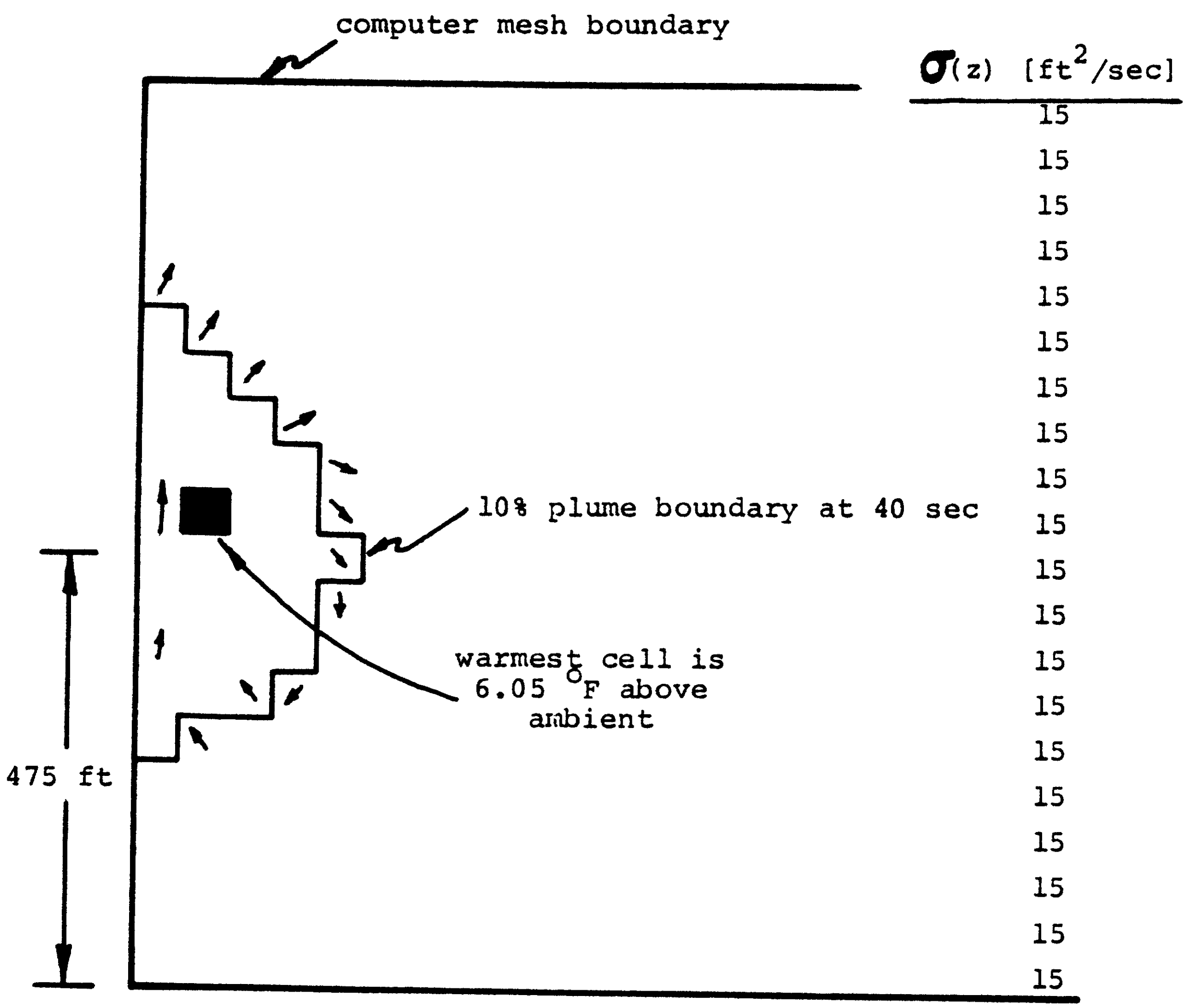

Fig. 5.2.1.9 Plume development in a moderately turbulent atmosphere. Mean flow field velocity vectors are shown.

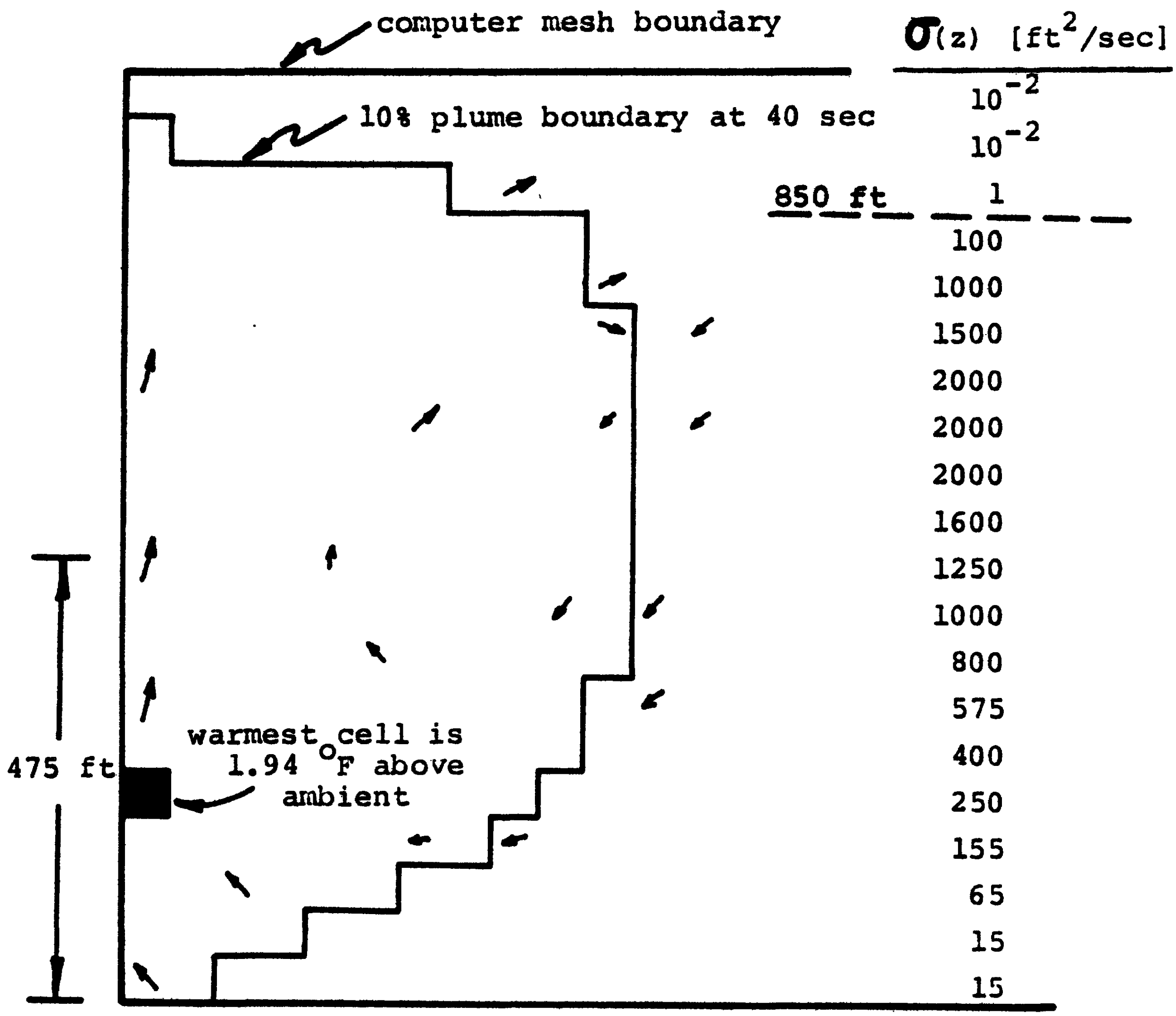

Fig. 5.2.1.10 Plume development in a very turbulent atmosphere. Mean flow field velocity vectors are shown.

eddy viscosity is maintained at a uniform 15 ft^2/sec. The resultant plume cross section at 40 seconds has developed the usual circulation, and its warmest cell is found to be 6.05°F above ambient. In strong contrast to this is the plume cross section of Fig. 5.2.1.10 which has a much stronger ambient turbulence field below 850 ft, and a much weaker turbulence field above 850 ft. The fictitious eddy viscosity profile quoted in Fig. 5.2.1.10 reflects a very turbulent boundary layer whose depth is about 850 ft. The resultant plume cross section at 40 sec is markedly different. The strong atmospheric dispersion has resulted in a much more diffuse plume whose maximum cell temperature is about one-third that of the previous run, although the plume rise is quite similar. This agrees with the notion that plume rise is dominated by the thermal stratification of the atmosphere (which is neutral in both cases here), and to a much lesser extent by other factors. Plume dispersion, which is very different in the two cases here, is affected strongly by the turbulent state of the atmosphere (which in turn is strongly affected by the thermal stratification of the atmosphere, among other factors).

The effects of using continuative outflow[68] versus free-slip solid walls for the top and right boundaries was studied. The alternative assumptions produce little difference between runs. The solid free-slip walls give more satisfactory results, although they are somewhat unrealistic physically, as are the continuative walls. Further refinement of the boundary conditions is expected to have little influence on the solutions.

5.2.2 Turbulent, Buoyant Line-Vortex Results

The results of the plume simulations in the plume dominated regime (see Fig. 5.1.1) are discussed here. To obtain these results, the ambient turbulence level should be less than one-tenth of the plume turbulence, so that the ambient turbulence will have only a small effect on the results. Plume simulations are compared to the experimental results of Richards[4] and Tsang.[33] Tsang's results are generally more accurate since his experimental technique is more sophisticated, but Richards was first to set down the basic similarity arguments.

Similarity and dimensional analyses by Richards and Tsang have revealed the formula for the plume top height, Z, versus the plume radius, R, and the formula for Z versus time, T. The concept of a virtual origin of Z and T simplifies the results in their analyses. Briefly, the virtual origin (T_*, Z_*) is the limit where the plume radius vanishes, much as if the plume had emanated from a single point at time T_*.

This is shown in Fig. 5.2.2.1, where the two formulas are quoted. Two universal constants, N and C, are found in the formulas. Tsang found that N = 3.0 and C = 1.9 provided a very good fit to dense salt water line thermals released in a tank of still, fresh water. The flow inside the line thermals is turbulent.

Tsang's results are simulated with the computer and presented in Fig. 5.2.2.2. Essentially, the virtual origin (T_*, Z_*) is free to be chosen to provide the best agreement between experimental and calculational results. The plume center height (not top height) is to be compared--the formula quoted in the figure is readily derived from the formulas in Fig. 5.2.2.1. The calculated values are represented by the points, and the experimental results (with an optimal T_* and Z_*) are represented by the solid line. Since ambient atmospheric turbulence is not important, the comparison serves to test the turbulence model by making sure that it can reproduce the self-similar plume development. The results are acceptably accurate through several hundred seconds of development. The calculated plume is found to rise a little too fast, so that a more "diffusive" turbulence model would be more accurate. The VARR turbulence constants, α, Γ, and Γ_1, were varied in an effort to accomplish this. The dissipation constant, α, was decreased tenfold to allow

$$Z - Z_* = NR \;, \quad (Z - Z_*)^{3/2} = C\left[\frac{A_o \Delta\rho\, g}{\rho}\right]^{1/2}(T - T_*)$$

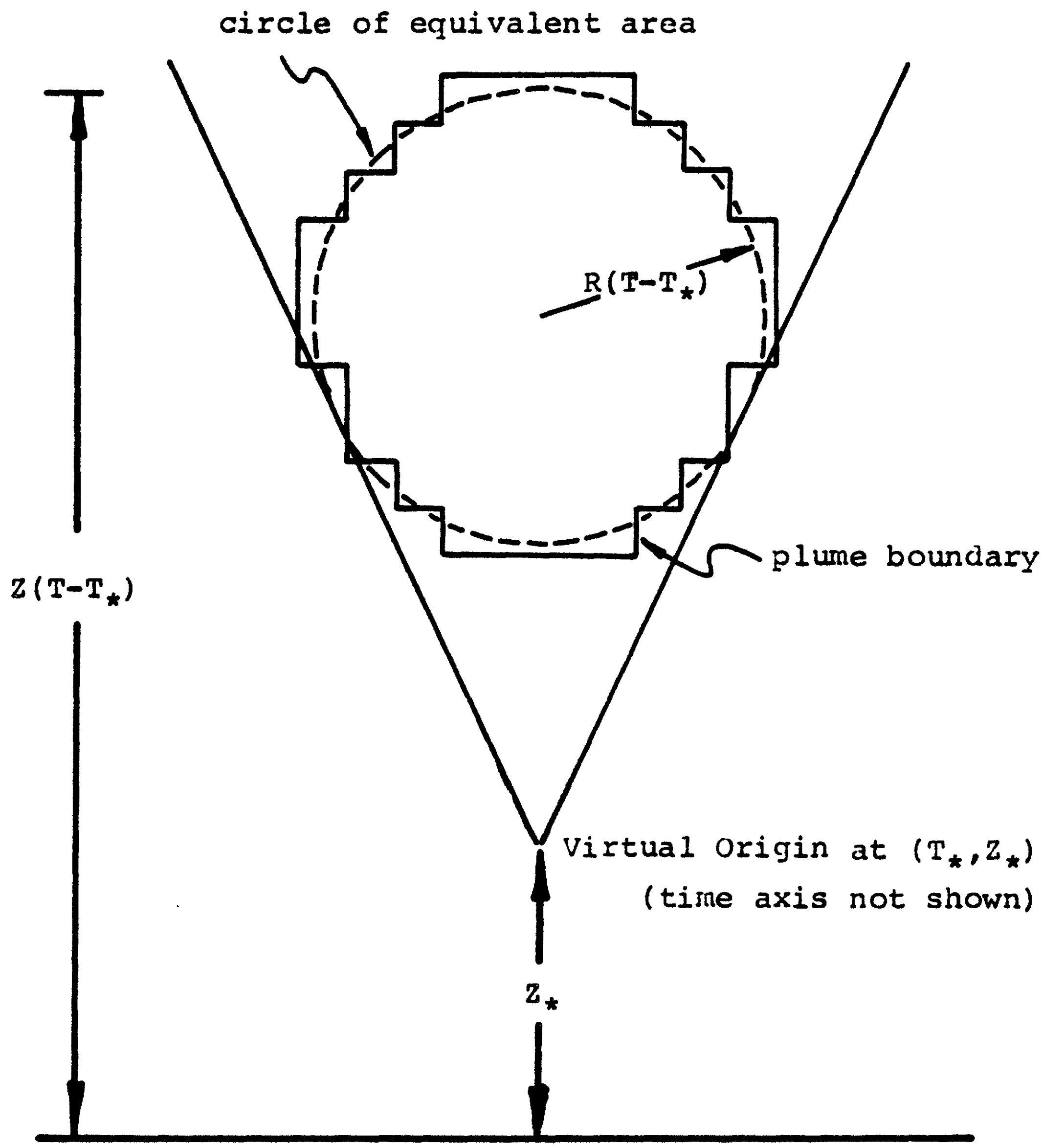

Fig. 5.2.2.1 Geometry for plume analyses.

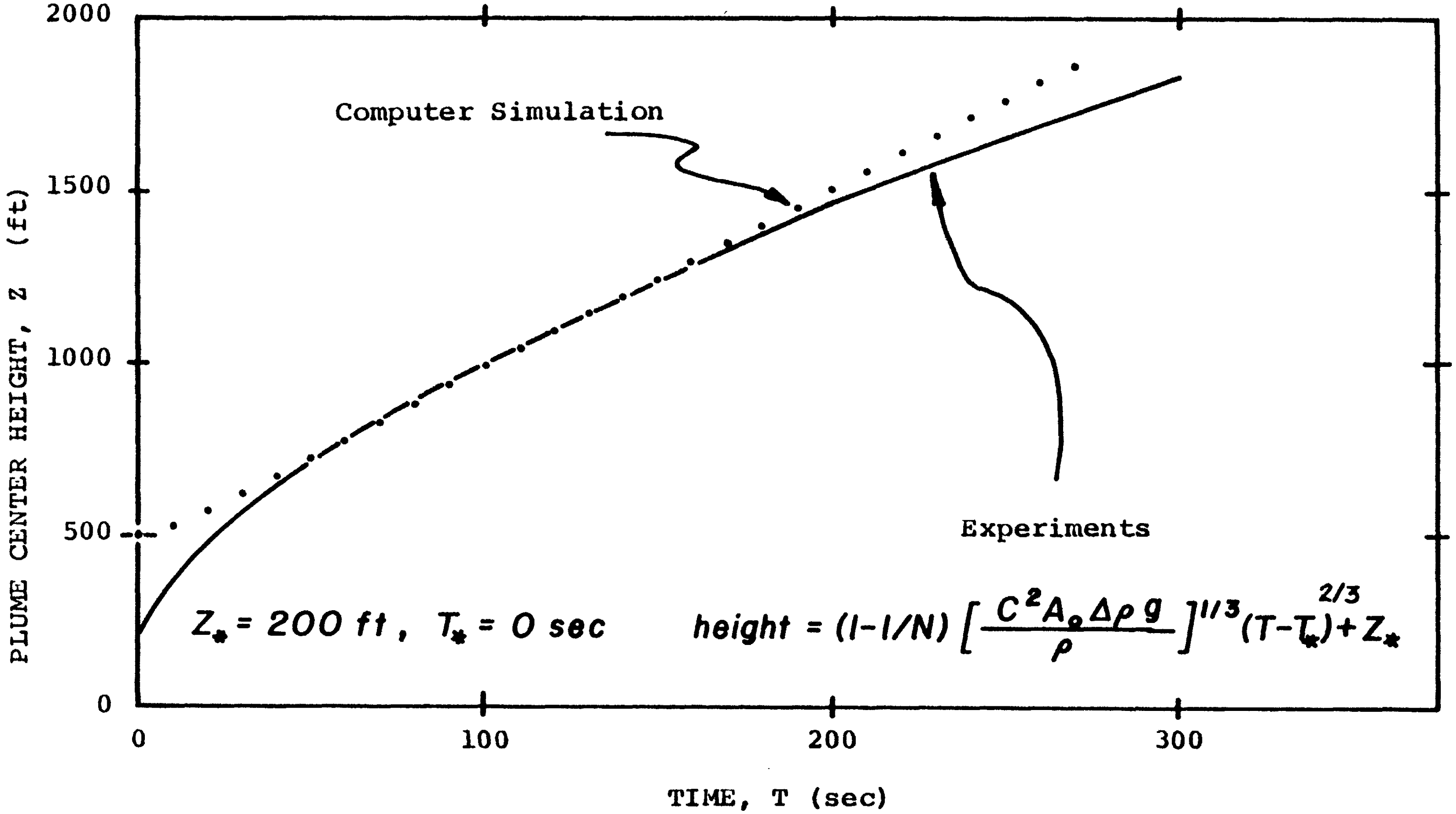

Fig. 5.2.2.2 Comparison of Computational and Experimental Results for Plume Rise versus Elapsed Time for Buoyant Line-Thermals.

the turbulence to persist with less dissipation. The turbulent transport constants, Γ and Γ_1, were increased tenfold to enhance turbulent diffusion. Alone or in any combination these variations produced little more than a 20 ft decrease of plume rise at 200 sec. Thus, these line-thermal results are largely independent of the model constants. The only term not associated with these constants (see Eq. 3.43) is the production term. It is suggested here that the production term is probably too small because it neglects buoyant production in favor of mechanical production alone. This hypothesis was not tested further in this work, however.

5.2.3 Brunt-Vaisala Period of a Turbulent, Buoyant Parcel

As a test of the hydrodynamic model, the Brunt-Vaisala period of a buoyant parcel in a stably stratified atmosphere is calculated. Briefly, the Brunt-Vaisala period is the period of the oscillation of a parcel of fluid that is perturbed from its equilibrium level in a stably stratified fluid. A consideration of the restoring force on the parcel yields the formula[69]

$$\text{Brunt-Vaisala period} = \frac{2\pi}{\sqrt{\frac{g}{T}\frac{d\theta}{dz}}} \quad [\text{sec}] \qquad (5.4)$$

For typical atmospheric values of T and $d\theta/dz$, the period is hundreds of seconds. Computer simulation to hundreds of seconds is too costly, so the stratification, $d\theta/dz$, is increased to $0.1^{o}F/ft$--about a twentyfold increase over typical atmospheric values--which decreases the predicted period to 81 sec and allows much more inexpensive simulations.

The entire computer mesh, 10^3 ft by 10^3 ft, was initialized to this stable stratification, and a warm parcel was placed at an elevation of 300 ft. The results of two different runs are shown in Fig. 5.2.3.1. In a first run, the parcel had a small buoyancy parameter:

$$\frac{F}{U} \equiv \frac{gQ_h}{\rho_s c_p T_s U} = 4.6 \times 10^3 \ ft^3/sec^2$$

which resulted in the lower curve. The curve exhibits a Brunt-Vaisala period of 92 seconds, and a fair amount of "jitteriness"--which is not surprising since the total parcel motion is much less than one cell spacing, so that the motion is not very well resolved on the mesh. In a second run, the parcel had a larger buoyancy parameter:

$$\frac{F}{U} = 4.6 \times 10^4 \ ft^3/sec^2$$

which resulted in the upper curve. The curve exhibits a Brunt-Vaisala period of 102 seconds, and a much smoother motion since several mesh cells have been traversed, and thus

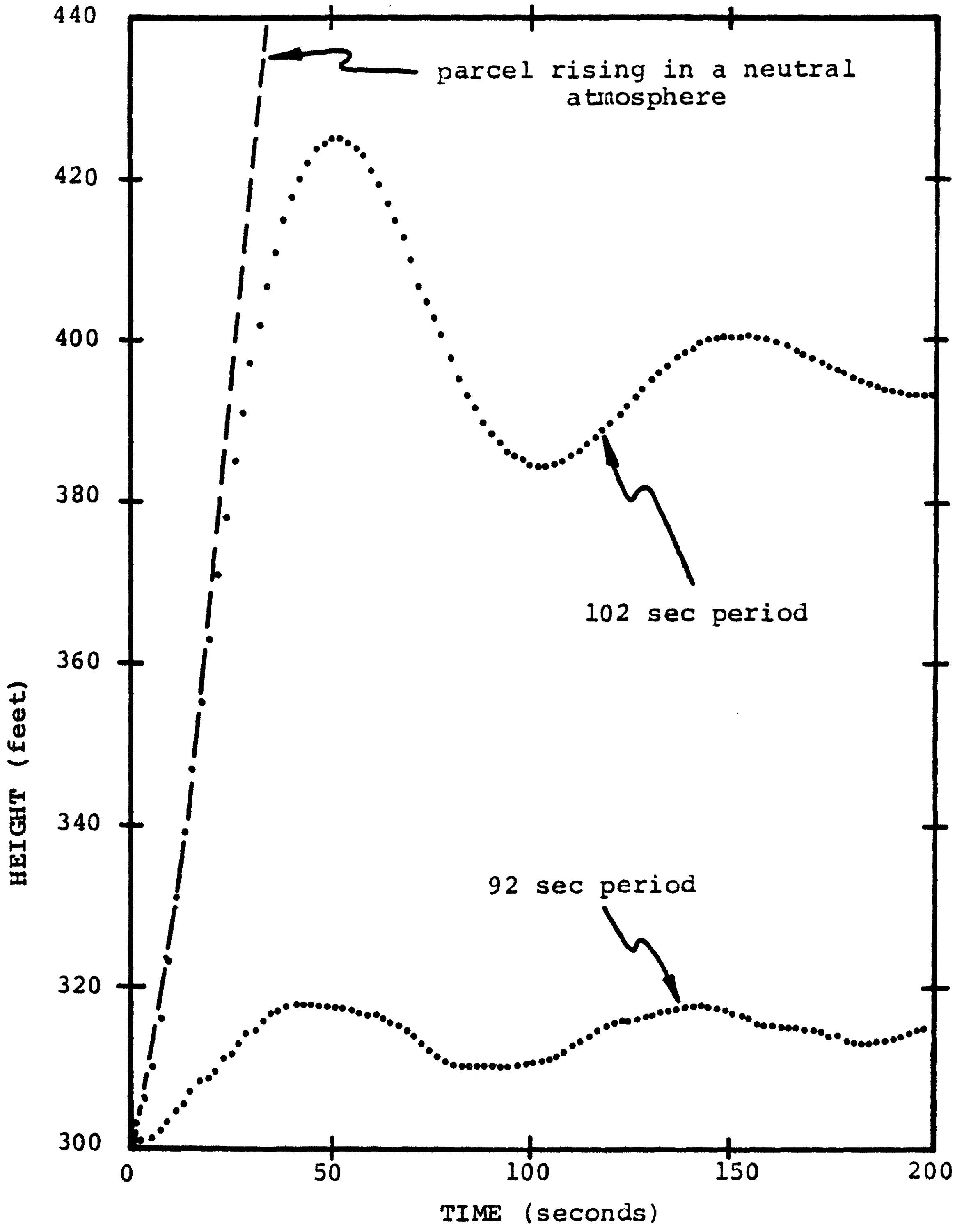

Fig. 5.2.3.1 Demonstration of the Brunt-Vaisala period. Parameters for these runs are discussed in the text.

the motion is better resolved on the mesh in this run.

Overall the agreement between calculated and observed values is good, considering that the classic Brunt-Vaisala problem allows no turbulent mixing, while the simulations in this work allow it. Generally, the action of turbulent mixing is to rapidly diffuse the temperature field and to slow the period of oscillation.

For comparison to these results, the parcel motion in a neutral atmosphere for the stronger ($F/U = 4.6 \times 10^4$ ft^3/sec^2) run has been included in Fig. 5.2.3.1. The stratification thus has a very strong effect on the motion.

5.3 Comparisons to Field Studies

5.3.1 Pasquill Dispersion and Briggs Plume Rise in Neutral Atmospheres

A comparison of plume simulation and experiments both in the plume and atmospheric dominated regimes (see Fig. 5.1.1) are discussed here for neutral atmospheres. To obtain these results, the ambient atmospheric turbulence is estimated from the discussion in Chapter Four. The plume simulations are started in the plume dominated regime and the simulations are run out to times where the plume excess temperature is very small, and the plumes are followed with the pollutant species concentration. The atmospheres in this section all have dry adiabatic lapse rates of temperature.

A comparison to Briggs'[70] plume rise for neutral atmospheres is made in Fig. 5.3.1.1. Briggs' work found that the plume rise and downwind distance, when nondimensionalized with a length L,

$$L \equiv \frac{F}{U^3} = \frac{gQ_h}{c_p \rho_s T_s U^3} \left[ft^4/sec^3 \right] \qquad (5.5)$$

yields a 2/3 power law relation between the plotted values for a wealth of field data. To interpret the data from the simulations, the plume rise is taken as the plume center height minus the virtual origin height (i.e., the rise from the virtual origin), and the downwind distance is then the product of the downwind velocity and the elapsed time from the virtual origin (see Fig. 5.2.2.1). For the run in Fig. 5.3.1.1, the distance, L, for a 1000MWt release in a 30 mph wind is 11.3 ft when calculated with Eq. 5.5. The agreement is generally good between calculation and experiment; the errors of estimation of Z, and T, and the undertainty in the ambient turbulence level all contribute to the discrepancy. Also, the data point at $x/L = 78$ is taken from the <u>initialized</u> plume cross section at time t = 0 which is <u>not</u> a physically accurate picture of the plume. The good agreement between calculation and experiment at this point is felt to be simply a cancellation of opposing errors.

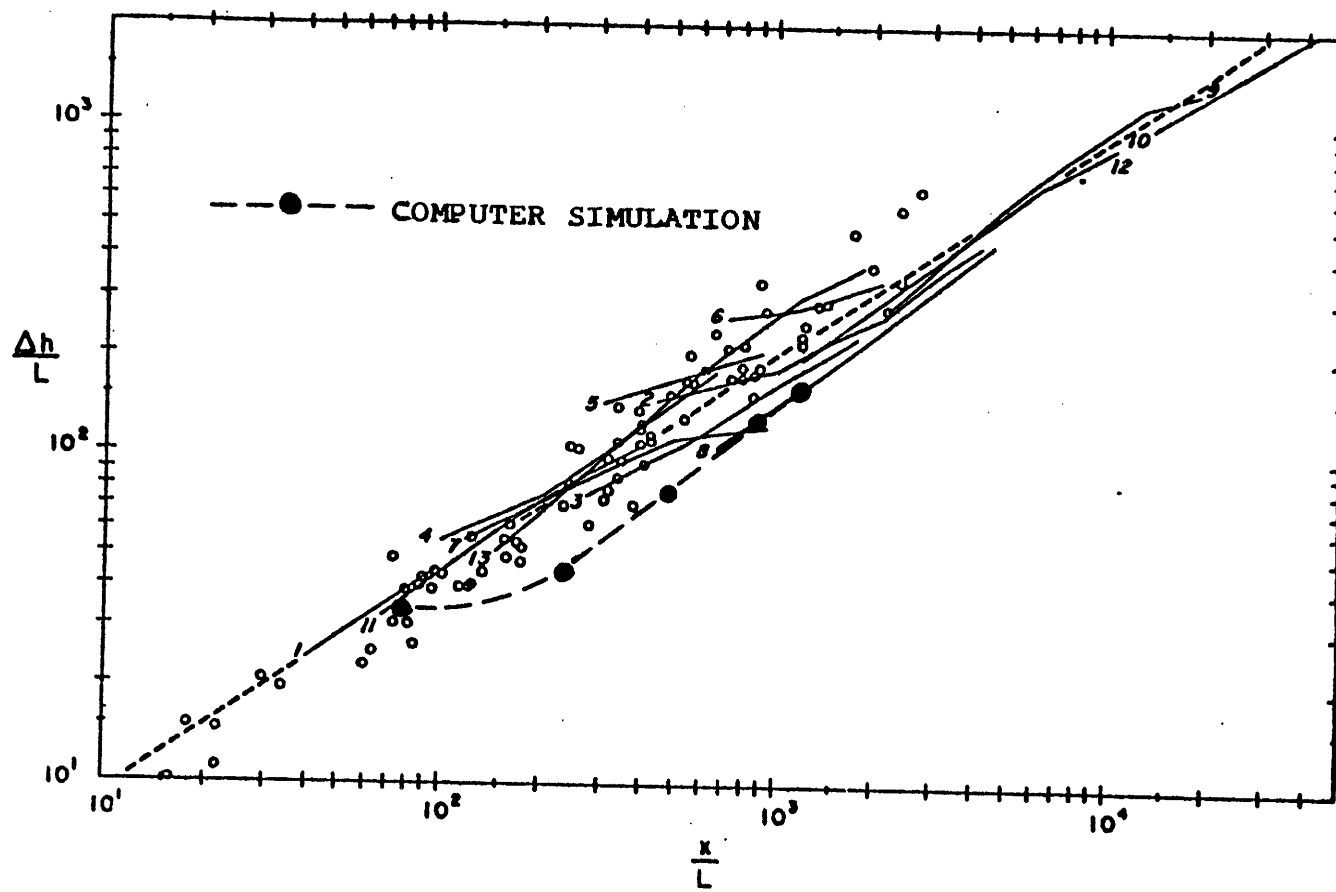

Fig. 5.3.1.1 Briggs'[70] Comparison of Plume Rise in Neutral Atmospheres Compared with a Computer Simulation of a 1000 MWt Release in a 30 mph Wind. From the analysis in the text, L = 11 ft, Δh is interpreted as $Z-Z_*$, and x is interpreted as $U(T-T_*)$.

A comparison to Pasquill's plume dispersion in neutral atmospheres (exactly the Pasquill D class) is made in Fig. 5.3.1.2. The Pasquill dispersion curves are taken from Turner's workbook[71], whose values are corrected from older sources of dispersion data. The calculated plume dispersion is taken from plume cross section printouts at four different times during the simulations. The calculated plume dispersion follows the Class D dispersion fairly well, but with a trend toward overpredicting the dispersion at points closer than the point 1/2 km downwind. This overprediction is again related to the finite plume size at time t = 0 in the initialization scheme. This error affects the earlier solution greatly, but has a decreasing effect on the solution at longer times. The error bars in the figure represent the error associated with increasing or decreasing the plume cross sectional area by one mesh cell. This gives a rough notion of the errors expected when the mesh cells are interpreted as being either entirely inside or outside of the plume. Note that these one-cell error bars decrease as the total number of cells in the plume increases with downwind distance. The trend to underpredict the dispersion at large distances reflects probable errors in the estimation of the ambient turbulence. Also note that since the turbulence is assumed to be isotropic, the calculated horizontal and vertical

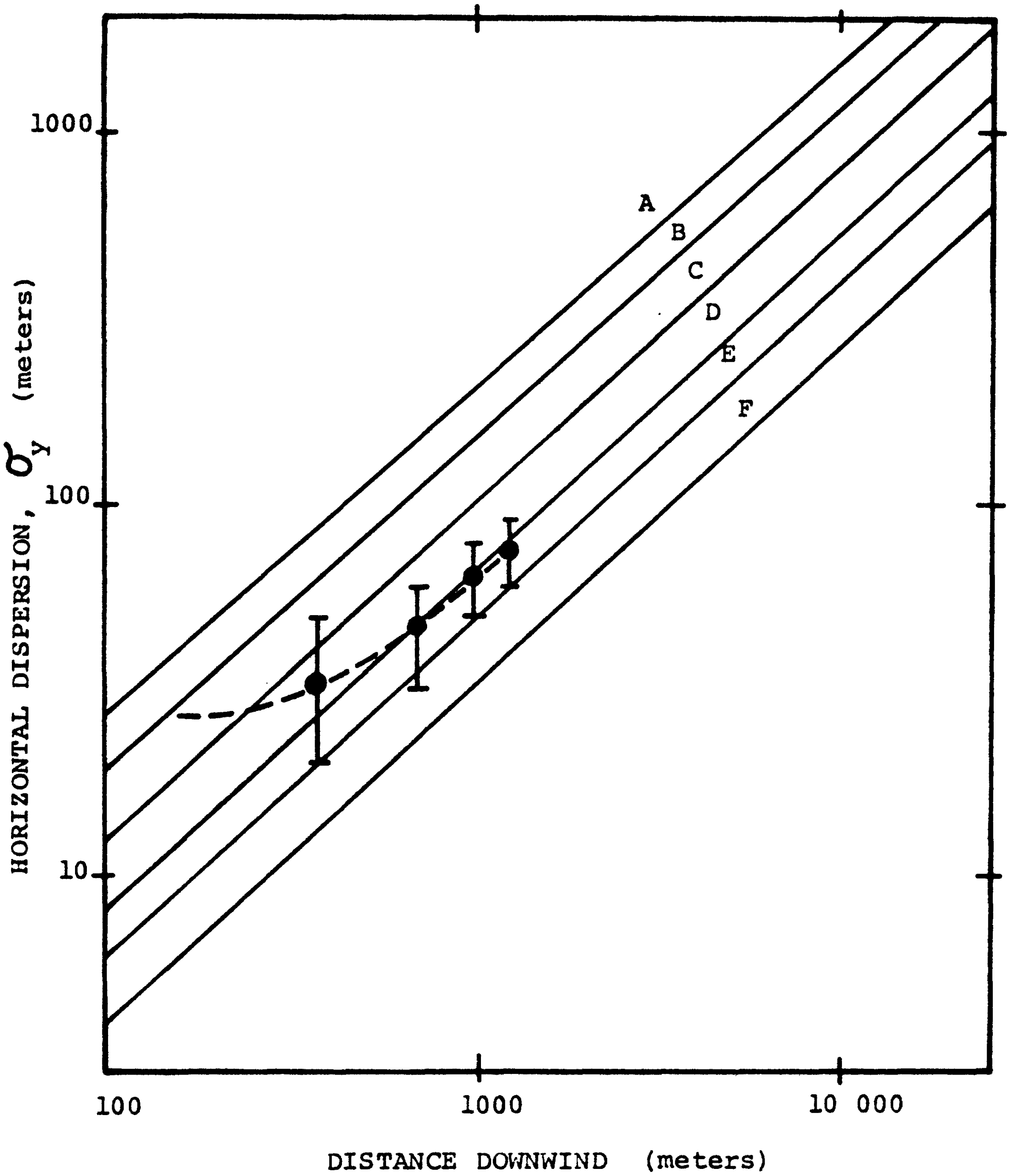

Fig. 5.3.1.2 Turner's[7] Horizontal Dispersion versus Distance Downwind Compared to a Computer Simulation of a 1000 MWt Release in a 30 mph Wind.

dispersion will not differ greatly; therefore, Pasquill dispersion cases that have significantly different σ_y's, and σ_z's (e.g., extreme stability) will be difficult for this model to duplicate.

5.3.2 LAPPES SO_2 Dispersion Studies

A number of comparisons to a well-studied plume from the LAPPES field experiments are made in this section. The plume emanating from stack No. 1 of the Keystone coal-fired generating station at about 8 a.m. on October 20, 1967 is modeled with a computer simulation. Information about the ambient weather and plant operating characteristics are provided in the LAPPES study. Experimental helicopter SO_2 plume cross sections and SO_2 bubbler data are available for comparison.

The computer simulation is initialized in Fig. 5.3.2.1 in the following way: The stack is releasing heat at 28.6×10^6 cal/sec. Half of this is to be arbitrarily put into three mesh cells that are 164 ft (50 m) high and 492 ft (150 m) wide. The other half of the heat resides in the mirror image of these cells. Using a Briggs plume rise correlation for the rise induced by the initial momentum of the effluent (20 m/sec exit velocity) yields a rise of about 100 ft. The three cells are then to be centered at the

```
XXXXX  0.0  XXXXXXXXX  0.0  XXXXXXXXX  0.0  XXXXXXXXX  0.0  XXXXXXXXX  0.0  XXXXX
X               X               X               X               X               X
X    ( 2,10)    X    ( 3,10)    X    ( 4,10)    X    ( 5,10)    X    ( 6,10)    X
X   49.902  F   X   49.902  F   X   49.902  F   X   49.902  F   X   49.902  F   X
X               X               X               X               X               X
0     1      0.0     1      0.0     1      0.0     1      0.0     1      0.0
X TNU= 2.741E+02 X TNU= 2.741E+02 X TNU= 2.741E+02 X TNU= 2.741E+02 X TNU= 2.741E+02 X
X TKE= 2.741E+00 X TKE= 2.741E+00 X TKE= 2.741E+00 X TKE= 2.741E+00 X TKE= 2.741E+00 X
X CHI= 5.293E-03 X CHI= 5.293E-03 X CHI= 5.293E-03 X CHI= 5.293E-03 X CHI= 5.293E-03 X
X VAP= 0.0       X VAP= 0.0       X VAP= 0.0       X VAP= 0.0       X VAP= 0.0       X
X LIQ= 0.0       X LIQ= 0.0       X LIQ= 0.0       X LIQ= 0.0       X LIQ= 0.0       X
XXXXX  0.0  XXXXXXXXX  0.0  XXXXXXXXX  0.0  XXXXXXXXX  0.0  XXXXXXXXX  0.0  XXXXX
X               X               X               X               X               X
X    ( 2, 9)    X    ( 3, 9)    X    ( 4, 9)    X    ( 5, 9)    X    ( 6, 9)    X
X   49.202  F   X   49.202  F   X   49.202  F   X   49.202  F   X   49.202  F   X
X               X               X               X               X               X
0     1      0.0     1      0.0     1      0.0     1      0.0     1      0.0
X TNU= 3.134E+02 X TNU= 3.134E+02 X TNU= 3.134E+02 X TNU= 3.134E+02 X TNU= 3.134E+02 X
X TKE= 3.134E+00 X TKE= 3.134E+00 X TKE= 3.134E+00 X TKE= 3.134E+00 X TKE= 3.134E+00 X
X CHI= 5.293E-03 X CHI= 5.293E-03 X CHI= 5.293E-03 X CHI= 5.293E-03 X CHI= 5.293E-03 X
X VAP= 0.0       X VAP= 0.0       X VAP= 0.0       X VAP= 0.0       X VAP= 0.0       X
X LIQ= 0.0       X LIQ= 0.0       X LIQ= 0.0       X LIQ= 0.0       X LIQ= 0.0       X
XXXXX  0.0  XXXXXXXXX  0.0  XXXXXXXXX  0.0  XXXXXXXXX  0.0  XXXXXXXXX  0.0  XXXXX
X               X               X               X               X               X
X    ( 2, 8)    X    ( 3, 8)    X    ( 4, 8)    X    ( 5, 8)    X    ( 6, 8)    X
X   49.098  F   X   48.599  F   X   48.599  F   X   48.599  F   X   48.599  F   X
X               X               X               X               X               X
0     1      0.0     1      0.0     1      0.0     1      0.0     1      0.0
X TNU= 1.000E+02 X TNU= 1.616E+00 X TNU= 1.616E+00 X TNU= 1.616E+00 X TNU= 1.616E+00 X
X TKE= 1.000E+02 X TKE= 1.600E-02 X TKE= 1.600E-02 X TKE= 1.600E-02 X TKE= 1.600E-02 X
X CHI= 2.300E-01 X CHI= 5.293E-03 X CHI= 5.293E-03 X CHI= 5.293E-03 X CHI= 5.293E-03 X
X VAP= 0.0       X VAP= 0.0       X VAP= 0.0       X VAP= 0.0       X VAP= 0.0       X
X LIQ= 0.0       X LIQ= 0.0       X LIQ= 0.0       X LIQ= 0.0       X LIQ= 0.0       X
XXXXX  0.0  XXXXXXXXX  0.0  XXXXXXXXX  0.0  XXXXXXXXX  0.0  XXXXXXXXX  0.0  XXXXX
X               X               X               X               X               X
X    ( 2, 7)    X    ( 3, 7)    X    ( 4, 7)    X    ( 5, 7)    X    ( 6, 7)    X
X   48.100  F   X   47.601  F   X   47.601  F   X   47.601  F   X   47.601  F   X
X               X               X               X               X               X
0     1      0.0     1      0.0     1      0.0     1      0.0     1      0.0
X TNU= 1.000E+02 X TNU= 2.450E+00 X TNU= 2.450E+00 X TNU= 2.450E+00 X TNU= 2.450E+00 X
X TKE= 1.000E+02 X TKE= 2.500E-02 X TKE= 2.500E-02 X TKE= 2.500E-02 X TKE= 2.500E-02 X
X CHI= 2.300E-01 X CHI= 5.293E-03 X CHI= 5.293E-03 X CHI= 5.293E-03 X CHI= 5.293E-03 X
X VAP= 0.0       X VAP= 0.0       X VAP= 0.0       X VAP= 0.0       X VAP= 0.0       X
X LIQ= 0.0       X LIQ= 0.0       X LIQ= 0.0       X LIQ= 0.0       X LIQ= 0.0       X
XXXXX  0.0  XXXXXXXXX  0.0  XXXXXXXXX  0.0  XXXXXXXXX  0.0  XXXXXXXXX  0.0  XXXXX
X               X               X               X               X               X
X    ( 2, 6)    X    ( 3, 6)    X    ( 4, 6)    X    ( 5, 6)    X    ( 6, 6)    X
X   42.098  F   X   41.598  F   X   41.598  F   X   41.598  F   X   41.598  F   X
X               X               X               X               X               X
0     1      0.0     1      0.0     1      0.0     1      0.0     1      0.0
X TNU= 1.000E+02 X TNU= 1.810E-01 X TNU= 1.810E-01 X TNU= 1.810E-01 X TNU= 1.810E-01 X
X TKE= 1.000E+02 X TKE= 2.000E-03 X TKE= 2.000E-03 X TKE= 2.000E-03 X TKE= 2.000E-03 X
X CHI= 2.300E-01 X CHI= 5.293E-03 X CHI= 5.293E-03 X CHI= 5.293E-03 X CHI= 5.293E-03 X
X VAP= 0.0       X VAP= 0.0       X VAP= 0.0       X VAP= 0.0       X VAP= 0.0       X
X LIQ= 0.0       X LIQ= 0.0       X LIQ= 0.0       X LIQ= 0.0       X LIQ= 0.0       X
XXXXX  0.0  XXXXXXXXX  0.0  XXXXXXXXX  0.0  XXXXXXXXX  0.0  XXXXXXXXX  0.0  XXXXX
X               X               X               X               X               X
X    ( 2, 5)    X    ( 3, 5)    X    ( 4, 5)    X    ( 5, 5)    X    ( 6, 5)    X
X   40.496  F   X   40.496  F   X   40.496  F   X   40.496  F   X   40.496  F   X
X               X               X               X               X               X
0     1      0.0     1      0.0     1      0.0     1      0.0     1      0.0
X TNU= 2.068E+00 X TNU= 2.068E+00 X TNU= 2.068E+00 X TNU= 2.068E+00 X TNU= 2.068E+00 X
X TKE= 2.100E-02 X TKE= 2.100E-02 X TKE= 2.100E-02 X TKE= 2.100E-02 X TKE= 2.100E-02 X
X CHI= 5.293E-03 X CHI= 5.293E-03 X CHI= 5.293E-03 X CHI= 5.293E-03 X CHI= 5.293E-03 X
X VAP= 0.0       X VAP= 0.0       X VAP= 0.0       X VAP= 0.0       X VAP= 0.0       X
X LIQ= 0.0       X LIQ= 0.0       X LIQ= 0.0       X LIQ= 0.0       X LIQ= 0.0       X
XXXXX  0.0  XXXXXXXXX  0.0  XXXXXXXXX  0.0  XXXXXXXXX  0.0  XXXXXXXXX  0.0  XXXXX
X               X               X               X               X               X
X    ( 2, 4)    X    ( 3, 4)    X    ( 4, 4)    X    ( 5, 4)    X    ( 6, 4)    X
X   39.595  F   X   39.595  F   X   39.595  F   X   39.595  F   X   39.595  F   X
X               X               X               X               X               X
0     1      0.0     1      0.0     1      0.0     1      0.0     1      0.0
X TNU= 6.710E+00 X TNU= 6.710E+00 X TNU= 6.710E+00 X TNU= 6.710E+00 X TNU= 6.710E+00 X
X TKE= 6.700E-02 X TKE= 6.700E-02 X TKE= 6.700E-02 X TKE= 6.700E-02 X TKE= 6.700E-02 X
X CHI= 5.293E-03 X CHI= 5.293E-03 X CHI= 5.293E-03 X CHI= 5.293E-03 X CHI= 5.293E-03 X
X VAP= 0.0       X VAP= 0.0       X VAP= 0.0       X VAP= 0.0       X VAP= 0.0       X
X LIQ= 0.0       X LIQ= 0.0       X LIQ= 0.0       X LIQ= 0.0       X LIQ= 0.0       X
XXXXX  0.0  XXXXXXXXX  0.0  XXXXXXXXX  0.0  XXXXXXXXX  0.0  XXXXXXXXX  0.0  XXXXX
```

Fig. 5.3.2.1 Initialized Plume Cross Section for the Keystone No. 1 Stack on 20 October 1967. DY = 150 m, DZ = 50 m.

stack height (800 ft) plus the momentum rise height (100 ft), or 900 ft. If the cells are all 164 ft high, then the center of cell (2,7) is at 902 ft--thus cells (2,6), (2,7), and (2,8), are to be initialized with half of the heat release. Checking the prevailing winds for cells (2,6), (2,7), and (2,8) finds that they sweep out 7.3 million cubic feet in one second. Releasing 14.3×10^6 cal into 7.3×10^6 ft^3 gives a temperature rise of 0.47°F, and this is added to the ambient air temperature in these cells in Fig. 5.3.2.1, which shows the computer initialization in the vicinity of the plume cells. This whole initialization process is admittedly crude, particularly in the treatment of momentum, but it gives very satisfactory answers.

The experimental results for this plume are found in Figs. 5.3.2.2 and 5.3.2.3. The former figure shows the prevailing wind speed, direction and potential temperature. The weather was clear on that morning, and a sizeable low-level inversion had formed during the night to about 250 m depth. The flow above 250 m was essentially neutrally stratified and flowed from the west. The turning of the wind with height is ignored in the computer simulation, but the wind speed and potential temperature values are input directly onto the computer mesh. The ambient humidity was fairly low due to a wide subsidence inversion over most of the computer mesh,

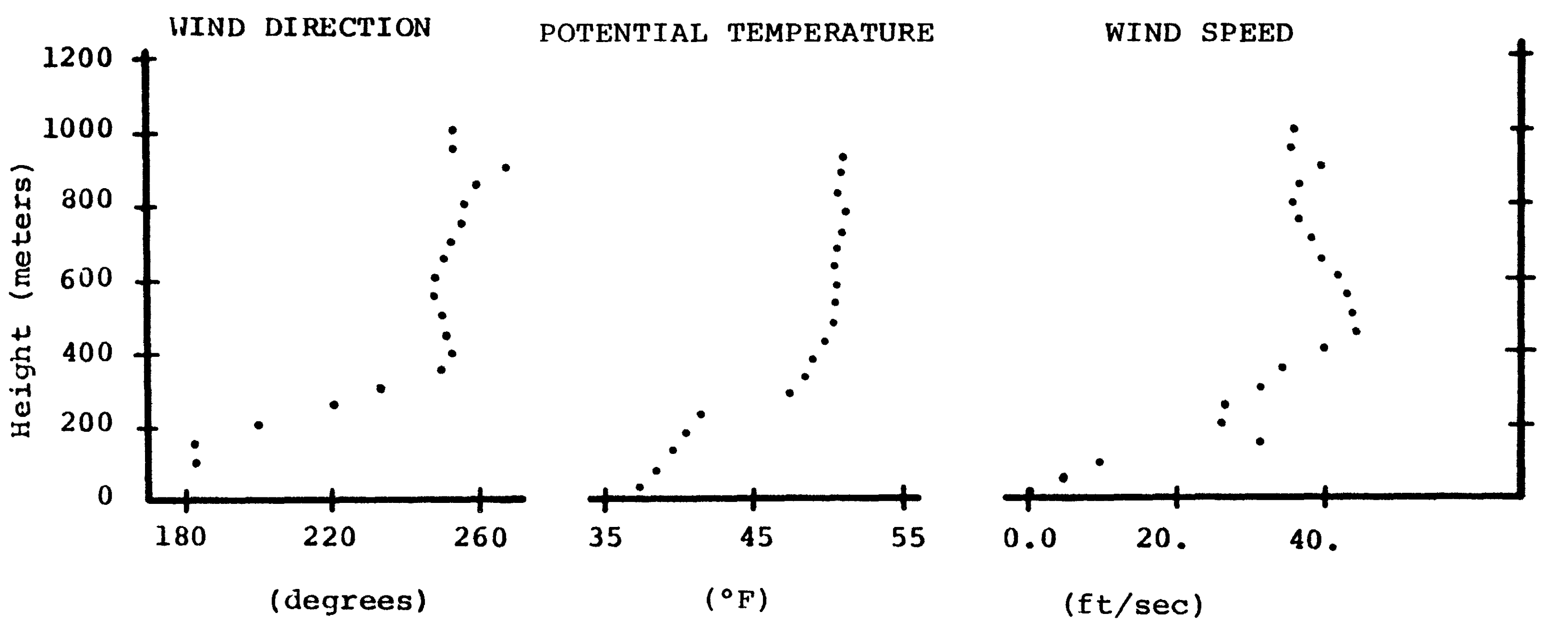

Fig. 5.3.2.2 Weather for 20 October 1967 at the Keystone Plant.

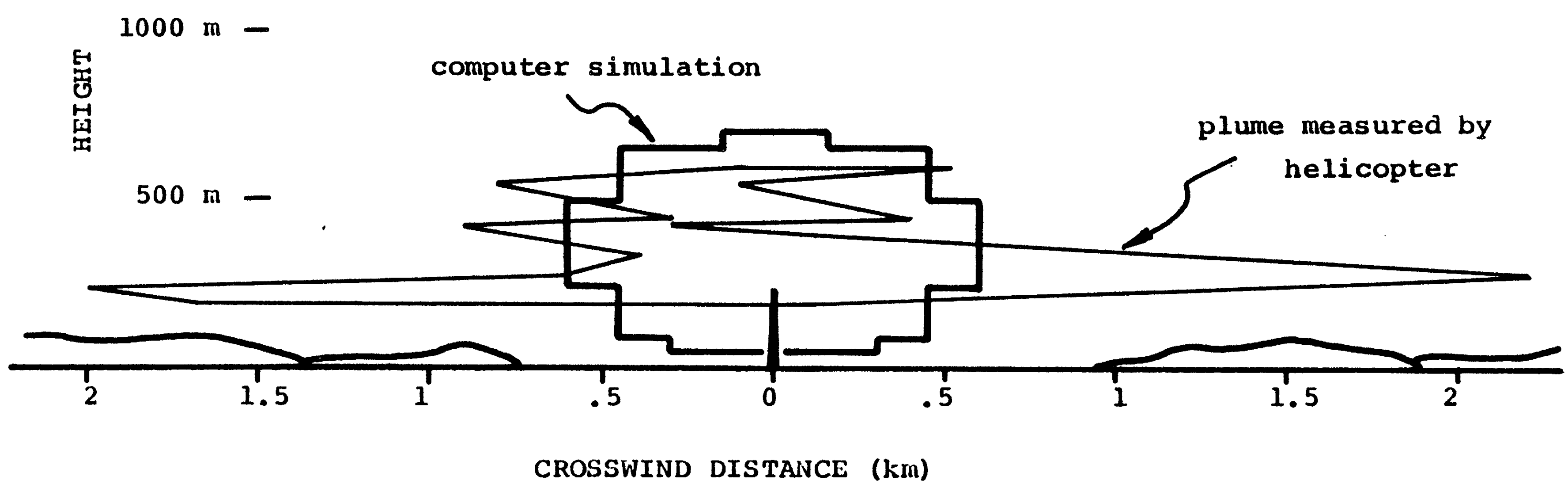

Fig. 5.3.2.3 Comparison of Computational and Helicopter Results at 4.8 km Downwind.

so humidity is neglected in this simulation. Turbulence values are calculated for a neutral atmosphere from Blackadar,[59] and the turbulence in the inversion layer is suppressed by a factor of 100 in the absence of any better information about the turbulence in the stably stratified region. The eddy viscosity is of the order of 100 ft^2/sec in the neutral region, and about 1 ft^2/sec in the stable region.

The helicopter plume cross section at 4.8 km downwind is drawn in Fig. 5.3.2.3 as the jagged outline. The outline connects the measured SO_2 horizontal traverses, and represents essentially a 1 percent boundary of SO_2. A mass balance of SO_2 in the plume cross section finds only 55 percent of the SO_2 that was emitted at the stack. It is suggested that much of the remaining 45 percent of the SO_2 could be found below 200 m, since the helicopters flew no lower than this (for safety) yet were still finding SO_2 at this level. The computer simulation at 600 sec is superposed on the experimental plume outline. Again, the computer trace represents about a 1 percent boundary of SO_2. Except for the two large "wings" of SO_2, the agreement is fairly good. The "wings" are likely produced by low frequency horizontal turbulent eddies generated in the region of the turning of the wind--but since the turbulence on the computer is assumed to be isotropic, this cannot be corrected in these runs in any simple way.

To put the computer and experimental results into perspective, a handbook calculation of the plume SO_2 is undertaken here. The trouble with the anlaysis of the plume of October 20 is to decide whether the stable or neutral conditions have the greatest effect on the behavior, since only one stratification can be used in handbook estimates. The plume rise and dispersion in an F class (stable inversion) is presented in Fig. 5.3.2.4. Note that the plume rise fits the data well, but the dispersion is too small (the dispersion is the 3σ, or 1 percent level value). The plume rise and dispersion in a D class (neutral layer) is presented in Fig. 5.3.2.5. Note that the plume rise is too large, while the dispersion is fairly close to the actual, but is also not able to reproduce the "wings" of SO_2. It is seen that either single choice of stability does not agree as well as the computer simulation (which was able to follow the plume through <u>both</u> regions of stability). This generality in the computer simulations appears to be a major source of improvement over the handbook estimates.

The comparison of experimental and computational plume cross sections is continued in Fig. 5.3.2.6 for the plume at 10.0 km. The helicopter results have the jagged outline in Fig. 5.3.2.6. A mass balance of SO_2 yields only 29 percent of the emitted SO_2, which brings the experimental

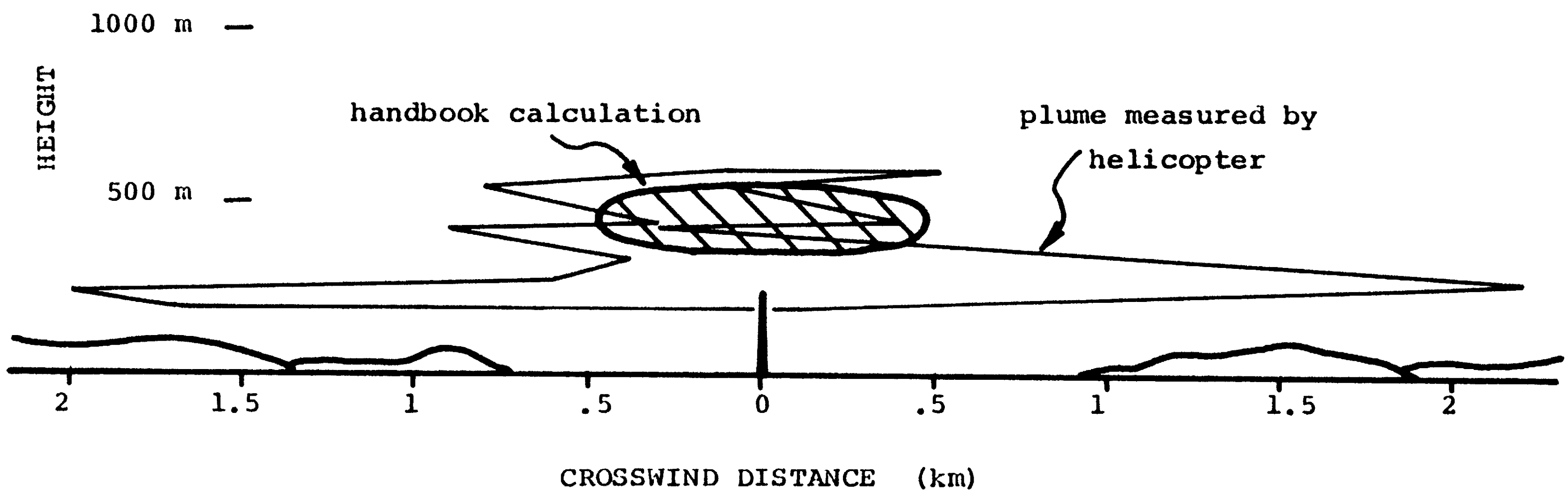

Fig. 5.3.2.4 Comparison of Handbook Calculations and Helicopter Results at 4.8 km Downwind. Pasquill stability class F.

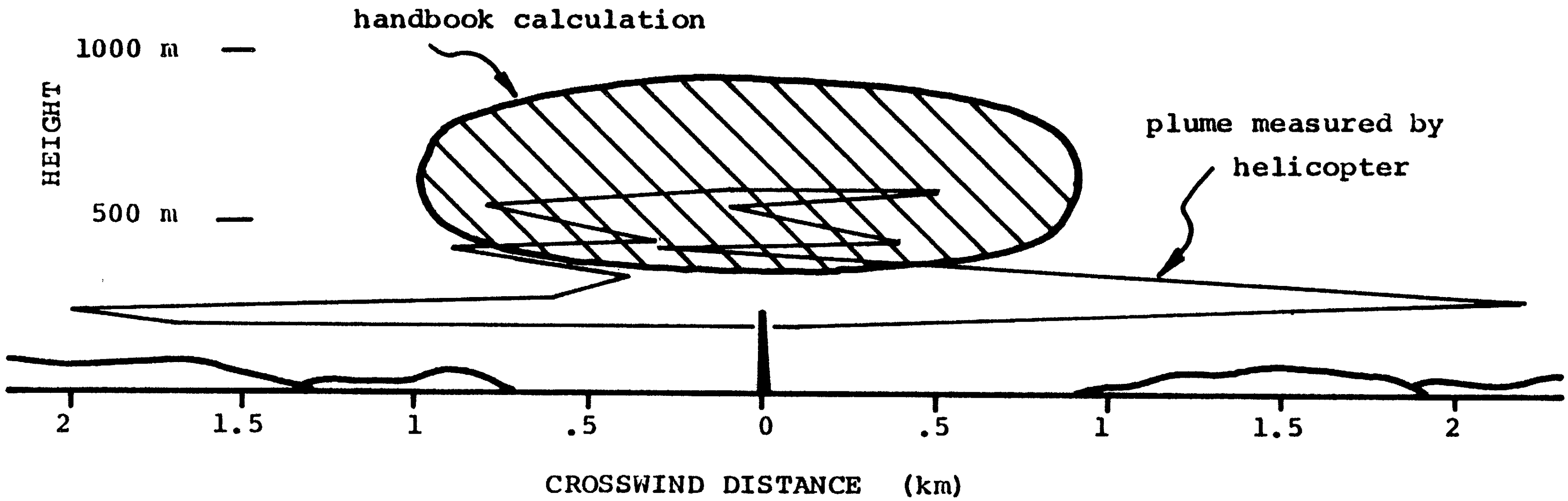

Fig. 5.3.2.5 Comparison of Handbook Calculations and Helicopter Results at 4.8 km Downwind. Pasquill stability class D.

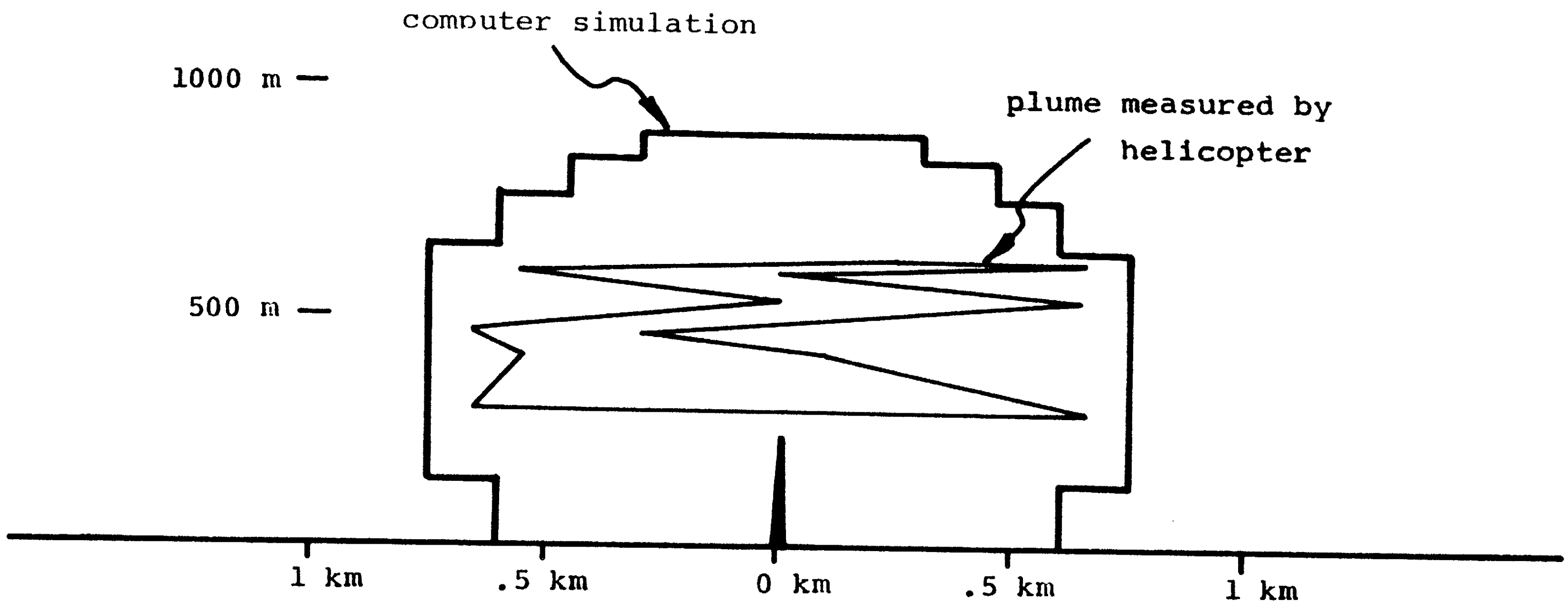

Fig. 5.3.2.6 Comparison of computational and experimental results at 10.0 km downwind for the 20 Oct 67 Keystone #1 plume.

results into question. The computer simulation is superposed, but not much emphasis should be placed on the comparison since the helicopter results appear to be inaccurate on the basis of the low mass balance.

Two other tests of the model with the October 20 plume are found in Figs. 5.3.2.7 and 5.3.2.8. Four SO_2 bubblers were placed on a small hill at 65 m elevation above the stack base, at 6.5 km downwind. The bubbler 1/2 hour averages were all averaged together to yield a 12 pphm ground-level SO_2 concentration. The central region of the simulated plume cross section is copied in Fig. 5.3.2.7. Each SO_2 concentration represents the value in a single computer mesh cell. The dashed line is drawn through the plume at the 65 m elevation, where the 12 pphm experimental value compares very well with the predicted values inside the plume

The entire simulation was carried to 12 km downwind. The maximum ground level SO_2 concentration is plotted at 2 km intervals in Fig. 5.3.2.8. Even at 12 km the SO_2 has not yet reached a maximum. However, the maximum SO_2 in the plume (calculated at 12 km) is 33 pphm, while the ground level is already 17 pphm--so the maximum calculated value will have to be between 17 and 33 pphm. A handbook estimate of the maximum ground level concentration (taken from Eq. 3.146 of Slade)[72] yields 47 pphm at 17 km downwind in neutral D class

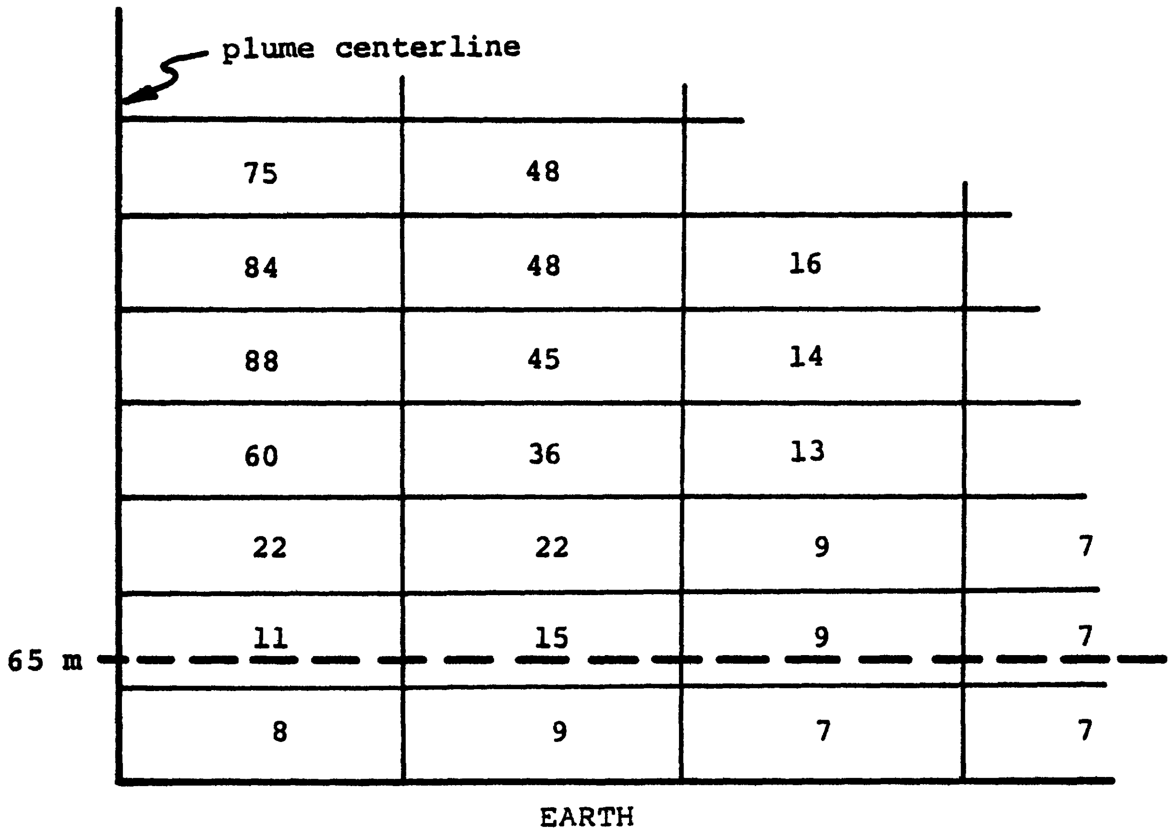

Fig. 5.3.2.7 Comparison of the computer simulation of the 20 Oct 67 Keystone #1 plume cross section with the half-hour average SO_2 concentration at 65 m. The values in the boxes are the mesh cell [SO_2] in pphm predicted by the code at 6.5 km downwind. An average [SO_2] of 12 pphm was recorded in four SO_2 bubblers at 65 m elevation and 6.5 km downwind. The dashed line at 65 m represents the bubbler elevation on the computer mesh.

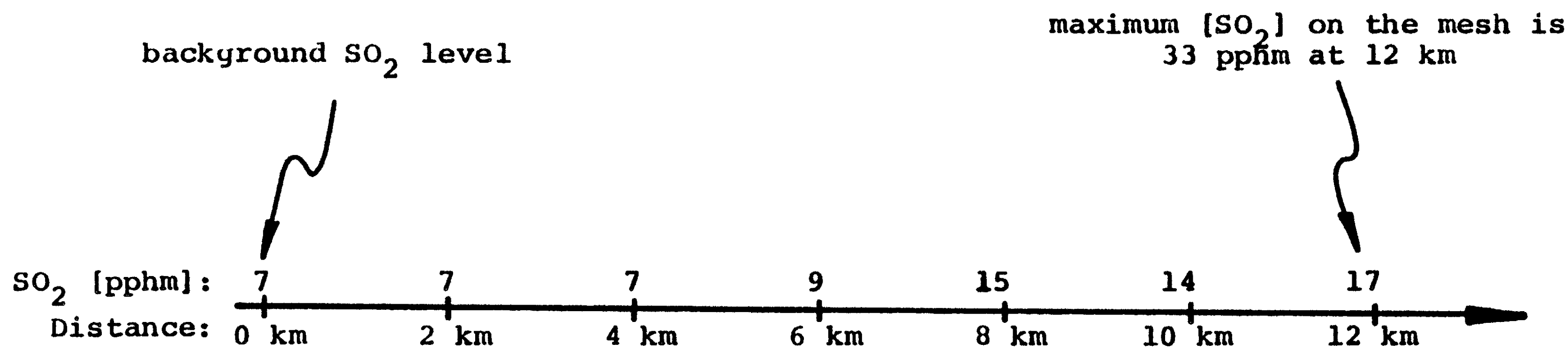

Fig. 5.3.2.8 Maximum ground-level SO_2 concentrations predicted in the computer simulation of the 20 Oct 67 Keystone #1 plume.

stability (which is roughly an upper bound for this value) and 22 pphm at 90 km downwind in stable E-class stability (which is roughly a lower bound for this value). The calculated value must therefore fall somewhere between these handbook estimates which lends credence to the results, even though the actual maximum ground level SO_2 value was not calculated.

5.4 Results of Model Extension

5.4.1 Fumigation Episode

A computer simulation that approximates a fumigation episode is presented in this section. No particular episode is intended to be represented by this run, but several of the general features of a fumigation episode near a shoreline site in the Great Lakes area are included.[73] These episodes are commonly characterized by a wind off of a large cool lake on a sunny spring day. The air that has traveled over the lake has developed a deep stable layer because of sensible heat exchange with the cool lake water. As this deep stable layer streams inland, the strong solar heating at the ground causes a deepening unstable thermal boundary layer to develop. This layer is characterized by strong mixing as vigorous turbulent thermal convection sets in. Plumes released in the stable air exhibit small plume rise and dispersion until they encounter the growing boundary layer from below. Quite rapidly they have their pollutants spread to the ground, in a sense "fumigating" a relatively small area with high pollutant concentration.

A rough calculation was performed to demonstrate this. The plume in a stable inversion from Sec. 5.3.2 was released over a deepening turbulent layer coming up from the ground. The situation is shown in Fig. 5.4.1.1. At 0, 20, 50, 100, and 200 seconds the turbulent layer (eddy viscosity = 1000 ft^2/sec) is deepened by an increment of 100 meters--this is represented by the staircase in Fig. 5.4.1. The plume that is released at 0 km is about half engulfed in the turbulent layer at 1 km, and almost entirely engulfed at 2 km. The strong turbulent mixing has produced ground level concentrations a factor of 4 and 8 times higher at these stations than the results of Sec. 5.3.2. This agrees qualitatively with actual fumigation episode results, and serves to demonstrate the ability of the model to extend into these important cases. A more refined calculation of the boundary layer, and actual weather and plume data from a shoreline site would be needed to more carefully test this type of simulation.

5.4.2 Plumes with Change of Phase

Model validation has not been carried out for plumes

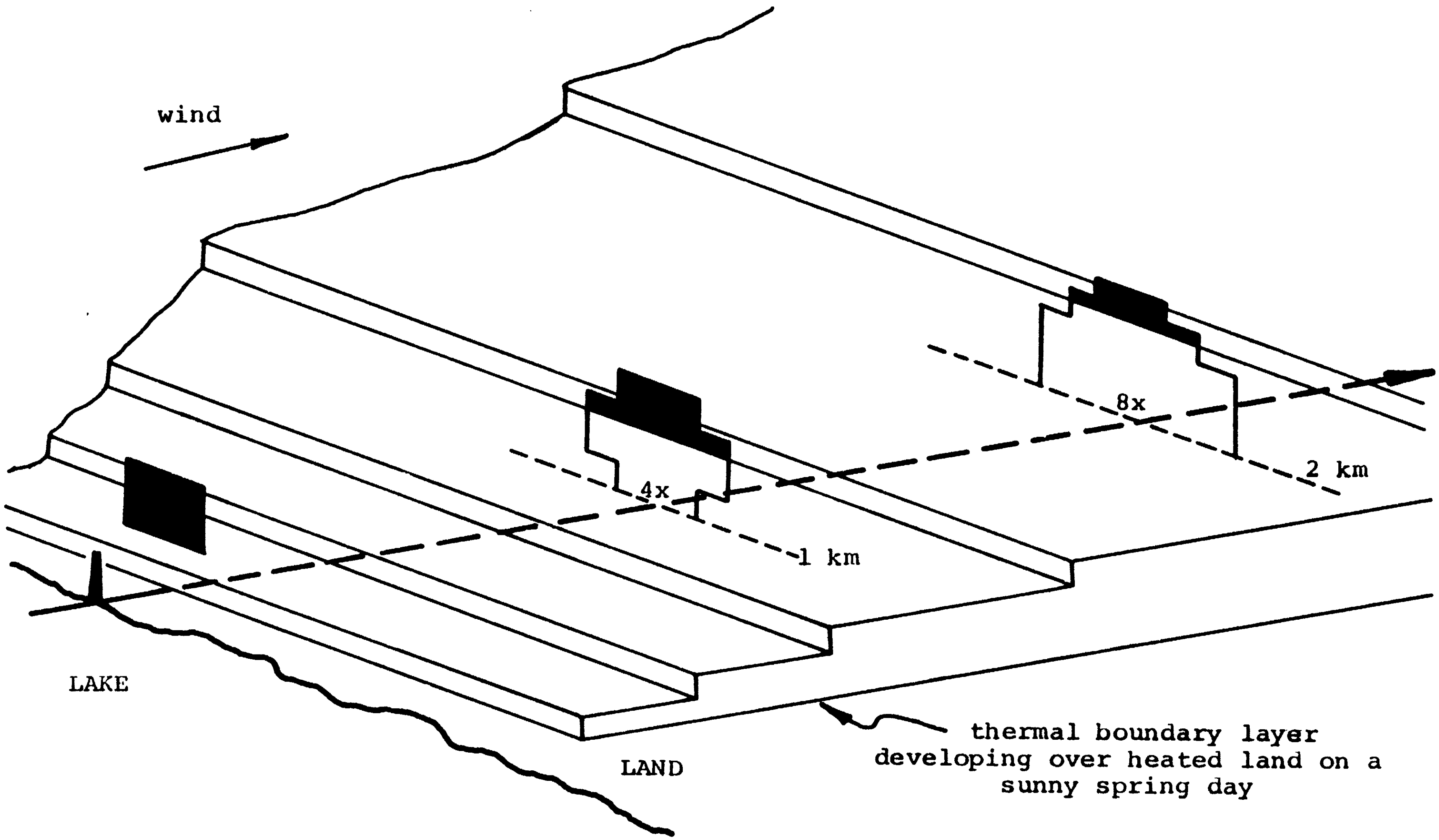

Fig. 5.4.1.1 Fumigation Episode at a Shoreline Site.
Cross sections are plume SO_2. Ground-level [SO_2] discussed in text.

with change of phase. The available Chalk Point data were incomplete during this work and could not be used. The balloon data from several mechanical draft towers at the Commanche plant[74] suffers from a lot of scatter from a variety of sources, and data were only obtained very close to the towers, which casts doubt on the ability of the simulations to handle this case.

From preliminary work with saturated parcels of air on the computer mesh, the model is found to suffer from oscillations that are due to the explicit nature of the moisture equilibrium calculation. The oscillations can be brought under control by reducing the timestep size, but a more fundamental solution to this problem is recommended in Sec. 6.2.3.

6. CONCLUSIONS AND RECOMMENDATIONS

6.1 Model Validation

A widely applicable calculational model of buoyant bent over plumes has been developed. The advantage of the model is its ability to treat problems outside the scope of existing plume models without greatly increasing the resources required for the analyses. The acceptance of the model, however, must begin with a demonstration of its ability to reproduce the solutions to problems that are known to be solvable. This demonstration has proceeded along two lines in this work--problems in which the plume properties dominate the flow, and problems in which the atmospheric turbulent mixing dominates the flow. Some overlap between these simple regimes occurs, but overall this organization serves to highlight the causes of the particular successes and discrepancies in the model validation work.

The results of Sec. 5.2 deal mainly with the plume dominated motions. Generally it is found that very good agreement with laboratory experiments is obtained. In particular, the buoyant line-vortex motions and the Brunt-Vaisala period of a buoyant cylinder of fluid are studied, and they compare very favorably with the predictions. However, the unsuccessful attempts to "tune" the turbulence model coefficients point out the rather limiting assumptions contained in the present turbulence model, particularly with regard to buoyant production of TKE. To the model's credit, it has been noted[75] that wall-free turbulent flows are the most difficult to "tune," and that the model does a credible job in its current form.

The results of Sec. 5.3 deal mainly with the atmospheric dominated motions. There is a large amount of overlap into the plume-dominated motions in the Briggs plume rise and Pasquill dispersion results, but these cases both represent experiments that were actually performed in the atmosphere, and they exhibit a fair amount of scatter in their data because of this. Again, the agreement between calculation and experiment is good. The results of the LAPPES individual plume study provides the best indication of where the calculational model is expected to benefit the modelers of plumes. In the limited number of calculations contained in that section, it is found that the calculational model agrees with the experimental results more closely than the current handbook estimates simply because it has made a more fundamental calculation, taking into account the actual micrometeorological profiles. Furthermore, the model provides a relatively accurate starting point for the detailed description of other important processes in a plume: chemical reactions, visibility, radiation dose rates, etc.

6.2 Recommendations

6.2.1 Calculational Scheme to Include Wind Shear Effects

A brief overview of a plausible calculational scheme that would address one of the important effects of wind shear on the plume dynamics is discussed here. The effect is that of the dilution of the plume properties as the plume rises into progressively stronger winds. The process is sketched in Fig. 6.2.1.1, and is well-known to plume modelers. A constant release of pollutant (illustrated in Fig. 6.2.1.1), momentum, sensible heat, moisture, etc., diluted into air that moves with a velocity $u(Z_o)$ will have a density proportional to the inverse of the velocity. A plume property that is released into a stronger wind, $u(Z)$, will be correspondingly more dilute. This effect is important in buoyant plumes when the plume updrafts and downdrafts in the presence of a wind shear cause parcels of the plume to change their downwind advection rate. Clearly, the problem is fully three-dimensional (though it can be in steady state), but a very restrictive assumption may afford a useful recasting of the two-dimensional problem. This assumption is discussed next.

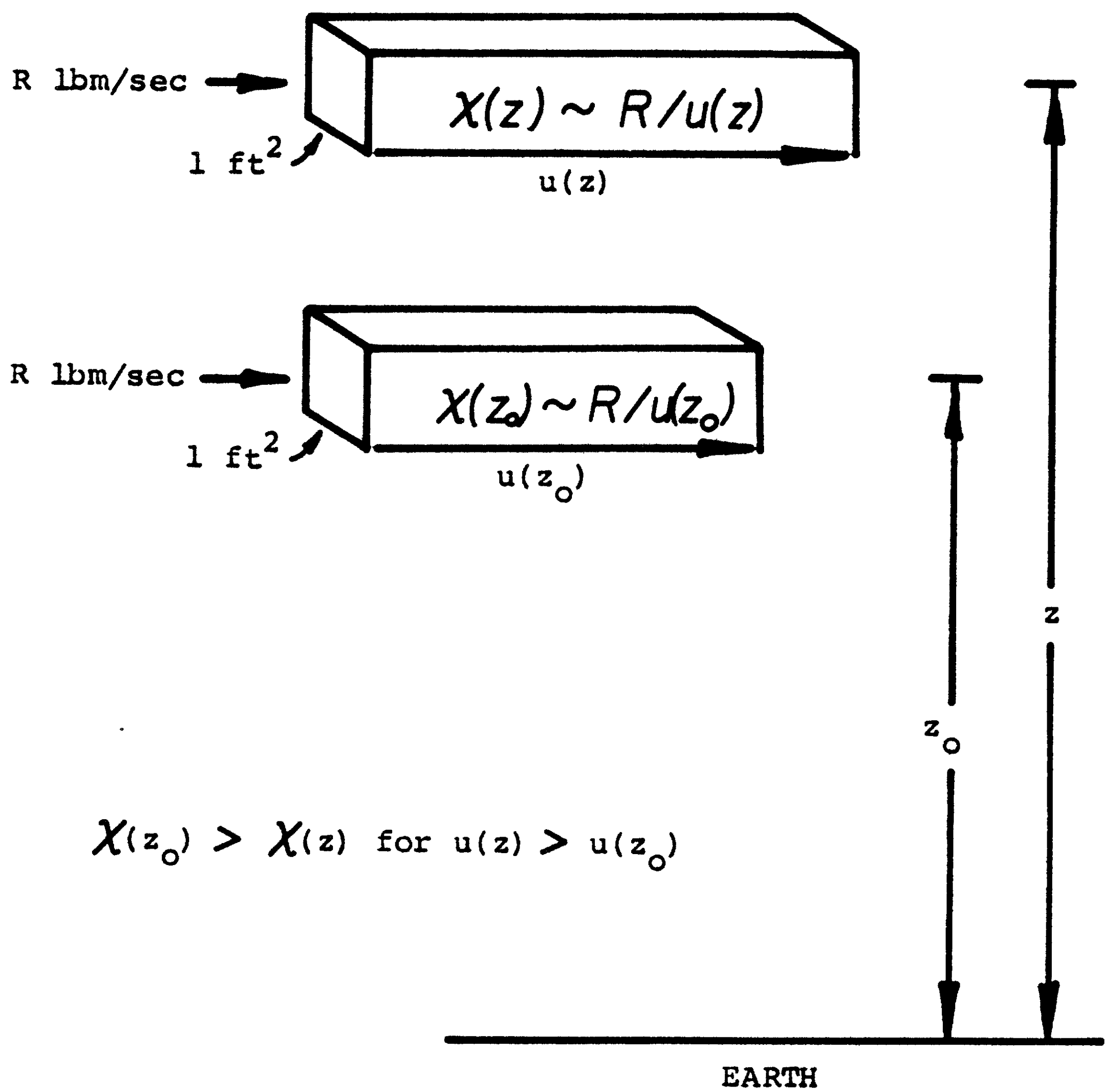

Fig. 6.2.1.1 Dilution of a Steady Release of Pollutant.

Consider the advection and turbulent diffusion of a pollutant in three dimensions (the results extend directly to momentum, sensible heat, etc.):

$$\frac{\partial \chi}{\partial t} + u\frac{\partial \chi}{\partial x} + v\frac{\partial \chi}{\partial y} + w\frac{\partial \chi}{\partial z} = \gamma_{\chi}\sigma\nabla^2\chi \tag{6.1}$$

Assuming that the system is in steady state, we have

$$u\frac{\partial \chi}{\partial x} + v\frac{\partial \chi}{\partial y} + w\frac{\partial \chi}{\partial z} = \gamma_{\chi}\sigma\nabla^2\chi \tag{6.2}$$

In the presence of a steady uniform wind field, u_o, the first term is commonly interpreted as the time-rate-of-change for an observer moving with the wind, and is written as $\frac{\partial \chi}{\partial t_o}$, where $u_o t_o = x$. This contains the important assumption that the plume <u>always</u> has the downwind velocity u_o--implying infinite accelerations at the stack exit, to be sure. In a strong wind field the downwind diffusion is commonly neglected with respect to the downwind advection, so the gradient operator has only y and z derivatives. If the wind field is allowed to have shears, then the first term may be represented as

$$u(z)\frac{\partial \chi}{\partial x} = \frac{u(z)}{u(z_o)}\left(u(z_o)\frac{\partial \chi}{\partial x}\right) = \frac{u(z)}{u(z_o)}\frac{\partial \chi}{\partial t_o} \tag{6.3}$$

where u_o has been arbitrarily chosen to be $u(z_o)$. This interpretation allows the equation to be formulated as

$$\frac{\partial \chi}{\partial t_o} + \frac{u(z_o)}{u(z)} (v \frac{\partial \chi}{\partial y} + \frac{\partial \chi}{\partial z}) = \frac{u(z_o)}{u(z)} \gamma_\chi \sigma (\frac{\partial^2 \chi}{\partial y^2} + \frac{\partial^2 \chi}{\partial z^2}) \qquad (6.4)$$

This equation holds the assumption that any parcel of air in the plume, when advected into a region of stronger wind, immediately takes on the local wind velocity and is correspondingly diluted. Note that it also causes parcels that are decelerated to concentrate their properties, which is physically unrealistic, but hopefully is not too serious an error since plume rise and updrafts are almost always stronger than downdrafts. The important feature that this scheme hopes to address is the dilution (usually by about 10 to 50 percent) of plume buoyancy, momentum, and moisture, which affect the plume dynamics. The procedure could be extended to every transport equation in the equation set--only the effect on the divergence condition in the fluid mechanics algorithm has not been studied. Its satisfaction would still be required as a constraint on the solution.

6.2.2 Calculational Scheme for Time-Dependent Release or Weather

The simulation of "mildly" time-dependent plumes can be made with the model. Essentially, the governing assumption here is that the prevailing weather or effluent properties will advect downwind, and never affect the flow that precedes or follows it. The situation is developed in Fig. 6.2.2.1, where a stack is assumed to have a set of exit properties, Ω, that are piecewise-constant in time over periods of 100 sec. To reconstruct the behavior, an initial simulation with the properties at time t_o, $\Omega(t_o)$ is made to 300 sec. The plume properties changed at time t_o to 100 sec, so a second simulation is made with properties $\Omega(t_o + 100)$ to 200 sec. Again the plume properties changed at time t_o + 200 sec, so a third simulation is made with properties $\Omega(t_o + 200)$ to 100 sec. The actual plume is then "cut and pasted" from the pertinent data in the simulations as shown at the bottom of the figure. The calculation is somewhat wasteful, since 600 sec of simulation produces only 300 sec of results--but the scheme surely saves time and storage over a fully three-dimensional calculation. Eventually, for sufficiently "strong" time-dependence the scheme becomes too laborious with respect to a three-dimensional calculation.

6.2.3 Cloud Microphysics Model

The limited success of the equilibrium moisture thermodynamics model is due to its explicit differencing. In short, the model is ignorant of the latent heat released in a current timestep, and it adjusts the equilibrium conditions without

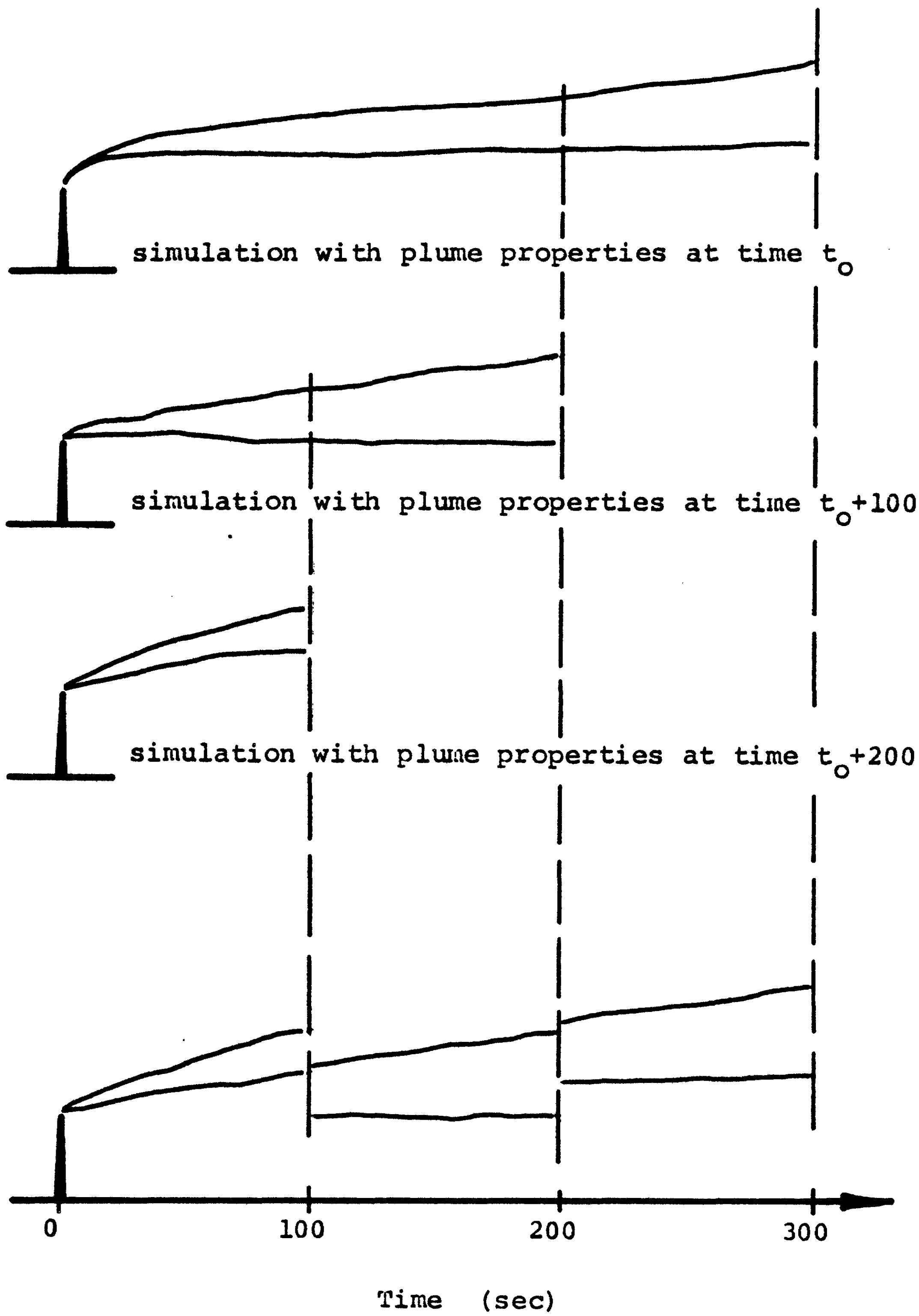

Fig. 6.2.2.1 Simulation of a Time-Dependent Plume in Steady-State Weather. Scheme is discussed in the text.

this knowledge. The resultant oscillations in the equilibrium conditions are not surprising, nor is the ability to control them with very small timesteps. If the calculation was made implicit--essentially iterating on the coupled latent heat release equation and Magnus' formula for liquid-vapor equilibrium--the timesteps could be relaxed back to their original size.

The prospect of incorporating a non-equilibrium moisture model is not investigated in this work. The limitations of the equilibrium model have not been sufficiently explored to justify the change at this point.

NOMENCLATURE

A_o	initial line-vortex area (ft^2)
C	experimental constant, 1.9
C_p	heat capacity at constant pressure (BTU/lb_m °R)
c_p^{moist}	heat capacity of moist air at constant pressure (BTU/lb_m °R)
DT	timestep size (sec)
DY	cell width (ft)
DZ	cell height (ft)
$e_{sat}(T)$	saturation vapor pressure of water (mb)
$E_\chi^{(i)}$	energy of the i^{th} decay channel from pollutant species χ (MeV)
$F_\chi^{(i)}$	fractional energy deposition for i^{th} radioactive decay channel from pollutant species χ)
g	acceleration due to gravity (ft/sec^2)
g_i	vector acceleration due to gravity (ft/sec^2)
I	specific internal energy (BTU/lbm)
k	thermal conductivity (BTU/ft-sec-°R)
L	buoyancy parameter (ft)
L_{eddy}	eddy length scale (ft)
L_{vap}	latent heat of vaporization of water (BTU/lb_m)
N	experimental constant, 3.0
$\tilde{p}$	physically measurable pressure (millibars)
p	pressure perturbation about an adiabatic reference state (mb)
p_o	pressure in a quiet adiabatic atmosphere (mb)

$\bar{p}$	time average pressure perturbation (mb)
p'	fluctuating pressure perturbation (mb)
Pr	Prandtl number
$q, q(y,z,t)$	turbulence kinetic energy per unit lb_m (ft^2/sec^2)
$q_{library}(Z)$	prescribed turbulence kinetic energy profile (ft^2/sec^2)
Q	heat (BTU)
Q_H	heat emitted at stack exit (BTU/sec)
$R(T)$	plume radius as a function of time (ft)
R_{dry}, Rd	gas constant for dry air $(ft^3\ mb/lb_m\ °R)$
R_{vap}, R_v	gas constant for water vapor $(ft^3 mb/lb_m\ °R)$
Sc_{liq}	Schmidt number for liquid water
Sc_{vap}	Schmidt number for water vapor
t, T	time (seconds)
t_o	x/u_o (sec)
T_*	time coordinate of virtual origin (sec)
$\tilde{T}$	physically measurable temperature (°R)
T	temperature perturbation about an adiabatic reference state (°R)
T_o	temperature in a quiet adiabatic atmosphere (°R)
T_s	temperature of stack effluent (°R)
$\tilde{T}_v$	virtual temperature (°R)
T_{vo}	virtual temperature in a quiet adiabatic atmosphere (°R)
u	downwind velocity (ft/sec)
u_o, U	windspeed, constant with height (ft/sec)
u_{eddy}	turbulent velocity scale in an eddy (ft/sec)
$\tilde{u}_i, \tilde{u}_j$	velocity (ft/sec)
u_i, u_j	velocity (ft/sec)

$\overline{u}_i, \overline{u}_j$	time average velocity (ft/sec)
u_i', u_j'	fluctuating velocity (ft/sec)
$\overline{u_i' \; u_j'}$	Reynolds stress tensor (ft^2/sec^2)
$\overline{u_i' \; \theta'}$	correlation of fluctuating velocity and temperature
$\overline{u_i' \; u_j' \; u_k'}$	triple correlation of fluctuating velocity (ft^3/sec^3)
v	crosswind velocity (ft/sec)
V_g	geostrophic wind (ft/sec)
w	vertical velocity (ft/sec)
$W_{mol,\chi}$	molecular weight of the pollutant species (lb_m/lb_m-mole)
X	downwind distance (ft)
X_i, X_j	cartesian coordinate (ft)
y	crosswind distance (ft)
z	height (ft)
z_*	height coordinate of virtual origin (ft)

α, α_1	turbulence constants
γ_L	reciprocal turbulent Schmidt number for liquid water
γ_T	reciprocal turbulent Prandtl number for heat
γ_V	reciprocal turbulent Schmidt number for water vapor
γ_χ	reciprocal turbulent Schmidt number for pollutant
Γ	turbulence constant
Γ_1	turbulence constant
Γ_d	dry adiabatic lapse rate (°R/ft)
ε_h	eddy diffusivity of heat (ft^2/sec)
ε_m	eddy diffusivity of momentum (ft^2/sec)
ε_χ	eddy diffusivity of pollutant (ft^2/sec)
$\tilde{\theta}$	potential temperature (°R)
θ	potential temperature perturbation about an adiabatic reference state (°R)
θ_o	potential temperature in a quiet adiabatic atmosphere (°R)
$\bar{\theta}$	time average potential temperature (°R)
θ'	fluctuating potential temperature (°R)
θ_v	virtual potential temperature (°R)
θ_{vo}	virtual potential temperature in a quiet adiabatic atmosphere (°R)
$\bar{\theta}_v$	time average virtual potential temperature (°R)
θ_v'	fluctuating virtual potential temperature (°R)
$\lambda_x^{(i)}$	decay constant for i^{th} radioactive decay channel from pollutant species χ (sec^{-1})

μ	dynamic viscosity (lb_m/sec. ft)
ν	kinematic viscosity (ft^2/sec)
ρ_{dry}	density of dry air (lbm/ft^3)
ρ_{liq}	liquid water density (lbm/ft^3)
$\bar{\rho}_{liq}$	time average liquid water density (lbm/ft^3)
ρ'_{liq}	fluctuating liquid water density (lbm/ft^3)
ρ_s	density of stack effluent (lbm/ft^3)
ρ_{sat}	saturation water vapor density (lbm/ft^3)
ρ_{vap}	water vapor density (lbm/ft^3)
$\bar{\rho}_{vap}$	time average water vapor density (lbm/ft^3)
ρ'_{vap}	fluctuating water vapor density (lbm/ft^3)
$\sigma, \sigma(y,z,t)$	eddy viscosity (same as ϵ_m) (ft^2/sec)
$\sigma_{library}(z)$	prescribed eddy viscosity profile (ft^2/sec)
χ	pollutant density (lbm/ft^3)

LIST OF FIGURES AND TABLES

REFERENCES

1. R. Scorer, Natural Aerodynamics, New York, Pergamon Press, 1958, p. 194.

2. J. Stuhmiller, "Development and Validation of a Two-Variable Turbulence Model," SAI-74-509-LJ, 1974.

3. F. Pasquill, Atmospheric Diffusion, Second Ed., England, Ellis Horwood Ltd., 1974.

4. J. Richards, "Experiments on the Motions of Isolated Cylindrical Thermals Through Unstratified Surroundings," Int. Jour. Air Water Poll., 7, pp 17-34, 1963.

5. F. Schiermeier, Large Power Plant Effluent Study, Vol. 1-4, Research Triangle Park, NC,EPA, Office of Air Programs, 1971.

6. R. Sklarew, and J. Wilson, "Air Quality Models Required Data Characterization," Palo Alto, CA, EPRI EC-137, May, 1976.

7. F. Hoffman, et. al., "Computer Codes for the Assessment of Radionuclides Released to the Environment," Nuclear Safety, Vol. 18, No. 3, pp 343-354, May-June, 1977.

8. M. Winton, "Computer Codes for Analyzing Nuclear Accidents," Nuclear Safety, Vol. 15, No. 5, pp 535-552, Sept.-Oct., 1973.

9. K. Rao, "Numerical Simulation of Turbulent Flows--A Review," ARATDL internal note, April, 1976.

10. C. Nappo, "The Detailed Numerical Simulation of Vorticity Concentration Downwind of Large Heat Sources," (unpublished notes).

11. C. DuP. Donaldson, "Construction of a Dynamic Model of the Production of Atmospheric Turbulence and the Dispersal of Atmospheric Pollutants," in D. Haugen, ed., Workshop on Micrometeorology, Ephrata, PA, Science Press, AMS, 1973, pp 313-392.

12. W. Lewellen, and M. Teske, "Second-Order Closure Modeling of Diffusion in the Atmospheric Boundary Layer," Boun. Lay. Met., 10, pp 69-90, March 1976.

13. S. Patankar, et. al., "Prediction of the Three-Dimensional Velocity Field of a Deflected Turbulent Jet," Trans. ASME, J. Flu. Eng., pp 758-762, Dec. 1977.

14. K. Rao, et. al., "Mass Diffusion from a Point Source in a Neutral Turbulent Shear Layer," Jour. Heat Transfer, 99, pp 433-438, Aug. 1977.

15. M. Dickerson, and R. Orphan, "Atmospheric Release Advisory Capability," Nuc. Safety, Vol. 17, No. 3, May-June, pp 281-289.

16. R. Lange, "ADPIC: A 3-D Computer Code for the Study of Pollutant Dispersal and Deposition Under Complex Conditions," UCRL-51462, Oct. 1973.

17. M. Dickerson, et. al., "Concept for an Atmospheric Release Advisory Capability," UCRL-51656, Oct. 1974.

18. J. Knox, "Numerical Modeling of the Transport, Diffusion, and Deposition of Pollutants for Regions and Extended Scales," UCRL-74666, Mar. 1973.

19. J. Knox, "Atmospheric Release Advisory Capability: Research and Progress," UCRL-75644 (Rev. 2), May 1974.

20. R. Lange, and J. Knox, "Adaptation of a 3-D Atmospheric Transport Diffusion Model to Rainout Assessments, UCRL-75731, Sep. 1974.

21. R. Lange, "ADPIC: A 3-D Transport-Diffusion Model for the Dispersal of Atmospheric Pollutants and its Validation Against Regional Tracer Studies," UCRL-76170, May 1975.

22. C. Sherman, "Mass-Consistent Model for Wind Fields Over Complex Terrain," UCRL-76171, May 1975.

23. R. Henninger, "A Two-Dimensional Dynamic Model for Cooling Tower Plumes," Trans. ANS, Vol. 17, 1973, pp 65-66.

24. J. Taft, "Numerical Model for the Investigation of Moist Buoyant Cooling-Tower Plumes," in S. Hanna and J. Pell, coords., Cooling Tower Environment-1974, ERDA Symposium Series No. 35, Oak Ridge, Tenn., USERDA, Conf-740302, April, 1975.

25. D. Lilly, "Numerical Solutions for the Shape-Preserving Two-Dimensional Thermal Convection Element," Jour. of the Atmos. Sci., 21, pp 83-98, Jan. 1964.

26. D. Johnson, et. al., "A Numerical Study of Fog Clearing by Helicopter Downwash," Jour. Appl. Met., 14, pp 1284-1292, 1975.

27. Y. Ogura, "The Evolution of a Moist Convective Element in a Shallow, Conditionally Unstable Atmosphere: A Numerical Calculation," Jour. Atmos. Sci., 20, pp 407-424, Sept. 1963.

28. G. Arnason, et. al., "A Numerical Experiment in Dry and Moist Convection Including the Rain Stage," Jour. Atmos. Sci., 25, pp 404-415, May 1968.

29. J. Liu, and H. Orville, "Numerical Modeling of Precipitation and Cloud Shadow Effects on Mountain-Induced Cumuli," Jour. Atmos. Sci., 26, pp 1283-1298, Nov. 1969.

30. W. Cotton, "Theoretical Cumulus Dynamics," Rev. Geophys. and Space Phys., Vol. 13, No. 2, pp 419-448, May 1975.

31. Chalk Point Cooling Tower Project, Vol. 1-3, PPSP-CPCTP-16, Applied Physics Lab., Johns Hopkins Univ., Laurel, MD, August, 1977.

32. Chalk Point Cooling Tower Project, PPSP-CPCTP-11 and PPSP-CPCTP-12, Applied Physics Lab., Johns Hopkins Univ., Laurel, MD, 1978.

33. G. Tsang, "Laboratory Study of Line Thermals," Atmos. Environ., 5, pp 445-471, 1971.

34. J. Deardorff, "Numerical Investigation of Neutral and Unstable Planetary Boundary Layers," Jour. Atmos. Sci., 29, pp 91-115, 1972.

35. J. Deardorff, "Three-Dimensional Numerical Modeling of the Planetary Boundary Layer," in D. Haugen, ed., Workshop on Micrometeorology, Ephrata, PA, Science Press, AMS, 1973.

36. J. Deardorff, "Three-Dimensional Numerical Study of the Height and Mean Structure of a Heated Planetary Boundary Layer," Boun. Lay. Met., 7, pp 81-106, 1974.

37. E. Spiegel, and G. Veronis, "On the Boussinesq Approximation for a Compressible Fluid," Astrophys. Jour., 131, pp 442-447, 1960.

38. L. Cloutman, C. Hirt, and N. Romero, "SOLA-ICE: A Numerical Algorithm for Transient Compressible Fluid Flows," UC-34, July, 1976.

39. J. Iribarne, and W. Godson, Atmospheric Thermodynamics, Holland, Reidel Publ. Co., 1973.

40. VARR-II--A Computer Program for Calculating Time-Dependent Turbulent Fluid Flows with Slight Density Variation, Vols 1,2,3, Madison, PA, Westinghouse Adv. React. Div., May 1975.

41. A. Amsden, and F. Harlow, "The SMAC Method: A Numerical Technique for Calculating Incompressible Fluid Flows," LA-4370, May 1970.

42. R. Gentry, et. al., "An Eulerian Differencing Method for Unsteady Compressible Flow Problems," Jour. of Comp. Phys., Vol. 1, 1966, pp 87-118.

43. E. Eckert, and R. Drake, Heat and Mass Transfer, New York, McGraw-Hill Book Co., 1959.

44. S. Hess, Introduction to Theoretical Meteorology, New York, Holt, Rinehart, and Winston, 1959, Chap 18.6.

45. Ibid., Chapter 18.7.

46. Ibid., Chapter 12.

47. H. Tennekes, "The Atmospheric Boundary Layer," Physics Today, Jan. 1974, pp 52-63.

48. C. Priestly, Turbulent Transfer in the Lower Atmosphere, Chicago, U. of Chicago Press, 1959.

49. R. Scorer, Natural Aerodynamics, New York, Pergamon Press, 1958.

50. A. Monin, "The Atmospheric Boundary Layer," in M. Van Dyke, ed., Ann. Rev. of Fluid Mechanics, Vol. 2, pp 225-250, 1970.

51. J. Businger, "The Atmospheric Boundary Layer," V. Derr, ed., Remote Sensing of the Troposphere, Washington, D.C., U.S.Dept. of Commerce, NOAA, Govt. Printing Office, Aug. 1972.

52. H. Panofsky, "The Boundary Layer Above 30 M," Bound. Lay. Met., 4, pp 251-264, 1973.

53. H. Panofsky, "The Atmospheric Boundary Layer Below 150 M," in Annual Review of Fluid Mechanics, pp 147-177, 1974.

54. G. Csanady, Turbulent Diffusion in the Environment, Boston, MA, Reidel Publ., 1973.

55. J. Lumley, and H. Panofsky, The Structure of Atmospheric Turbulence, New York, John Wiley & Sons, 1964.

56. A. Monin, and A. Yaglom, Statistical Fluid Mechanics, Vol. 1, Cambridge, MA, MIT Press, 1971.

57. A. Monin, and A. Yaglom, Statistical Fluid Mechanics, Vol. 2, Cambridge, MA, MIT Press, 1975.

58. Ibid., Vol. 1, p 280.

59. A. Blackadar, "The Vertical Distribution of Wind and Turbulent Exchange in a Neutral Atmosphere," Jour. Geophys. Res., 67, pp 3095-3102, 1962.

60. A. Blackadar, and J. Ching, "Wind Distribution in a Steady State Planetary Boundary Layer of the Atmosphere with Upward Heat Flux," AF(604)-6641, Dept. of Meteor., Penn. State Univ., pp 23-48, 1965.

61. G. Yamamoto, and A. Shimanuki, "Turbulent Transfer in Diabatic Conditions," J. Meteor. Soc. Japan, Ser. 2, 44, pp 301-307, 1966.

62. J. O'Brien, "A Note on the Vertical Structure of the Eddy Exchange Coefficient in the Planetary Boundary Layer," J. Atmos. Sci., 27, pp 1213-1215, Nov. 1970.

63. R. Bornstein, "The Two-Dimensional URBMET Urban Boundary Layer Model," J. Appl. Met., 14, pp 1459-1477, Dec. 1975.

64. F. Nieuwstadt, "The Computation of the Friction Velocity, u_*, and the Temperature Scale, T_*, from Temperature and Wind Velocity Profiles by Least-Square Methods," Bound. Lay. Met., 14, pp 235-246, 1978.

65. H. Tennekes, and J. Lumley, A First Course in Turbulence, Cambridge, MA, MIT Press, 1972.

66. A. Monin, Weather Forecasting as a Problem in Physics, Cambridge, MA, MIT Press, 1972.

67. VARR-II Users' Guide, Op. Cit., p. 88.

68. Ibid., p. 37.

69. J. Holton, An Introduction to Dynamic Meteorology, New York, Academic Press, 1978, pp 167-169.

70. G. Briggs, "A Plume Rise Model Compared with Observations," Jour. Air Poll. Con. Assoc., Vol. 15, No. 9, pp 433-438, Sep. 1965.

71. D. Turner, Workbook of Atmospheric Dispersion Estimates, Cincinnati, Ohio, Us. Dept. HEW, 1969.

72. D. Slade, ed., Meteorology and Atomic Energy--1968, Oak Ridge, Tenn., USAEC, TID-24190, July, 1968.

73. R. Meroney and J. Cermak, "Modeling of Atmospheric Transport and Fumigation at Shoreline Sites," Bound. Lay. Met., 9, pp 69-90, 1975.

74. R. West, "Field Investigation of Cooling Tower and Cooling Pond Plumes," EPA-600/7-78-059, Corvallis, Oregon, April, 1978.

75. J. Lumley, and B. Khajeh-nouri, "Computational Modeling of Turbulent Transport," in Advances in Geophysics, 18A, New York, Academic Press, 1974, pp 169-192.

APPENDIX

Computer Code Listing

```
*********************************************************************** ERAS0010
*                                                                     * ERAS0020
*       TO SET ELEMENTS OF REAL OR INTEGER ARRAYS TO ZERO. A1,A2,...  * ERAS0030
*       ARE ARRAY NAMES AND N1,N2,... ARE INTEGER VALUES OR           * ERAS0040
*       EXPRESSIONS GIVING THE ARRAY SIZES.                           * ERAS0050
**      I.E. - CALL ERASE(C,26*31,N,7*31,E,254)                      ** ERAS0060
*                                                                     * ERAS0070
*********************************************************************** ERAS0080
ERASE   START 0                                                         ERAS0090
        SAVE  (14,12),,*                                                ERAS0100
        BALR  12,0                                                      ERAS0110
        USING *,12                                                      ERAS0120
        SR    0,0                                                       ERAS0130
        SR    2,2           PARAMETER LIST INDEX=0                      ERAS0140
        L     6,=F'4'                                                   ERAS0150
E1      L     3,0(2,1)      LOAD 3 WITH ARRAY ADDRESS                   ERAS0160
        L     4,4(2,1)      LOAD 4 WITH ADDRESS OF ARRAY LENGTH         ERAS0170
        L     7,0(4)        LOAD 7 WITH ARRAY LENGTH-1 TIMES 4          ERAS0180
        SLA   7,2                                                       ERAS0190
        SR    7,6                                                       ERAS0200
        SR    5,5                                                       ERAS0210
E2      ST    0,0(5,3)      STORE ZERO                                  ERAS0220
        BXLE  5,6,E2                                                    ERAS0230
        LTR   4,4           TEST FOR LAST ARGUMENT IN LIST              ERAS0240
        BM    RETN                                                      ERAS0250
        A     2,=F'8'                                                   ERAS0260
        B     E1            PICK UP NEXT ARGUMENT PAIR                  ERAS0270
RETN    RETURN (14,12),T                                                ERAS0280
        END                                                             ERAS0290
      INTEGER BUFL,CF,CF1,CFB,CFC,CFI,CFL,CFR,CFS,CFT,CQF,ERF,TD,VNTP,
     1   VTP
      REAL NU,LIQ,LIQO,LIQI,LOUT                                        RGBMN60A
      DIMENSION CF(1),CQ(1),QCON(1),P(1),RX(1),RZ(1),TQ(1),TS(1),U(1),
     1   W(1),ER(1),FFX3(102),FFY3(102),PBTIM(2),UO(1),WO(1),TQO(1),
     2   TSO(1),SIE(1),SIEO(1),CHI(1),CHIO(1)                           RGBMN01A
     A,VAP(1),VAPO(1),LIQ(1),LIQO(1)                                    RGBMN60A
```

```
3    ,TYMF(25),FN(25),TYMT1(25),T1N(25),TYMT2(25),T2N(25),
4    COFBA(25),COFBB(25),COFBC(25),COFTA(25),COFTB(25),COFTC(25),
5    COFRA(25),COFRB(25),COFRC(25),COFLA(25),COFLB(25),COFLC(25),
6    OFOBTA(25),OFOBTB(25),OFOBTC(25),
7    OFOBRA(25),OFOBRB(25),OFOBRC(25),TAU(10),USL(32),USLOB(20),
8    USROB(20),USTOB(20),USBOB(20)
9,COFBD(25),COFBE(25),COFTD(25),COFTE(25),COFTF(25),COFBF(25),
*COFRD(25),COFRE(25),COFLD(25),COFLE(25),COFRF(25),COFLF(25),
AOFOBTD(25),OFOBTE(25),OFOBRD(25),OFOBRE(25),
B  OFOBTF(25),OFOBRF(25),
CTYMT3(25),TYMT4(25),TYMT5(25),T3N(25),T4N(25),T5N(25),
*  IICFR(1),IICFL(1),IICFT(1),IICFB(1)
*    ,ZERO1(1165),ZERO2(608),ZERO3(16),ZERO4(3)
 DIMENSION ZSIE(22),ZTQ(22),ZTS(22),ZVP(22),ZLQ(22),ZAP(22),WSP(22) RGBVM62A
 DIMENSION TRSTRT(5),WZSIE(100),WZTQ(100),WZTS(100)                 RGBVM55A
A,WZVP(100),WZLQ(100),WZAP(100),WWSP(100)                            RGBVM62A
 COMMON/VRCOM/A(14000)                                               RGBMN60A
 COMMON/RGB/RLAMB,CHII,GAMX,NRSTRT,TRSTRT,ZSIE,ZTQ,ZTS,WZSIE,WZTQ,   RGBVM55A
AWZTS,NPROF,WZVP,WZLQ,ZVP,ZLQ,GAML,GAMV,VAPI,LIQI                    RGBMN60A
B,WSP,WWSP,BKGND,DWNDS                                               RGBMN60B
 COMMON /VRCON/ ALP,ALP0,ALX,ALZ,B0,BETA,BUFL,CFI(9),CFS(9),CYL,
1    DT,DX,DZ,EM6,EPS,ERF,FSLIP,GAM,GAM1,GX,GZ,HDX,HDZ,I,I1,I2,I2K2,
2    IBP1,IBP2,IBR,IDATIN,IDIAG,IKP2,IOBS,IRSTRT,ITAPW,ITER,IVDI,
3    IVDO,K,K1,K2,K2NC,KBP1,KBP2,KBF,KNC,KWB,KWL,KWR,KWT,LABEL(20),
4    LPR,NCYC,NCYCB,NPRT,NU,NWPC,RDT,RDX,RDZ,RDZS,RIBKB,ROI,TD,TFIN,
5    TIMET,TIOSUM,TPL,TPLT,TPR,TPRT,TQI,TSI,TTD,TWTD,UI,WI
*   ,USR(32),UST(22),USB(22),USO(10),FFX3,FFY3
6    ,AW,BW,CW,EPSB,UBLI,UBRI,WBBI,WBTI,WEPS,WOBI,NTPAS,TGAM,CSUBP,
7    T0,SIEI,IDG,KDG,TI,MAT,RHO0,AT,TMU,TK,TYMF,FN,TYMT1,T1N,TYMT2,
8    T2N,RPRAN,NRESEX,NFLOW,NT1,NT2,TSTEP,KDERBC,UOBI,COFBA,COFBB,
9    COFBC,COFTA,COFTB,COFTC,COFRA,COFRB,COFRC,COFLA,COFLB,COFLC,
*    OFOBTA,OFOBTB,OFOBTC,OFOBRA,OFOBRB,OFOBRC,TAU,NTAU,USL,
1    USLOB,USROB,USTOB,USBOB,UMAX,WMAX
*   ,CSUBPO,EPSO,RDXDZS,RLENGH ,TQJET,TSJET
 COMMON /FLMCON/ DROU,DROUO,IPRFM
 COMMON /VRMAT3/ AI,BI,CI,AR,BR,CR,AMU,BMU,CMU,AK,BK,CK,ACP,BCP,CCP
```

```
 1                   ,VMIN
   COMMON/PROP/SIGN
  COMMON/EXTRA/NT3,NT4,NT5,TYMT3,TYMT4,TYMT5,T3N,T4N,T5N,COFBD,
 1COFBE,COFBF,COFTD,COFTE,COFTF,COFRD,COFRE,COFRF,COFLD,COFLE,
 2COFLF,OFOBTD,OFOBTE,OFOBTF,OFOBRD,OFOBRE,OFOBRF,IRESET,
 *NCYCLS,TADD,NIV,IOBRAN
   COMMON/INDEX/NWPCL,K2NCL
   COMMON/LARGE/DIFFCO(2400)
  EQUIVALENCE (A(1),CF),(A(2),U),(A(3),W),(A(4),P),(A(5),TQ),
 1   (A(6),TS),(A(7),ER,CQ),(A(8),UO),(A(9),WO),(A(10),TQO),
 2   (A(11),TSO),(A(12),SIE),(A(13),SIEO),(A(14),RX),(A(15),RZ),
 3   (A(16),IICFR),(A(17),IICFL),(A(18),IICFT),(A(19),IICFB),
 A   (A(20),CHI),(A(21),CHIO),                                    RGBMN01A
 B   (A(22),VAP),(A(23),VAPO),(A(24),LIQ),(A(25),LIQO),           RGBMN60A
 4   (ZERO1(1),ALP),(ZERO2(1),NT3),(ZERO3(1),AI),(ZERO4(1),DROU)
C NOTE. END - END OF NON-EXECUTABLE STATEMENTS .
C
C NOTE. NWPC = NUMBER OF WORDS PER MESH CELL .
      CALL ERASE (ZERO1,1165,ZERO2,608,ZERO3,16,ZERO4,3,A,14000)  RGBMN60A
      NWPC=25                                                     RGBMN60A
      NWPCL = 4
      IVDI=5
      IVDO=6
  100 WRITE(IVDO,1)
      READ(IVDI,2) IBR,KBR,IPRFM,NCYCLS,TADD,IRESET
      ERF=0
      IF( IPRFM.GT.0 ) CALL FLMINI
      IF( IBR ) 700,400,400
 400  PRINT 11
      CALL VSET
      WRITE(IVDO,3)
      IF( ERF.EQ.1 ) GO TO 700                                    VRC42002
      PRINT 12
      CALL VM
      IF( ERF.EQ.1 ) GO TO 700                                    VRC50002
      GO TO 100
```

```
700 IF( IPRFM.GT.0 ) CALL FLMFIN
C ***** FORMATS ***** FORMATS ***** FORMATS ***** .
  1 FORMAT(1H1,22H MAIN PROGRAM CALLED .)
 2  FORMAT(2(5X,I5),7X,I2,I11,F10.4,5X,I5)
3   FORMAT(1H ,27H SUBROUTINE VSET FINISHED .)
11  FORMAT(1H ,25H SUBROUTINE VSET CALLED .)
12  FORMAT(1H ,23H SUBROUTINE VM CALLED .)
    STOP
    END                                                          VRC70004
    BLOCK DATA
    COMMON/LARGE/DIFFCO(2400)
    REAL DIFFCO/2400*1.0/
    END
    SUBROUTINE IDLE
    INTEGER BUFL,CF,CF1,CFB,CFC,CFI,CFL,CFR,CFS,CFT,CQF,ERF,TD,VNTP,
   1   VTP
    REAL NU,LIQ,LIQO,LIQI,LOUT                                   RGBMN60A
    DIMENSION CF(1),CQ(1),QCON(1),P(1),RX(1),RZ(1),TQ(1),TS(1),U(1),
   1   W(1),ER(1),FFX3(102),FFY3(102),PBTIM(2),UO(1),WO(1),TQO(1),
   2   TSO(1),SIE(1),SIEO(1),CHI(1),CHIO(1)                      RGBMN01A
   A,VAP(1),VAPO(1),LIQ(1),LIQO(1)                               RGBMN60A
   3   ,TYMF(25),FN(25),TYMT1(25),T1N(25),TYMT2(25),T2N(25),
   4   COFBA(25),COFBB(25),COFBC(25),COFTA(25),COFTB(25),COFTC(25),
   5   COFRA(25),COFRB(25),COFRC(25),COFLA(25),COFLB(25),COFLC(25),
   6   OFOBTA(25),OFOBTB(25),OFOBTC(25),
   7   OFOBRA(25),OFOBRB(25),OFOBRC(25),TAU(10),USL(32),USLOB(20),
   8   USROB(20),USTOB(20),USBOB(20)
   9,COFBD(25),COFBE(25),COFTD(25),COFTE(25),COFTF(25),COFBF(25),
   *COFRD(25),COFRE(25),COFLD(25),COFLE(25),COFRF(25),COFLF(25),
   AOFOBTD(25),OFOBTE(25),OFOBRD(25),OFOBRE(25),
   B  OFOBTF(25),OFOBRF(25),
   CTYMT3(25),TYMT4(25),TYMT5(25),T3N(25),T4N(25),T5N(25),
   *  IICFR(1),IICFL(1),IICFT(1),IICFB(1)
   *   ,ZERO1(1165),ZERO2(608),ZERO3(16),ZERO4(3)
    DIMENSION ZSIE(22),ZTQ(22),ZTS(22),ZVP(22),ZLQ(22),ZAP(22),WSP(22)RGBVM62A
    DIMENSION TRSTRT(5),WZSIE(100),WZTQ(100),WZTS(100)           RGBVM55A
```

```
A,WZVP(100),WZLQ(100),WZAP(100),WWSP(100)                          RGBVM62A
 COMMON/VRCOM/A(14000)                                             RGBMN60A
 COMMON/RGB/RLAMB,CHII,GAMX,NRSTRT,TRSTRT,ZSIE,ZTQ,ZTS,WZSIE,WZTQ, RGBVM55A
AWZTS,NPROF,WZVP,WZLQ,ZVP,ZLQ,GAML,GAMV,VAPI,LIQI                  RGBMN60A
B,WSP,WWSP,BKGND,DWNDS                                             RGBMN60B
 COMMON /VRCON/ ALP,ALP0,ALX,ALZ,B0,BETA,BUFL,CFI(9),CFS(9),CYL,
1   DT,DX,DZ,EM6,EPS,ERF,FSLIP,GAM,GAM1,GX,GZ,HDX,HDZ,I,I1,I2,I2K2,
2   IBP1,IBP2,IBR,IDATIN,IDIAG,IKP2,IOBS,IRSTRT,ITAPW,ITER,IVDI,
3   IVDO,K,K1,K2,K2NC,KBP1,KBP2,KBR,KNC,KWB,KWL,KWR,KWT,LABEL(20),
4   LPR,NCYC,NCYCB,NPRT,NU,NWPC,RDT,RDX,RDZ,RDZS,RIBKB,ROI,TD,TFIN,
5   TIMET,TIOSUM,TPL,TPLT,TPR,TPRT,TQI,TSI,TTD,TWTD,UI,WI
*  ,USR(32),UST(22),USB(22),USO(10),FFX3,FFY3
6   ,AW,BW,CW,EPSB,UBLI,UBRI,WBBI,WBTI,WEPS,WOBI,NTPAS,TGAM,CSUBP,
7   TO,SIEI,IDG,KDG,TI,MAT,RHOO,AT,TMU,TK,TYMF,FN,TYMT1,T1N,TYMT2,
8   T2N,RPRAN,NRESEX,NFLOW,NT1,NT2,TSTEP,KDERBC,UOBI,COFBA,COFBB,
9   COFBC,COFTA,COFTB,COFTC,COFRA,COFRB,COFRC,COFLA,COFLB,COFLC,
*   OFOBTA,OFOBTB,OFOBTC,OFOBRA,OFOBRB,OFOBRC,TAU,NTAU,USL,
1   USLOB,USROB,USTOB,USBOB,UMAX,WMAX
*  ,CSUBPO,EPS0,RDXDZS,RLENGH ,TQJET,TSJET
 COMMON /FLMCON/ DROU,DROU0,IPRFM
 COMMON /VRMAT3/ AI,BI,CI,AR,BR,CR,AMU,BMU,CMU,AK,BK,CK,ACP,BCP,CCP
1                ,VMIN
  COMMON/PROP/SIGN
 COMMON/EXTRA/NT3,NT4,NT5,TYMT3,TYMT4,TYMT5,T3N,T4N,T5N,COFBD,
1COFBE,COFBF,COFTD,COFTE,COFTF,COFRD,COFRE,COFRF,COFLD,COFLE,
2COFLF,OFOBTD,OFOBTE,OFOBTF,OFOBRD,OFOBRE,OFOBRF,IRESET,
*NCYCLS,TADD,NIV,IOBRAN
  COMMON/INDEX/NWPCL,K2NCL
  COMMON/LARGE/DIFFCO(2400)
 EQUIVALENCE (A(1),CF),(A(2),U),(A(3),W),(A(4),P),(A(5),TQ),
1   (A(6),TS),(A(7),ER,CQ),(A(8),UO),(A(9),WO),(A(10),TQO),
2   (A(11),TSO),(A(12),SIE),(A(13),SIEO),(A(14),RX),(A(15),RZ),
3   (A(16),IICFR),(A(17),IICFL),(A(18),IICFT),(A(19),IICFB),
A   (A(20),CHI),(A(21),CHIO),                                      RGBMN01A
B   (A(22),VAP),(A(23),VAPO),(A(24),LIQ),(A(25),LIQO),             RGBMN60A
4   (ZERO1(1),ALP),(ZERO2(1),NT3),(ZERO3(1),AI),(ZERO4(1),DROU)
```

```
      ENTRY TAPREA
      REWIND 8
       READ(8) A,ZERO1,ZERO2,ZERO4,NWPCL
      WRITE(IVDO,50) TD,TIMET,NCYC
      IDATIN=1
      NCYCB=NCYC
      IRSTRT=1
C *****FORMATS ***** FORMATS ***** FORMATS *****
  50  FORMAT(1H ,19H TAPE FILE NUMBER =,I4,9H  TIMET =,1PE12.4,
     1   16H  CYCLE NUMBER =,I6)
      RETURN
      ENTRY TAPWRI
      TD=TD+1
      ITW=ITAPW
      REWIND 8
      WRITE(8) A,ZERO1,ZERO2,ZERO4,NWPCL
      WRITE(IVDO,51) TD,TIMET,NCYC
C *****FORMATS ***** FORMATS ***** FORMATS *****
  51  FORMAT(1H ,19H TAPE FILE NUMBER =,I4,9H  TIMET =,1PE12.4,
     1   16H  CYCLE NUMBER =,I6)
      RETURN
      ENTRY COARSE                                                      RGBID55A
C  RESTART ON A COARSER MESH FOR IBR AND KBR EVEN ONLY                  RGBID55A
      IHALF=IBP2/2                                                      RGBID55A
      KHALF=KBP2/2                                                      RGBID55A
C  MANAGES ATMOSPHERIC PROFILES DURING RESTARTS ON A COARSER MESH       RGBID55A
      DO 90 K=2,KHALF                                                   RGBID55A
      ZTQ(K)=(ZTQ(2*K-2)+ZTQ(2*K-1))/2.0                                RGBID55A
      ZTS(K)=(ZTS(2*K-2)+ZTS(2*K-1))/2.0                                RGBID55A
      ZLQ(K)=(ZLQ(2*K-2)+ZLQ(2*K-1))/2.0                                RGBID70A
      ZVP(K)=(ZVP(2*K-2)+ZVP(2*K-1))/2.0                                RGBID70A
      ZAP(K)=(ZAP(2*K-2)+ZAP(2*K-1))/2.0                                RGBID70A
      WSP(K)=(WSP(2*K-2)+WSP(2*K-1))/2.0                                RGBID70A
  90  ZSIE(K)=(ZSIE(2*K-2)+ZSIE(2*K-1))/2.0                             RGBID55A
      ZSIE(1)=ZSIE(2)                                                   RGBID55A
      ZTS(1)=ZTS(2)                                                     RGBID55A
```

```
      ZTQ(1)=ZTQ(2)                                                     RGBID55A 0217
      ZLQ(1)=ZLQ(2)                                                     RGBID70A 0218
      ZVP(1)=ZVP(2)                                                     RGBID70A 0219
      ZAP(1)=ZAP(2)                                                     RGBID70A 0220
      WSP(1)=WSP(2)                                                     RGBID70A 0221
      KHP1=KHALF+1                                                      RGBID55A 0222
      DO 95 K=KHP1,KBP1                                                 RGBID55A 0223
      ZTQ(K)=WZTQ((NRSTRT*KBR/2)+K-1)                                   RGBID55A 0224
      ZTS(K)=WZTS((NRSTRT*KBR/2)+K-1)                                   RGBID55A 0225
      ZLQ(K)=WZLQ((NRSTRT*KBR/2)+K-1)                                   RGBID70A 0226
      ZVP(K)=WZVP((NRSTRT*KBR/2)+K-1)                                   RGBID70A 0227
      ZAP(K)=WZAP((NRSTRT*KBR/2)+K-1)                                   RGBID70A 0228
      WSP(K)=WWSP((NRSTRT*KBR/2)+K-1)                                   RGBID70A 0229
   95 ZSIE(K)=WZSIE((NRSTRT*KBR/2)+K-1)                                 RGBID55A 0230
      ZSIE(KBP2)=ZSIE(KBP1)                                             RGBID55A 0231
      ZTS(KBP2)=ZTS(KBP1)                                               RGBID55A 0232
      ZTQ(KBP2)=ZTQ(KBP1)                                               RGBID55A 0233
      ZLQ(KBP2)=ZLQ(KBP1)                                               RGBID70A 0234
      ZVP(KBP2)=ZVP(KBP1)                                               RGBID70A 0235
      ZAP(KBP2)=ZAP(KBP1)                                               RGBID70A 0236
      WSP(KBP2)=WSP(KBP1)                                               RGBID70A 0237
C  RECOMPUTES DATA ASSOCIATED WITH DZ, DX FOR USE IN VM                 RGBID55A 0238
      DX=2.0*DX                                                         RGBID55A 0239
      DZ=2.0*DZ                                                         RGBID55A 0240
      RDX=1./DX                                                         RGBID55A 0241
      RDZ=1./DZ                                                         RGBID55A 0242
      HDX=.5*DX                                                         RGBID55A 0243
      HDZ=.5*DZ                                                         RGBID55A 0244
      RDZS=1./(DZ*DZ)                                                   RGBID55A 0245
      BETA=.5*RO/(RDX*RDX+RDZ*RDZ)                                      RGBID55A 0246
      EPSB=4.*NU/AMIN1(DX,DZ)                                           RGBID55A 0247
      RDXDZS=1./(RDX*RDX+RDZ*RDZ)                                       RGBID55A 0248
      X1=FLOAT(IBR)*DX                                                  RGBID55A 0249
      Z1=FLOAT(KBR)*DZ                                                  RGBID55A 0250
      RLENGH=1./AMAX1(X1,Z1)                                            RGBID55A 0251
C  BEGINS CELL BY CELL AVERAGING                                        RGBID55A 0252
```

```
      DO 100 I=2,IBP1                                                   RGBID55A
      DO 100 K=2,KBP1                                                   RGBID55A
      IK=1+NWPC*(((I-1)*KBP2)+K-1)                                      RGBID55A
      IF(I.GT.IHALF.OR.K.GT.KHALF) GO TO 200                            RGBID55A
C   COMPUTES INDICES FOR FLUID CELLS                                    RGBID55A
      J=2*(I-1)                                                         RGBID55A
      L=2*(K-1)                                                         RGBID55A
      IKR=1+NWPC*(((J-1)*KBP2)+L-1)                                     RGBID55A
      J=2*I-1                                                           RGBID55A
      IPKR=1+NWPC*(((J-1)*KBP2)+L-1)                                    RGBID55A
      L=2*K-1                                                           RGBID55A
      IPKPR=1+NWPC*(((J-1)*KBP2)+L-1)                                   RGBID55A
      J=2*(I-1)                                                         RGBID55A
      IKPR=1+NWPC*(((J-1)*KBP2)+L-1)                                    RGBID55A
C   COMPUTES FLUID CELL DENSITIES FOR CELL MASS AVERAGING               RGBID55A
      CIT=CI-SIE(IKR)                                                   RGBID55A
      TEMPLL=SI(AI,BI,CIT,-1)                                           RGBID55A
      CIT=CI-SIE(IPKR)                                                  RGBID55A
      TEMPLR=SI(AI,BI,CIT,-1)                                           RGBID55A
      CIT=CI-SIE(IKPR)                                                  RGBID55A
      TEMPUL=SI(AI,BI,CIT,-1)                                           RGBID55A
      CIT=CI-SIE(IPKPR)                                                 RGBID55A
      TEMPUR=SI(AI,BI,CIT,-1)                                           RGBID55A
      RHOLL=AR*TEMPLL*TEMPLL+BR*TEMPLL+CR                               RGBID55A
      RHOLR=AR*TEMPLR*TEMPLR+BR*TEMPLR+CR                               RGBID55A
      RHOUL=AR*TEMPUL*TEMPUL+BR*TEMPUL+CR                               RGBID55A
      RHOUR=AR*TEMPUR*TEMPUR+BR*TEMPUR+CR                               RGBID55A
      RHOSUM=RHOLL+RHOLR+RHOUL+RHOUR                                    RGBID55A
C   MASS AVERAGING OF FLUID CELLS FOR RESTART ON COARSER MESH           RGBID55A
      U(IK)=(U(IKR)*RHOLL+U(IPKR)*RHOLR+U(IKPR)*RHOUL+U(IPKPR)*RHOUR)/RHRGBID55A
     AOSUM                                                              RGBID55A
      UO(IK)=(UO(IKR)*RHOLL+UO(IPKR)*RHOLR+UO(IKPR)*RHOUL+UO(IPKPR)     RGBID55A
     A*RHOUR)/RHOSUM                                                    RGBID55A
      W(IK)=(W(IKR)*RHOLL+W(IPKR)*RHOLR+W(IKPR)*RHOUL+W(IPKPR)*RHOUR)/RHRGBID55A
     AOSUM                                                              RGBID55A
      WO(IK)=(WO(IKR)*RHOLL+WO(IPKR)*RHOLR+WO(IKPR)*RHOUL+WO(IPKPR)     RGBID55A
```

```
     A*RHOUR)/RHOSUM                                                      RGBID55A
      TS(IK)=(TS(IKR)+TS(IPKR)+TS(IKPR)+TS(IPKPR))/4.00                   RGBID55A
      TSO(IK)=(TSO(IKR)+TSO(IPKR)+TSO(IKPR)+TSO(IPKPR))/4.0               RGBID55A
      TQ(IK)=(TQ(IKR)*RHOLL+TQ(IPKR)*RHOLR+TQ(IKPR)*RHOUL+TQ(IPKPR)       RGBID55A
     A*RHOUR)/RHOSUM                                                      RGBID55A
      TQO(IK)=(TQO(IKR)*RHOLL+TQO(IPKR)*RHOLR+TQO(IKPR)*RHOUL+TQO(IPKPR)RGBID55A
     A*RHOUR)/RHOSUM                                                      RGBID55A
      SIE(IK)=(SIE(IKR)*RHOLL+SIE(IPKR)*RHOLR+SIE(IKPR)*RHOUL+SIE(IPKPR)RGBID55A
     A*RHOUR)/RHOSUM                                                      RGBID55A
      SIEO(IK)=(SIEO(IKR)*RHOLL+SIEO(IPKR)*RHOLR+SIEO(IKPR)*RHOUL+SIEO(IRGBID55A
     APKPR)*RHOUR)/RHOSUM                                                 RGBID55A
      CHI(IK)=(CHI(IKR)+CHI(IPKR)+CHI(IKPR)+CHI(IPKPR))/4.0               RGBID55A
      CHIO(IK)=(CHIO(IKR)+CHIO(IPKR)+CHIO(IKPR)+CHIO(IPKPR))/4.0          RGBID55A
      VAP(IK)=(VAP(IKR)+VAP(IPKR)+VAP(IKPR)+VAP(IPKPR))/4.0               RGBID70A
      VAPO(IK)=(VAPO(IKR)+VAPO(IPKR)+VAPO(IKPR)+VAPO(IPKPR))/4.0          RGBID70A
      LIQ(IK)=(LIQ(IKR)+LIQ(IPKR)+LIQ(IKPR)+LIQ(IPKPR))/4.0               RGBID70A
      LIQO(IK)=(LIQO(IKR)+LIQO(IPKR)+LIQO(IKPR)+LIQO(IPKPR))/4.0          RGBID70A
      P(IK)=0.0                                                           RGBID55A
      GO TO 100                                                           RGBID55A
C  INITIALIZATION OF CELLS THAT WEREN'T IN THE PREVIOUS RUN               RGBID55A
  200 U(IK)=0.0                                                           RGBID55A
      UO(IK)=0.0                                                          RGBID55A
      W(IK)=0.0                                                           RGBID55A
      WO(IK)=0.0                                                          RGBID55A
      SIE(IK)=ZSIE(K)                                                     RGBID55A
      SIEO(IK)=ZSIE(K)                                                    RGBID55A
      TS(IK)=ZTS(K)                                                       RGBID55A
      TSO(IK)=ZTS(K)                                                      RGBID55A
      TQ(IK)=ZTQ(K)                                                       RGBID55A
      TQO(IK)=ZTQ(K)                                                      RGBID55A
      CHI(IK)=BKGND                                                       RGBVM70A
      CHIO(IK)=BKGND                                                      RGBVM70A
      LIQ(IK)=ZLQ(K)                                                      RGBVM70A
      LIQO(IK)=ZLQ(K)                                                     RGBVM70A
      VAP(IK)=ZVP(K)                                                      RGBVM70A
      VAPO(IK)=ZVP(K)                                                     RGBVM70A
```

```
      P(IK)=0.0                                          RGBID55A
  100 CONTINUE                                           RGBID55A
      RETURN                                             RGBID55A
      ENTRY FILMCO
      RETURN
      ENTRY FLMCAL
      RETURN
      ENTRY FLMINI
      RETURN
      ENTRY FLMFIN
      RETURN
      ENTRY FLMGEN
      RETURN
      ENTRY VREQ
      RETURN
      ENTRY VRFLM
      RETURN
      END
      FUNCTION SI(XTBL,YTBL,X,N)
      COMMON/PROP/SIGN
      DIMENSION XTBL(1),YTBL(1)
      IF( N.LT.0 ) GO TO 200
      IF(X.LT.XTBL(1)) GO TO 16
      IF(X.GT.XTBL(N)) GO TO 31
      DO 10 I=1,N
      IF(X.EQ.XTBL(I)) GO TO 21
      IF(X.LT.XTBL(I)) GO TO 26
   10 CONTINUE
   16 J1 = 1
      J2 = 2
      GO TO 50
   21 SI = YTBL(I)
      GO TO 100
   26 J1 = I-1
      J2 = I
      GO TO 50
```

```
 31 J1 = N-1
    J2 = N
 50 SI=YTBL(J1)+(YTBL(J2)-YTBL(J1))*(X-XTBL(J1))/(XTBL(J2)-XTBL(J1))
100 RETURN
C NOTE. ROOTS OF QUADRATIC EQUATION - A*X**2 + B*X + C =0.0 .
200 A=XTBL(1)
    B=YTBL(1)
    C=X
     IF(A.NE.0.0) GO TO 205
     SI=-1.0*C/B
     RETURN
205  CONTINUE
    D=B*B - 4.*A*C
    IF( D ) 210,220,220
210 PRINT 211
    RETURN
220 DS=SQRT( D )
    IF (SIGN) 224,224,226
224 SI = -1.0 * (B + DS) / (2.0 * A)
    GO TO 230
226 SI = (DS - B) / (2.0 * A)
    GO TO 230
230 CONTINUE
    RETURN
C ***** FORMATS ***** FORMATS ***** FORMATS ***** .                    OLAY0029
211 FORMAT(1H ,28H ERROR - ROOTS ARE COMPLEX .)
    END
    SUBROUTINE VRPRT
    DIMENSION TPT(50,50)
    INTEGER BUFL,CF,CF1,CFB,CFC,CFI,CFL,CFR,CFS,CFT,CQF,ERF,TD,VNTP,
   1VTP,CFOUT
    REAL NU,LIQ,LIQO,LIQI,LOUT                                         RGBMN60A
    DIMENSION UOUT(7),VOUT(7),IOUT(7),KOUT(7),CFOUT(7),QOUT(7),
   1SOUT(7),TOUT(7),XOUT(7),GOUT(7),LOUT(7)                            RGBMO60A
    DIMENSION CF(1),CQ(1),QCON(1),P(1),RX(1),RZ(1),TQ(1),TS(1),U(1),
   1   W(1),ER(1),FFX3(102),FFY3(102),PBTIM(2),UO(1),WO(1),TQO(1),
```

```
2   TSO(1),SIE(1),SIEO(1),CHI(1),CHIO(1)                                RGBMN01A
A,VAP(1),VAPO(1),LIQ(1),LIQO(1)                                         RGBMN60A
3   ,TYMF(25),FN(25),TYMT1(25),T1N(25),TYMT2(25),T2N(25),
4   COFBA(25),COFBB(25),COFBC(25),COFTA(25),COFTB(25),COFTC(25),
5   COFRA(25),COFRB(25),COFRC(25),COFLA(25),COFLB(25),COFLC(25),
6   OFOBTA(25),OFOBTB(25),OFOBTC(25),
7   OFOBRA(25),OFOBRB(25),OFOBRC(25),TAU(10),USL(32),USLOB(20),
8   USROB(20),USTOB(20),USBOB(20)
9,COFBD(25),COFBE(25),COFTD(25),COFTE(25),COFTF(25),COFBF(25),
*COFRD(25),COFRE(25),COFLD(25),COFLE(25),COFRF(25),COFLF(25),
AOFOBTD(25),OFOBTE(25),OFOBRD(25),OFOBRE(25),
B  OFOBTF(25),OFOBRF(25),
CTYMT3(25),TYMT4(25),TYMT5(25),T3N(25),T4N(25),T5N(25),
*  IICFR(1),IICFL(1),IICFT(1),IICFB(1)
*   ,ZERO1(1165),ZERO2(608),ZERO3(16),ZERO4(3)
 DIMENSION ZSIE(22),ZTQ(22),ZTS(22),ZVP(22),ZLQ(22),ZAP(22),WSP(22)RGBVM62A
 DIMENSION TRSTRT(5),WZSIE(100),WZTQ(100),WZTS(100)                    RGBVM55A
A,WZVP(100),WZLQ(100),WZAP(100),WWSP(100)                               RGBVM62A
 COMMON/VRCOM/A(14000)                                                  RGBMN60A
 COMMON/RGB/RLAMB,CHII,GAMX,NRSTRT,TRSTRT,ZSIE,ZTQ,ZTS,WZSIE,WZTQ,      RGBVM55A
AWZTS,NPROF,WZVP,WZLQ,ZVP,ZLQ,GAML,GAMV,VAPI,LIQI                      RGBMN60A
B,WSP,WWSP,BKGND,DWNDS                                                  RGBMN60B
 COMMON /VRCON/ ALP,ALPO,ALX,ALZ,BO,BETA,BUFL,CFI(9),CFS(9),CYL,
1   DT,DX,DZ,EM6,EPS,ERF,FSLIP,GAM,GAM1,GX,GZ,HDX,HDZ,I,I1,I2,I2K2,
2   IBP1,IBP2,IBR,IDATIN,IDIAG,IKP2,IOBS,IRSTRT,ITAPW,ITER,IVDI,
3   IVDO,K,K1,K2,K2NC,KBP1,KBP2,KBR,KNC,KWB,KWL,KWR,KWT,LABEL(20),
4   LPR,NCYC,NCYCB,NPRT,NU,NWPC,RDT,RDX,RDZ,RDZS,RIBKB,ROI,TD,TFIN,
5   TIMET,TIOSUM,TPL,TPLT,TPR,TPRT,TQI,TSI,TTD,TWTD,UI,WI
*  ,USR(32),UST(22),USB(22),USO(10),FFX3,FFY3
6   ,AW,BW,CW,EPSB,UBLI,UBRI,WBBI,WBTI,WEPS,WOBI,NTPAS,TGAM,CSUBP,
7   TO,SIEI,IDG,KDG,TI,MAT,RHOO,AT,TMU,TK,TYMF,FN,TYMT1,T1N,TYMT2,
8   T2N,RPRAN,NRESEX,NFLOW,NT1,NT2,TSTEP,KDERBC,UOBI,COFBA,COFBB,
9   COFBC,COFTA,COFTB,COFTC,COFRA,COFRB,COFRC,COFLA,COFLB,COFLC,
*   OFOBTA,OFOBTB,OFOBTC,OFOBRA,OFOBRB,OFOBRC,TAU,NTAU,USL,
1   USLOB,USROB,USTOB,USBOB,UMAX,WMAX
*  ,CSUBPO,EPSO,RDXDZS,RLENGH ,TQJET,TSJET
```

```
      COMMON /VRMAT3/ AI,BI,CI,AR,BR,CR,AMU,BMU,CMU,AK,BK,CK,ACP,BCP,CCP
     1                ,VMIN
       COMMON/PROP/SIGN
      COMMON/EXTRA/NT3,NT4,NT5,TYMT3,TYMT4,TYMT5,T3N,T4N,T5N,COFBD,
     1COFBE,COFBF,COFTD,COFTE,COFTF,COFRD,COFRE,COFRF,COFLD,COFLE,
     2COFLF,OFOBTD,OFOBTE,OFOBTF,OFOBRD,OFOBRE,OFOBRF,IRESET,
     *NCYCLS,TADD,NIV,IOBRAN
       COMMON/INDEX/NWPCL,K2NCL
      COMMON /FLMCON/ DROU,DROUO,IPRFM
       COMMON/LARGE/DIFFCO(2400)
      EQUIVALENCE (A(1),CF),(A(2),U),(A(3),W),(A(4),P),(A(5),TQ),
     1   (A(6),TS),(A(7),ER,CQ),(A(8),UO),(A(9),WO),(A(10),TQO),
     2   (A(11),TSO),(A(12),SIE),(A(13),SIEO),(A(14),RX),(A(15),RZ),
     3   (A(16),IICFR),(A(17),IICFL),(A(18),IICFT),(A(19),IICFB),
     A   (A(20),CHI),(A(21),CHIO),                                    RGBMN01A
     B   (A(22),VAP),(A(23),VAPO),(A(24),LIQ),(A(25),LIQO),           RGBMN60A
     4   (ZERO1(1),ALP),(ZERO2(1),NT3),(ZERO3(1),AI),(ZERO4(1),DROU)
C NOTE. END - END OF NON-EXECUTABLE STATEMENTS .
C     PRODUCES A CELL BY CELL OUTPUT OF STORED VARIABLES (22 X 22 ONLY)
      WRITE(IVDO,5)
   96 DO 103 ILOOP=1,4
      IREST=(ILOOP-1)*5
   97 DO 102 KLOOP=1,5
      KREST=(KLOOP-1)*5
   98 DO 100 KINV=1,5
      K=23-KINV-KREST
      IF(K.EQ.0) GO TO 101
      DO 99 IPART=1,7
      I=IPART+IREST
      IK=1+NWPC*(((I-1)*KBP2)+K-1)
      UOUT(IPART)=U(IK)
      VOUT(IPART)=W(IK)
      IOUT(IPART)=I
      KOUT(IPART)=K
      CFOUT(IPART)=CF(IK)
      QOUT(IPART)=TQ(IK)
```

```
      SOUT(IPART)=TS(IK)
      XOUT(IPART)=CHI(IK)                                      RGBM001A
      GOUT(IPART)=VAP(IK)                                      RGBM060A
      LOUT(IPART)=LIQ(IK)                                      RGBM060A
      SIEC=SIE(IK)
      CIT=CI-SIEC
      TOUT(IPART)=SI(AI,BI,CIT,-1)
      IF(CF(IK).GE.30)  TOUT(IPART)=P(IK)
   99 CONTINUE
      WRITE(IVDO,20)  (VOUT(L),L=1,7)
      WRITE(IVDO,10)
      WRITE(IVDO,30)  (IOUT(L),KOUT(L),L=1,7)
      WRITE(IVDO,40)  (TOUT(L),L=1,7)
      WRITE(IVDO,10)
      WRITE(IVDO,50)  (CFOUT(L),UOUT(L),L=1,7)
      WRITE(IVDO,70)  (SOUT(L),L=1,7)
      WRITE(IVDO,60)  (QOUT(L),L=1,7)
      WRITE(IVDO,80)  (XOUT(L),L=1,7)                          RGBM001A
      WRITE(IVDO,85)  (GOUT(L),L=1,7)                          RGBM060A
      WRITE(IVDO,90)  (LOUT(L),L=1,7)                          RGBM060A
  100 CONTINUE
  101 WRITE(IVDO,7)  TIMET,NCYC,ITER,DT
      WRITE(IVDO,5)
  102 CONTINUE
  103 CONTINUE
      RETURN
    5 FORMAT('1')
    7 FORMAT(1H ,5HTIME=,1PE12.4,3H  , ,14HCYCLE NUMBER =,I5,3H  , ,
     1 28H PRESSURE ITERATION NUMBER =,I4,3H  , ,4HDT =,E12.4)
   10 FORMAT(' ',7('X',17X))
   20 FORMAT(' ',7(5HXXXXX,1X,F7.3,1X,4HXXXX))
   30 FORMAT(' ',7(1HX,5X,'(',I2,',',I2,')',5X))
   40 FORMAT(' ',7(1HX,3X,F7.3,1X,' F',4X))
   50 FORMAT(' ',3X,7(4X,I2,5X,F7.3))
   60 FORMAT(' ',7(1HX,2X,'TKE=',1PE10.3,1X))
   70 FORMAT(' ',7(1HX,2X,'TNU=',1PE10.3,1X))
```

```
80   FORMAT(' ',7(1HX,2X,'CHI=',1PE10.3,1X))                     RGBM001A
85   FORMAT(' ',7(1HX,2X,'VAP=',1PE10.3,1X))                     RGBM060A
90   FORMAT(' ',7(1HX,2X,'LIQ=',1PE10.3,1X))                     RGBM060A
     END
     SUBROUTINE VSET
     INTEGER BUFL,CF,CF1,CFB,CFC,CFI,CFL,CFR,CFS,CFT,CQF,ERF,TD,VNTP,
    1   VTP
     REAL NU,LIQ,LIQO,LIQI,LOUT                                    RGBMN60A
     DIMENSION CF(1),CQ(1),QCON(1),P(1),RX(1),RZ(1),TQ(1),TS(1),U(1),
    1   W(1),ER(1),FFX3(102),FFY3(102),PBTIM(2),UO(1),WO(1),TQO(1),
    2   TSO(1),SIE(1),SIEO(1),CHI(1),CHIO(1)                     RGBMN01A
    A,VAP(1),VAPO(1),LIQ(1),LIQO(1)                                RGBMN60A
    3   ,TYMF(25),FN(25),TYMT1(25),T1N(25),TYMT2(25),T2N(25),
    4   COFBA(25),COFBB(25),COFBC(25),COFTA(25),COFTB(25),COFTC(25),
    5   COFRA(25),COFRB(25),COFRC(25),COFLA(25),COFLB(25),COFLC(25),
    6   OFOBTA(25),OFOBTB(25),OFOBTC(25),
    7   OFOBRA(25),OFOBRB(25),OFOBRC(25),TAU(10),USL(32),USLOB(20),
    8   USROB(20),USTOB(20),USBOB(20)
    9,COFBD(25),COFBE(25),COFTD(25),COFTE(25),COFTF(25),COFBF(25),
     COFRD(25),COFRE(25),COFLD(25),COFLE(25),COFRF(25),COFLF(25),
    AOFOBTD(25),OFOBTE(25),OFOBRD(25),OFOBRE(25),
    B  OFOBTF(25),OFOBRF(25),
    CTYMT3(25),TYMT4(25),TYMT5(25),T3N(25),T4N(25),T5N(25),
      IICFR(1),IICFL(1),IICFT(1),IICFB(1)
    *   ,ZERO1(1165),ZERO2(608),ZERO3(16),ZERO4(3)
     DIMENSION ZSIE(22),ZTQ(22),ZTS(22),ZVP(22),ZLQ(22),ZAP(22),WSP(22)RGBVM62A
     DIMENSION TRSTRT(5),WZSIE(100),WZTQ(100),WZTS(100)            RGBVM55A
    A,WZVP(100),WZLQ(100),WZAP(100),WWSP(100)                      RGBVM62A
     COMMON/VRCOM/A(14000)                                         RGBMN60A
     COMMON/RGB/RLAMB,CHII,GAMX,NRSTRT,TRSTRT,ZSIE,ZTQ,ZTS,WZSIE,WZTQ, RGBVM55A
    AWZTS,NPROF,WZVP,WZLQ,ZVP,ZLQ,GAML,GAMV,VAPI,LIQI              RGBMN60A
    B,WSP,WWSP,BKGND,DWNDS                                         RGBMN60B
     COMMON /VRCON/ ALP,ALPO,ALX,ALZ,BO,BETA,BUFL,CFI(9),CFS(9),CYL,
    1   DT,DX,DZ,EM6,EPS,ERF,FSLIP,GAM,GAM1,GX,GZ,HDX,HDZ,I,I1,I2,I2K2,
    2   IBP1,IBP2,IBR,IDATIN,IDIAG,IKP2,IOBS,IRSTRT,ITAPW,ITER,IVDI,
    3   IVDO,K,K1,K2,K2NC,KBP1,KBP2,KBR,KNC,KWB,KWL,KWR,KWT,LABEL(20),
```

```
     4   LPR,NCYC,NCYCB,NPRT,NU,NWPC,RDT,RDX,RDZ,RDZS,RIBKB,ROI,TD,TFIN,
     5   TIMET,TIOSUM,TPL,TPLT,TPR,TPRT,TQI,TSI,TTD,TWTD,UI,WI
        ,USR(32),UST(22),USB(22),USO(10),FFX3,FFY3
     6   ,AW,BW,CW,EPSB,UBLI,UBRI,WBBI,WBTI,WEPS,WOBI,NTPAS,TGAM,CSUBP,
     7   TO,SIEI,IDG,KDG,TI,MAT,RHOO,AT,TMU,TK,TYMF,FN,TYMT1,T1N,TYMT2,
     8   T2N,RPRAN,NRESEX,NFLOW,NT1,NT2,TSTEP,KDERBC,UOBI,COFBA,COFBB,
     9   COFBC,COFTA,COFTB,COFTC,COFRA,COFRB,COFRC,COFLA,COFLB,COFLC,
     *   OFOBTA,OFOBTB,OFOBTC,OFOBRA,OFOBRB,OFOBRC,TAU,NTAU,USL,
     1   USLOB,USROB,USTOB,USBOB,UMAX,WMAX
     *  ,CSUBPO,EPSO,RDXDZS,RLENGH ,TQJET,TSJET
      COMMON /FLMCON/ DROU,DROUO,IPRFM
      COMMON /VRMAT3/ AI,BI,CI,AR,BR,CR,AMU,BMU,CMU,AK,BK,CK,ACP,BCP,CCP
     1               ,VMIN
       COMMON/PROP/SIGN
      COMMON/EXTRA/NT3,NT4,NT5,TYMT3,TYMT4,TYMT5,T3N,T4N,T5N,COFBD,
     1COFBE,COFBF,COFTD,COFTE,COFTF,COFRD,COFRE,COFRF,COFLD,COFLE,
     2COFLF,OFOBTD,OFOBTE,OFOBTF,OFOBRD,OFOBRE,OFOBRF,IRESET,
      NCYCLS,TADD,NIV,IOBRAN
       COMMON/INDEX/NWPCL,K2NCL
       COMMON/LARGE/DIFFCO(2400)
      EQUIVALENCE (A(1),CF),(A(2),U),(A(3),W),(A(4),P),(A(5),TQ),
     1   (A(6),TS),(A(7),ER,CQ),(A(8),UO),(A(9),WO),(A(10),TQO),
     2   (A(11),TSO),(A(12),SIE),(A(13),SIEO),(A(14),RX),(A(15),RZ),
     3   (A(16),IICFR),(A(17),IICFL),(A(18),IICFT),(A(19),IICFB),
     A   (A(20),CHI),(A(21),CHIO),                                      RGBMN01A
     B   (A(22),VAP),(A(23),VAPO),(A(24),LIQ),(A(25),LIQO),             RGBMN60A
     4   (ZERO1(1),ALP),(ZERO2(1),NT3),(ZERO3(1),AI),(ZERO4(1),DROU)
C NOTE. END - END OF NON-EXECUTABLE STATEMENTS .
C
C
C NOTE. VSET IS RESPONSIBLE FOR MESH,PARTICLE AND FILM INITIALIZATION .
C
      IDATIN=0
      IF( IBR.EQ.0 ) CALL TAPREA
C NOTE. READS,WRITES PRIMARY INPUT DATA .
      READ(IVDI,1) LABEL
```

```
      READ(IVDI,2)     DT,TPRT,TPLT,TWTD,TFIN,ITAPW,NPRT,IDIAG,LPR,IOBS
     1 ,IDG,KDG
      WRITE(IVDO,50) IBR,KBR,IPRFM,NCYCLS,TADD,IRESET
      WRITE(IVDO,1) LABEL
      WRITE(IVDO,51) DT,TPRT,TPLT,TWTD,TFIN,ITAPW,NPRT,IDIAG,LPR,IOBS
     1 ,IDG,KDG
      RDT=1./DT
      IF( IPRFM.LT.1 ) TPLT=2.*TFIN
      TPL=TPLT
      TPR=TPRT
      TTD=TWTD
      IF( IDATIN.LT.1 ) GO TO 100
      TIMET=TIMET+TADD
      TWTD=TIMET
      TPRT=TWTD
      TPLT=TPRT
      CALL MESHMK
      IF (IPRFM.LT.1) GO TO 500
      CALL FLMGEN
      CALL FILMCO
      GO TO 500
C NOTE. INITIALIZES CONSTANTS .
  100 TIMET=0.0
      IRSTRT=0
      TD=0                                                              VRS12001
      NCYC=0                                                            VRS12002
      NCYCB=0
      EM6=1.E-6                                                         VRS12014
C NOTE. INITIALIZES CELL INDEX QUANTITIES .
      IBP1=IBR + 1
      KBP1=KBR+1                                                        VRS12402
      IBP2=IBR+2                                                        VRS12404
      KBP2=KBR+2                                                        VRS12406
      I2K2=IBP2*KBP2*NWPC                                               VRS12408
      KNC=KBR*NWPC
      K2NC=KBP2*NWPC                                                    VRS12412
```

```
      K2NCL = KBP2 * NWPCL
      IKP2=IBR*K2NC                                                   VRS12420
      IKMK=I2K2 + 2*K2NC
      RIBKB=1./FLOAT(IBR*KBR)
C NOTE. GENERATES BOTH MESH AND FILM REGIONS , RESPECTIVELY .
      CALL MESHMK
      IF( IPRFM.LT.1 ) GO TO 2000
      CALL FLMGEN
      CALL FILMCO
 2000 WRITE(IVDO,60)
  500  K2NCL=KBP2*NWPCL
      WRITE(IVDO,70)
       WRITE(IVDO,80)
      I1=2
      K1=2
      I2=IBP1
      K2 = KBP1
      KKL = 0
      KK = 0
      DO 511 I=I1,I2
      KK = KK + K2NC
      KKL = KKL + K2NCL
      LWPC = 1
      LWPCL = 1
      DO 510 K=K1,K2
      LWPC = LWPC + NWPC
      LWPCL = LWPCL + NWPCL
      IK = KK + LWPC
      IKL = KKL + LWPCL
      IPK = IK + K2NC
      IMK = IK - K2NC
      IKP = IK + NWPC
      IKM = IK - NWPC
      CPC = CP(IK)
      CPR = CP(IPK)
      CPL = CP(IMK)
```

```
      CFT = CF(IKP)
      CFB = CF(IKM)
      IF (CFC.NE.1) GO TO 510
      IF (CFR.NE.1) DIFFCO( IKL  ) = 0.0
      IF (CFL.NE.1) DIFFCO(IKL+2)= 0.0
      IF (CFT.NE.1) DIFFCO( IKL+1) = 0.0
      IF (CFB.NE.1) DIFFCO( IKL+3) = 0.0
      DCR = DIFFCO(IKL)
      DCT = DIFFCO(IKL+1)
      DCL = DIFFCO(IKL+2)
      DCB = DIFFCO(IKL+3)
       WRITE(IVDO,75) I,K,IK,IKL,CFC,CFR,CFT,CFL,CFB,DCR,DCT,DCL,DCB
  510 CONTINUE
 511  CONTINUE
  520 RETURN
C ***** FORMATS ***** FORMATS ***** FORMATS ***** .
    1 FORMAT(20A4)
    2 FORMAT(5F8.3,5I2,2I3)
 50   FORMAT(1H ,4X,4HIBR=,I5,/,5X,4HKBR=,I5,/,3X,6HIPRFM=,I2,/,5X,
     1 8HNCYCLST=,I10,/,5X,5HTADD=,E12.5,5X,7HIRESET=,I5)
   51 FORMAT(1H ,5X,3HDT=,1PE12.5/4X,5HTPRT=,E12.5/4X,5HTPLT=,E12.5/
     1 4X,5HTWTD=,E12.5/4X,5HTFIN=,E12.5/3X,6HITAPW=,I2/4X,5HNPRT=,I2/
     2 3X,6HIDIAG=,I2/5X,4HLPR=,I2/4X,5HIOBS=,I2/5X,4HIDG=,I3/5X,4HKDG=,
     3 I3)
   52 FORMAT(1H ,104H *** ERROR 001 - MESH ARRAY A() IS DIMENSIONED TOO
     1SMALL FOR MESH PARAMETERS ,I.E.   IBR  AND  KBR . ***)
   60 FORMAT(1H ,63H NOTE. COMPLETION OF     VSET     - VARR II SET UP G
     1ENERATION .)
  70  FORMAT(1H1)
 75    FORMAT(1H ,9I6,4F6.1)
 80    FORMAT(1H ,5X,1HI,5X,1HK,4X,2HIK,3X,3HIKL,3X,3HCFC,3X,3HCFR,3X,
     1 3HCFT,3X,3HCFL,3X,3HCFB,3X,3HDCR,3X,3HDCT,3X,3HDCL,3X,3HDCB)
      END                                                               VRS99999
      SUBROUTINE MESHMK
      INTEGER BUFL,CF,CF1,CFB,CFC,CFI,CFL,CFR,CFS,CFT,CQF,ERF,TD,VNTP,
     1   VTP
```

```
      REAL NU,LIQ,LIQO,LIQI,LOUT                                        RGBMN60A
      DIMENSION CF(1),CQ(1),QCON(1),P(1),RX(1),RZ(1),TQ(1),TS(1),U(1),
     1   W(1),ER(1),FFX3(102),FFY3(102),PBTIM(2),UO(1),WO(1),TQO(1),
     2   TSO(1),SIE(1),SIEO(1),CHI(1),CHIO(1)                           RGBMN01A
     A,VAP(1),VAPO(1),LIQ(1),LIQO(1)                                    RGBMN60A
     3   ,TYMP(25),FN(25),TYMT1(25),T1N(25),TYMT2(25),T2N(25),
     4   COFBA(25),COFBB(25),COFBC(25),COFTA(25),COFTB(25),COFTC(25),
     5   COFRA(25),COFRB(25),COFRC(25),COFLA(25),COFLB(25),COFLC(25),
     6   OFOBTA(25),OFOBTB(25),OFOBTC(25),
     7   OFOBRA(25),OFOBRB(25),OFOBRC(25),TAU(10),USL(32),USLOB(20),
     8   USROB(20),USTOB(20),USBOB(20)
     9,COFBD(25),COFBE(25),COFTD(25),COFTE(25),COFTF(25),COFBF(25),
     *COFRD(25),COFRE(25),COFLD(25),COFLE(25),COFRF(25),COFLF(25),
     AOFOBTD(25),OFOBTE(25),OFOBRD(25),OFOBRE(25),
     B  OFOBTF(25),OFOBRF(25),
     CTYMT3(25),TYMT4(25),TYMT5(25),T3N(25),T4N(25),T5N(25),
     *  IICFR(1),IICFL(1),IICFT(1),IICFB(1)
     *   ,ZERO1(1165),ZERO2(608),ZERO3(16),ZERO4(3)
      DIMENSION ZSIE(22),ZTQ(22),ZTS(22),ZVP(22),ZLQ(22),ZAP(22),WSP(22) RGBVM62A
      DIMENSION TRSTRT(5),WZSIE(100),WZTQ(100),WZTS(100)                RGBVM55A
     A,WZVP(100),WZLQ(100),WZAP(100),WWSP(100)                          RGBVM62A
      COMMON/VRCOM/A(14000)                                             RGBMN60A
      COMMON/RGB/RLAMB,CHII,GAMX,NRSTRT,TRSTRT,ZSIE,ZTQ,ZTS,WZSIE,WZTQ, RGBVM55A
     AWZTS,NPROP,WZVP,WZLQ,ZVP,ZLQ,GAML,GAMV,VAPI,LIQI                  RGBMN60A
     B,WSP,WWSP,BKGND,DWNDS                                             RGBMN60B
      COMMON /VRCON/ ALP,ALPO,ALX,ALZ,BO,BETA,BUFL,CFI(9),CFS(9),CYL,
     1   DT,DX,DZ,EM6,EPS,ERF,FSLIP,GAM,GAM1,GX,GZ,HDX,HDZ,I,I1,I2,I2K2,
     2   IBP1,IBP2,IBR,IDATIN,IDIAG,IKP2,IOBS,IRSTRT,ITAPW,ITER,IVDI,
     3   IVDO,K,K1,K2,K2NC,KBP1,KBP2,KBR,KNC,KWB,KWL,KWR,KWT,LABEL(20),
     4   LPR,NCYC,NCYCB,NPRT,NU,NWPC,RDT,RDX,RDZ,RDZS,RIBKB,ROI,TD,TFIN,
     5   TIMET,TIOSUM,TPL,TPLT,TPR,TPRT,TQI,TSI,TTD,TWTD,UI,WI
        ,USR(32),UST(22),USB(22),USO(10),FFX3,FFY3
     6   ,AW,BW,CW,EPSB,UBLI,UBRI,WBBI,WBTI,WEPS,WOBI,NTPAS,TGAM,CSUBP,
     7   TO,SIET,IDG,KDG,TI,MAT,RHOO,AT,TMU,TK,TYMP,FN,TYMT1,T1N,TYMT2,
     8   T2N,RPRAN,NRESEX,NFLOW,NT1,NT2,TSTEP,KDERBC,UOBI,COFBA,COFBB,
     9   COFBC,COFTA,COFTB,COFTC,COFRA,COFRB,COFRC,COFLA,COFLB,COFLC,
```

```
*   OFOBTA,OFOBTB,OFOBTC,OFOBRA,OFOBRB,OFOBRC,TAU,NTAU,USL,
1   USLOB,USROB,USTOB,USBOB,UMAX,WMAX
*   ,CSUBPO,EPSO,RDXDZS,RLENGH ,TQJET,TSJET
     COMMON /FLMCON/ DROU,DROUO,IPRFM
     COMMON /VRMAT3/ AI,BI,CI,AR,BR,CR,AMU,BMU,CMU,AK,BK,CK,ACP,BCP,CCP
1                  ,VMIN
      COMMON/PROP/SIGN
     COMMON/EXTRA/NT3,NT4,NT5,TYMT3,TYMT4,TYMT5,T3N,T4N,T5N,COFBD,
    1COFBE,COFBF,COFTD,COFTE,COFTF,COFRD,COFRE,COFRF,COFLD,COFLE,
    2COFLF,OFOBTD,OFOBTE,OFOBTF,OFOBRD,OFOBRE,OFOBRF,IRESET,
    *NCYCLS,TADD,NIV,IOBRAN
      COMMON/INDEX/NWPCL,K2NCL
      COMMON/LARGE/DIFFCO(2400)
     EQUIVALENCE (A(1),CF),(A(2),U),(A(3),W),(A(4),P),(A(5),TQ),
    1   (A(6),TS),(A(7),ER,CQ),(A(8),UO),(A(9),WO),(A(10),TQO),
    2   (A(11),TSO),(A(12),SIE),(A(13),SIEO),(A(14),RX),(A(15),RZ),
    3   (A(16),IICFR),(A(17),IICFL),(A(18),IICFT),(A(19),IICFB),
    A   (A(20),CHI),(A(21),CHIO),                                        RGBMN01A
    B   (A(22),VAP),(A(23),VAPO),(A(24),LIQ),(A(25),LIQO),               RGBMN60A
    4   (ZERO1(1),ALP),(ZERO2(1),NT3),(ZERO3(1),AI),(ZERO4(1),DROU)
C NOTE. END - END OF NON-EXECUTABLE STATEMENTS .
C
C NOTE. MESHMK IS RESPONSIBLE FOR GENERATION OF MESH SUBREGIONS .
C NOTE. READS,WRITES PRIMARY MESH INPUT DATA .
     READ(IVDI,1)    DX,DZ,GX,GZ,ALX,ALZ,CYL,BO,EPS,VMIN                 MESH    6
     READ (IVDI,2) KWR,KWL,KWT,KWB,FSLIP,ALP,GAM,ALPO,GAM1,NU,TQJET,
    * TSJET
     READ(IVDI,7)    AW,BW,CW,WEPS,KDERBC,UBRI,UBLI,WBTI,WBBI
     READ(IVDI,8)    WOBI,UOBI,CSUBPO
     READ(IVDI,10)    TGAM,TO,TI,TSTEP,MAT,NRESEX
     READ(IVDI,1)    AI,BI,CI,AR,BR,CR,AMU,BMU,CMU
     READ (IVDI,1) AK,BK,CK,ACP,BCP,CCP,SIGN
     READ(IVDI,11) NFLOW,NT1,NT2,NT3,NT4,NT5,NTAU
     WRITE(IVDO,61) NFLOW,NT1,NT2,NT3,NT4,NT5,NTAU
      IF(NFLOW.GT.0) GO TO 190
      NIV=1.0
```

```
      NFLOW =- NFLOW
 190  CONTINUE
      READ (IVDI,12)    ( TYMF(I),FN(I),I=1,NFLOW )
      READ(IVDI,12)     ( TYMT1(I),T1N(I),I=1,NT1 )
      READ (IVDI,12)    ( TYMT2(I),T2N(I),I=1,NT2 )
       IF(NT3.EQ.0) GO TO 195
      READ (IVDI,12) (TYMT3(I),T3N(I),I=1,NT3)
       IF(NT4.EQ.0) GO TO 195
      READ (IVDI,12) (TYMT4(I),T4N(I),I=1,NT4)
       IF(NT5.EQ.0) GO TO 195
      READ(IVDI,12) (TYMT5(I),T5N(I),I=1,NT5)
 195  CONTINUE
      IF( NTAU.LT.1 ) GO TO 200
      READ (IVDI,12)    ( TAU (I),I=1,NTAU )
C NOTE. READ COEFFICIENTS A,B, AND C FOR THE BOTTOM EXTERIOR BOUNDARY .
 200  READ(IVDI,13) I,COFA,COFB,COFC,COFD,COFE,COFF
      IF( I.LT.1 ) GO TO 210
      COFBA(I)=COFA
      COFBB(I)=COFB
      COFBC(I)=COFC
      COFBD(I)=COFD
      COFBE(I)=COFE
      COFBF(I)=COFF
      WRITE(IVDO,64) I,COFBA(I),COFBB(I),COFBC(I),COFBD(I),COFBE(I),
     1  COFBF(I)
      GO TO 200
C NOTE. READ COEFFICIENTS A,B, AND C FOR THE   TOP  EXTERIOR BOUNDARY .
 210  READ(IVDI,13) I,COFA,COFB,COFC,COFD,COFE,COFF
      IF( I.LT.1 ) GO TO 220
      COFTA(I)=COFA
      COFTB(I)=COFB
      COFTC(I)=COFC
      COFTD(I)=COFD
      COFTE(I)=COFE
      COFTF(I)=COFF
      WRITE(IVDO,64) I,COFTA(I),COFTB(I),COFTC(I),COFTD(I),COFTE(I),
```

```
    1  COFTF(I)
      GO TO 210
C NOTE. READ COEFFICIENTS A,B, AND C FOR THE RIGHT  EXTERIOR BOUNDARY .
  220 READ(IVDI,13) I,COFA,COFB,COFC,COFD,COFE,COFF
      IF( I.LT.1 ) GO TO 230
      COFRA(I)=COFA
      COFRB(I)=COFB
      COFRC(I)=COFC
      COFRD(I)=COFD
      COFRE(I)=COFE
      COFRF(I)=COFF
      WRITE(IVDO,64) I,COFRA(I),COFRB(I),COFRC(I),COFRD(I),COFRE(I),
    1  COFRF(I)
      GO TO 220
C NOTE. READ COEFFICIENTS A,B, AND C FOR THE  LEFT  EXTERIOR BOUNDARY .
  230 READ(IVDI,13) I,COFA,COFB,COFC,COFD,COFE,COFF
      IF( I.LT.1 ) GO TO 240
      COFLA(I)=COFA
      COFLB(I)=COFB
      COFLC(I)=COFC
      COFLD(I)=COFD
      COFLE(I)=COFE
      COFLF(I)=COFF
      WRITE(IVDO,64) I,COFLA(I),COFLB(I),COFLC(I),COFLD(I),COFLE(I),
    1  COFLF(I)
      GO TO 230
C NOTE. READ COEFFICIENTS A,B, AND C FOR THE   TOP INTERIOR OBSTACLE .
  240 READ(IVDI,13) I,COFA,COFB,COFC,COFD,COFE,COFF
      IF( I.LT.1 ) GO TO 250
      OFOBTA(I)=COFA
      OFOBTB(I)=COFB
      OFOBTC(I)=COFC
      OFOBTD(I)=COFD
      OFOBTE(I)=COFE
      OFOBTF(I)=COFF
      WRITE(IVDO,64) I,OFOBTA(I),OFOBTB(I),OFOBTC(I),OFOBTD(I),
```

```
     1OFOBTE(I),OFOBTF(I)
      GO TO 240
C NOTE. READ COEFFICIENTS A,B, AND C FOR THE RIGHT INTERIOR OBSTACLE .
 250  READ(IVDI,13) I,COFA,COFB,COFC,COFD,COFE,COFF
      IF( I.LT.1 ) GO TO 310
      OFOBRA(I)=COFA
      OFOBRB(I)=COFB
      OFOBRC(I)=COFC
      OFOBRD(I)=COFD
       OFOBRE(I)=COFE
      OFOBRF(I)=COFF
      WRITE(IVDO,64) I,OFOBRA(I),OFOBRB(I),OFOBRC(I),OFOBRD(I),
     1OFOBRE(I),OFOBRF(I)
      GO TO 250
  310 READ(IVDI,14)    I,K,RXC,RZC
      WRITE(IVDO,65)   I,K,RXC,RZC
      IF( I.LT.1 ) GO TO 320
      IK=(K-1)*NWPC + (I-1)*K2NC + 1
      RX(IK)=RXC
      RZ(IK)=RZC
      GO TO 310
  320 CONTINUE
      WRITE(IVDO,50) DX,DZ,GX,GZ,ALX,ALZ,CYL,BO,EPS,VMIN                MESH   8
      WRITE (IVDO,51) KWR,KWL,KWT,KWB,FSLIP,ALP,GAM,ALPO,GAM1,NU,TQJET,
     * TSJET
      WRITE(IVDO,59) AW,BW,CW,WEPS,KDERBC,UBRI,UBLI,WBTI,WBBI
      WRITE(IVDO,58) WOBI,UOBI,CSUBPO
      WRITE(IVDO,60)  TGAM,TO,TI,TSTEP,MAT,NRESEX
      WRITE(IVDO,52) AI,BI,CI,AR,BR,CR,AMU,BMU,CMU
      WRITE (IVDO,53) AK,BK,CK,ACP,BCP,CCP,SIGN
      WRITE(IVDO,61)  NFLOW,NT1,NT2,NTAU
      WRITE(IVDO,57)    ( TAU(I),I=1,NTAU )
      NMAX=AMAX0( NFLOW,NT1,NT2 )
      WRITE(IVDO,62)
      DO 319 I=1,NMAX
      WRITE(IVDO,63)  I,TYMF(I),FN(I),TYMT1(I),T1N(I),TYMT2(I),T2N(I)
```

```
  319 CONTINUE
       NMAX=AMAX0(NT3,NT4,NT5)
       DO 321 I=1,NMAX
      WRITE(IVDO,66) TYMT3(I),T3N(I),TYMT4(I),T4N(I),TYMT5(I),T5N(I)
 321   CONTINUE
C NOTE. GENERATION OF MESH CELL SIZES .
      RDX=1./DX                                                    VRS12004
      RDZ=1./DZ                                                    VRS12006
      HDX=.5*DX                                                    VRS12018
      HDZ=.5*DZ                                                    VRS12020
      RDZS=1./(DZ*DZ)
      BETA=.5*B0/(RDX*RDX + RDZ*RDZ)                               VRS12022
      IF( KDERBC.GT.0 ) FSLIP=1.0
      IF( CYL.GT.1.E-6 ) KWL=1
      EPSB=4.*NU/AMIN1( DX,DZ )
      NTPAS=1
      IF( ALX.LT.EM6 .OR. ALZ.LT.EM6 ) NTPAS=2
      RDXDZS=1./( RDX*RDX + RDZ*RDZ )
      X1=FLOAT(IBR)*DX
      Z1=FLOAT(KBR)*DZ
      RLENGH=1./AMAX1( X1,Z1 )
      EPS0=EPS
      TP=TI + 459.7
C NOTE. CALCULATION OF SPECIFIC MATERIAL FOR SIE INITIAL AND RHOO .
      GO TO( 400,420,440,460 ),MAT
C NOTE. COMPUTATION FOR SODIUM MATERIAL .
  400 SIEII=0.38935*TR - 0.553E-4*TR**2 + 0.1137E-7*TR**3 - 29.02
      RHOII=59.566 - 7.9504E-3*TI - .2872E-6*TI**2 + 0.06035E-9*TI**3
      RHO0=59.566 - 7.9504E-3*T0 - 0.2872E-6*T0**2 + 0.06035E-9*T0**3
      AT=397.17/TR + 1.0203
      TMU=(10.0**AT/3600.)/TR**0.4925
      NU=TMU/RHOII
      TK=0.015085 - 5.2167E-6*TI + 5.809E-10*TI**2
      CSUBP=0.38935 - 1.106E-4*TI + 0.3411E-7*TI**2
      RPRAN=TK/( CSUBP*TMU )
      GO TO 500
```

```
C NOTE. COMPUTATION FOR WATER MATERIAL .
  420 SIEII=1.0004*TI - 32.013
      RHOII=62.742 - 0.372E-2*TI - 0.44E-4*TI**2
      RHOO =62.742 - 0.372E-2*TO - 0.44E-4*TO**2
      BT=446.0/( TI+207.0 ) - 5.0
      TMU=1.622*10.**BT
      NU=TMU/RHOII
      TK=8.369E-5 + 2.368E-7*TI - 5.89E-10*TI**2
      CSUBP=1.0004
      RPRAN=TK/( CSUBP*TMU )
      GO TO 590
  440 SIEII=  AI*TI*TI  +  BI*TI + CI
      RHOII=  AR*TI*TI  +  BR*TI +  CR
      RHOO =  AR*TO*TO  +  BR*TO +  CR
      TMU  = AMU*TI*TI  + BMU*TI + CMU
      TK   =  AK*TI*TI  +  BK*TI +  CK
      CSUBP= ACP*TI*TI  + BCP*TI + CCP
      NU=TMU/RHOII
      RPRAN=TK/( CSUBP*TMU )
      GO TO 590
  460  CONTINUE
      NU=TMU/RHOII
      RPRAN=TK/( CSUBP*TMU )
C NOTE. NL=NUMBER OF LEFT MOST CELL , NR=NUMBER OF RIGHT MOST CELL ,
C NOTE. GENERATION OF INTERIOR MESH CELLS ,I.E. FLUID AND OBSTACLE .
  590 IF(IDATIN.GT.0.AND.IRESET.EQ.0) GO TO 590
      READ(IVDI,5)    NL,NR,NB,NT,ICELTY
      WRITE(IVDO,54) NL,NR,NB,NT,ICELTY
      IF( NL.EQ.0 ) GO TO 700
      READ(IVDI,6) SIEI,TQI,TSI,UI,WI,CHII,VAPI,LIQI                 RGBMK60A
      WRITE(IVDO,55) SIEI,TQI,TSI,UI,WI,CHII,VAPI,LIQI               RGBMK60A
      I1=NL
      I2=NR
      K1=NB
      K2=NT
      KK=1 + (I1-2)*K2NC
```

```
      DO 589 I=I1,I2
      KK=KK + K2NC
      LWPC=(K1-2)*NWPC
      DO 579 K=K1,K2
      LWPC=LWPC + NWPC
      IK=KK + LWPC
      CF(IK)=ICELTY
C NOTE. FOR OBSTACLES WITH TAU FACTORS - SET SIEI = OBSTACLE TEMPERA -
C NOTE. TURE IN F DEGREES .
      SIE(IK)=SIEI                                                 RGBMK01A
      IF( ICELTY.GE.30 .AND. NTAU.GT.0 ) P(IK)=SIEI
      TQ(IK)=TQI
      TS(IK)=TSI
      U(IK)=UI
      W(IK)=WI
      CHI(IK)=CHII                                                 RGBMK02A
      VAP(IK)=VAPI                                                 RGBMK60A
      LIQ(IK)=LIQI                                                 RGBMK60A
      SIEO(IK)=SIE(IK)
      TQO(IK)=TQ(IK)
      TSO(IK)=TS(IK)
      UO(IK)=U(IK)
      WO(IK)=W(IK)
      CHIO(IK)=CHI(IK)                                             RGBMK02A
      VAPO(IK)=VAP(IK)                                             RGBMK60A
      LIQO(IK)=LIQ(IK)                                             R3BMK60A
  578 CONTINUE
  579 CONTINUE
  589 CONTINUE
      GO TO 500
 590  CONTINUE
C NOTE. GENERATION OF EXTERIOR BOUNDRY MESH CELLS .
  700 I1=1
      TSMAX=-1.0E+20
      TMAX=TSMAX
      WMAX=TMAX
```

```
      UMAX=WMAX
      TSMIN=+1.0E+20
      TMIN=TSMIN
      WMIN=TMIN
      UMIN=WMIN
      TQMAX=-1.E+20
      I2=IBP2
      K1=1
      K2=KBP2
      KK=1 + (I1-2)*K2NC
      DO 789 I=I1,I2
      KK=KK + K2NC
      LWPC=(K1-2)*NWPC
      DO 779 K=K1,K2
      LWPC=LWPC + NWPC
      IK=KK + LWPC
      UMAX=AMAX1( UMAX,U(IK) )
      WMAX=AMAX1( WMAX,W(IK) )
      UMIN=AMIN1( UMIN,U(IK) )
      WMIN=AMIN1( WMIN,W(IK) )
      TSMAX=AMAX1( TSMAX,TS(IK) )
      TSMIN=AMIN1( TSMIN,TS(IK) )
      TQMAX=AMAX1( TQMAX,TQ(IK) )
      CFC= CF(IK)
      IF( K.EQ.K1 .AND. CFC.LT.11 ) CF(IK)=10
      IF( K.EQ.K2 .AND. CFC.LT.11 ) CF(IK)=10
      IF( I.EQ.I1 .AND. CFC.LT.11 ) CF(IK)=10
      IF( I.EQ.I2 .AND. CFC.LT.11 ) CF(IK)=10
      IF( I.EQ.I1 .AND. K.EQ.K1 ) CF(IK)=2
      IF( I.EQ.I1 .AND. K.EQ.K2 ) CF(IK)=2
      IF( I.EQ.I2 .AND. K.EQ.K1 ) CF(IK)=2
      IF( I.EQ.I2 .AND. K.EQ.K2 ) CF(IK)=2
      IF( CFC.LT.20 .OR. IOBS.EQ.0 ) GO TO 770
C NOTE. FLAGS CELLS SURROUNDING THE OBSTACLE CELL.
      CFR=CF(IK+K2NC)
      CFL=CF(IK-K2NC)
```

```
      CFT=CF(IK+NWPC)
      CFB=CF(IK-NWPC)
      IICFR(IK)=1
      IICFL(IK)=1
      IICFT(IK)=1
      IICFB(IK)=1
      IF (CFR.NE.1) IICFR(IK)=0
      IF (CFL.NE.1) IICFL(IK)=0
      IF (CFT.NE.1) IICFT(IK)=0
      IF (CFB.NE.1) IICFB(IK)=0
770   CONTINUE
  779 CONTINUE
  789 CONTINUE
      RETURN
C ***** FORMATS ***** FORMATS ***** FORMATS ***** .
    1 FORMAT (10F8.3)
    2 FORMAT (4I2,8F8.3)
    5 FORMAT (4I5,I2)
   6  FORMAT (8F8.3)
    7 FORMAT (4F8.3,I2,4F8.3)                                       RGBMK60A
    8 FORMAT (3F8.3)
   10 FORMAT (4F8.3,2I2)
 11   FORMAT (7X,I3,5(5X,I3),7X,I3)
   12 FORMAT (8F8.3)
 13   FORMAT (3X,I3,2X,6F8.3)
   14 FORMAT (2(3X,I3),2(5X,F8.3))
   50 FORMAT (1H ,5X,3HDX=,1PE12.5/6X,3HDZ=,E12.5/6X,3HGX=,E12.5/
     1 6X,3HGZ=,E12.5/5X,4HALX=,E12.5/5X,4HALZ=,E12.5/5X,4HCYL=,E12.5/
     2 6X,3HB0=,E12.5/5X,4HEPS=,E12.5/4X,5HVMIN=,E12.5)
   51 FORMAT (1H ,4X,4HKWR=,I2/5X,4HKWL=,I2/5X,4HKWT=,I2/5X,4HKWB=,I2/
     1 3X,6HFSLIP=,1PE12.5/5X,4HALP=,E12.5/5X,4HGAM=,E12.5/4X,5HALP0=,
     2E12.5/4X,5HGAM1=,E12.5/6X,3HNU=,E12.5/3X,6HTQJET=,E12.5/3X,
     36HTSJET=,E12.5)
   52 FORMAT (1H ,5X,3HAI=,1PE12.5/6X,3HBI=,E12.5/6X,3HCI=,E12.5/
     1 6X,3HAR=,E12.5/6X,3HBR=,E12.5/6X,3HCR=,E12.5/5X,4HAMU=,E12.5/
     2 5X,4HBMU=,E12.5/5X,4HCMU=,E12.5)
```

```
 53 FORMAT(1H ,5X,3HAK=,1PE12.5/6X,3HBK=,E12.5/6X,3HCK=,E12.5/5X,
   14HACP=,E12.5/5X,4HBCP=,E12.5/,5X,4HCCP=,E12.5/5X,5HSIGN=,E12.5)
 54 FORMAT(1H ,3HNL ,I5,3HNR ,I5,3HNB ,I5,3HNT ,I5,8HICELTYP ,I2)
 55 FORMAT(1H ,3X,5HSIEI=,1PE12.5/5X,4HTQI=,E12.5/5X,4HTSI=,E12.5/
   16X,3HUI=,E12.5/6X,3HWI=,E12.5/5X,4HCHI=,E12.5/5X,4HVAP=,E12.5/5X,4RGBMK60A
   2HLIQ=,E12.5)                                                 RGBMK60A
 57 FORMAT(1H ,20H TAU FOR OBSTACLES =,7(2X,1PE12.5))
 58 FORMAT(1H ,3X,5HWOBI=,1PE12.5/4X,5HUOBI=,E12.5/1X,8HCSUBPOB=,
   1 E12.5)
 59 FORMAT(1H ,5X,3HAW=,1PE12.5/6X,3HBW=,E12.5/6X,3HCW=,E12.5/
   1 4X,5HWEPS=,E12.5/2X,7HKDERBC=,I2/4X,5HUBRI=,E12.5/4X,5HUBLI=,
   2 E12.5/4X,5HWBTI=,E12.5/4X,5HWBBI=,E12.5)
 60 FORMAT(1H ,3X,5HTGAM=,1PE12.5/6X,3HTO=,E12.5/6X,3HTI=,E12.5/
   1 3X,6HTSTEP=,E12.5/5X,4HMAT=,I2/1X,8HNRESEXP=,I2)
61   FORMAT(1H ,7H NFLOW ,I3,5H NT1 ,I3,5H NT2 ,I3,5H NT3 ,I3,5H NT4 ,
   1  I3,5H NT5 ,I3,6H NTAU ,I3)
 62 FORMAT(1H ,3X,1HI,9X,4HTYMF,12X,2HFN,11X,5HTYMT1,11X,3HT1N,11X,
   1 5HTYMT2,11X,3HT2N)
 63 FORMAT(1H ,2X,I3,2X,6(2X,1PE11.4,2X))
64   FORMAT(1H ,3H I ,I3,2X,6F8.3)
 65 FORMAT(1H ,3H I ,I3,3H K ,I3,5H RXC ,F8.3,5H RZC ,F8.3)
66   FORMAT(1H ,///,22X,6(2X,1PE11.4,2X))
     END
     SUBROUTINE VM
     INTEGER BUFL,CF,CF1,CFB,CFC,CFI,CFL,CFR,CFS,CFT,CQF,ERF,TD,VNTP,
    1   VTP
     REAL NU,LIQ,LIQO,LIQI,LOUT                                 RGBMN60A
     REAL LIQL,LIQR,LIQT,LIQB,LIQC,LIQCO                        RGBVM60A
     DIMENSION EFRAC(5),RLAM(5),ELAM(5)                         RGBVM56A
     DIMENSION CF(1),CQ(1),QCON(1),P(1),RX(1),RZ(1),TQ(1),TS(1),U(1),
    1   W(1),ER(1),FFX3(102),FFY3(102),PBTIM(2),UO(1),WO(1),TQO(1),
    2   TSO(1),SIE(1),SIEO(1),CHI(1),CHIO(1)                    RGBMN01A
    A,VAP(1),VAPO(1),LIQ(1),LIQO(1)                             RGBMN60A
    3   ,TYMF(25),FN(25),TYMT1(25),T1N(25),TYMT2(25),T2N(25),
    4   COFBA(25),COFBB(25),COFBC(25),COFTA(25),COFTB(25),COFTC(25),
    5   COFRA(25),COFRB(25),COFRC(25),COFLA(25),COFLB(25),COFLC(25),
```

```
6    OFOBTA(25),OFOBTB(25),OFOBTC(25),
7    OFOBRA(25),OFOBRB(25),OFOBRC(25),TAU(10),USL(32),USLOB(20),
8    USROB(20),USTOB(20),USBOB(20)
9,COFBD(25),COFBE(25),COFTD(25),COFTE(25),COFTF(25),COFBF(25),
*COFRD(25),COFRE(25),COFLD(25),COFLE(25),COFRF(25),COFLF(25),
AOFOBTD(25),OFOBTE(25),OFOBRD(25),OFOBRE(25),
B   OFOBTF(25),OFOBRF(25),
CTYMT3(25),TYMT4(25),TYMT5(25),T3N(25),T4N(25),T5N(25),
*   IICFR(1),IICFL(1),IICFT(1),IICFB(1)
*     ,ZERO1(1165),ZERO2(608),ZERO3(16),ZERO4(3)
  DIMENSION ZSIE(22),ZTQ(22),ZTS(22),ZVP(22),ZLQ(22),ZAP(22),WSP(22) RGBVM62A
  DIMENSION TRSTRT(5),WZSIE(100),WZTQ(100),WZTS(100)                 RGBVM55A
A,WZVP(100),WZLQ(100),WZAP(100),WWSP(100)                             RGBVM62A
  COMMON/VRCOM/A(14000)                                               RGBMN60A
  COMMON/RGB/RLAMB,CHII,GAMX,NRSTRT,TRSTRT,ZSIE,ZTQ,ZTS,WZSIE,WZTQ,   RGBVM55A
AWZTS,NPROF,WZVP,WZLQ,ZVP,ZLQ,GAML,GAMV,VAPI,LIQI                     RGBMN60A
B,WSP,WWSP,BKGND,DWNDS                                                RGBMN60B
  COMMON /VRCON/ ALP,ALPO,ALX,ALZ,BO,BETA,BUFL,CFI(9),CFS(9),CYL,
1    DT,DX,DZ,EM6,EPS,ERF,FSLIP,GAM,GAM1,GX,GZ,HDX,HDZ,I,I1,I2,I2K2,
2    IBP1,IBP2,IBR,IDATIN,IDIAG,IKP2,IOBS,IRSTRT,ITAPW,ITER,IVDI,
3    IVDO,K,K1,K2,K2NC,KBP1,KBP2,KBR,KNC,KWB,KWL,KWR,KWT,LABEL(20),
4    LPR,NCYC,NCYCB,NPRT,NU,NWPC,RDT,RDX,RDZ,RDZS,RIBKB,ROI,TD,TFIN,
5    TIMEP,TTOSUM,TPL,TPLT,TPR,TPRT,TQI,TSI,TTD,TWTD,UI,WI
   ,USR(32),UST(22),USB(22),USO(10),FFX3,FFY3
6    ,AW,BW,CW,EPSB,UBLI,UBRI,WBBI,WBTI,WEPS,WOBI,NTPAS,TGAM,CSUBP,
7    T0,SIEI,IDG,KDG,TI,MAT,RHOO,AT,TMU,TK,TYMP,PN,TYMT1,T1N,TYMT2,
8    T2N,RPRAN,NRESEX,NFLOW,NT1,NT2,TSTEP,KDERBC,UOBI,COFBA,COFBB,
9    COFBC,COFTA,COFTB,COFTC,COFRA,COFRB,COFRC,COFLA,COFLB,COFLC,
*    OFOBTA,OFOBTB,OFOBTC,OFOBRA,OFOBRB,OFOBRC,TAU,NTAU,USL,
1    USLOB,USROB,USTOB,USBOB,UMAX,WMAX
*   ,CSUBPO,EPSO,RDXDZS,RLENGH ,TQJET,TSJET
  COMMON /FLMCON/ DROU,DROUO,IPRFM
  COMMON /VRMAT3/ AI,BI,CI,AR,BR,CR,AMU,BMU,CMU,AK,BK,CK,ACP,BCP,CCP
1                ,VMIN
  COMMON/PROP/SIGN
  COMMON/EXTRA/NT3,NT4,NT5,TYMT3,TYMT4,TYMT5,T3N,T4N,T5N,COFBD,
```

```
     1COFRE,COFBF,COFTD,COFTE,COFTF,COFRD,COFRE,COFRF,COFLD,COFLE,
     2COFLF,OFOBTD,OFOBTE,OFOBTF,OFOBRD,OFOBRE,OFOBRF,IRESET,
     *NCYCLS,TADD,NIV,IOBRAN
      COMMON/INDEX/NWPCL,K2NCL
      COMMON/LARGE/DIFFCO(2400)
      EQUIVALENCE (A(1),CF),(A(2),U),(A(3),W),(A(4),P),(A(5),TQ),
     1   (A(6),TS),(A(7),ER,CQ),(A(8),UO),(A(9),WO),(A(10),TQO),
     2   (A(11),TSO),(A(12),SIE),(A(13),SIEO),(A(14),RX),(A(15),RZ),
     3   (A(15),IICFR),(A(17),IICFL),(A(18),IICFT),(A(19),IICFB),
     A   (A(20),CHI),(A(21),CHIO),                                      RGBMN01A
     B   (A(22),VAP),(A(23),VAPO),(A(24),LIQ),(A(25),LIQO),             RGBMN60A
     4   (ZERO1(1),ALP),(ZERO2(1),NT3),(ZERO3(1),AI),(ZERO4(1),DROU)
C NOTE. END - END OF NON-EXECUTABLE STATEMENTS .
C NOTE. VM IS RESPONSIBLE FOR CALCULATION OF BOUNDARY CONDITIONS
C NOTE. AND EQUATIONS .
      NRSTRT=1                                                          R3BVM55A
      READ(IVDI,57) GAMX,NCHAN,WMOLX,GAMV,GAML,BKGND,DWNDS              RGBVM60B
   57 FORMAT(F8.3,I8,5F8.3)                                             RGBVM60B
      WRITE(IVDO,58) GAMX,NCHAN,WMOLX,GAMV,GAML,BKGND                   RGBVM60A
   58 FORMAT(10H  GAMX =  ,F8.4,I5,' DECAY CHANNELS  MOLEC WT = ',F8.3/RGBVM60A
     110H  GAMV =  ,F8.4/10H  GAML =  ,F8.4/10H  BKGND = ,E8.4)         RGBVM60A
      WRITE(IVDO,64)                                                    RGBVM56A
   64 FORMAT(54H  DECAY CHANNEL   LAMBDA (1/SEC)  ENERGY (MEV) FRACT.)  RGBVM56A
      READ(IVDI,65) (RLAM(J),ELAM(J),EFRAC(J),J=1,NCHAN)                RGBVM56A
   65 FORMAT(3F8.3)                                                     R3BVM56A
      WRITE(IVDO,66) (J,RLAM(J),ELAM(J),EFRAC(J),J=1,NCHAN)             RGBVM56A
   66 FORMAT(8X,I1,13X,F8.5,7X,F8.5,3X,F6.4)                            RGBVM56A
      RLAMB=0.0                                                         RGBVM56A
      SER=0.0                                                           R3BVM56A
      DO 98 J=1,NCHAN                                                   RGBVM56A
      SER=SER+RLAM(J)*ELAM(J)*EFRAC(J)                                  RGBVM56A
   98 RLAMB=RLAMB+RLAM(J)                                               RGBVM56A
      WRITE(IVDO,67) RLAMB,SER                                          RGBVM56A
   67 FORMAT(' RLAMB = ',E10.5,' SPEC. ENERGY RELEASE = ',E10.5)        RGBVM56A
      READ(IVDI,62) NPROF,(TRSTRT(L),L=1,5)                             RGBVM55A
   62 FORMAT(I8,5F8.3)                                                  RGBVM55A
```

```
      READ(IVDI,56)  (WZSIE(K),WZTQ(K),WZTS(K),WZVP(K),WZLQ(K),WZAP(K),WWRGBVM62A
     ASP(K),K=1,NPROF)                                                  RGBVM62A
   56 FORMAT(7F8.3,24X)                                                 RGBVM62A
      WRITE(IVDO,59) (WZSIE(K),WZTQ(K),WZTS(K),WZVP(K),WZLQ(K),WZAP(K),WWRGBVM62A
     ASP(K),K=1,NPROF)                                                  RGBVM62A
   59 FORMAT(' ',7F10.3)                                                RGBVM62A
C  TRANSFER OF PROFILES BEFORE ANY RESTART CASES                        RGBVM55A
      DO 99 K=2,KBP1                                                    RGBVM55A
      WSP(K)=WWSP(K-1)                                                  RGBVM70A
      ZAP(K)=WZAP(K-1)                                                  RGBVM62A
      ZVP(K)=WZVP(K-1)                                                  RGBVM60A
      ZLQ(K)=WZLQ(K-1)                                                  RGBVM60A
      ZSIE(K)=WZSIE(K-1)                                                RGBVM55A
      ZTQ(K)=WZTQ(K-1)                                                  RGBVM55A
   99 ZTS(K)=WZTS(K-1)                                                  RGBVM55A
      WSP(1)=0.0                                                        RGBVM70A
      ZAP(1)=0.0                                                        RGBVM62A
      ZVP(1)=ZVP(2)                                                     RGBVM60A
      ZLQ(1)=ZLQ(2)                                                     RGBVM60A
      ZSIE(1)=ZSIE(2)                                                   RGBVM55A
      ZTQ(1)=ZTQ(2)                                                     RGBVM55A
      ZTS(1)=ZTS(2)                                                     RGBVM55A
      WSP(KBP2)=0.0                                                     RGBVM70A
      ZAP(KBP2)=0.0                                                     RGBVM62A
      ZVP(KBP2)=ZVP(KBP1)                                               RGBVM60A
      ZLQ(KBP2)=ZLQ(KBP1)                                               RGBVM60A
      ZSIE(KBP2)=ZSIE(KBP1)                                             RGBVM55A
      ZTQ(KBP2)=ZTQ(KBP1)                                               RGBVM55A
      ZTS(KBP2)=ZTS(KBP1)                                               RGBVM55A
C NOTE. CALCULATION OF CONSTANTS AND PREASSIGNED BRANCHES .
      IF( IRSTRT.EQ.0 ) GO TO 100
      CALL VRPRT
      IF( IDROU.GT.0 ) DROU=DROU0*AMIN1(DX,DZ)/AMAX1(UMAX,WMAX,EM6)
      IF( IPRFM.GT.0 ) CALL VRFLM
      IRSTRT=0
  100 ITER=0
```

```
      ICALI=1
      X1=AMAX1( UMAX, WMAX )
      VELOLD=X1
      EPS=EPS0*X1*RLENGH
      IF( X1.LT.VMIN )  EPS=EPS0*VMIN*RLENGH
      IF( EPS0.LT.EM6 )  EPS=ABS( EPS0 )
      ASSIGN 2000 TO KBC
C NOTE. COMPUTATION OF FNTAU,T1NTAU AND T2NTAU .
      FNTAU=SI( TYMF,FN,TIMET,NFLOW )
      T1NTAU=SI( TYMT1,T1N,TIMET,NT1 )
       IF(NT2.EQ.0) GO TO 107
      T2NTAU=SI( TYMT2,T2N,TIMET,NT2 )
       IF(NT3.EQ.0) GO TO 107
      T3NTAU=SI(TYMT3,T3N,TIMET,NT3)
       IF(NT4.EQ.0) GO TO 107
      T4NTAU=SI(TYMT4,T4N,TIMET,NT4)
       IF(NT5.EQ.0) GO TO 107
      T5NTAU=SI(TYMT5,T5N,TIMET,NT5)
 107   CONTINUE
C NOTE. ZERO OUT THE CQ(IK) ARRAY FOR TAU FACTORS IN SIE EQUATION .
      I1=2
      I2=IBP1
      K1=2
      K2=KBP1
      KK=1
      ITAUCN=0
      DO 109 I=I1,I2
      KK=KK + K2NC
      LWPC=0
      DO 109 K=K1,K2
      LWPC=LWPC + NWPC
      IK=KK + LWPC
      CQ(IK)=0.0
  109 CONTINUE
      IF( NCYCB.LT.NCYC ) GO TO 1000
C NOTE. CALCULATION OF DIAGNOSTIC CONSTANTS .
```

```
      ASSIGN 12500 TO KDAGTU
C NOTE. PREASSIGN BRANCHES FOR RESISTANCE EQUATIONS , I.E. RX AND RZ .
      RXC=0.0
      RZC=0.0                                                  VM212002
      ASSIGN 2300 TO KRXRZ                                     VM212004
      IF( NWPC.GT. 13 ) ASSIGN 2250 TO KRXRZ
C NOTE. PREASSIGN BRANCHES FOR PLANE - CYL=0.0 - OR CYLINDRICAL
C NOTE. - CYL=1.0 - COORDINATES .
      FCU=0.0
      FCW=0.0                                                  VM215002
      RL=1.0
      RC=RL
      RR=RC
      DR=DX
      RRL=1.0
      RRC=RRL
      RRR=RRC
      RRRC=1.0
      RRP=RRRC
      RDR=RDX
      RDRS=1./( DR*DR )
      RDRM=RDR
      RDRP=RDRM
      RDZM=RDZ
      RDZP=RDZM
      ASSIGN 2400 TO KCLU                                      VM215006
      ASSIGN 2500 TO KCLW
      ASSIGN 2220 TO KRU                                       VM215010
      IF( CYL.LT.EM6 ) GO TO 120
      ASSIGN 2370 TO KCLU                                      VM215014
      ASSIGN 2470 TO KCLW                                      VM215016
      ASSIGN 2215 TO KRU                                       VM215018
  120 ASSIGN 13000 TO KDIAG
      IF( IDIAG.LT.1 ) GO TO 200
      ASSIGN 12200 TO KDIAG
      IF( IDIAG.GT.1 ) ASSIGN 12500 TO KDIAG
```

```
  200 TSUM=0.0
      TIOSUM=0.0
C
C NOTE. COMPUTATION OF BOUNDARY CONDITIONS .
C
1000  LWPC=1 - NWPC
      IF( KDERBC.LT.1 ) GO TO 1100
C
C NOTE. COMPUTATION OF RIGHT AND LEFT BOUNDARY CONDITIONS .
1100  LWPC=1 - NWPC
      I1=1
      I2=IBP2
      K1=1
      K2=KBP2
      NDERR=0
      NDERL=0
      NCOFR=0
      NCOFL=0
      DO 1289 K=K1,K2
      LWPC=LWPC+NWPC                                                    VM111002
      IMK=LWPC
      CFL= CF(IMK)
      ICFL=CFL
      IPK=IMK + IKP2
      IPPK=IPK + K2NC
      IMKT=IMK + K2NC
      IPKT=IPK
      CFR= CF(IPPK)
      ICFR=CFR
      IF( CFL.NE.2 ) GO TO 1105
      IF( K.EQ.K2 ) GO TO 1103
      IMKT=IMK + K2NC + NWPC
      IPKT=IPK + NWPC
      CFL= CF(IMK+NWPC)
      CFR= CF(IPPK+NWPC)
      GO TO 1105
```

```
1103  IMKT=IMK + K2NC - NWPC
      IPKT=IPK - NWPC
      CFL= CF(IMK-NWPC)
      CFR= CF(IPPK-NWPC)
 1105 W(IMK)=W(IMKT)                                              RGBVM51A
      W(IPPK)=W(IPK)                                              RGBVM02A
C NOTE. COMPUTATION OF REFLECTIVE BOUNDARY CONDITIONS ON TQ AND TS .
      SIE(IMK)=SIE(IMKT)
      SIE(IPPK)=ZSIE(K)                                           RGBVM51A
      TQ(IMK)=TQ(IMKT)
      TQ(IPPK)=ZTQ(K)                                             RGBVM51A
      TS(IMK)=TS(IMKT)
      TS(IPPK)=ZTS(K)                                             RGBVM51A
      CHI(IMK)=CHI(IMKT)                                          RGBVM52A
      CHI(IPPK)=0.0                                               RGBVM52A
      IF(U(IPKT).GT.0.0) CHI(IPPK)=CHI(IPKT)                      RGBVM52A
      VAP(IMK)=VAP(IMKT)                                          RGBVM60A
      VAP(IPPK)=ZVP(K)                                            RGBVM60A
      LIQ(IMK)=LIQ(IMKT)                                          RGBVM60A
      LIQ(IPPK)=ZLQ(K)                                            RGBVM60A
      GO TO ( 1120,1130,1140,1150 ),KWL
C NOTE. COMPUTATION OF RIGID  LEFT  WALL BOUNDARY CONDITION .
1120  U(IMK)=0.0
      GO TO 1180                                                  VM114002
C NOTE. COMPUTATION OF CONTINUATIVE  LEFT  WALL BOUNDARY CONDITION .
1130  IF( ITER.GT.0 ) GO TO 1180
      U(IMK)=U(IMK+K2NC)
      W(IMK) = -W(IMK+K2NC)
      W(IMK-NWPC) = -W(IMK+K2NC-NWPC)
      GO TO 1180                                                  VM115004
C NOTE. COMPUTATION OF PERIODIC  LEFT  WALL BOUNDARY CONDITION .
1140  U(IMK)=U(IPK)
      GO TO 1180
C NOTE. VARIABLE BOUNDARY OPTION AT LEFT WALL .
1150  NCFL=CFL - 9
      GO TO ( 1152,1130,1155,1160 ),NCFL
```

```
C NOTE. RIGID BOUNDARY SECTION AT LEFT WALL .
1152  NRIGID=KDERBC + 1
      GO TO( 1120,1153 ),NRIGID
C NOTE. DERIVED BOUNDARY CONDITION AT LEFT WALL .
1153  WC=W(IMKT)
      IF( K.EQ.1 ) GO TO 1120
      IF (K.GE.(KBR+1)) GO TO 1120
      ICF1=CF(IMKT)
      IF (ICF1.GE.30) GO TO 1120
      QC=TQ(IMKT)
      SC=TS(IMKT)
      NDERL=NDERL + 1
      WSA=USL(NDERL)
      QW=5.*WSA*WSA
      W(IMK) = -WC
      SW = WSA * WSA * HDX/WC
      TQ(IMK)=2.*QW - QC
      TS(IMK)=2.*SW - SC
      GO TO 1120
C NOTE. CONSTANT INFLOW AT LEFT WALL .
1155  U(IMK)=UBLI
      GO TO 1180
C NOTE. VARIABLE OR FUNCTIONAL INFLOW AT LEFT WALL .
1160  IF( ICFL.EQ.2 ) GO TO 1180
      NCOFL=NCOFL + 1
      TI=COFLB(NCOFL)*T1NTAU + COFLC(NCOFL)*T2NTAU
     1+COFLD(NCOFL)*T3NTAU+COFLE(NCOFL)*T4NTAU+COFLF(NCOFL)*T5NTAU
      ASSIGN 1162 TO KIROBC
      SIEX=SIE(IMKT)                                        RGBVM01A
      GO TO 1500
1162  AREAK=3.14159265*FLOAT(2*K-3)*DZ*DZ
      IF( CYL.LT.1.0 ) AREAK=DZ
      FLK=COFLA(NCOFL)*PNTAU
      UBAR=FLK/RHOII
      U(IMK)=UBAR/AREAK
       IF(NIV.EQ.1) U(IMK)=FLK
```

```
      SIE(IMK)=SIEII                                                    RGBVM02A
      TS(IMK)=TS(IPK)                                                   RGBVM02A
      TQ(IMK)=TQ(IPK)                                                   RGBVM02A
 1180 GO TO( 1220,1230,1240,1250 ),KWR
C NOTE. COMPUTATION OF RIGID RIGHT  WALL BOUNDARY CONDITION .
 1220 U(IPK)=0.0
      GO TO 1280                                                        VM124002
C NOTE. COMPUTATION OF CONTINUATIVE RIGHT  WALL BOUNDARY CONDITION .
 1230 IF( ITER.GT.0 ) GO TO 1280
      U(IPPK)=U(IPK-K2NC)
      W(IPPK-NWPC)=W(IPK-NWPC)                                          RGBVM02A
      GO TO 1280                                                        VM125004
C NOTE. COMPUTATION OF PERIODIC RIGHT  WALL BOUNDARY CONDITION .
 1240 U(IPPK)=U(IMK+K2NC)
      W(IPPK)=W(IMK+K2NC)
      GO TO 1280
C NOTE. VARIABLE BOUNDARY OPTION AT RIGHT WALL .
 1250 NCFR=CFR - 9
      GO TO( 1252,1230,1255,1260 ),NCFR
C NOTE. RIGID BOUNDARY SECTION AT RIGHT WALL .
 1252 NRIGID=KDERBC + 1
      GO TO( 1220,1253 ),NRIGID
C NOTE. DERIVED BOUNDARY CONDITION AT RIGHT WALL .
 1253 WC=W(IPKT)
      IF (K.GE.(KBR+1)) GO TO 1220
      IF( K.EQ.1 ) GO TO 1220
      ICF2=CF(IPKT)
      IF (ICF2.GE.30) GO TO 1220
      QC=TQ(IPKT)
      SC=TS(IPKT)
      NDERR=NDERR + 1
      WSA=USR(NDERR)
      QW=5.*WSA*WSA
 1256 SW = WSA * WSA * HDX/WC
      W(IPPK) = -WC
      TQ(IPPK)=2.*QW-QC
```

```
      TS(IPPK)=2.*SW-SC
      GO TO 1220
C NOTE. CONSTANT INFLOW AT RIGHT WALL .
1255  U(IPK)=UBRI
      GO TO 1280
C NOTE. VARIABLE OR FUNCTIONAL INFLOW AT RIGHT WALL .
1260  IF( ICFR.EQ.2 ) GO TO 1280
      NCOFR=NCOFR + 1
      TI=COFRB(NCOFR)*T1NTAU + COFRC(NCOFR)*T2NTAU
     1+COFRD(NCOFR)*T3NTAU+COFRE(NCOFR)*T4NTAU+COFRF(NCOFR)*T5NTAU
      ASSIGN 1262 TO KIROBC
      SIEK=SIE(IPKT)                                              R3BVM01A
      GO TO 1500
 1262 AREAK = 3.14159265 * 2 * IBR * DR * DZ
      IF( CYL.LT.1.0 ) AREAK=DZ
      FLK=COFRA(NCOFR)*FNTAU
      UBAR=FLK/RHOII
      U(IPK)=UBAR/AREAK
       IF(NIV.EQ.1) U(IPK)=FLK
       SIEC=SIE(IPKT)
       SIEW=SIEII
       SIE(IPPK)=(2*SIEW+(ALX-1.0)*SIEC)/(1.0+ALX)
      QC = TQ(IPKT)
      QW = TQJET * U(IPK)*U(IPK)
      SC = TS(IPKT)
      SW = TSJET * U(IPK) * DZ
       SW=ABS(SW)
       QW=AMAX1(QW,1.0E-5)
       SW=AMAX1(SW,NU)
       TQ(IPPK)=(2*QW+(ALX-1.0)*QC)/(1.0+ALX)
       TS(IPPK)=(2*SW+(ALX-1.0)*SC)/(1.0+ALX)
1280  CONTINUE                                                    VM128000
1289  CONTINUE                                                    VM128900
C NOTE. COMPUTATION OF TOP AND BOTTOM BOUNDARY CONDITIONS .
      NDERB=0
      NDERT=0
```

```
      NCOFB=0
      NCOFT=0
      KK=1 - K2NC
      DO 1489 I=I1,I2
      KK=KK+K2NC                                                      VM131002
      IKM=KK
      CFB= CF(IKM)
      ICFB=CFB
      IKP=IKM + KNC
      IKPP=IKP + NWPC
      CFT= CF(IKPP)
      ICFT=CFT
      IKMT=IKM + NWPC
      IKPT=IKP
      IF( CFB.NE.2 ) GO TO 1305
      IF( I.EQ.I2 ) GO TO 1303
      IKMT=IKM + K2NC + NWPC
      IKPT=IKP + K2NC
      CFB= CF(IKM+K2NC)
      CFT= CF(IKPP+K2NC)
      GO TO 1305
 1303 IKMT=IKM - K2NC + NWPC
      IKPT=IKP - K2NC
      CFB= CF(IKM-K2NC)
      CFT= CF(IKPP-K2NC)
 1305 U(IKM)=-U(IKMT)                                                 RGBVM50A
      U(IKPP)=U(IKP)                                                  RGBVM51A
C NOTE. COMPUTATION OF REFLECTIVE BOUNDARY CONDITIONS ON TQ AND TS .
      SIE(IKM)=SIE(IKMT)
      SIE(IKPP)=SIE(IKPT)
      TQ(IKM)=TQ(IKMT)
      TQ(IKPP)=TQ(IKPT)
      TS(IKM)=TS(IKMT)
      TS(IKPP)=TS(IKPT)
      CHI(IKM)=CHI(IKMT)                                              RGBVM52A
      CHI(IKPP)=0.0                                                   RGBVM52A
```

```
      IF(W(IKPT).GT.0.0)  CHI(IKPP)=CHI(IKPT)                           RGBVM52A
      VAP(IKM)=VAP(IKMT)                                                RGBVM60A
      VAP(IKPP)=VAP(IKPT)                                               RGBVM60A
      LIQ(IKM)=LIQ(IKMT)                                                RGBVM60A
      LIQ(IKPP)=LIQ(IKPT)                                               RGBVM60A
      GO TO( 1320,1330,1340,1350 ),KWT
C NOTE. COMPUTATION OF RIGID  TOP   WALL BOUNDARY CONDITION .
1320  W(IKP)=0.0
      GO TO 1380                                                        VM134002
C NOTE. COMPUTATION OF CONTINUATIVE  TOP   WALL BOUNDARY CONDITION .
1330  IF( ITER.GT.0 ) GO TO 1380
      W(IKPP)=W(IKP-NWPC)
      U(IKPP-K2NC)=U(IKP-K2NC)                                          RGBVM51A
      GO TO 1380                                                        VM135004
C NOTE. COMPUTATION OF PERIODIC  TOP   WALL BOUNDARY CONDITION .
1340  W(IKPP)=W(IKM+NWPC)
      U(IKPP)=U(IKM+NWPC)
      GO TO 1380
C NOTE. VARIABLE BOUNDARY OPTION AT TOP WALL .
1350  NCFT=CFT - 9
      GO TO( 1352,1330,1355,1360 ),NCFT
C NOTE. RIGID BOUNDARY SECTION AT TOP WALL .
1352  NRIGID=KDERBC + 1
      GO TO( 1320,1353 ),NRIGID
C NOTE. DERIVED BOUNDARY CONDITION AT TOP WALL .
1353  UCT=U(IKP)
      IF( I.EQ.1 ) GO TO 1320
      IF (I.GE.(IBR+1)) GO TO 1320
      ICF3=CF(IKP)
      IF (ICF3.GE.30) GO TO 1320
      QCT=TQ(IKP)
      SCT=TS(IKP)
      NDERT=NDERT + 1
      USAT=UST(NDERT)
      QWT=5.*USAT*USAT
 1356 SWT = USAT * USAT * HDZ /UCT
```

```
      U(IKPP) = -UCT
      TQ(IKPP)=2.*QWT - QCT
      TS(IKPP)=2.*SWT - SCT
      GO TO 1320
C.NOTE  CONSTANT INFLOW AT TOP WALL .                                RGB/03/78
1355  W(IKP)=WBTI
      GO TO 1380
C NOTE. VARIABLE OR FUNCTIONAL INFLOW AT TOP WALL .
1360  IF( ICFT.EQ.2 ) GO TO 1380
      NCOFT=NCOFT + 1
      TI=COFTB(NCOFT)*T1NTAU + COFTC(NCOFT)*T2NTAU
     1+COFTD(NCOFT)*T3NTAU+COFTE(NCOFT)*T4NTAU+COFTF(NCOFT)*T5NTAU
      ASSIGN 1362 TO KIROBC
      SIEX=SIE(IKPT)                                                 RGBVM01A
      GO TO 1500
1362  AREAI=3.14159265*FLOAT(2*I-3)*DR*DR
      IF( CYL.LT.1.0 ) AREAI=DX
      FLI=COFTA(NCOFT)*FNTAU
      WBAR=FLI/RHOII
      W(IKP)=WBAR/AREAI
       IF(NIV.EQ.1) W(IKP)=FLI
       SIEC=SIE(IKP )
       SIEW=SIEII
       SIE(IKPP)=(2*SIEW+(ALZ-1.0)*SIEC)/(1.0+ALZ)
      QCT=TQ(IKP)
      QWT=TQJET*W(IKP)*W(IKP)
      SCT=TS(IKP)
      SWT=TSJET*W(IKP)*DR
       SWT=ABS(SWT)
       QWT=AMAX1(QWT,1.0E-5)
       SWT=AMAX1(SWT,NU)
       TQ(IKPP)=(2*QWT+(ALZ-1.0)*QCT)/(1.0+ALZ)
       TS(IKPP)=(2*SWT+(ALZ-1.0)*SCT)/(1.0+ALZ)
1380  GO TO( 1420,1430,1440,1450 ),KWB
C NOTE. COMPUTATION OF RIGID BOTTOM WALL BOUNDARY CONDITION .
1420  W(IKM)=0.0
```

```
      GO TO 1480
C NOTE. COMPUTATION OF CONTINUATIVE BOTTOM WALL BOUNDARY CONDITION .
1430  IF( ITER.GT.0 ) GO TO 1480
      W(IKM)=W(IKM+NWPC)
      U(IKM)=-U(IKM+NWPC)
      U(IKM-K2NC)=-U(IKM+NWPC-K2NC)
      GO TO 1480                                                VM145004
C NOTE. COMPUTATION OF PERIODIC BOTTOM WALL BOUNDARY CONDITION .
1440  W(IKM)=W(IKP)
      GO TO 1480
C NOTE. VARIABLE BOUNDARY OPTION AT BOTTOM WALL .
1450  NCFB=CFB - 9
      GO TO( 1452,1430,1455,1460 ),NCFB
C NOTE. RIGID BOUNDARY SECTION AT BOTTOM WALL .
1452  NRIGID=KDERBC + 1
      GO TO( 1420,1453 ),NRIGID
C NOTE. DERIVED BOUNDARY CONDITION AT BOTTOM .
1453  IK=IKM + NWPC
      IF( I.EQ.1 ) GO TO 1420
      IF (I.GE.(IBR+1)) GO TO 1420
      ICF4=CF(IK)
      IF (ICF4.GE.30) GO TO 1420
      UCB=U(IK)
      QCB=TQ(IK)
      SCB=TS(IK)
      NDERB=NDERB + 1
      USAB=USB(NDERB)
      QWB=5.*USAB*USAB
 1456 SWB=USAB*USAB*HDZ/UCB
      U(IKM)=-UCB
      TQ(IKM)=2.*QWB - QCB
      TS(IKM)=2.*SWB - SCB
      GO TO 1420
C NOTE. CONSTANT INFLOW AT BOTTOM WALL .
1455  W(IKM)=WBBI
      GO TO 1480
```

```
C NOTE. VARIABLE OR FUNCTIONAL INFLOW AT BOTTOM WALL .
1460  IF( ICFB.EQ.2 ) GO TO 1480
      NCOFB=NCOFB + 1
      TI =COFBB(NCOFB)*T1NTAU + COFBC(NCOFB)*T2NTAU
     1+COFBD(NCOFB)*T3NTAU+COFBE(NCOFB)*T4NTAU+COFBF(NCOFB)*T5NTAU
      ASSIGN 1462 TO KIROBC
      SIEX=SIE(IKMT)                                             RGBVM01A
      GO TO 1500
1462  AREAI=3.14159265*FLOAT(2*I-3)*DR*DR
      IF( CYL.LT.1.0 ) AREAI=DX
      FLI=COFBA(NCOFB)*FNTAU
      WBAR=FLI/RHOII
      W(IKM)=WBAR/AREAI
       IF(NIV.EQ.1) W(IKM)=FLI
       SIEC=SIE(IK  )
       SIEW=SIEII
       SIE(IKM )=(2*SIEW+(ALZ-1.0)*SIEC)/(1.0+ALZ)
      QCB=TQ(IK)
      QWB=TQJET*W(IKM)*W(IKM)
      SCB=TS(IK)
      SWB=TSJET*W(IKM)*DR
       QWB=AMAX1(QWB,1.0E-5)
       SWB=AMAX1(SWB,NU)
       TQ(IKM )=(2*QWB+(ALZ-1.0)*QCB)/(1.0+ALZ)
       TS(IKM )=(2*SWB+(ALZ-1.0)*SCB)/(1.0+ALZ)
1480  CONTINUE                                                   VM148000
1489  CONTINUE                                                   VM148900
      GO TO 1700
C NOTE. COMPUTATION OF SIE AND RHO FOR VARIABLE OR FUNCTIONAL INFLOW
C NOTE. AT A BOUNDARY WALL .
1500  TR=TI + 459.7
      GO TO( 1510,1520,1530,1540 ),MAT
C NOTE. COMPUTATION FOR SODIUM MATERIAL .
1510  SIEII=0.38935*TR - 0.553E-4*TR*TR + 0.1137E-7*TR*TR*TR-29.02
      RHOII=59.566 - 7.9504E-3*TI - .2872E-6*TI*TI + 0.06035E-9*TI*TI*TI
      AT=397.17/TR + 1.0203
```

```
      TMU=(10.0**AT/3600.)/TR**0.4925
      TK=0.015085 - 5.2167E-6*TI + 5.809E-10*TI*TI
      TEMP =-385.27 + 2.6602*SIEX + 5.9894E-04*SIEX*SIEX +
     1      1.5575E-06*SIEX*SIEX*SIEX-2.9048E-09*SIEX*SIEX*SIEX*SIEX+
     2      1.15427E-12*SIEX*SIEX*SIEX*SIEX*SIEX
      IF( ICSUBP.GT.0 ) TI=TEMP
      CSUBP=0.38935 - 1.106E-4*TI + 0.3411E-7*TI*TI
      GO TO 1550
C NOTE. COMPUTATION FOR WATER MATERIAL .
 1520 SIEII=1.0004*TI - 32.013
      RHOII=62.742 - 0.372E-2*TI - 0.44E-4*TI*TI
      BT=446.0/( TI+207.0 ) - 5.0
      TMU=1.622*10.**BT
      TK=8.369E-5 + 2.368E-7*TI - 5.89E-10*TI*TI
      TEMP=0.9996*SIEX + 32.0002
      CSUBP=1.0004
      GO TO 1550
 1530 SIEII=  AI*TI*TI +  BI*TI + CI
      RHOII=  AR*TI*TI +  BR*TI +  CR
      TMU  = AMU*TI*TI + BMU*TI + CMU
      TK   =  AK*TI*TI +  BK*TI +  CK
      CIT=CI-SIEX
      TEMP=SI( AI,BI,CIT,-1 )
      CSUBP= ACP*TI*TI + BCP*TI + CCP
      GO TO 1550
 1540 CONTINUE
 1550 NU=TMU/RHOII
      RPRAN=TK/( CSUBP*TMU )
      GO TO KIROBC,( 1162,1262,1362,1462,1605,1615,1625,1635,1736,1756 )
C
C NOTE. COMPUTATION OF THE TAU FACTOR FOR USE IN THE SIE EQUATION .
C
C NOTE. FLUID CELL TO THE   LEFT OF THE IK OBSTACLE .
 1600 ICSUBP=0
      IF( ITAUCN.GT.1 .OR. NTAU.LT.1 ) GO TO 1714
      ASSIGN 1605 TO KIROBC
```

```
      SIEX=SIE(IMK)
      ICSUBP=1
      GO TO 1500
1605  NTAU=CFC - 29
      RTAU=1./TAU(NTAU)
      P(IK)=1./(1.+DT*RTAU)*( P(IK) + DT*RTAU*TEMP )
      CQ(IMK)=CSUBPO*RTAU*( TEMP-P(IK) )
      ICSUBP=0
      GO TO 1714
C NOTE. FLUID CELL TO THE BOTTOM OF THE IK OBSTACLE .
1610  ICSUBP=0
      IF( ITAUCN.GT.1 .OR. NTAU.LT.1 ) GO TO 1724
      ASSIGN 1615 TO KIROBC
      SIEX=SIE(IKM)
      ICSUBP=1
      GO TO 1500
1615  NTAU=CFC - 29
      RTAU=1./TAU(NTAU)
      P(IK)=1./(1.+DT*RTAU)*( P(IK) + DT*RTAU*TEMP )
      CQ(IKM)=CSUBPO*RTAU*( TEMP-P(IK) )
      ICSUBP=0
      GO TO 1724
C NOTE. FLUID CELL TO THE   TOP  OF THE IK OBSTACLE .
1620  ICSUBP=0
      IF( ITAUCN.GT.1 .OR. NTAU.LT.1 ) GO TO 1744
      ASSIGN 1625 TO KIROBC
      SIEX=SIE(IKP)
      ICSUBP=1
      GO TO 1500
1625  NTAU=CFC - 29
      RTAU=1./TAU(NTAU)
      CQ(IKP)=CSUBPO*RTAU*(TI-P(IK))                            R3BVM03A
      ICSUBP=0
      GO TO 1744
C NOTE. FLUID CELL TO THE  RIGHT OF THE IK OBSTACLE .
1630  ICSUBP=0
```

```
      IF ( ITAUCN.GT.1 .OR. NTAU.LT.1 ) GO TO 1764
      ASSIGN 1635 TO KIROBC
      SIEX=SIE(IPK)
      ICSUBP=1
      GO TO 1500
 1635 NTAU=CFC - 29
      RTAU=1./TAU(NTAU)
      P(IK)=1./(1.+DT*RTAU)*( P(IK) + DT*RTAU*TEMP )
      CQ(IPK)=CSUBPO*RTAU*( TEMP-P(IK) )
      ICSUBP=0
      GO TO 1764
C
C NOTE. COMPUTATUON OF OBSTACLE SUBREGIONS BOUNDARY CONDITIONS .
C
 1700 KK=1
      ITAUCN=ITAUCN + 1
      I1=2
      I2=IBP1
      K1=2
      K2=KBP1
      IF( IOBS.EQ.0 ) GO TO 1990
      NDERR=0
      NDERL=0
      NDERB=0
      NDERT=0
      NCOFT=0
      NCOFR=0
      DO 1789 I=I1,I2
      KK=KK + K2NC
      LWPC=0
      DO 1779 K=K1,K2
      LWPC=LWPC + NWPC
      IK=KK + LWPC
      IMK=IK - K2NC
      IKM=IK - NWPC
      IKP=IK + NWPC
```

```
      IPK=IK + K2NC
      ICFC=CF(IK)
      CFC=ICFC
      IF( CFC.EQ.1 ) GO TO 1778
      CFT=IICFT(IK)+1
      CFB=IICFB(IK)+1
      CFR=IICFR(IK)+1
      CFL=IICFL(IK)+1
      IF( CFT.GT.1 ) GO TO 1710
      IF( CFB.GT.1 ) GO TO 1710
      IF( CFR.GT.1 ) GO TO 1710
      IF( CFL.GT.1 ) GO TO 1710
      U(IK)=0.0
      U(IMK)=0.0
      W(IK)=0.0
      W(IKM)=0.0
      TS(IK)=0.0
      TQ(IK)=0.0
      SIE(IK)=0.0
      GO TO 1770
C NOTE. OBSTACLE BOUNDARY CONDITION AT THE  LEFT  FACE .
1710  GO TO( 1720,1600 ),CFL
C NOTE. NON-FLUID CELL TO THE  LEFT  OF THE IK OBSTACLE .
1712  U(IMK)=0.0
      GO TO 1720
C NOTE. FLUID CELL TO THE   LEFT OF THE IK OBSTACLE .
1714  U(IMK)=0.0
      NRIGID=KDERBC + 1
      GO TO ( 1715,1716 ),NRIGID
C NOTE. RIGID BOUNDARY AT THE   LEFT FACE .
1715  W(IK)=FSLIP*W(IMK)
      SIE(IK)=SIE(IMK)
      TQ(IK)=TQ(IMK)
      TS(IK)=TS(IMK)
      GO TO 1720
C NOTE. DERIVED BOUNDARY CONDITION AT THE  LEFT  FACE .
```

```
1716  WC=W(IMK)
      QC=TQ(IMK)
      SC=TS(IMK)
      NDERL=NDERL + 1
      WSA=USLOB(NDERL)
      QW=5.*WSA*WSA
      SW=WSA*WSA*HDX/WC
      W(IK)=-WC
      TQ(IK)=2.*QW - QC
      TS(IK)=2.*SW - SC
      GO TO 1712
C NOTE. OBSTACLE BOUNDARY CONDITION AT THE BOTTOM FACE .
1720  GO TO( 1730,1610 ),CFB
C NOTE. NON-FLUID CELL TO THE BOTTOM OF THE IK OBSTACLE .
1722  W(IKM)=0.0
      GO TO 1730
C NOTE. FLUID CELL TO THE BOTTOM OF THE IK OBSTACLE .
1724  W(IKM)=0.0
      NRIGID=KDERBC + 1
      GO TO( 1725,1726 ),NRIGID
C NOTE. RIGID BOUNDARY AT THE BOTTOM FACE .
1725  U(IK)=FSLIP*U(IKM)
      SIE(IK)=SIE(IKM)
      TQ(IK)=TQ(IKM)
      TS(IK)=TS(IKM)
      GO TO 1730
C NOTE. DERIVED BOUNDARY CONDITION AT THE BOTTOM FACE .
1726  UCT=U(IKM)
      QCT=TQ(IKM)
      SCT=TS(IKM)
      NDERB=NDERB + 1
      USAT=USBOB(NDERB)
      QWT=5.*USAT*USAT
      SWT=USAT*USAT*HDZ/UCT
      U(IK)=-UCT
      TQ(IK)=2.*QWT - QCT
```

```
      TS(IK)=2.*SWT - SCT
      GO TO 1722
C NOTE. OBSTACLE BOUNDARY CONDITION AT THE   TOP  FACE .
1730  IF( CFC.GE.30 ) GO TO 1740
C NOTE. VARIABLE BOUNDARY OPTION AT THE  TOP  FACE .
      NCFT=CFC - 21
      GO TO( 1732,1734,1740,1740,1740 ),NCFT
C NOTE. CONSTANT INFLOW AT THE  TOP  FACE .
1732  W(IK)=WOBI
      GO TO 1745
C NOTE. VARIABLE OR FUNCTIONAL INFLOW AT THE TOP FACE .
1734  NCOFT=NCOFT + 1
      TI=OFOBTB(NCOFT)*T1NTAU + OFOBTC(NCOFT)*T2NTAU
     1+OFOBTD(NCOFT)*T3NTAU+OFOBTE(NCOFT)*T4NTAU+OFOBTF(NCOFT)*T5NTAU
      ASSIGN 1736 TO KIROBC
      SIEX=SIE(IKP)                                            RGBVM01A
      GO TO 1500
1736  AREAI=3.14159265*FLOAT(2*I-3)*DR*DR
      IF( CYL.LT.1.0 ) AREAI=DX
      FLI=OFOBTA(NCOFT)*FNTAU
      WBAR=FLI/RHOII
      W(IK)=WBAR/AREAI
       IF(NIV.EQ.1) W(IK)=FLI
       SIEC=SIE(IKP )
       SIEW=SIEII
       SIE(IK  )=(2*SIEW+(ALZ-1.0)*SIEC)/(1.0+ALZ)
      QCT = TQ(IKP)
      QWT = TQJET * W(IK)*W(IK)
      SCT = TS(IKP)
      SWT = TSJET * W(IK) * DR
       QWT=AMAX1(QWT,1.0E-5)
       SWT=AMAX1(SWT,NU)
       TQ(IK  )=(2*QWT+(ALZ-1.0)*QCT)/(1.0+ALZ)
       TS(IK  )=(2*SWT+(ALZ-1.0)*SCT)/(1.0+ALZ)
      U(IK)=FSLIP*U(IKP)
      GO TO 1750
```

```
C NOTE. OBSTACLE BOUNDARY CONDITION AT THE   TOP  FACE .
1740   GO TO( 1750,1620 ),CFT
C NOTE. NON-FLUID CELL TO THE   TOP  OF THE IK OBSTACLE .
1742   W(IK)=0.0
       GO TO 1750
C NOTE. FLUID CELL TO THE   TOP  OF THE IK OBSTACLE .
1744   W(IK)=0.0
       NRIGID=KDERBC + 1
       GO TO( 1745,1746 ),NRIGID
C NOTE. RIGID BOUNDARY AT THE   TOP  FACE .
 1745  U(IK)=-U(IKP)                                          RGBVM50A
       SIE(IK)=SIE(IKP)
       TQ(IK)=TQ(IKP)
       TS(IK)=TS(IKP)
       GO TO 1750
C NOTE. DERIVED BOUNDARY CONDITION AT THE   TOP  FACE .
1746   UCT=U(IKP)
       QCT=TQ(IKP)
       SCT=TS(IKP)
       NDERT=NDERT + 1
       USAT=USTOB(NDERT)
       QWT=5.*USAT*USAT
       SWT = USAT * USAT * HDZ/UCT
       U(IK) = -UCT
       TQ(IK)=2.*QWT - QCT
       TS(IK)=2.*SWT - SCT
       GO TO 1742
C NOTE. OBSTACLE BOUNDARY CONDITION AT THE  RIGHT FACE .
1750   IF( CFC.GE.30 ) GO TO 1760
C NOTE. VARIABLE BOUNDARY OPTION AT THE RIGHT FACE .
       NCFR=CFC - 21
       GO TO( 1776,1776,1776,1752,1754 ),NCFR
C NOTE. CONSTANT INFLOW AT THE RIGHT FACE .
1752   U(IK)=UOBI
       GO TO 1765
C NOTE. VARIABLE OR FUNCTIONAL INFLOW AT THE RIGHT FACE .
```

```
1754  NCOFR=NCOFR + 1
      TI=OFOBRB(NCOFR)*T1NTAU + OFOBRC(NCOFR)*T2NTAU
     1+OFOBRD(NCOFR)*T3NTAU+OFOBRE(NCOFR)*T4NTAU+OFOBRF(NCOFR)*T5NTAU
      ASSIGN 1756 TO KIROBC
      SIEX=SIE(IPK)                                                     RGBVM01A
      GO TO 1500
 1756 AREAK = 3.14159265 * 2*(I-1) * DR * DZ
      IF( CYL.LT.1.0 ) AREAK=DZ
      FLK=OFOBRA(NCOFR)*FNTAU
      UBAR=FLK/RHOII
      U(IK)=UBAR/AREAK
       IF(NIV.EQ.1) U(IK)=FLK
       SIEC=SIE(IPK )
       SIEW=SIEII
       SIE(IK  )=(2*SIEW+(ALX-1.0)*SIEC)/(1.0+ALX)
      QC = TQ(IPK)
      QW = TQJET * U(IK)*U(IK)
      SC = TS(IPK)
      SW = TSJET * U(IK) * DZ
       QW=AMAX1(QW,1.0E-5)
       SW=AMAX1(SW,NU)
       TQ(IK  )=(2*QW+(ALX-1.0)*QC)/(1.0+ALX)
       TS(IK  )=(2*SW+(ALX-1.0)*SC)/(1.0+ALX)
      W(IK)=FSLIP*W(IPK)
      GO TO 1770
C NOTE. OBSTACLE BOUNDARY CONDITION AT THE  RIGHT FACE .
1760  GO TO( 1770,1630 ),CFR
C NOTE. NON-FLUID CELL TO THE  RIGHT OF THE IK OBSTACLE .
1762  U(IK)=0.0
      GO TO 1770
C NOTE. FLUID CELL TO THE  RIGHT OF THE IK OBSTACLE .
1764  U(IK)=0.0
      NRIGID=KDERBC + 1
      GO TO( 1765,1766 ),NRIGID
C NOTE. RIGID BOUNDARY AT THE  RIGHT FACE .
1765  W(IK)=FSLIP*W(IPK)
```

```
      SIE(IK)=SIE(IPK)
      TQ(IK)=TQ(IPK)
      TS(IK)=TS(IPK)
      GO TO 1770
C NOTE. DERIVED BOUNDARY CONDITION AT THE  RIGHT FACE .
1766  WC=W(IPK)
      QC=TQ(IPK)
      SC=TS(IPK)
      NDERR=NDERR + 1
      WSA=USROB(NDERR)
      QW=5.*WSA*WSA
      SW = WSA * WSA * HDX/WC
      W(IK)  = -WC
      TQ(IK)=2.*QW - QC
      TS(IK)=2.*SW - SC
      GO TO 1762
1770  IF( CFT.EQ.2 .AND. CFC.GE.30 ) W(IK)=0.0
1776  IF( CFR.EQ.2 .AND. CFC.LT.25 ) U(IK)=0.0
1778  CONTINUE
1779  CONTINUE
1789  CONTINUE
1990  GO TO KBC,( 2000,2990,4100,5000,5060 )
C
C NOTE. CHECKS FOR INITIAL CYCLES PRINTS ,I.E. NPRT=0 NO PRINT,
C NOTE. NPRT=1 CYCLE 0 PRINT AND NPRT=2 CYCLE 0,1 PRINTS .
C
2000  IF( NCYC.LT.NPRT ) GO TO 2010
      GO TO 2030                                               VM200004
2010  CALL VRPRT
      IF( IPRFM.GT.0 ) CALL VRFLM
C NOTE. CALL TO THE VARIABLE RESISTANCE SUBROUTINE .
C NOTE. BEGIN THE N PASS PHASE OF THE TILDE EQUATION SECTION .
2030  DO 2999 NTE=1,NTPAS
      IF( NWPC.GT.11 ) CALL VREQ
C
C NOTE. U AND W TILDE VELOCITY EQUATIONS SECTION .
```

```
C
C NOTE. TRANSFERS VELOCITIES TO STORAGE ARRAY( AT TIME=N ) .
      K1=1
      K2=KBP2
      LWPC=1 - NWPC
      DO 2109 K=K1,K2
      LWPC=LWPC+NWPC                                                    VM210008
      IK=LWPC
      IKS=I2K2 + IK
      SIE(IKS)=SIE(IK)
      U(IKS)=U(IK)
      W(IKS)=W(IK)
      TQ(IKS)=TQ(IK)
      TS(IKS)=TS(IK)
      CHI(IKS)=CHI(IK)                                                  RGBVM52A
      VAP(IKS)=VAP(IK)                                                  RGBVM60A
      LIQ(IKS)=LIQ(IK)                                                  RGBVM60A
 2109 CONTINUE                                                          VM210900
      I1=2
      I2=IBP1
      K1=2
      K2=KBP2
      KK=0
      KKL = 0
      DO 2989 I=I1,I2
      KK=KK+K2NC                                                        VM221002
      KKL = KKL + K2NCL
      LWPCL = 1
      LWPC=1
      IKMS=I2K2 + 1
      SIE(1)=SIE(IKMS)
      U(1)=U(IKMS)
      W(1)=W(IKMS)
      TQ(1)=TQ(IKMS)
      TS(1)=TS(IKMS)
      CHI(1)=CHI(IKMS)                                                  RGBVM52A
```

```
      VAP(1)=VAP(IKMS)                                          RGBVM60A
      LIQ(1)=LIQ(IKMS)                                          R3BVM60A
      SIE(IKMS)=SIE(KK+1)
      U(IKMS)=U(KK+1)
      W(IKMS)=W(KK+1)
      TQ(IKMS)=TQ(KK+1)
      TS(IKMS)=TS(KK+1)
      CHI(IKMS)=CHI(KK+1)                                       RGBVM52A
      VAP(IKMS)=VAP(KK+1)                                       R3BVM60A
      LIQ(IKMS)=LIQ(KK+1)                                       RGBVM60A
      GO TO KRU,( 2215,2220 )                                   VM221012
C NOTE. COMPUTATION OF RADIUS CONSTANTS IN THE I DIRECTION .
2215  RR=FLOAT(I-1)*DX
      RC=RR-HDX
      RL=RR-DX
      RRR=1./RR
      RRC=1./RC
      RRC1=RR + HDX
      RRRC=1./RRC1
      RRP=RR + DR
2220  DO 2979 K=K1,K2
C NOTE. COMPUTATION OF CELL INDICES .
      LWPC=LWPC+NWPC                                            VM222002
      IK=KK + LWPC
      LWPCL = LWPCL + NWPCL
      IKL = KKL + LWPCL
      DCR = DIFFCO(IKL)
      DCT = DIFFCO(IKL+1)
      DCL = DIFFCO(IKL+2)
      DCB = DIFFCO(IKL+3)
C NOTE. BYPASS OBSTACLE CELLS .
      CPC=CP(IK)
      IPK=IK + K2NC
      IKP=IK + NWPC
      IMKS=I2K2 + LWPC
      IKMS=IMKS - NWPC
```

```
      UR=U (IPK)
      UC=U (IK)
      UL=U (IMKS)
      WT=W (IKP)
      WC=W (IK)
      WB=W (IKMS)
      PC=P (IK)
      PR=P (IPK)
      PT=P (IKP)
      SIEC=SIE (IK)
      SIER=SIE (IPK)
      SIET=SIE (IKP)
      SIEL=SIE (IMKS)
      SIEB=SIE (IKMS)
      SIECO=SIEO (IK)
      UCO=UO (IK)
      WCO=WO (IK)
C NOTE. COMPUTATION OF TQ AND TS CONSTANTS .
      TQC=TQ (IK)
      TQR=TQ (IPK)
      TQT=TQ (IKP)
      TQL=TQ (IMKS)
      TQB=TQ (IKMS)
      TQCO=TQO (IK)
      TSC=TS (IK)
      TSR=TS (IPK)
      TST=TS (IKP)
      TSL=TS (IMKS)
      TSB=TS (IKMS)
      TSCO=TSO (IK)
      CHIC=CHI (IK)                                         RGBVM52A
      CHIR=CHI (IPK)                                        R3BVM52A
      CHIT=CHI (IKP)                                        RGBVM52A
      CHIL=CHI (IMKS)                                       R3BVM52A
      CHIB=CHI (IKMS)                                       RGBVM52A
      CHICO=CHIO (IK)                                       R3BVM52A
```

```
      VAPC=VAP(IK)                                                      RGBVM60A
      VAPR=VAP(IPK)                                                     RGBVM60A
      VAPT=VAP(IKP)                                                     RGBVM60A
      VAPL=VAP(IMKS)                                                    RGBVM60A
      VAPB=VAP(IKMS)                                                    RGBVM60A
      VAPCO=VAPO(IK)                                                    RGBVM60A
      LIQC=LIQ(IK)                                                      RGBVM60A
      LIQR=LIQ(IPK)                                                     RGBVM60A
      LIQT=LIQ(IKP)                                                     RGBVM60A
      LIQL=LIQ(IMKS)                                                    RGBVM60A
      LIQB=LIQ(IKMS)                                                    RGBVM60A
      LIQCO=LIQO(IK)                                                    RGBVM60A
      IF( CPC.NE.1 )  GO TO 2700
      TSTR=.25*( TSR + TSC + TST + TS(IKP+K2NC) )
      TSBR=.25*( TSR + TSC + TSB + TS(IPK-NWPC) )
      TSTL=.25*( TSL + TSC + TST + TS(IMKS+NWPC) )
      IF( ICALI.EQ.2 ) GO TO 2500
      GO TO KRXRZ, ( 2250,2300 )                                        VM222028
C NOTE. STORAGE OF SUBSCRIPTED RX(),RZ() TO CONSTANT RXC AND RZC .
2250  RXC=RX(IK)*ABS( UC )**NRESEX
      RZC=RZ(IK)*ABS( WC )**NRESEX
C NOTE. COMPUTATION OF U TILDE FLUXES .
2300  URA=.5*(UC+UR)                                                    VM230000
      URAA=ABS(URA)                                                     VM230002
      ULA=.5*(UL+UC)                                                    VM230004
      ULAA=ABS(ULA)                                                     VM230006
      FUX=.5*RDX*( URA*(UC+UR) + ALX*URAA*(UC-UR) - ULA*(UL+UC)         VM230008
     1            -ALX*ULAA*(UL-UC) )                                   VM230010
      WTA=.5*(WC+W(IPK))
      WTAA=ABS(WTA)                                                     VM230014
      WBA=.5*(WB+W(IPK-NWPC))
      WBAA=ABS(WBA)                                                     VM230018
      FUZ=.5*RDZ*( WTA*(UC+U(IKP)) + ALZ*WTAA*(UC-U(IKP))
     1             - WBA*(U(IKMS)+UC) - ALZ*WBAA*(U(IKMS)-UC) )
C NOTE. CALCULATION OF THE U TILDE DIFFUSION TERMS .
      DURR=RDRP*RRRC*TSR*( RRP*UR - RR*UC )
```

```
      DURL=RDR*RRC*TSC*( RR*UC - RL*UL )
      DUR=RDR*( DURR - DURL )
      DUZ=RDZ*( TSTR*(U(IKP)-UC)*RDZP - TSBR*(UC-U(IKMS))*RDZM )
      FUT=DUR + DUZ
      GO TO KCLU,( 2370,2400 )
C NOTE. COMPUTATION OF THE U TILDE CYLINDRICAL FLUX TERM .
2370  FCU=.5*RRR*( URA*URA + ULA*ULA + .5*ALX*URAA*(UC-UR)
     1            + .5*ALX*ULAA*(UL-UC) )                            VM237002
C NOTE. COMPUTATION OF W TILDE FLUXES .
2400  UTA=.5*(UC+U(IKP))
      UTAA=ABS(UTA)                                                  VM240002
      ULT=.5*(UL+U(IMKS+NWPC))
      ULTA=ABS(ULT)                                                  VM240006
      WTA=.5*( WC+WT )
      WTAA=ABS( WTA )
      WBA=.5*( WB+WC )
      WBAA=ABS( WBA )
      FWX=.5*RDX*( UTA*(WC+W(IPK)) + ALX*UTAA*(WC-W(IPK))
     1          - ULT*(W(IMKS)+WC) - ALX*ULTA*(W(IMKS)-WC) )
      FWZ=.5*RDZ*( WTA*(WC+WT) + ALZ*WTAA*(WC-WT)                    VM240012
     1          - WBA*(WB+WC) - ALZ*WBAA*(WB-WC) )                   VM240014
C NOTE. CALCULATION OF THE W TILDE DIFFUSION TERMS .
      DWRR=RDRP*RR*TSTR*(W(IPK)-WC)
      DWRL=RDRM*RL*TSTL*(WC-W(IMKS))
      DWR=RRC*RDR*( DWRR - DWRL )
      DWZ=RDZP*( TST*(WT-WC)*RDZ - TSC*(WC-WB)*RDZ )
      FWT=DWR + DWZ
      GO TO KCLW,( 2470,2500 )
C NOTE. COMPUTATION OF THE W TILDE CYLINDRICAL FLUX TERM .
2470  FCW=.25*RRC*( UTA*(WC+W(IPK)) + ULT*(W(IMKS)+WC)
     1            + ALX*UTAA*(WC-W(IPK)) + ALX*ULTA*(W(IMKS)-WC) )
C NOTE. COMPUTATION  OF BOTH  Q AND SIGMA TURBULANCE QUANTITIES .
2500  TQRA=.5*(TQC+TQR)
      IF( ICALI.EQ.1 ) GO TO 2591
      TQLA=.5*(TQC+TQL)
      TQTA=.5*(TQC+TQT)
```

```
      TQBA=.5*(TQC+TQB)
      TSRA=.5*(TSC+TSR)
      TSLA=.5*(TSC+TSL)
      TSTA=.5*(TSC+TST)
      TSBA=.5*(TSC+TSB)
C NOTE. CALCULATION OF THE SIJ  TERM,I.E. THE SOURCE TERM .
      SIJ=RDRS*(UC-UL)**2 + RDZS*(WC-WB)**2 + .25*CYL*(RRC*(UC+UL))**2 +
     1    0.03125*( RDZ*( U(IKP)+U(IMKS+NWPC)-U(IKMS)-U(1) )
     2              + RDR*( W(IPK)+W(IPK-NWPC)-W(IMKS)-W(1) ) )**2
C NOTE. CALCULATION OF THE Q EQUATION CONVECTION TERMS .
      CQR=-.5*RRC*RDR*( RR*( UC*(TQC+TQR) + ALX*ABS(UC)*(TQC-TQR) )
     1                - RL*( UL*(TQL+TQC) + ALX*ABS(UL)*(TQL-TQC) ) )
      CQZ=-.5*RDZ*(WC*(TQC+TQT) + ALZ*ABS(WC)*(TQC-TQT)
     1            - WB*(TQB+TQC) - ALZ*ABS(WB)*(TQB-TQC) )
C NOTE. CALCULATION OF THE Q EQUATION DIFFUSION TERM .
      DQRR = RRC * RDR * (RR * TSRA * (TQR - TQC)) * DCR
      DQRL = RRC * RDR * (RL * TSLA * ( TQC - TQL)) * DCL
      DQR = RDR * ( DQRR - DQRL)
      DQZT = RDZ * ( TSTA * ( TQT - TQC )) * DCT
      DQZB = RDZ * ( TSBA * ( TQC - TQB )) * DCB
      DQZ = RDZ * ( DQZT - DQZB)
C NOTE. CALCULATION OF THE Q EQUATION DECAY TERM .
      DQ=4.*ALP*TQC/( TSC+1.E-20 )
C NOTE. CALCULATION OF THE NEW Q AT TIME N+1 .
      TQ(IK)=(1./(1.+DT*DQ))*( TQCO + DT*(CQR+CQZ+2.*TSC*SIJ +
     1                         GAM*(DQR+DQZ)) )
C NOTE. COMPUTATION  OF SIGMA QUANTITIES .
C NOTE. CALCULATION OF THE SIGMA EQUATION CONVECTION TERMS .
      CSR=-.5*RRC*RDR*( RR*( UC*(TSC+TSR) + ALX*ABS(UC)*(TSC-TSR) )
     1                - RL*( UL*(TSL+TSC) + ALX*ABS(UL)*(TSL-TSC) ) )
      CSZ=-.5*RDZ*( WC*(TSC+TST) + ALZ*ABS(WC)*(TSC-TST)
     1             - WB*(TSB+TSC) - ALZ*ABS(WB)*(TSB-TSC) )
C NOTE. CALCULATION OF THE SIGMA EQUATION DIFFUSION TERM .
      IF( I.LT.I2 ) GO TO 2502
      IFLGS=0
      IFLGQ=0
```

```
      IF( TQR.LT.0.0 ) IFLGQ=1
      IF( TSR.LT.0.0 ) IFLGS=1
      IFLG1=IFLGQ+IFLGS
      IF( IFLG1.EQ.2 ) TQR=-TQR
 2502 IF( K.GT.K1 ) GO TO 2504
      IFLGS=0
      IFLGQ=0
      IF( TQB.LT.0.0 ) IFLGQ=1
      IF( TSB.LT.0.0 ) IFLGS=1
      IFLG1=IFLGQ + IFLGS
      IF( IFLG1.EQ.2 ) TQB=-TQB
 2504 IF( K.LT.KBP1 ) GO TO 2506
      IFLGS=0
      IFLGQ=0
      IF( TQT.LT.0.0 ) IFLGQ=1
      IF( TST.LT.0.0 ) IFLGS=1
      IFLG1=IFLGQ + IFLGS
      IF( IFLG1.EQ.2 ) TQT=-TQT
 2506 IF( I.GT.I1 ) GO TO 2508
      IFLGS=0
      IFLGQ=0
      IF( TQL.LT.0.0 ) IFLGQ=1
      IF( TSL.LT.0.0 ) IFLGS=1
      IFLG1=IFLGQ + IFLGS
      IF( IFLG1.EQ.2 ) TQL=-TQL
 2508 CONTINUE
      DSRR = RRC * RDR * ( RR * TQRA * ( TQR/TSR - TQC/TSC )) * DCR
      DSRL = RRC * RDR * ( RL * TQLA * (TQC/TSC - TQL/TSL )) * DCL
      DSR = RDR * ( DSRR - DSRL)
      DSZT = RDZ * ( TQTA * ( TQT/TST - TQC/TSC)) * DCT
      DSZB = RDZ * ( TQBA * ( TQC/TSC - TQB/TSB )) * DCB
      DSZ = RDZ * ( DSZT - DSZB)
C     DIJ=GAM*TSC/TQC*( DQR+DQZ ) - GAM1*TSC*TSC*TSC/TQC*TQC*(DSR+DSZ)  RGBVM000
      DIJ=GAM*TSC/TQC*( DQR+DQZ ) - GAM1*TSC*TSC*TSC/TQC**2*(DSR+DSZ)   RGBVM000
C     DS=4.*ALPO*TQC/( TSC+1.E-20 )                                     MWG04/78
      DS=ALP*TQC/(TSC+1.E-20)                                           MWG04/78
```

```
C NOTE. CALCULATION OF THE NEW SIGMA AT N+1 .
      TS(IK)=(1./(1.+DT*DS))*( TSCO+DT*(CSR+CSZ+TSC*TSC/TQC*SIJ+DIJ) )
      IF(TQ(IK).LT.ZTQ(K))  TQ(IK)=ZTQ(K)                                RGBVM51A
      IF(TS(IK).LT.ZTS(K))  TS(IK)=ZTS(K)                                RGBVM51A
C  CALCULATION OF TERMS IN THE VAP TRANSPORT EQUATION                    RGBVM61A
      CVR=.5*RRC*RDR*( RR*( UC*(VAPC+VAPR)  + ALX*ABS(UC)*(VAPC-VAPR) )  RGBVM61A
     1              - RL*( UL*(VAPL+VAPC)  + ALX*ABS(UL)*(VAPL-VAPC) ) )RGBVM61A
      CVZ=.5*RDZ*( WC*(VAPC+VAPT)  + ALZ*ABS(WC)*(VAPC-VAPT)             RGBVM61A
     1           - WB*(VAPB+VAPC)  - ALZ*ABS(WB)*(VAPB-VAPC) )           RGBVM61A
        DVRR=RDR*(RR*GAMV*TSRA*DCR*(VAPR-VAPC))                          RGBVM61A
        DVRL=RDR*(RL*GAMV*TSLA*DCL*(VAPC-VAPL))                          RGBVM61A
        DVR=RRC*RDR*(DVRR-DVRL)                                          RGBVM61A
        DVZT=RDZ*(GAMV*TSTA*DCT*(VAPT-VAPC))                             RGBVM61A
        DVZB=RDZ*(GAMV*TSBA*DCB*(VAPC-VAPB))                             RGBVM61A
        DVZ=RDZ*(DVZT-DVZB)                                              RGBVM61A
      VAP(IK)=VAPCO+DT*(-CVR-CVZ+DVR+DVZ)                                RGBVM61A
C  CALCULATION OF TERMS IN THE LIQ TRANSPORT EQUATION                    RGBVM61A
      CLR=.5*RRC*RDR*( RR*( UC*(LIQC+LIQR)  + ALX*ABS(UC)*(LIQC-LIQR) )  RGBVM61A
     1              - RL*( UL*(LIQL+LIQC)  + ALX*ABS(UL)*(LIQL-LIQC) ) )RGBVM61A
      CLZ=.5*RDZ*( WC*(LIQC+LIQT)  + ALZ*ABS(WC)*(LIQC-LIQT)             RGBVM61A
     1           - WB*(LIQB+LIQC)  - ALZ*ABS(WB)*(LIQB-LIQC) )           RGBVM61A
        DLRR=RDR*(RR*GAML*TSRA*DCR*(LIQR-LIQC))                          RGBVM61A
        DLRL=RDR*(RL*GAML*TSLA*DCL*(LIQC-LIQL))                          RGBVM61A
        DLR=RRC*RDR*(DLRR-DLRL)                                          RGBVM61A
        DLZT=RDZ*(GAML*TSTA*DCT*(LIQT-LIQC))                             RGBVM61A
        DLZB=RDZ*(GAML*TSBA*DCB*(LIQC-LIQB))                             RGBVM61A
        DLZ=RDZ*(DLZT-DLZB)                                              RGBVM61A
      LIQ(IK)=LIQCO+DT*(-CLR-CLZ+DLR+DLZ)                                RGBVM61A
C                                                                        RGBVM62A
C  EQUILIBRIUM MOISTURE THERMODYNAMICS SECTION                           RGBVM62A
      CIT=CI-SIEC                                                        RGBVM56A
      TEMPC=SI(AI,BI,CIT,-1)                                             RGBVM56A
      RHOC=AR*TEMPC*TEMPC+BR*TEMPC+CR                                    RGBVM56A
C  CALCULATE THE ABSOLUTE THERMODYNAMIC TEMPERATURE  (DEG C)             RGBVM62A
      ABT=(TEMPC+459.7)*((ZAP(K)/1000.)**.2856)/(1.+0.61*VAP(IK)/RHOC)/1RGBVM62A
```

```
C  CALCULATE THE SATURATION VAPOR PRESSURE  (MB)                         RGBVM62A
      EVAP=10.**(-2937.4/ABT-4.9283*ALOG10(ABT)+23.5518)                  RGBVM62A
C  CALCULATE THE VAPOR DENSITY AT SATURATION  (LBM/CU FT)                 RGBVM62A
      RHOS=RHOC*0.61*EVAP/ZAP(K)                                          RGBVM62A
      IF(VAP(IK).LT.RHOS) GO TO 300                                       RGBVM62A
      IF(VAP(IK).EQ.RHOS) GO TO 320                                       RGBVM62A
C  CONDENSE VAPOR AND RELEASE LATENT HEAT                                 RGBVM62A
      LIQ(IK)=LIQ(IK)+VAP(IK)-RHOS                                        RGBVM62A
      CQ(IK)=CQ(IK)-((VAP(IK)-RHOS)*1075.0)/(DT*RHOC)                     RGBVM62A
      VAP(IK)=RHOS                                                        RGBVM62A
      GO TO 320                                                           RGBVM62A
C  EVAPORATE LIQUID AND ABSORB LATENT HEAT                                RGBVM62A
  300 IF(LIQ(IK).LE.0.0) GO TO 320                                        RGBVM62A
      IF(LIQ(IK).LE.RHOS-VAP(IK)) GO TO 310                               RGBVM62A
      LIQ(IK)=LIQ(IK)-RHOS+VAP(IK)                                        RGBVM62A
      CQ(IK)=CQ(IK)+((RHOS-VAP(IK))*1075.0)/(DT*RHOC)                     RGBVM62A
      VAP(IK)=RHOS                                                        RGBVM62A
      GO TO 320                                                           RGBVM62A
  310 CQ(IK)=CQ(IK)+(LIQ(IK)*1075.0)/(DT*RHOC)                            RGBVM62A
      VAP(IK)=VAP(IK)+LIQ(IK)                                             RGBVM62A
      LIQ(IK)=0.0                                                         RGBVM62A
  320 CONTINUE                                                            RGBVM62A
C                                                                         RGBVM62A
C
C NOTE. COMPUTATION OF SPECIFIC INTERNAL ENERGY .
C
C NOTE. CALCULATION OF THE SIE EQUATION CONVECTION TERMS .
2590  CIR=.5*RRC*RDR*( RR*( UC*(SIEC+SIER) + ALX*ABS(UC)*(SIEC-SIER) )
     1             - RL*( UL*(SIEL+SIEC) + ALX*ABS(UL)*(SIEL-SIEC) ) )
      CIZ=.5*RDZ*( WC*(SIEC+SIET) + ALZ*ABS(WC)*(SIEC-SIET)
     1          - WB*(SIEB+SIEC) - ALZ*ABS(WB)*(SIEB-SIEC) )
C NOTE. CALCULATION OF THE SIE EQUATION DIFFUSION TERMS .
      GAMT=TGAM
      IF( TSC.LE.NU ) GAMT=RPRAN
       DIFR=RDR*(RR*GAMT*TSRA*DCR*(SIER-SIEC))
       DIFL=RDR*(RL*GAMT*TSLA*DCL*(SIEC-SIEL))
```

```
      DIR=RRC*RDR*(DIRR-DIRL)
      DIZT=RDZ*(GAMT*TSTA*DCT*(SIET-SIEC))
      DIZB=RDZ*(GAMT*TSBA*DCB*(SIEC-SIEB))
      DIZ=RDZ*(DIZT-DIZB)
C  CALCULATION OF DECAY HEAT  (BTU/LBM*SEC)                         RGBVM56A
      DECHT=4.150934E10*CHI(IK)*SER/(RHOC*WMOLX)                    RGBVM56A
C NOTE. COMPUTATION OF THE NEW SPECIFIC INTERNAL ENTERGY AT N+1 .
      SIE(IK)=SIECO + DT*( -CIR - CIZ + DIR + DIZ - CQ(IK)+DECHT)  RGBVM56A
C  CALCULATION OF TERMS IN THE CHI TRANSPORT EQUATION               RGBVM52C
      CXR=.5*RRC*RDR*( RR*( UC*(CHIC+CHIR) + ALX*ABS(UC)*(CHIC-CHIR) )  RGBVM52C
     1            - RL*( UL*(CHIL+CHIC) + ALX*ABS(UL)*(CHIL-CHIC) ) )RGBVM52C
      CXZ=.5*RDZ*( WC*(CHIC+CHIT) + ALZ*ABS(WC)*(CHIC-CHIT)         RGBVM52C
     1          - WB*(CHIB+CHIC) - ALZ*ABS(WB)*(CHIB-CHIC) )         RGBVM52C
      DXRR=RDR*(RR*GAMX*TSRA*DCR*(CHIR-CHIC))                        RGBVM52C
      DXRL=RDR*(RL*GAMX*TSLA*DCL*(CHIC-CHIL))                        RGBVM52C
      DXR=RRC*RDR*(DXRR-DXRL)                                        RGBVM52C
      DXZT=RDZ*(GAMX*TSTA*DCT*(CHIT-CHIC))                           RGBVM52C
      DXZB=RDZ*(GAMX*TSBA*DCB*(CHIC-CHIB))                           RGBVM52C
      DXZ=RDZ*(DXZT-DXZB)                                            RGBVM52C
      CHI(IK)=CHICO*(1.0-RLAMB*DT)+DT*(-CXR-CXZ+DXR+DXZ)            RGBVM52C
      GO TO 2650
C NOTE. CALCULATION OF SPECIFIC MATERIAL FOR TEMPERATURE AND
C NOTE. RELATIVE DENSITY .
2591  GO TO ( 2592,2594,2596,2598 ),MAT
C NOTE. CALCULATION OF SODIUM MATERIAL FOR TEMPERATURE AND RHO .
2592  TEMPC=-385.27 + 2.6602*SIEC + 5.9894E-04*SIEC*SIEC +
     1      1.5575E-06*SIEC**3 - 2.9048E-09*SIEC**4 +
     2      1.15427E-12*SIEC**5
      TEMPT=-385.27 + 2.6602*SIET + 5.9894E-04*SIET*SIET +
     1      1.5575E-06*SIET**3 - 2.9048E-09*SIET**4 +
     2      1.15427E-12*SIET**5
      TEMPR=-385.27 + 2.6602*SIER + 5.9894E-04*SIER*SIER +
     1      1.5575E-06*SIER**3 - 2.9048E-09*SIER**4 +
     2      1.15427E-12*SIER**5
      RHOC=59.566 - 7.9504E-3*TEMPC - 0.2872E-6*TEMPC*TEMPC +
     1     0.06035E-9*TEMPC*TEMPC*TEMPC
```

```
      RHOT=59.566 - 7.9504E-3*TEMPT - 0.2872E-6*TEMPT*TEMPT +
     1     0.06035E-9*TEMPT*TEMPT*TEMPT
      RHOR=59.566 - 7.9504E-3*TEMPR - 0.2872E-6*TEMPR*TEMPR +
     1     0.06035E-9*TEMPR*TEMPR*TEMPR
      RHOA=0.5*( RHOC+RHOT )
      RHOAX=0.5*( RHOC+RHOR )
      RHOX=( RHOAX-RHOO )/RHOO
      RHOZ=( RHOA-RHOO )/RHOO
      GO TO 2600
C NOTE. CALCULATION OF WATER  MATERIAL FOR TEMPERATURE AND RHO .
 2594 TEMPC=0.9996*SIEC + 32.0002
      TEMPT=0.9996*SIET + 32.0002
      TEMPR=0.9996*SIER + 32.0002
      RHOC=62.742 -0.372E-2*TEMPC - 0.44E-4*TEMPC*TEMPC
      RHOT=62.742 -0.372E-2*TEMPT - 0.44E-4*TEMPT*TEMPT
      RHOA=0.5*( RHOC+RHOT )
      RHOA=0.5*( RHOC+RHOR )
      RHOZ=( RHOA-RHOO )/RHOO
      RHOR=62.742 -0.372E-2*TEMPR - 0.44E-4*TEMPR*TEMPR
      RHOX=( RHOA-RHOO )/RHOO
      GO TO 2600
 2596 CIT=CI - SIEC
      TEMPC=SI( AI,BI,CIT,-1 )
      CIT=CI-SIET
      TEMPT=SI( AI,BI,CIT,-1 )
      CIT=CI-SIER
      TEMPR=SI( AI,BI,CIT,-1 )
      RHOC=AR*TEMPC*TEMPC + BR*TEMPC + CR
      RHOT=AR*TEMPT*TEMPT + BR*TEMPT + CR
      RHOR=AR*TEMPR*TEMPR + BR*TEMPR + CR
      RHOA=0.5*( RHOC+RHOT )
      RHOZ=( RHOA-RHOO )/RHOO
      RHOA=0.5*( RHOC+RHOR )
      RHOX=( RHOA-RHOO )/RHOO
      GO TO 2600
 2598 CONTINUE
```

```
C NOTE. COMPUTATION OF FULL TILDE EQUATIONS AT TIME=N+1 .
2600  IF( ICALI.EQ.2 ) GO TO 2650
      U(IK)=(1./(1.+DT*RXC))*( UCO + DT*( RDX*(PC-PR) + RHOX*GX
     1                           - FUX - FUZ - FCU + FUT ) )
      W(IK)=(1./(1.+DT*RZC))*( WCO + DT*( RDZ*(PC-PT) + RHOZ*GZ
     1                           - FWX - FWZ - FCW + FWT ) )
2650  IF( ICALI.EQ.1 ) GO TO 2700
C NOTE. UPDATING THE Q EQUATION WITH THE RESISTANCE FACTORS .
      RXC=RX(IK)*ABS( UO(IK) )**NRESEX
      RXL=RX(IMK)*ABS( UO(IMK) )**NRESEX
      RZC=RZ(IK)*ABS( WO(IK) )**NRESEX
      RZB=RZ(IKM)*ABS( WO(IKM) )**NRESEX
2700  U(1)=U(IMKS)
      W(1)=W(IMKS)
      TQ(1)=TQ(IMKS)
      TS(1)=TS(IMKS)
      SIE(1)=SIE(IMKS)
      CHI(1)=CHI(IMKS)                                       RGBVM52B
      VAP(1)=VAP(IMKS)                                       RGBVM60A
      LIQ(1)=LIQ(IMKS)                                       RGBVM60A
      SIE(IMKS)=SIEC
      U(IMKS)=UC
      W(IMKS)=WC
      TQ(IMKS)=TQC
      TS(IMKS)=TSC
      CHI(IMKS)=CHIC                                         RGBVM52B
      VAP(IMKS)=VAPC                                         RGBVM60A
      LIQ(IMKS)=LIQC                                         RGBVM60A
2979  CONTINUE
2989  CONTINUE
      ASSIGN 2990 TO KBC
      IF( NTE.LT.NTPAS ) GO TO 1100
2990  CONTINUE
2999  CONTINUE
      IF( ICALI.EQ.2 ) GO TO 5050
C NOTE. IMPLICIT PRESSURE ITERATION .
```

```
4050  IFC=0
      ASSIGN 4100 TO KBC
      GO TO 1100                                                        VM452002
C NOTE. BEGIN PRESSURE ITERATION AFTER SETING BOUNDARY CONDITIONS .
4100  I1=2
      I2=IBP1
      K1=2
      K2=KBP1
      KK=1
      DO 4489 I=I1,I2
      KK=KK + K2NC
      LWPC=0
      RADD=(FLOAT(I)-1.5)*DX                                            VM412006
      RRADD=1./RADD                                                     VM412008
      IF( CYL.LT.EM6 ) RRADD=0.0                                        VM412010
      DO 4479 K=K1,K2
      LWPC=LWPC + NWPC
      IK=KK + LWPC
      IMK=IK - K2NC
      IKM=IK - NWPC
      CFC=CF(IK)
      IF( CFC.NE.1 ) GO TO 4470
      D=RDX*(U(IK)-U(IMK)) + RDZ*(W(IK)-W(IKM)) +.5*RRADD*(U(IK)+U(IMK))
      DTP=-BETA*D                                                       VM420002
      RXC=RX(IK)*ABS( UO(IK) )**NRESEX
      RXL=RX(IMK)*ABS( UO(IMK) )**NRESEX
      RZC=RZ(IK)*ABS( WO(IK) )**NRESEX
      RZB=RZ(IKM)*ABS( WO(IKM) )**NRESEX
      U(IK)=U(IK) + RDX*DTP/(1.+DT*RXC)
      U(IMK)=U(IMK) - RDX*DTP/(1.+DT*RXL)
      W(IK)=W(IK) + RDZ*DTP/(1.+DT*RZC)
      W(IKM)=W(IKM) - RDZ*DTP/(1.+DT*RZB)
      P(IK)=P(IK) + RDT*DTP
C NOTE. CHECKS FOR CONVERGENCE OF PRESSURE FIELD .
      IF( ABS(D).GT.EPS ) IFC=1
4470  CONTINUE
```

```
4479  CONTINUE
4489  CONTINUE
      ITER=ITER + 1
       IF(ITER.LT.1500) GO TO 4510
C NOTF. PRESSURES FAILED TO CONVERGE WITHIN 999 ITERATIONS .
      WRITE(IVDO,50)
       ERP=AMIN1(1.0,.1*NCYC)
      GO TO 4600
4510  IF( IFC.EQ.1 ) GO TO 4050
4600  ASSIGN 5000 TO KBC
      ITERC=ITER
      ITER=0
      GO TO 1100                                        VM452002
C
C NOTF. COMPUTES THE DIVERGENCE ERRORS - ER(IK) .
C
5000  ICALI=2
      GO TO 2030
5050  ASSIGN 5060 TO KBC
      GO TO 1100
5060  ITER=ITERC
      I1=1
      I2=IBP2
      K1=1
      K2=KBP2
      KK=1 - K2NC
      DMX=0.0
      TSMAX=-1.E+20
      TMAX=TSMAX
      WMAX=TMAX
      UMAX=WMAX
      TMIN=+1.E+20
      WMIN=TMIN
      UMIN=WMIN
      PMAX=-1.E+20
      TQMAX=PMAX
```

```
      DO 5029 I=I1,I2
      KK=KK + K2NC
      LWPC=-NWPC
      RRADD=1./( (FLOAT(I)-1.5)*DX )
      DO 5019 K=K1,K2
      LWPC=LWPC + NWPC
      IK=KK + LWPC
      IMK=IK - K2NC
      IKM=IK - NWPC
      CFC=CF(IK)
      IF( CFC.NE.1 ) GO TO 5001
      ER(IK)= RDX*( U(IK)-U(IMK)) + RDZ*( W(IK)-W(IKM))
      DMX=AMAX1( DMX,ABS(ER(IK)) )
     1              + .5*CYL*RRADD*( U(IK)+U(IMK))
 5001 SIEO(IK)=SIE(IK)
      TQO(IK)=TQ(IK)
      TSO(IK)=TS(IK)
      UO(TK)=U(IK)
      WO(IK)=W(IK)
      SIEO(IK)=SIE(IK)
      CHIO(IK)=CHI(IK)                                           RGBVM52B
      VAPO(IK)=VAP(IK)                                           RGBVM60A
      LIQO(IK)=LIQ(IK)                                           RGBVM60A
      SIEC=SIE(IK)
      IF( CFC.GE.30 ) GO TO 5018
      GO TO( 5002,5004,5006,5008 ),MAT
C NOTE. COMPUTATION OF TEMPERATURE FOR SODIUM MATERIAL .
 5002 TEMP =-385.27 + 2.6602*SIEC + 5.9894E-04*SIEC*SIEC +
     1         1.5575E-06*SIEC**3 - 2.9048E-09*SIEC**4 +
     2         1.15427E-12*SIEC**5
      GO TO 5010
C NOTE. COMPUTATION OF TEMPERATURE FOR WATER MATERIAL .
 5004 TEMP=0.9996*SIEC + 32.0002
      GO TO 5010
 5006 CIT=CI-SIEC
      TEMP=SI( AI,BI,CIT,-1 )
```

```
      GO TO 5010
5008  CONTINUE
5010  UMAX=AMAX1( UMAX,U(IK) )
      WMAX=AMAX1( WMAX ,W(IK) )
      TMAX=AMAX1( TMAX,TEMP )
      TSMAX=AMAX1( TSMAX,TS(IK) )
      UMIN=AMIN1( UMIN,U(IK) )
      WMIN=AMIN1( WMIN,W(IK) )
      TMIN=AMIN1( TMIN,TEMP )
      TQMAX=AMAX1( TQMAX,TQ(IK) )
      PMAX=AMAX1( PMAX,P(IK) )
      IF( I.EQ.IDG .AND. K.EQ.KDG ) GO TO 5012
      GO TO 5018
5012  UDG=U(IK)
      WDG=W(IK)
      TDG=TEMP
      TIM=TIMET + DT
5018  CONTINUE
5019  CONTINUE
5029  CONTINUE
      IF( ERF.LT.1 ) GO TO 10000
      CALL VRPRT
      IF( IPRFM.GT.0 ) CALL VRFLM
      RETURN
C
C NOTE. UPDATES TIME AND NUMBER OF CYCLES .
C
10000 TIMET=TIMET + DT
      NCYC=NCYC + 1
      SMSIE=0.0                                                    RGBVM70A
      SMCHI=0.0                                                    RGBVM70A
      FCHI=0.0                                                     RGBVM70A
      VELCHI=0.0                                                   RGBVM70A
C     COMPUTE PLUME CENTER AND SIGMA (HEIGHT) FOR CHI DISTRIBUTION  RGBVM54B
      DO 11150 K=2,KBP1                                            RGBVM54A
      DO 11160 I=2,IBP1                                            RGBVM54A
```

```
      IK=1+NWPC*(((I-1)*KBP2)+K-1)                                      RGBVM54A
      CIT=CI-SIE(IK)                                                    RGBVM70A
      TEMPC=SI(AI,BI,CIT,-1)                                            RGBVM70A
      RHOC=AR*TEMPC*TEMPC+BR*TEMPC+CR                                   RGBVM70A
      SMSIE=SMSIE+(RHOC*DX*DZ*SIE(IK))                                  RGBVM70A
      SMCHI=SMCHI+(CHI(IK)-BKGND)                                       RGBVM70A
      FCHI=FCHI+(FLOAT(K)-1.5)*DZ*(CHI(IK)-BKGND)                       RGBVM70A
      VELCHI=VELCHI+WSP(K)*(CHI(IK)-BKGND)                              RGBVM70A
11160 CONTINUE                                                          RGBVM54A
11150 CONTINUE                                                          RGBVM54A
      YPLUME=FCHI/SMCHI                                                 RGBVM70A
      VELCHI=VELCHI/SMCHI                                               RGBVM70A
      DWNDS=DWNDS+VELCHI*DT                                             RGBVM70A
      IF( IDIAG.GT.0 ) WRITE(IVDO,51)  TIMET,NCYC,ITER,DT,DMX
      IF( IDIAG.EQ.0 ) GO TO 11000
C NOTE. CHECKS ON TIME WHEN TO PRINT AND/OR PLOT FILM .
      IF (IDATIN.EQ.1)  GO TO 11001
11000 IF( TIMET+1.0E-5 .LT. TPRT )  GO TO 11100
      TPRT=TPRT + TPR
      CALL  VRPRT
      GO TO 11100
11001 TPRT=TPRT+TPR
11100 IF( IPRFM.LT.1 .OR. TIMET+1.0E-5.LT.TPLT ) GO TO 11200
      TPLT=TPLT + TPL
      WRITE(IVDO,60) YPLUME,VELCHI,DWNDS                                RGBVM54B
   60 FORMAT(' ',15HPLUME CENTER AT,F8.2,6H FEET.,15H PLUME SPEED IS,   RGBVM54A
     1F8.2,22H  DOWNWIND DISTANCE IS,F6.0)                              RGBVM54B
      WRITE(IVDO,63)  SMSIE                                             RGBVM55B
   63 FORMAT(4H    ,'TOTAL  ENERGY   ON MESH IS  ',E12.5)               RGBVM55B
      WRITE(IVDO,51)  TIMET,NCYC,ITER,DT,DMX                            RGBVM55B
      CALL  VRFLM
11200 CONTINUE
C  TIMING SECTION FOR RESTARTING PROGRAM ON A COARSER MESH              RGBVM55A
11300 IF(TIMET+1.0E-5.LT.TRSTRT(NRSTRT)) GO TO 11400                    RGBVM55A
      CALL COARSE                                                       RGBVM55A
      NRSTRT=NRSTRT+1                                                   RGBVM55A
```

```
      DR=DX                                                             RGBID55B
      RDR=RDX                                                           RGBID55B
      RDRS=1./(DR*DR)                                                   RGBID55B
      RDRM=RDR                                                          RGBID55B
      RDRP=RDRM                                                         RGBID55B
      RDZM=RDZ                                                          RGBID55B
      RDZP=RDZM                                                         RGBID55B
      WRITE(IVDO,40) TIMET,DX,DZ                                        RGBVM55A
   40 FORMAT(22H  PROGRAM RESTART AT  ,F10.3,12H SECONDS    ,'  DX = ', RGBVM55A
     AF6.2,'  DZ = ',F6.2)                                              RGBVM55A
      CALL VRPRT                                                        RGBVM55A
11400 CONTINUE                                                          RGBVM55A
C NOTE. CHECKS ON TIME WHEN TO WRITE MAG TAPE FILE .
12000 IF( TWTD.GE.1.E+5 ) GO TO 12100
      IF (IDATIN.EQ.1) GO TO 12001
      IF( TIMET+1.0E-5 .LT. TWTD ) GO TO 12100
      TWTD=TWTD + TTD
      CALL TAPWRI
      GO TO 12100
12001 TWTD=TWTD+TTD
C NOTE. COMPUTATION OF SPECIFIC DIAGNOSTIC VARIABLES .
12100 GO TO KDIAG,( 12200,12500,13000 )
C NOTE. OUTPUT OF DIAGNOSTIC VARIABLES IF IDIAG=1 FROM CARD NO. 3 .
12200 WRITE(IVDO,54) IDG,KDG,UDG,WDG,TDG,UMAX,UMIN,WMAX,WMIN,TMAX,TMIN
     1 ,TSMAX,EPS
C
C NOTE. COMPUTATION OF TIMING IN VARIOUS PORTIONS OF THE PROGRAM .
C
12500  IF( TIMET+1.E-10 .LT. TFIN ) GO TO 13000
C
C NOTE. CHECKS ON TIME WHEN TO FINISH .
C
13000 IF( TSTEP.LT.EM6 ) GO TO 13010
      IF( NCYC.LT.2 ) GO TO 13010
      ALENG=AMIN1( DX,DZ )
      VEL=AMAX1( UMAX,WMAX )
```

```
      IF ( VEL.GT.EM6 )  DT=TSTEP*ALENG/VEL
      DTDIF=TSTEP*RDXDZS/TSMAX
      VELNEW=AMAX1( UMAX,WMAX )
      TAUDT=0.20*VELNEW/( VELNEW-VELOLD+EM6 )
      TAUDT=ABS( TAUDT )
      DT=AMIN1( DT,DTDIF,TAUDT )
      RDT=1./DT
13010 IDATIN=0
      IF( TIMET+1.0E-5 .LT. TFIN ) GO TO 100
      RETURN
C **** * FORMATS ***** FORMATS ***** FORMATS ***** .
   50 FORMAT(1H ,75H *** ERROR 004 - PRESSURES FAILED TO CONVERGE WITHIN
     1 1500  ITERATIONS . ***)
   51 FORMAT(1H ,5HTIME=,1PE12.4,3H , ,14HCYCLE NUMBER =,I5,3H , ,
     1 28H PRESSURE ITERATION NUMBER =,I4,3H , ,4HDT =,E12.4,3H , ,
     2 16HMAX DIVERGENCE =,E12.4)
   52 FORMAT(1H ,5X,62H THE FOLLOWING DIAGNOSTICS OCCUR AFTER TIME HAS B
     1EEN UPDATED .)
   54 FORMAT(1H ,5X,2HI=,I3,3H K=,I3,4H  U=,1PE12.5,4H  W=,E12.5,
     1 4H  T=,E12.5,3H * ,6H UMAX=,E12.5,6H UMIN=,E12.5/6H WMAX=,E12.5,
     2 6H WMIN=,E12.5,17X,7H  TMAX=,E12.5,7H  TMIN=,E12.5,7H TSMAX=,
     3 E12.5/7H   EPS=,E12.5)
   55 FORMAT(1H ,5X,10HTIME/CYC =,1PE10.3,10H TOT TIME=,E10.3,
     1 10HI/O T/CYC=,E10.3,10H TOT I/O =,E10.3)
      END                                                        VM999991
```